

EVOLUTION AND DEVELOPMENT OF PETALS IN AIZOACEAE (CARYOPHYLLALES)

By

SAMUEL FRASER BROCKINGTON

A DISSERTATION PRESENTED TO THE GRADUATE SCHOOL
OF THE UNIVERSITY OF FLORIDA IN PARTIAL FULFILLMENT
OF THE REQUIREMENTS FOR THE DEGREE OF
DOCTOR OF PHILOSOPHY

UNIVERSITY OF FLORIDA

2009

© 2009 Samuel Fraser Brockington

To my ma and pa

ACKNOWLEDGMENTS

I acknowledge the assistance of numerous people and organizations that have contributed to this doctoral work. First and foremost, I thank my advisors Douglas and Pamela Soltis for their patient support and example. I thank Walter S. Judd for inspiring my interest in the evolution of angiosperms and for his insight into various aspects of this project. I thank David Oppenheimer and Paris Gray for their expertise and use of their *in-situ* facilities. I thank Elena M. Kramer for her advice and expertise at various stages of this project. The morphological development work would not have been possible without the help of Paula J Rudall at the Royal Botanic Gardens, Kew and Michael Frohlich at the Natural History Museum, London. I thank my supervisory committee for taking the time to read this dissertation. I thank Mark Whitten for taking so many superb photos and sharing his photographic equipment. Kurt Neubig kindly shared equipment. I thank my two undergraduate helpers Alexandre Roolse and Jeremy Ramdial for putting in some long hours and collecting substantial amounts of data.

The research was funded by an Assembling the Tree of Life grant EF-0431266 (NSF) to D. E. Soltis and P. S. Soltis, Floral Genome Project NSF grant PGR-0115684 to D. E. Soltis and P. S. Soltis, and a DDIG grant DEB-0808342 (NSF) to D. E. Soltis and S. F. Brockington, and a Botanical Society of America Karling Award to S. F. Brockington.

Finally I thank my friends in Florida and England, and my siblings Dan, Alice and Grace for their endless support and encouragement. Above all I thank my parents for their love and dedication over so many years.

TABLE OF CONTENTS

	<u>page</u>
ACKNOWLEDGMENTS.....	4
LIST OF TABLES.....	9
LIST OF FIGURES	11
LIST OF ABBREVIATIONS.....	13
ABSTRACT.....	14
CHAPTER	
1 INTRODUCTION.....	16
The Angiosperm Perianth as a System for Evolutionary Developmental Biology (Evo-Devo).....	16
An Evo-Devo Framework for the Study of Petal Evolution.....	17
Caryophyllales: A Model Clade for the Study of Perianth Evolution.....	18
Dissertation Outline: Developing the Caryophyllales as a System for Evo-Devo Research.....	18
2 PHYLOGENY OF THE CARYOPHYLLALES <i>SENSU LATO</i> : REVISITING HYPOTHESES ON POLLINATION BIOLOGY AND PERIANTH DIFFERENTIATION IN THE CORE CARYOPHYLLALES	20
Introduction	21
Materials and Methods.....	26
Taxon Sampling.....	26
DNA Isolation and Amplification	27
Alignment and Phylogenetic Analysis	28
Character Reconstructions	30
Results.....	34
Individual Plastid Single Copy Data Sets	34
Inverted Repeat Data Set.....	35
Combined Plastid Genes from the Single Copy Region	35
Combined Plastid Single Copy and Nuclear Genes	36
Total Evidence Data Set.....	36
Discussion.....	37
Phylogenetic Analyses	38
Reconstruction of Pollination Mechanism	42
Reconstruction of Perianth Differentiation	44
Multiple Origins of Perianth Differentiation	46
Recruitment of Preceding Bracts	47
Petaloid Modification of the Androecium.....	50

	Differentiation of Homologous Perianth Parts	51
	Caryophyllales as a System for Floral Evo-Devo.....	52
3	LABILE EVOLUTION OF PIGMENTATION IN THE CORE CARYOPHYLLALES	85
	Introduction	86
	The Unique Origin of Betalains.....	87
	The Intercalation of Betalain and Anthocyanin Lineages.....	88
	Mutual Exclusion of Anthocyanins and Betalains.....	89
	Biosynthetic Inhibition	89
	Materials And Methods	91
	Taxon Sampling and Data Assembly	91
	Phylogenetic Analyses	91
	Character Coding	93
	Character-state Reconstruction	93
	Stochastic Mapping	94
	Prior Specification	94
	Rates of Transformation and Ancestral State Reconstruction	95
	Results.....	96
	Phylogenetic Relationships	96
	Character Mapping with Unordered Coding.....	97
	Character Mapping with Ordered Coding.....	98
	Discussion.....	99
	Polyphyletic Molluginaceae.....	99
	Early-Diverging Anthocyanic Lineages.....	100
	Derived Anthocyanic Lineages.....	101
	Evidence for Reversals to Anthocyanin Pigmentation.....	102
	Effect of Ordered Character Coding - Support for Ehrendorfer (1976.....	103
	The Occurrence of Unpigmented Lineages.....	104
	Multiple Origins of Betalain Pigmentation	105
	Conclusion	107
4	KEEP THE DNA ROLLING: MULTIPLE DISPLACEMENT AMPLIFICATION OF ARCHIVAL PLANT DNA EXTRACTS	122
	Introduction	122
	Materials and Methods.....	124
	DNA Extractions from Herbarium Specimens	124
	Multiple Displacement Amplification.....	124
	PCR.....	125
	PCR Cleanup and Sequencing	126
	Results.....	126
	Multiple Displacement Amplification.....	126
	PCR.....	127
	Sequencing	128
	Discussion.....	128

5	PHYLOGENY OF MADS-BOX GENE LINEAGES IN AIZOACEAE (CARYOPHYLLALES).....	133
	Introduction	133
	MIKC Genes and ABCDE Functions in Floral Organ Identity.....	134
	Phylogenetic Analyses Reveal the Evolutionary History of MIKC-type Genes.....	135
	Phylogeny of A-Function MIKC-type Genes	136
	B-Function MIKC-type Genes.....	137
	C and D-Function MIKC-type Genes.....	137
	E-function MIKC-type Genes.....	138
	Duplications in Association with Morphological Variation and Novelty.....	139
	Methods	141
	Taxon Sampling.....	141
	RNA Isolation and Gene Amplification.....	142
	Alignments	142
	Phylogenetic Analyses	143
	Results and Discussion	144
	Caryophyllid MIKC Complement.....	144
	Polygonales-specific Duplication in the <i>EuAP3</i> Lineage	146
	Absence of the <i>euPLE</i> Lineage in Caryophyllales	147
	Absence of Duplications Coinciding with the Inferred Origin of Petaloid Staminodes	148
6	PERIANTH EVOLUTION IN AIZOACEAE: NOT ALL CORE EUDICOT PETALS WERE CREATED EQUAL.....	162
	Introduction	163
	Methods	169
	Plant Materials	169
	Scanning Electron Microscopy.....	169
	RNA-RNA <i>In-situ</i> Hybridisation.....	169
	Relative-Quantitative RT-PCR.....	170
	Results.....	171
	Floral Ontogeny in <i>Sesuvium portulacastrum</i>	171
	Floral Ontogeny in <i>Delosperma napiforme</i>	172
	Expression of <i>AGAMOUS</i> Homologs	173
	Expression of <i>PISTILLATA</i> Homologs	174
	Expression of <i>APETALA3</i> Homologs.....	175
	Discussion.....	176
	Perianth Ontogeny and Historical Homology of Petaloid Organs in Aizoaceae.....	176
	Petal Identity: A Morphological or Functional Concept?	177
	Implications of Correspondence between Leaf Sheath and Petaloid Tepal.....	178
	Assessing Morphological Homology between Different Petaloid Organs in Aizoaceae	180
	Assessing Process Homology between Petaloid Staminodes and Petaloid Tepals	181
	Implications of <i>AP3</i> and <i>PI</i> Homolog Expression Patterns	182
	Implications of <i>AG</i> Homolog Expression Patterns.....	184

Evolution of the Aizoaeae Perianth in the Context of the Caryophyllales	186
Conclusion.....	188
REFERENCES	197
BIOGRAPHICAL SKETCH	213

LIST OF TABLES

<u>Table</u>	<u>page</u>
2-1 Table showing for each data partition: aligned and analysed length of data partitions.....	70
2-2 Voucher, Citation, and GenBank Accession No. for <i>rbcL</i>	71
2-3 Voucher, Citation, and GenBank Accession No. for <i>rpoC2</i>	72
2-4 Voucher, Citation, and GenBank Accession No. for <i>atpB</i>	73
2-5 Voucher, Citation, and GenBank Accession No. for <i>psbBTN</i>	74
2-6 Voucher, Citation, and GenBank Accession No. for <i>rps4</i>	75
2-8 Voucher, Citation, and GenBank Accession No. for 18S rDNA	77
2-9 Voucher, Citation, and GenBank Accession No. for 26S rDNA	78
2-10 Voucher, Citation, and GenBank Accession No. for IR.....	79
2-11 Primers used for PCR and Sequencing	80
2-12 Coding of Perianth for Parsimony Reconstruction and Stochastic Character Mapping, with references used to code taxa.....	81
2-13 Coding of Pollination for Parsimony Reconstruction and Stochastic Character Mapping, with references used to code taxa.	82
2-14 Estimations of the posterior probability of ancestral perianth character states at each node.....	83
2-15 Estimations of the posterior probability of ancestral pollination character states at each node. Coding Strategy for Pollination: Anemophilous = 0, Entomophilous = 1.....	84
3-1 Summary of hypotheses historically proposed to explain the evolution of pigmentation in the Caryophyllales, with limitations of each.....	115
3-2 Frequencies of each transformation for four alternative reconstructions employing unordered character coding.	116
3-3 Frequencies of each transformation for four alternative reconstructions employing ordered character coding.....	117
3-4 Voucher, citation, and GenBank accession No. for <i>rbcL</i> (Voucher information not shown for previously published sequences).	118

3-5	Voucher, citation, and GenBank accession No. for <i>matK</i> (voucher information not shown for previously published sequences)	119
3-6	The estimations of the posterior probability of ancestral characters for the ordered and unordered evolution of pigments for all nodes presented graphically in Fig. 3.....	120
3-7	Pigment coding for each terminal and sources of information used to designate characters states. Coding Strategy: Anthocyanin (0), Unpigmented (1), Betalain (2), Unknown (?).	121
4-1	Species of Caryophyllales used in this study: family, source, collection date, accession number and DNA extraction method.	132

LIST OF FIGURES

<u>Figure</u>	<u>page</u>
2-1	Maximum likelihood (ML) tree resulting from GARLI analysis of total evidence data set 55
2-2	Phylogram of single most parsimonious tree based on the total evidence data set..... 56
2-3	Parsimony reconstruction (illustrated on an MP tree) and stochastic character mapping (illustrated on Bayesian consensus tree): A) Reconstruction of perianth evolution; B) Pollination syndromes. 57
2-4	The diverse forms of the perianth in the core Caryophyllales..... 58
2-5	Trees derived from analyses of the <i>atpB</i> data set..... 59
2-6	Trees derived from analyses of the <i>matK</i> data set..... 60
2-7	Trees derived from analyses of the <i>ndhF</i> data set..... 61
2-8	Trees derived from analyses of the <i>psbBTN</i> data set 62
2-9	Trees derived from analyses of the <i>rbcL</i> data set..... 63
2-10	Trees derived from analyses of the <i>rpoC2</i> data set 64
2-11	Trees derived from analyses of the <i>rps4</i> data set 65
2-12	Trees derived from analyses of the IR data set 66
2-13	Trees derived from analyses of the combined plastid single-copy gene data set..... 67
2-14	Trees derived from analyses of the combined single copy plastid gene and nuclear gene data sets. 68
2-15	Posterior probabilities of each rate category given each combination of E(T) and SD(T) and sampled from the prior with 10,000 realizations..... 69
3-1	Phylogram of one of twelve most parsimonious trees based on the <i>matK</i> and <i>rbcL</i> data set for 11 genera of Molluginaceae 109
3-2	Maximum likelihood (ML) tree resulting from GARLI analysis of <i>matK</i> and <i>rbcL</i> data set for 11 genera of Molluginaceae 110
3-3	Reconstruction of pigment evolution. 111
3-4	Prior simulations for ordered data set. 112

3-5	Prior simulations for unordered data set.....	113
3-6	Parsimony reconstruction of pigment evolution using unordered data sets and ordered data sets.....	114
4-1	MDA-treated reaction products (M1-8) and corresponding untreated genomic equivalent (G1-8).....	131
4-2	Amplification of 1363 bp fragment of <i>psbB</i> , fragment of <i>nad7</i> gene, fragment of ITS for two of the eight species.....	131
5-1	ML tree derived from analysis of a DNA dataset comprising 121 MADS-box gene loci (including 54 loci isolated by this study).....	149
5-2	Trees derived from analyses of the ‘A-function’ DNA dataset comprising 82 MADS-box gene loci (including 12 loci isolated by the study).....	150
5-3	Trees derived from analyses of the ‘B-function’ DNA dataset comprising 127 MADS-box gene loci (including 19 loci isolated by the study).....	152
5-4	Trees derived from analyses of the <i>APETALA3</i> DNA dataset comprising 69 MADS-box gene loci (including ten loci isolated by the study).....	154
5-5	Trees derived from analyses of the <i>PISTILLATA</i> DNA dataset comprising 47 MADS-box gene loci (including 6 loci isolated by the study).....	156
5-6	Trees derived from analyses of the ‘C and D-function’ DNA dataset comprising 104 MADS-box gene loci (including nine loci isolated by the study).....	158
5-7	Trees derived from analyses of the ‘E-function’ DNA dataset comprising 151 MADS-box gene loci (including eight loci isolated by the study).....	160
6-1	Floral Development in <i>Sesuvium portulacastrum</i>	190
6-2	Floral development in <i>Delosperma napiforme</i>	191
6-3	Correspondence between perianth and leaf sheath in <i>Sesuvium portulacastrum</i>	192
6-4	Expression of <i>AGAMOUS</i> (<i>AG</i>) homologs in <i>Sesuvium portulacastrum</i>	193
6-5	Expression of <i>PISTILLATA</i> (<i>PI</i>) homologs in <i>Sesuvium portulacastrum</i>	194
6-6	Expression of <i>APETALA3</i> (<i>AP3</i>) homologs in <i>Sesuvium portulacastrum</i>	195
6-6	RQ-RT-PCR data for four species of Aizoaceae and three gene homologs (<i>AG</i> , <i>AP3</i> , and <i>PI</i>).....	196

LIST OF ABBREVIATIONS

bp	Base Pair
ML	Maximum Likelihood
MP	Maximum Parsimony
μl	micro-litre

Abstract of Dissertation Presented to the Graduate School
of the University of Florida in Partial Fulfillment of the
Requirements for the Degree of Doctor of Philosophy

EVOLUTION AND DEVELOPMENT OF PETALS IN AIZOACEAE (CARYOPHYLLALES)

By

SAMUEL FRASER BROCKINGTON

August 2009

Chair: Douglas E. Soltis

Cochair: Pamela S. Soltis

Major: Botany

In this dissertation, the Caryophyllales *sensu lato* are explored and developed as a system for studying the evolutionary development of the angiosperm perianth. The phylogenetic context of the Caryophyllales is defined with a molecular phylogenetic analysis employing eight plastid genes, two nuclear genes and the entire plastid Inverted Repeat for forty taxa representing the major families within the Caryophyllales *sensu lato*. Stochastic character mapping and parsimony reconstruction analyses reveal a minimum of nine independent origins of the differentiated perianth within the core Caryophyllales clade. Molluginaceae are revealed to be polyphyletic such that two genera, *Hypertelis* and *Macarthuria*, form disparate lineages with respect to Molluginaceae *sensu stricto*. The implications of this resolved polyphyly for our understanding of the evolution of pigmentation within the core Caryophyllales was explored by stochastic character mapping and parsimony reconstruction analyses. Multiple origins of betalains are suggested, with reversals to anthocyanins. The value of Multiple Displacement Amplification is demonstrated as a means to augment rare archival DNA stocks for molecular phylogenetic analysis. The evolution of various lineages of MADS-box transcription factors was explored in relation to the novel evolution of petaloid staminodes within the plant family Aizoaceae. Fifty-four new MADS-box gene loci were sequenced from six species of Caryophyllales. Phylogenetic analyses of these loci demonstrate an absence of gene duplication,

therefore, increases in MADS-box gene complement do not play a role in the evolution of the novel petaloid staminodes in Aizoaceae. Finally the evidence for a shared genetic pathway for petal development was assessed by examining the morphological structure and genetic processes in two distinct petaloid organs in Aizoaceae, the petaloid staminodes and petaloid tepals. It is determined that at multiple levels the petaloid staminodes and petaloid tepals are not-homologous. There is no morphological or genetic evidence to recommend the concept of a conserved petal identity program in Aizoaceae. The petaloid organs in Aizoaceae should therefore be regarded as convergent evolutionary events that have occurred independently of a hypothesized petal identity program. Thus, the concept of a conserved petal identity program across all core eudicot angiosperms is refuted.

CHAPTER 1 INTRODUCTION

The Angiosperm Perianth as a System for Evolutionary Developmental Biology (Evo-Devo)

The perianth is a near-constant characteristic of angiosperms, giving many flowers their distinctive appearance and playing an important role in plant-pollinator interactions (Baum and Whitlock 1999). The importance of the perianth for angiosperm biology has ensured a long and rich history of research. More recently, research into perianth evolution has been invigorated by the discipline of evolutionary developmental biology, which seeks to integrate new data from molecular phylogenetic analyses, comparative developmental morphology, and comparative analyses of gene expression and function. In the context of the perianth, the evolution of the petal in particular has become the focus of evolutionary developmental study.

Several factors motivate evolutionary developmental research into the petal: 1) The genetic pathways underlying petal development in model organisms are relatively well understood (Coen and Meyerowitz, 1991). 2) Homologs of the MADS-box genes that are critical in petal developmental pathways have been isolated across the angiosperms (Kramer and Irish, 2000; Kim et al., 2005). 3) MADS-box gene homologs function in a spatially dependent fashion and so are amenable to comparative expression techniques (Kramer and Jaramillo, 2007). 4) Diverse perianth structures provide the necessary variation to explore how the evolution of developmental genetic pathways relates to the evolution of morphology and allow various principles of evolutionary developmental biology to be tested (Endress, 1996). In the context of petal evolution, these principles include: the role of heterotopy in morphological evolution; the developmental basis of homoplasy and homology; the relative frequency of parallel and convergent evolution; and the role of gene duplication in the origin of morphological novelty.

An Evo-Devo Framework for the Study of Petal Evolution

Classical theory of petal evolution suggests that petals have evolved multiple times independently (Takhtajan, 1991). This theory arose from the assumption that the ancestor to the angiosperms was apetalous (Sun et al. 1998), and that petals in different lineages of angiosperms exhibit distinct suites of morphological traits reminiscent of either bracts or stamens.

Bracteopetals describe petals that generally exhibit leaf-like characteristics: they initiate and develop earlier than the stamens; they are often spirally arranged on the same parastichies as the subtending bracts; their primordia are distinctly crescent-shaped; and they are supplied by three vascular traces. In contrast, andropetals exhibit stamen-like characteristics: they are developmentally delayed relative to the stamens; arranged on the same parastichies as the stamens; similar in appearance to stamen primordia at inception; and are supplied by a single vascular trace (Endress 1994).

In an effort to synthesize these classical observations with contemporary developmental genetic data, Kramer and Irish (1999) proposed the concept of an ancestral petal identity program. Their hypothesis rests on the observation that petal development pathways are conserved between distant core eudicot lineages, and that the MADS-box gene components within these petal developmental programs are frequently associated with petals and petaloid organs across angiosperms. Kramer and Irish hypothesized that de-activation and subsequent repeated re-activation of an ancestral genetic petal identity program, together with spatial redeployment in either bracts or stamens, generated petaloid organs of differing historical and positional homology in different lineages of angiosperms. Consequently, angiosperm petals, although appearing to have evolved independently many times, may actually share latent genetic homology in the form of a common petal identity pathway. This hypothesis is considered to be

testable through the comparative analysis of the developmental genetic pathways that specify petal identity in bracteopetals and andropetals in distinct lineages of angiosperms.

Caryophyllales: A Model Clade for the Study of Perianth Evolution

The Caryophyllales is a group long recognized by its distinctive placentation and embryology, and is a major order of angiosperms representing about 5% of core eudicot diversity. The order exhibits diverse variation in perianth structure and morphology and is consequently a valuable clade in which to assess the concepts of a petal identity program. In essence, the patterns of perianth evolution in Caryophyllales imitate, on a smaller phylogenetic scale, the evolutionary trends traditionally thought to have taken place across the angiosperms as a whole (Bessey, 1915; Takhtajan, 1991). The perianth varies from an undifferentiated to differentiated structure with the concomitant evolution of petals from either bracts or stamens, in varying positions in the flower. More recently, molecular phylogenetics has improved our understanding of intra-ordinal relationships within the Caryophyllales (Cuenoud et al., 2002), allowing more accurate interpretations of polarity in perianth evolution and enabling clearer understanding of homology between different perianth structures. This improved phylogenetic resolution, combined with novel evolutionary developmental approaches has the potential to shed much light on the evolution of floral morphology in the Caryophyllales. In the following chapters, I take the first steps in developing the Caryophyllales as a system for the study of the evolutionary development of the angiosperm perianth, with special reference to the evolution of petals.

Dissertation Outline: Developing the Caryophyllales as a System for Evo-Devo Research

Chapter 2 defines the phylogenetic concept of Caryophyllales with a molecular phylogenetic analysis employing eight plastid genes, two nuclear genes and the entire plastid Inverted Repeat (~42,000bp) for 40 taxa representing the major families within the

Caryophyllales *sensu lato*. Stochastic character mapping and parsimony reconstruction analyses reveal a minimum of nine independent origins of the differentiated perianth within the core Caryophyllales clade. Chapter 3 addresses the problem of the anthocyanic yet polyphyletic Molluginaceae, revealing that two genera, *Hypertelis* and *Macarthuria*, form disparate lineages with respect to Molluginaceae *sensu stricto*. The implications of this resolved polyphyly for our understanding of the evolution of pigmentation within the core Caryophyllales is explored by stochastic character mapping and parsimony reconstruction analyses. Chapter 4 illustrates the value of Multiple Displacement Amplification as a means to augment rare archival DNA stocks for molecular phylogenetic analysis – a strategy employed in Chapters 2 and 3. Chapter 5 describes the isolation of 54 MADS-box gene loci representing 10 clades of MADS-box genes, from all four subfamilies within the family Aizoaceae, as well representatives from Portulacaceae and Polygonaceae. Phylogenetic analyses using Parsimony, Likelihood and Bayesian criteria are employed to determine orthology and paralogy in these MADS-box gene lineages and to identify putative gene losses and duplication. Chapter 6 tests the concept of the petal identity program in the context of the family Aizoaceae (Caryophyllales), combining developmental morphological data and gene expression analyses of MADS-box gene homologs.

CHAPTER 2
PHYLOGENY OF THE CARYOPHYLLALES *SENSU LATO*: REVISITING HYPOTHESES
ON POLLINATION BIOLOGY AND PERIANTH DIFFERENTIATION IN THE CORE
CARYOPHYLLALES

Molecular phylogenetics has revolutionized our understanding of the Caryophyllales, and yet many relationships have remained uncertain, particularly at deeper levels. We have performed parsimony and maximum likelihood analyses on separate and combined data sets comprising eight plastid genes (~12,000bp), two nuclear genes (~5000bp) and the plastid inverted repeat (~24,000bp) giving a combined analyzed length of 42006bp for 36 species of Caryophyllales and four outgroups. We have recovered strong support for deep-level relationships across the order. Two major subclades are well-supported - the non-core and core Caryophyllales; *Rhabdodendron* followed by *Simmondsia* are sisters to the core Caryophyllales; *Limeum* and *Stegnosperma* are successive sisters to the ‘globular inclusion’ clade; *Gisekia* is a distinct lineage well separated from *Rivina* within the ‘raphide’ clade; and *Rivina* and Phytolaccaceae are disparate lineages with *Rivina* sister to Nyctaginaceae. The placement of *Sarcobatus* and relationships within the portulacaceous cohort remain problematic. Within the latter, *Halophytum* is sister to Basellaceae and Didiereaceae, and the clade comprising *Portulaca*, *Talinum* and Cactaceae is well supported. Classical hypotheses argued that the early Caryophyllales had evolved in open, dry, marginal environments at a time when pollinators were scarce and as such the ancestral caryophyllid flower was wind-pollinated with an undifferentiated perianth. We re-evaluated these hypotheses in light of our phylogeny and find little support for anemophily as the ancestral condition, however the early caryophyllid flower is suggested to have possessed an undifferentiated perianth. There has been a subsequent minimum of nine origins of differentiated perianth. We discuss the evidence for independent origins of

differentiated perianth and highlight the research opportunities that this pattern offers to the field of evolutionary developmental genetics.

Introduction

Research interest in Caryophyllales has a long and rich history; core members of this lineage correspond to the old Centrospermae ('central seeded'), a group long recognized by its distinctive placentation and embryology (Braun, 1864; Eichler, 1875-78). Centrospermae became the focus of research and debate in the 1960s as one of the first groups whose circumscription was modified based on phytochemistry (Cronquist and Thorne, 1994). All but two of the ten families then recognized as belonging to the Centrospermae were discovered to possess betalain pigments instead of anthocyanins (Cronquist and Thorne, 1994). On the basis of this chemosystematic character, Cactaceae and Didiereaceae were reassigned to the Centrospermae, and several families of dubious affiliation were excluded (Cronquist and Thorne, 1994). Subsequent classifications recognized the Caryophyllales as a well-defined group on the basis of numerous morphological, ultrastructural and chemical characters (Cronquist, 1981, 1988; Dahlgren, 1975; Tahktajan, 1980; Thorne, 1976). Just prior to the emergence of DNA-based molecular systematics, the Caryophyllales *sensu stricto* comprised 12 families (Cronquist, 1988; Tahktajan, 1980; Thorne, 1992a): Phytolaccaceae, Achatocarpaceae, Nyctaginaceae, Aizoaceae, Didiereaceae, Cactaceae, Chenopodiaceae, Amaranthaceae, Portulacaceae, Basellaceae, Molluginaceae, and Caryophyllaceae. In addition, Polygonaceae and Plumbaginaceae have been regarded as closely related to these 12 families by numerous systematists (Cronquist and Thorne, 1994).

A series of molecular phylogenetic investigations has altered the concept of Caryophyllales provided in earlier classifications. Giannasi et al. (1992) confirmed the close relationship of Polygonaceae and Plumbaginaceae with the Caryophyllales. Albert et al. (1992) and Williams et

al. (1994) demonstrated the association of Droseraceae, Nepenthaceae and Drosophyllaceae with Polygonaceae and Plumbaginaceae. The carnivorous clade plus Polygonaceae/Plumbaginaceae was further expanded to include Ancistrocladaceae, Dioncophyllaceae, Frankeniaceae and Tamaricaceae (Fay et al., 1997). Numerous analyses have recognized this expanded clade, which is variously termed the ‘non-core Caryophyllales’ (APGII, 2003; Cuénoud et al., 2002), Caryophyllales II (Hilu et al., 2003), and ‘Polygonales’ (Judd et al., 1999), as sister to Caryophyllales *sensu stricto* (Soltis et al., 2000; Soltis et al., 1999).

Within Caryophyllales *s.s.* or the ‘core Caryophyllales’, molecular data have resulted in several refinements in phylogeny and classification. Additional families recognized as belonging to the core Caryophyllales include Physenaceae and Asteropeiaceae (Morton et al., 1997), Rhabdodendraceae and Simmondsiaceae (Fay et al., 1997). Simmondsiaceae are supported as sister to the core Caryophyllales (Cuénoud et al., 2002) with Physenaceae and Asteropeiaceae forming a strongly supported sister group (combined *rbcL/matK* analysis: Cuénoud et al., 2002). Rhabdodendraceae have been associated with Simmondsiaceae as sister to the core Caryophyllales or as sister to both core and non-core Caryophyllales, but with little support for either position (*matK* analysis: Cuénoud et al., 2002).

Molecular studies have also identified and confirmed a number of polyphyletic groups within the core Caryophyllales. Recognition that Phytolaccaceae are polyphyletic (initially by Rettig et al., 1992) supports the delimitation of four families: Achatocarpaceae, Barbeuiaceae, Gisekiaceae and Stegnospermataceae (APG II, 2003; Cuénoud et al., 2002). Achatocarpaceae may form a clade together with Caryophyllaceae and Amaranthaceae (combined *matk/rbcL* analysis: Cuénoud et al., 2002). Stegnospermataceae are placed without support as a successive sister lineage to the remainder of the core Caryophyllales (Cuénoud et al., 2002), following the

divergence of Asteropeiaceae, Physenaceae, Achatocarpaceae, Caryophyllaceae and Amaranthaceae. *Barbeuia* represents a distinct, isolated lineage within the core Caryophyllales but of uncertain position (Cuénoud et al., 2002). *Rivina* and *Petiveria*, formerly both of Phytolaccaceae, are paraphyletic (combined *matK/rbcL* analysis: Cuénoud et al., 2002) with respect to *Phytolacca*. *Rivina* has been allied with the family Gisekiaceae, and *Petiveria* is placed sister to *Rivina*, and Gisekiaceae (combined *matK/rbcL* analysis: Cuénoud et al., 2002). Similarly in the *matK* analyses *Hillieria* is placed sister to *Rivina* and *Ledenbergia* is sister to these two taxa. *Lophiocarpus*, originally placed within Phytolaccaceae, is now separated and placed sister to *Corbichonia* (Cuénoud et al., 2002). *Sarcobatus*, originally placed in the Chenopodiaceae, was recognized as the family Sarcobataceae (Behnke, 1997; APG II, 2003) on the basis of distinct sieve-element plastids with respect to Chenopodiaceae (Behnke, 1997). This separation was supported by molecular analyses in which Sarcobataceae form a distinct lineage allied with the clade containing Aizoaceae, Phytolaccaceae and Nyctaginaceae, Gisekiaceae and *Agdestis* (Cuénoud et al., 2002; Downie et al., 1997). The circumscription of Molluginaceae remains problematic; the family is likely to be polyphyletic. Previous authors have suggested that the inclusion of *Macarthuria* and *Polpoda* is unlikely based on morphological observations, however, two genera have not been included in previous molecular analyses (Cuénoud et al., 2002). Genera previously included within Molluginaceae (*Corbichonia*, *Limeum*, *Gisekia*) form disparate lineages with respect to the type genus. However, the position of *Limeum* outside Molluginaceae is unsupported (*rbcL/matK*: Cuénoud et al., 2002). *Mollugo*, *Adenogramma*, *Glischrothamnus*, *Glinus*, *Pharnaceum* and *Suessenguthiella* constitute a monophyletic group that is sister to the portulacaceous cohort (Cuénoud et al., 2002).

The portulacaceous cohort of Basellaceae, Cactaceae, Didiereaceae and Portulacaceae was initially proposed by Thorne (1976) and is supported by non-DNA characters such as presence of a floral involucre, succulent tissue, mucilage and CAM photosynthesis (Cuénoud et al., 2002; Nyffeler, 2007). The monophyly of the cohort was implied by early molecular analyses (Downie et al., 1997; Rettig et al., 1992); however, relationships within the group are unclear, and complicated by the gross paraphyly of Portulacaceae (suggested by Carolin, 1987 and Hershkovitz, 1993). The addition of molecular data has resulted in some clarification. In an analysis of ITS sequences, Hershkovitz and Zimmer (1997) suggested that Cactaceae were embedded within Portulacaceae and sister to *Portulaca*, *Anacampseros* and relatives, and portions of *Talinum* (the ACPT clade; from Anacampseroteae, Cactaceae, *Portulaca* and *Talinum*: Nyffeler, 2007). These findings were confirmed and extended by Applequist and Wallace (2001) in an analysis of *ndhF* sequences; *Talinum* with *Talinella*, *Portulaca* with *Anacampseros*, and the Cactaceae form three distinct lineages within a well-supported clade. Although the monophyly of the ACPT clade seems clear, as summarized by Nyffeler (2007), the pattern of branching within the clade has varied among analyses. Outside of the ACPT clade, Hershkovitz and Zimmer (1997) found that Basellaceae and Didiereaceae form a distinct monophyletic group and are sister to portulacaceous genera *Portulacaria* and *Ceraria*. In addition, Applequist and Wallace (2001) described this same clade as consisting of three distinct lineages: Basellaceae; Didiereaceae with *Calyptrorhiza*, *Ceraria* and *Portulacaria*; and a strongly supported assemblage of genera including *Claytonia*, *Montia*, *Calandrinia*, *Montiopsis*, *Cistanthe*, *Calyptridium* and *Phemeranthus*.

Despite these advances in the understanding of subordinal relationships in Caryophyllales, a number of uncertainties remain. The positions of *Limeum*, *Stegnosperma* and *Barbeuia* are all

ambiguous. The relative position of *Rhabdodendron* and *Simmondsia* as possible sisters to either the core Caryophyllales or Caryophyllales *s.l.* is unclear. Relationships within the portulacaceous cohort are largely unresolved, particularly within the clade containing Basellaceae, Didiereaceae and allied genera (Appelquist and Wallace, 2001). The clade including Phytolaccaceae, Sarcobataceae, Nyctaginaceae, Gisekiaceae and Agdestidaceae also lacks internal resolution. Additionally, some relationships have only been suggested on the basis of single-gene analyses (Cuénoud et al., 2002) with many nodes scattered throughout the Caryophyllales lacking strong support.

In an effort to resolve the remaining problematic deep-level relationships within Caryophyllales, we constructed a much larger data set than employed previously. Our data set comprised eight plastid genes from single-copy (SC) regions, two nuclear genes and the entire plastid Inverted Repeat (IR; a combined analyzed length of 42,006 base pairs) for 40 taxa representing 31 families of the Caryophyllales and three families as outgroups.

The unusual morphological and biochemical variation found within the Caryophyllales has fueled much speculation as to its evolutionary origins. Ehrendorfer (1976) outlined a plausible scenario to explain the coincident evolution of several unique characteristics found in the Caryophyllales, including floral variation and betalain pigmentation. He proposed that ancestral taxa in Caryophyllales occupied “open, warm, dry and windy habitats with mineral soils.” Reasons for assuming this ancestral habitat derive from the observation that many of the families in Caryophyllales currently inhabit xeric, marginal environments. Ehrendorfer (1976) argued that if the ancestral habitats were xeric, there would be strong selection for anemophily as pollinating insects would have been scarce in areas of little pioneer plant growth. He states that pollinators may have been scarce, as the time of the origin of the core Caryophyllales (104-111 MYBP:

Wikstrom, 2001) predates the major diversification of insect pollinator lineages. He then argues that much of the floral variation and novel pigmentation in the core Caryophyllales could be interpreted as the consequence of this anemophilous ancestry with reversals to zoophily in extant lineages. However, as this study will demonstrate, the phylogenetic concept of the Caryophyllales has changed considerably since Ehrendorfer (1976). We evaluate Ehrendorfer's hypotheses in light of a much-altered phylogeny by examining patterns of pollination biology and perianth differentiation. We discuss the evolution of perianth differentiation in the context of the literature on perianth development within Caryophyllales and use our phylogeny to identify broad trends in perianth evolution across the clade. Finally, we discuss the research opportunities that these patterns of morphological variation offer to the field of evolutionary developmental genetics.

Materials and Methods

Taxon Sampling

In this analysis 31 families of Caryophyllales *sensu* APGII (2003; Cuénoud et al., 2002) were represented. Some families are monotypic (e.g. Drosophyllaceae, Halophytaceae, Stegnospermataceae), others comprise only one genus (e.g. Asteropeiaceae, Nepenthaceae, Ancistrocladaceae, Frankeniaceae), or two or three genera (Achatocarpaceae, Dioncophyllaceae, Droseraceae, Limeaceae, Talinaceae). For larger potentially polyphyletic or paraphyletic families (e.g. Portulacaceae), multiple genera were sampled to represent more of the phylogenetic diversity. The final data set included 36 taxa of Caryophyllales with an additional four taxa (*Tetracera* and *Hibbertia* representing Dilleniaceae, *Berberidopsis* and *Vitis*) sampled as outgroups. Species, voucher information and GenBank accession numbers are given in tables 2-2 to 2-10). In some instances sequence data was combined from multiple species to represent a family - this was judged not to significantly affect a family-level analysis but the instances are

listed here: Aizoaceae (*Delosperma napiforme*, *Delosperma echinatum*, *Delosperma cooperi*); Amaranthaceae (*Celosia argentea* and *Celosia cristata*); Cactaceae (*Opuntia microdasys* and *Opuntia dillenii*); Didiereaceae (*Alluaudia ascendens* and *Alluaudia procera*); Dilleniaceae (*Hibbertia volubilis* and *Hibbertia cuneiformis*); Gisekiaceae (*Gisekia africana* and *Gisekia pharnacioides*); Molluginaceae (*Limeum africanum* and *Limeum aetheopicum*); Plumbaginaceae (*Limonium gibertii* and *Limonium arborescens*, *Plumbago zeylanica* and *Plumbago auriculata*); Polygonaceae (*Polygonum sagittatum* and *Polygonum virginicum*); Portulacaceae (*Claytonia virginica* and *Claytonia perfoliata*).

DNA Isolation and Amplification

We isolated DNA following standard CTAB protocols (Doyle and Doyle, 1987) and Qiagen DNA extraction kits (Qiagen, Valencia, CA, USA). To augment depleted DNA stocks we carried out Multiple Displacement Amplification (MDA) using the Genomiphi kit (Amersham, Piscataway, NJ, USA) according to the manufacturer's instructions (Brockington et al., 2008). MDA-treated DNA was diluted 1:10 before further PCR amplification of targeted genes.

We targeted 10 specific genes for sequencing – eight plastid genes from the large and small SC regions and two nuclear genes; all targeted genes and primers used for PCR and sequencing are provided in table 2-11. All PCR reactions contained *Taq* DNA polymerase (New England Biolabs MA, USA) and 10X Thermopol Reaction Buffer supplied by the manufacturer. The reaction volume was 25 μ l, and the final concentration of the components was *Taq* buffer (pH 8.8), MgCl₂ (1.5 mM), 200 μ M dNTP, forward and reverse primers (1 μ M), 1U *Taq* polymerase, and 1 μ l of DNA. PCR cycling was carried out in an Eppendorf Mastercycler (Eppendorf, Westbury, NJ, USA (95°C for 3 min, followed by 30-35 cycles of 94°C for 30 sec, 50°C for 30 sec, and 72°C for 1 min with a final extension time of 7 min at 72°C). PCR products

were purified using ExoSAP, and sequences were generated on an ABI 3730 XL DNA sequencer (Applied Biosystems, Inc., Fullerton, CA, USA) following the manufacturer's protocol.

Sequences were submitted to GenBank (numbers given in tables 2-2 to 2-10)

The Amplification, Sequencing and Annotation of Plastomes (ASAP) method (Dhingra and Folta, 2005) was used to obtain the sequence of the plastid genome Inverted Repeat (IR) for 35 genera of Caryophyllales (the IR for *Physena* was not sequenced) and two members of Dilleniaceae. The published complete plastid sequence of *Spinacia* (Schmitz-Linneweber et al., 2001) and *Plumbago* (Moore et al., 2007) provided the IR sequence for these two taxa. The IR sequences were subsequently annotated using DOGMA (Wyman et al., 2004). IR sequences were submitted to GenBank (numbers given in tables 2-2 to 2-10).

Alignment and Phylogenetic Analysis

Sequences were automatically aligned using Clustal X (Thompson et al., 1997) and then manually adjusted. Coding regions were aligned by predicted amino acid sequence. Regions at the beginning and ends of genes for which sequences were incomplete, together with regions that were difficult to align, were excluded from the analysis. The total aligned lengths and the analyzed aligned lengths are given in table 1. Using the new sequences generated here together with those previously published (cited in tables 2-2 to 2-10), we constructed six different data partitions: 1) individual plastid genes from the SC regions; 2) combined plastid genes from the SC regions; 3) two nuclear ribosomal RNA genes (18S rDNA and 26S rDNA); 4) plastid IR; 5) combined plastid SC and nuclear genes; 6) total evidence data set (all plastid and nuclear genes).

All data partitions were subject to the following phylogenetic analyses. We used maximum parsimony (MP) and maximum likelihood (ML) to infer phylogeny. MP analyses were implemented in PAUP*4.0 (Swofford, 2000). Shortest trees were obtained using a heuristic search and 1,000 replicates of random taxon addition with tree-bisection-reconnection (TBR)

branch swapping, saving all shortest trees per replicate. Bootstrap support (BS) for relationships (Felsenstein, 1985) was estimated from 1,000 bootstrap replicates using 10 random taxon additions per replicate, with TBR branch swapping and saving all trees.

For ML analyses we employed the program GARLI (Genetic Algorithm for Rapid Likelihood Inference; version 0.942) (Zwickl, 2000). GARLI conducts ML heuristic phylogenetic searches under the GTR model of nucleotide substitution, in addition to models that incorporate among-site rate variation, either assuming a gamma distribution (Γ) or a proportion of invariable sites (I), or both. Analyses were run with default options, except that the “significanttopochange” parameter was reduced to 0.01 to make searches more stringent. ML bootstrap analyses were conducted with the default parameters and 100 replicates. We performed a strict consensus of five replicate GARLI analyses and topological differences resulting in collapsed nodes were annotated on the representative ML tree.

Bayesian analyses were performed on the combined partition to generate trees for stochastic character mapping. Models of nucleotide substitution were determined using MrModeltest (Nylander, 2004). The Akaike information criterion (AIC) was used to select GTR+I+G as an appropriate model based on the relative informational distance between the ranked models. Analyses were implemented in MrBayes, version 3.1.2 (Huelsenbeck and Ronquist, 2001; Ronquist and Huelsenbeck, 2003). Two independent analyses each ran for 5 million generations, using four Markov chains, and with all other parameters at default values; trees were sampled every thousandth generation, with a burn-in of 200,000 generations. Stationarity of the Markov Monte Carlo chain was determined by the average standard deviation of split frequencies between runs (after 5 million generations the average standard deviation was 0.004%) and by examination of the posterior in Tracer, version 1.3 (Rambaut and Drummond,

2003). A majority rule consensus of post burn-in trees were generated in PAUP*4.0 (Swofford, 2000), using the resulting posterior distribution of the trees.

Character Reconstructions

Parsimony-based reconstructions were achieved using standard unweighted parsimony character optimization and performed within Mesquite (Maddison and Maddison, 2008). Reconstructions focus on the core Caryophyllales. And were carried out using the MP topology derived from the total evidence data set. Reconstructions were further modeled by means of stochastic mapping techniques as described by Huelsenbeck et al. (2003) and implemented in SIMMAP (Bollback, 2006). This approach estimates the rates at which a discrete character undergoes state changes as it evolves through time. Bayesian estimation has several advantages over traditional parsimony-based reconstruction. First, it allows one to average over equally likely topologies, which is valuable as the position of some taxa are poorly supported (e.g. *Limeum*) or poorly resolved (e.g. taxa within the portulacaceous cohort and ‘raphide’ clade). Second, it allows more than one character change per branch and is therefore a useful methodology for character reconstruction in the Caryophyllales - a clade in which long branches are common.

Posterior mapping requires the specification of prior values. The prior on the bias parameter was fixed at $1/k$, where k is the number of states (this being the recommended approach in SIMMAP for characters of more than two states; (Renner et al., 2007). We applied an empirical Bayesian approach in choosing appropriate priors for the substitution rate parameters following the method of (Couvreur et al., 2008a, 2008b). The gamma distribution of the substitution rate is governed by two hyperparameters defining the mean $E(T)$ and the standard deviation $SD(T)$. The values of these hyperparameters for the prior gamma distribution were selected independently for each character using the ‘number of realizations sampled from

priors' function in SIMMAP with 10,000 draws. A series of trials was performed (10,000 realizations in each) that systematically sampled for values of $E(T)$ between 1 and 30, in combination with $SD(T)$ values of either 1 and 5. The posterior distribution these combinations were visualized in Tracer v. 1.3 and further plotted as graphs of frequency against rate (see figure. 2-15). The posterior distribution curves derived from these trials allowed the selection of values of $E(T)$ that gave highest sampling and allowed optimization of the $E(T)$ value (Couvreur et al., 2008a, 2008b). A trial was also performed without specifying priors and allowing rates to be determined by branch lengths (as performed by Renner et al., 2007); however, the posterior distribution curves were generally highly skewed (see figure. 2-15), and thus this form of prior selection was not employed in subsequent analyses. Following exploration of different combinations of $E(T)$ and $SD(T)$, the prior $E(T)$ values chosen for the characters were as follows: Perianth $E(T) = 17$, Pollination $E(T) = 7$ (marked with an asterix in figure. 2-15). For all of these values of $E(T)$, an $SD(T)$ value of 5 was applied in subsequent analyses, allowing a large standard deviation to accommodate uncertainty in mean rate of substitution.

Following specification of priors, the rate and number of state transformations were estimated by 100 realizations on the 4800 post burn-in trees (with branch lengths) from the Bayesian analyses. As recommended, branch lengths were rescaled so that the total tree length was 1 but the branch length proportions were maintained. The ancestral state at different nodes was assessed using a hierarchical Bayesian ancestral state reconstruction method implemented in the 'posterior ancestral states' function of SIMMAP (Bollback, 2006). The nodes for which ancestral states were estimated are labeled in figure 2-3. The estimations of the posterior probability of ancestral character states at each node are listed in tables 2-14 and 2-15 and presented graphically on the nodes in figure 2-3.

With parsimony reconstruction analyses, when more than one character state was present in the family the representative taxon was coded as having more than one character state. In stochastic mapping analyses using SIMMAP terminals cannot be coded as having more than one state so in instances where more than one character state was present in the family, the representative taxon was coding as unknown (?). Information on pollination was derived primarily from entries in Kubitzki et al. (1993, 2003, 2007); pollination was coded as entomophilous or anemophilous. In the case where observations on pollinators have not been made, the character-state determination was ‘unknown’ (?). All coding information is listed in tables 2-12 and 2-13.

Our approach to coding perianth requires further clarification as there are many types of differentiated perianth within Caryophyllales, and their homology is not always clear. Occurrences of differentiated perianth were given different character states where there are clear documented differences in development of the differentiated perianth. Data on perianth and development were collated from the available literature (see figure 2-15). As reviewed by Ronse De Craene, 2008 criteria used to determine these differences in the literature include: meristic variation, sequence of organ initiation, difference in appearance at maturity, and presence of morphological intermediates. We were however interested in estimating the minimum number of origins of the differentiated perianth under parsimony and therefore applied a stringent approach to character coding, minimizing the number of character states to four: undifferentiated (0), differentiated with stamen-derived petaloid organs (1), differentiated with an involucre-derived outer whorl (2), and differentiated perianth of uncertain affinity (3). We employed a conservative approach to character coding, only assigning states 1 and 2 to taxa in which developmental morphological data was most conclusive. Where we were uncertain we assigned taxa to character

state 3 ‘differentiated perianth of uncertain affinity’. We emphasize that this coding does not reflect our belief that these instances of differentiated perianth are necessarily homologous, but in coding them as identical we ensure that estimation of the number of origins of differentiated perianth is conservative.

The differentiated perianths of Caryophyllaceae and Molluginaceae were assigned character state 2 due to the similar androecial nature of the petaloid perianth parts despite notable developmental differences (Ronse De Craene, 1998; 2007). In Aizoaceae, in the subfamilies Mesembryanthemoideae and Ruschoideae, the differentiated perianth is also the result of sterilization of outer members of a centrifugally initiating androecium and concomitant sepaldoidy in the outer quincuncial whorl. Morphological intermediates clearly link the petaloid staminodes with fertile stamens (Brockington SF, unpublished observations; Ronse de Craene 2007). A similar form of perianth differentiation exists in *Glinus* in the Molluginaceae (Hofmann, 1994; Ronse de Craene 2007). However it is clear that Mesembryanthemoideae and Ruschoideae are derived within Aizoaceae and that the early diverging families do not have a differentiated perianth – thus in contrast to Caryophyllaceae and Molluginaceae, the family is coded as undifferentiated for the purpose of this reconstruction. Ronse de Craene (1998) describes the strong affinity of the petaloid members of the differentiated perianth to the androecium, in Caryophyllaceae. The involucre perianths of Nyctaginaceae and the portulacaceous cohort were given the same character states in recognition of similar recruitment of bracteoles or bracts as a calyx, but again there are notable developmental differences (as described in Rohweder and Huber, 1974; Hofmann, 1994; Ronse De Craene, 2008). The quincuncial differentiated perianth in *Mirabilis jalapa* is most likely the result of floral loss within an involucre (Vanvinckenroye et al. 1993) while the differentiated perianth in the portulacaceous cohort is probably the result of

two additional phyllomes inserted between the bracteoles and inner petaloid quincuncial perianth members (Hofmann, 1994). The petals of *Limeum* and *Stegnosperma* are similar (and probably homologous to the petals in Caryophyllaceae (Hofmann 1973, 1977; Ronse de Craene pers. comm) and are coded as such. The nature of the perianth in both *Asteropeia* and *Rhabdodendron* is uncertain due to lack of detailed investigations and is coded as ‘differentiated perianth of uncertain affinity’. Cactaceae exhibit a great increase in perianth parts and these increases in floral merism and generally modified floral form make it challenging to determine correspondence between perianth in Cactaceae and its closest relatives – in this study, *Portulaca* and *Talinum*. Cactaceae was also therefore coded as of uncertain homology. Non-core Caryophyllales and Outgroup taxa were coded as ‘differentiated perianth of uncertain homology’ because the nature of the perianth relative to that within the core Caryophyllales is uncertain.

Results

Individual Plastid Single Copy Data Sets

MP and ML trees from individual data sets are largely congruent with each other (figures 2-5 to 2-11; tree statistics shown in table 2-1). Consistent with the approximate nature of the GARLI approach to ML phylogeny estimation, replicate GARLI analyses on the individual gene data sets do on occasion recover slightly different topologies. Taking into account nodes that are either unsupported or that collapse in the strict consensus however there are few instances of conflicting relationships between trees derived from different individual gene data sets. These examples of conflict include the following: in the *matK* MP tree, *Delosperma* and *Gisekia* were recovered as sister groups (51%); in the MP and ML *ndhF* tree, *Spinacia* and *Stellaria* were resolved as sister groups to the exclusion of *Celosia* (MP BS=100%); in the *rbcL* MP and ML tree *Gisekia* are sister to *Rivina* (MP BS=100%), *Delosperma* was sister to *Phytolacca* MP (BS=89%) and *Stellaria* was sister to the Amaranthaceae (MP BS = 53%); in the *rpoC2* ML tree

alone, *Phytolacca* and *Sarcobatus* are recovered as sister groups (ML BS = 79%). Importantly, these anomalous relationships are not recovered or not supported in any other data sets, in either single-gene or combined partitions. None of the trees derived from these individual plastid gene data sets gives good resolution across the tree, and deeper-level relationships in particular are poorly supported.

Inverted Repeat Data Set

As with the individual plastid gene data sets, the IR partition generates MP and ML trees that are congruent (figure 2-12). Parsimony analyses recovered a single tree; replicate GARLI analyses recovered trees that differed only in the topology of the ‘succulent’ clade. The IR tree differs from the previous analyses in the placement of *Sarcobatus*, which is resolved as sister to Nyctaginaceae and Phytolaccaceae with strong support (ML BS = 100%). Furthermore, analyses of individual plastid genes resolve *Talinum* as sister to *Portulaca* and Cactaceae whereas the IR data set recovers *Portulaca* and *Talinum* as sister to each other.

Combined Plastid Genes from the Single Copy Region

The combined plastid gene data set generated a single most parsimonious tree. Replicate GARLI analyses recovered the same ML topology (figure 2-13). Levels of bootstrap support are higher in general in the ML tree than in the MP tree. Again, the MP and ML trees are largely congruent, although in the MP tree *Sarcobatus* and *Rivina* are sister to each other whereas in the ML tree *Sarcobatus* is placed without support with Phytolaccaceae and Nyctaginaceae. In the MP tree *Limeum* is placed without support as sister to *Mollugo* and the ‘succulent’ clade and *Stegnosperma* is placed as sister to the ‘globuloid inclusion’ clade; in the ML tree, *Limeum* and *Stegnosperma* are placed as successive sisters to the ‘globular inclusion’ clade. As with the individual plastid gene trees, *Talinum* is resolved as sister to *Portulaca* and Cactaceae, but

relationships among Didiereaceae, Basellaceae, *Halophytum* and *Claytonia* are either poorly supported or unresolved.

Combined Plastid Single Copy and Nuclear Genes

The addition of the nuclear gene data set to the combined plastid genes has little effect on topology (figure 2-14). In contrast to analyses of the combined plastid gene data set, both the MP and ML analyses with the nuclear data recover *Stegnosperma* and *Limeum* as successive sisters to the ‘globular inclusion’ clade. Again the MP and ML trees differ in their placement of *Sarcobatus* in the same way as in the combined plastid tree topologies, i.e. as sister to *Rivina* in the MP tree but sister to *Rivina* and Nyctaginaceae in the ML tree; both placements have low bootstrap support (~60%). As in the IR ML tree topology, the MP recovers *Portulaca* and *Talinum* as sister to Cactaceae but without support; in the ML tree, however, *Talinum* is sister to *Portulaca* plus Cactaceae.

Total Evidence Data Set

The total evidence data partition generated a single MP (figure 2-2) tree that agrees in topology with the ML tree (figure 2-1), except for the placement of *Sarcobatus*. The MP and ML trees derived from the ‘total evidence’ data set show more congruence with each other than the congruence found between MP and ML trees derived for any other data partition. As in previous combined analyses, in the MP tree, *Sarcobatus* and *Rivina* are placed sister to each other (BS=63%) while in the ML tree *Sarcobatus* is placed without support as sister to Nyctaginaceae plus *Rivina*. The position of *Sarcobatus* therefore remains uncertain in these analyses. The ML topology was chosen as the basis of subsequent character reconstruction analyses because it is less prone to the problem of long-branch attraction (Felsenstein, 1978) and because the bootstrap values are higher than in the MP tree. The full topology of the tree is therefore described in detail here.

Non-core Caryophyllales form a strongly supported (BS=100%) monophyletic group with two subclades. One clade comprises Plumbaginaceae with Polygonaceae resolved as sister to Frankeniaceae plus Tamaricaceae (all with BS of 100%). The second clade, containing the carnivorous taxa and relatives, comprises Drosophyllaceae with Ancistrocladaceae and Dioncophyllaceae (BS=100%), and Nepenthaceae with Droseraceae (BS=59%).

Core Caryophyllales form a strongly supported group (BS=100%) with Rhabdodendraceae as sister to the rest (BS=100%). Following the divergence of Rhabdodendraceae, the backbone of the tree is strongly supported and characterized by a grade of successively branching taxa, in the following order: Simmondsiaceae; Asteropeiaceae with Physenaceae; a clade comprising Caryophyllaceae, Achatocarpaceae, and Amaranthaceae (BS=100%); and Stegnospermataceae (BS=100%). Subsequently, *Limeum* is placed as sister to the remaining members of Caryophyllales, which form two clades. In the first of these two clades, the topology is as follows: the earliest-diverging group is Aizoaceae, followed by *Gisekia*, *Phytolacca*, *Sarcobatus*, *Rivina* and Nyctaginaceae. In the second clade, Molluginaceae are sister to a group comprising Cactaceae, Portulacaceae, Didiereaceae, Basellaceae, *Halophytum* and *Claytonia*. Within this group, *Portulaca* and *Talinum* are strongly supported as sister to Cactaceae; however, relationships among Didiereaceae, Basellaceae, *Halophytum* and *Claytonia* are poorly supported.

For each of the character reconstructions, multiple state transitions are inferred within the core Caryophyllales. The patterns of character evolution derived from parsimony reconstruction and the inferred ancestral states derived from stochastic mapping analyses are illustrated in figure 2-3.

Discussion

Several broad molecular phylogenetic analyses have examined intra-ordinal relationships across the entire Caryophyllales *sensu lato*. Rettig et al. (1992) conducted an *rbcL* analysis of 12

families; Downie and Palmer (1994) inferred phylogeny from chloroplast genome structural changes and Inverted Repeat restriction site variation in 11 families of Caryophyllales; Downie et al. (1997) compared sequences of ORF2280 (*ycf2*) across 11 families. However, the most comprehensive study is that of Cuénoud et al. (2002), who generated a partial *matK* sequence phylogeny (30 families, 121 genera). In Cuénoud et al. (2002) a subset of the *matK* data was combined with previously published genes to generate a combined *rbcL/matK* phylogeny (19 families, 53 genera) and a four-gene analysis that also incorporated *atpB* and 18S rDNA sequences (19 families, 25 genera). Although the taxonomic sampling of the *matK* phylogeny was extensive and dramatically improved our understanding of the Caryophyllales phylogeny, the study suffered from restricted taxon sampling in the combined analyses, with just over half of the families in the core Caryophyllales represented in the *rbcL/matK* and *rbcL/matK/atpB/18S* data sets. Parsimony was the only optimality criterion used in these analyses and there were several soft incongruences among the *matK*, *rbcL/matK*, and *rbcL/matK/atpB/18S* trees. Our analyses resolve many of these remaining uncertainties.

Phylogenetic Analyses

The earliest-diverging lineages in the core Caryophyllales are clarified and are well supported. Notably, Rhabdodendraceae followed by Simmondsiaceae are supported as sisters to the rest of the core Caryophyllales (both with 100% BS; figure 2-1). The position of *Rhabdodendron* had previously been ambiguous, recovered either as sister to both core and non-core Caryophyllales (in combined *matK* and *rbcL* analyses: Cuénoud et al., 2002) or weakly supported as sister to *Simmondsia*, at the base of the core Caryophyllales (in *matK* analysis: Cuénoud et al., 2002). Following the divergence of Rhabdodendraceae and Simmondsiaceae, our analyses strongly support a clade of Physenaceae and Asteropeiaceae (100% BS) as sister to the remaining core Caryophyllales. Relatively little is known about these early-diverging lineages of

core Caryophyllales from the perspective of morphology, and lack of data for these critical early lineages prevents a clear understanding of ancestral states within the core Caryophyllales.

In the *matK* analysis of Cuénoud et al. (2002), Caryophyllaceae and Achatocarpaceae plus Amaranthaceae *s.l.* branch successively as sister to the rest of the core Caryophyllales and do not form a clade with Achatocarpaceae and Amaranthaceae *s.l.* as suggested in the *rbcL/matK* analyses. In our analyses, the clade comprising Caryophyllaceae, Achatocarpaceae and Amaranthaceae *s.l.* receives strong support (100% BS), agreeing with the combined analyses of Cuénoud et al. (2002). Morphological synapomorphies for this clade remain elusive, probably in part because Achatocarpaceae are poorly studied.

Molecular studies have consistently recovered a distinct clade within the core Caryophyllales (Cuénoud et al., 2002; Downie et al., 1997; Giannasi et al., 1992; Rettig et al., 1992) termed the ‘globular inclusion’ clade (Aizoaceae, Phytolaccaceae, Nyctaginaceae, Gisekiaceae, Molluginaceae, Portulacaceae, Didiereaceae, Basellaceae, Cactaceae; Cuénoud et al., 2002) on account of distinctive P-plastid characteristics (as found by Behnke, 1993). Consistent with previous analyses, *Stegnosperma* and *Limeum* are recovered as successive sisters to this ‘globular inclusion’ clade but with greater support (BS 98%) than in earlier studies. Within the ‘globular inclusion’ clade, two subclades are recovered that correspond to the ‘raphide’ clade (Judd et al., 1999) and the ‘succulent’ clade (Rettig et al., 1992). Molluginaceae are maximally supported as sister to this succulent clade (BS 100%). In Cuénoud et al. (2002), Molluginaceae were placed as sister to the succulent clade but with no support in the *matK* and *matK/rbcL* analyses and moderate support (BS 70%) in the four-gene analysis.

Within the ‘raphide’ clade, *Gisekia* is strongly supported as sister to Phytolaccaceae, *Rivina*, *Sarcobatus* and Nyctaginaceae (BS 100%). This contradicts the findings of Cuénoud et

al. (2002) whose single-gene analyses variously place *Gisekia* as sister to Aizoaceae (*matK*) or *Rivina* (*rbcL* and *rbcL/matK*) analyses. Out of the eight plastid genes that we analyzed, only *rbcL* supports a sister relationship between *Gisekia* and *Rivina*. In addition, we provide further evidence and support for the separation of *Rivina* (Rivinioidae) from Phytolaccaceae and its placement as sister to Nyctaginaceae (BS=77%). The placement of *Sarcobatus* in our analyses is problematic and its position varies in relation to Nyctaginaceae, *Rivina* and Phytolaccaceae. The ‘raphide’ clade is under-sampled in this study and while we suggest alternative placements for *Gisekia* and *Sarcobatus*, we recognize that increased taxon sampling (e.g. *Agdestis* which has been associated with *Sarcobatus* by Cuénoud et al., 2002) could affect these findings.

Taxa within the portulacaceous cohort have traditionally been treated at the rank of family; however, the degree of paraphyly in Portulacaceae suggests that phylogenetic resolution should be conceptually envisioned as an intrafamilial problem (HersHKovitz and Zimmer, 1997). For example, in analyses of ITS, the genetic divergence of Cactaceae from Portulacaceae is equal to or less than that between many pairs of genera in Portulacaceae (HersHKovitz and Zimmer, 1997). Two methodological constraints limited our ability to address the question of phylogenetic relationships among Cactaceae and its portulacaceous relatives. First, the large amount of sequencing for each taxon limited the total number of taxa that could be sampled – this under-sampling is particularly acute in the succulent clade, given the degree of paraphyly inherent in Portulacaceae. Second, the broad scope of the taxon sampling, i.e. the whole of Caryophyllales *s.l.*, meant that only slower-evolving coding genes rather than more rapidly evolving regions such as intergenic spacers could be sampled to permit alignment across the order. Consistent with the low levels of genetic divergence in this clade, very little informative variation was obtained for members of the portulacaceous cohort from these coding regions

(despite sequencing over 40,000 base pairs). There are fewer than 20 substitutions on the branches leading to the clade containing *Halophytum*, *Alluaudia* and *Basella* and fewer than 50 substitutions on the branch leading to *Portulaca* and *Talinum*.

Limitations aside, within the portulacaceous cohort, the monophyly of the ACPT clade comprising Cactaceae (*Pereskia* plus *Opuntia*), *Portulaca* and *Talinum* is strongly supported (100% BS) in analyses of all partitions with the exception of the IR partition. Historically, however, different analyses have recovered different patterns within the ACPT clade depending on taxon sampling and phylogenetic markers used (reviewed in Nyffeler, 2007). In our analyses, different partitions and analytical methods also gave different branching patterns within the ACPT clade. Parsimony analyses of the IR partition recovered a branching pattern (with support less than 50%) similar to the morphological cladistic analysis of Carolin (1987). Parsimony and GARLI analyses of the plastid gene partition found *Talinum* sister to *Portulaca* plus Cactaceae as proposed by the morphological cladistic analyses of Hershkovitz (1993) and the Bayesian molecular analysis of Nyffeler (2007). Parsimony and GARLI analyses of the total evidence and GARLI analyses of IR data sets recovered a well-supported branching pattern not found in previous analyses – Cactaceae sister to *Portulaca* plus *Talinum*.

Total evidence, plastid gene, plastid plus nuclear and IR data sets all place *Halophytum* as sister to Basellaceae and Didiereaceae. This affiliation is consistent with Savolainen et al.'s (2000) analysis of *rbcL* sequences (albeit with low taxon sampling in the Caryophyllales), and was suggested by Bittrich (1993) on the basis of pollen morphology and by Hunziker et al. (2000) due to shared similarities in basic chromosome number ($x=12$). The position of *Claytonia*, however, is unstable in our analyses and is generally not in agreement with studies with better taxon sampling (Applequist and Wallace, 2001; Hershkovitz and Zimmer, 1997; Nyffeler, 2007).

Claytonia, together with associated portulacaceous genera, were placed in a clade with Basellaceae and Didiereaceae with reasonable support (80% BS; Applequist and Wallace, 2001). However, in our study only MP analyses of the *matK* and IR data sets were able to recover this relationship. Individual plastid genes placed *Claytonia* in a variety of positions while the combined data sets invariably placed *Claytonia* as sister to the rest of the portulacaceous cohort. Notably, our phylogeny derived from *ndhF* alone (the same gene employed by Applequist and Wallace, 2001) also recovered *Claytonia* as sister to the rest of the portulacaceous cohort. This suggests that the apparent instability in the placement of *Claytonia* may be the result of limited taxon sampling in our study; pruning the data set from Applequist and Wallace (2001) to match our taxon sampling generated a similarly anomalous placement of *Claytonia* (data not shown).

Reconstruction of Pollination Mechanism

Our phylogeny differs considerably from the concept of the Caryophyllales that stimulated the speculations of Ehrendorfer (1976). The Caryophyllales *sensu* Ehrendorfer essentially correspond to the core Caryophyllales presented in this study; however, the composition and phylogeny of this clade has changed considerably. None of the four of the currently recognized early-diverging lineages were recognized as belonging to the Caryophyllales in the 1970s. Ehrendorfer was strongly influenced by the idea that the Chenopodiaceae (Amaranthaceae *s.l.*) with their reduced anemophilous flowers were representative of the ancestral Caryophyllid type. Consequently, he argued that anemophily was the ancestral condition because the early Caryophyllales had evolved in open, dry, marginal environments at a time when pollinators were scarce. These hypotheses to prove or disprove (Clement and Mabry, 1996); however, our phylogeny confirms that the Amaranthaceae constitute a relatively derived lineage. If pollinators were scarce at the time of origin of the Caryophyllales, this might also apply as a general limitation to other lineages of eudicots diverging at that time, but in any case, the relative timing

and location of diversification in eudicot lineages and their respective pollinator lineages is unclear at present. Friedman and Barrett (2008) demonstrate a strong correlation between the occurrence of open habitat and anemophily and provide support for the prevalence of anemophily in open habitats; however, this correlation may not necessarily be due to pollinator scarcity but rather to the selective advantage of wind pollination in an open environment. Moreover, parsimony reconstruction of the ancestral habitat would be ambiguous given that the extant members of early-diverging lineages of the core Caryophyllales occupy tropical understory (Asteropeiaceae and Rhabdodendraceae) or have a global holarctic distribution (Caryophyllaceae).

Using the current phylogeny, parsimony-based character reconstruction and stochastic character mapping do not provide support for the hypothesis that the Caryophyllales were ancestrally wind-pollinated. *Rhabdodendron*, which is sister to all other core Caryophyllales, is described as visited by pollen-collecting bees (Prance, 2003) while extensive field observations suggest that Asteropeiaceae are also entomophilous (Birkinshaw et al., 2004). It is notable, however, that together with the wind-pollinated *Simmondsia*, two other early-diverging lineages do at least exhibit morphological characteristics that are reminiscent of wind-pollinated flowers. Despite reports of bee visitation, *Rhabdodendron* exhibits very long anthers and sepaloïd petals, lacks a nectary, possesses a gynoeceium with only 1 or 2 ovules and a single seed in fruit, and has a relatively long stigma (P.K Endress, pers. comm.); perianth parts also fall off as the flower opens (Nelson and Prance, 1984). *Physena* exhibits very long anthers and no petaloïd organs, lacks a nectary and has a large stigmatic surface. Coding *Physena* as wind-pollinated, however, does not alter the conclusion of the character mapping analyses, and thus there is little support for an anemophilous ancestry in the core Caryophyllales. Indeed, as noted by Clement and

Mabry (1996), even if one accepts the highly reduced inconspicuous flowers of *Amaranthaceae s.l.* as archetypal, it is not necessary to invoke wind pollination as it has already been noted that many of the diminutive flowers in *Amaranthaceae* are probably entomophilous (Blackwell and Powell, 1981; Kuhn, 1993).

Reconstruction of Perianth Differentiation

Despite recovering entomophily as ancestral, our character reconstruction analyses suggest that an undifferentiated perianth arose early within the core Caryophyllales (in agreement with Ehrendorfer, 1976; Ronse De Craene, 2008). This perianth type has been strongly correlated with anemophily (Friedman and Barret 2008). Parsimony reconstruction infers that the evolution of this undifferentiated, uniseriate condition evolved after the divergence of *Rhabdodendron* while the stochastic mapping analyses recovers the basalmost node in core Caryophyllales as either undifferentiated or differentiated, with equal probability. Subsequent nodes along the backbone of the tree until the divergence of Molluginaceae are recovered as undifferentiated (with greater than 0.99 posterior probability).

A discussion of perianth evolution within the core Caryophyllales is complicated by the great diversity of floral structure within the order and uncertainty in defining the correspondence of these structures both within Caryophyllales and with respect to floral organs in other eudicots. Observations by Ronse De Craene (2007, 2008) suggest that although petal organs in eudicots may appear homologous with respect to position and superficial appearance, the variable expression of features reminiscent of either stamens or bracts means that petals in different lineages of core eudicots are of uncertain homology and may have been differently derived. This viewpoint argues against the widespread notion that the petals within eudicots are invariably derived from stamens and makes it difficult to homologize between perianth parts even within the core eudicots (Ronse De Craene, 2007; 2008). In the Caryophyllales, these difficulties are

compounded by different floral structures and the limitations of established terminology. The specific terms petal, sepal, corolla and calyx are not usefully applied to Caryophyllid taxa as they imply not only the characteristics and function of an organ but also the position of the organ (Endress, 1994; Jaramillo and Kramer, 2007). In core eudicots, for example, the term petal implies both the showiness of the perianth part and the position of the organ in the second whorl of the flower (Jaramillo and Kramer, 2007). However, in comparing the differentiated perianth found in many Caryophyllales with the bipartite perianth of most core eudicots, the positional feature alone is not necessarily a sufficient criterion of homology, and terms such as ‘petal’ that imply positional correspondence are misleading. Similarly, the term ‘bipartite perianth’ should also be avoided, as this implies the presence of distinct perianth whorls. While distinct perianth whorls may be found in some families in the Caryophyllales e.g Limeaceae (Hofmann, 1973) and Caryophyllaceae (Rohweder, 1967), differentiation in a spiral phyllotaxis occurs in Cactaceae. For the purposes of this discussion, therefore, we use the term ‘differentiated’ to describe a perianth that comprises at least two distinct types of organ that perform the functions commonly ascribed to the calyx and corolla. We refer to members of a differentiated perianth as either petaloid or sepaloid (i.e., resembling the petals or sepals of other core eudicots and putatively performing similar functions without necessarily being homologous by positional criterion alone). Finally, because the terms petaloid and sepaloid refer only to a superficial resemblance and putatively similar function, within Caryophyllales we apply these terms to structures that are clearly non-homologous in other respects. The terms sepaloid ‘tepal’ and petaloid ‘tepal’ are applied to the quincuncial perianth parts that are present in core Caryophyllales while ‘petaloid staminodes’ refer to perianth parts that are clearly androecium-derived.

Multiple Origins of Perianth Differentiation

Our analyses suggest that there have subsequently been a minimum of nine independent origins of a differentiated perianth within the Caryophyllales. This is more than the minimum suggested by Ronse De Craene (2008) who, in a broad survey of eudicots, cites five origins of ‘petals’ in the core Caryophyllales, occurring in ‘Stegnospermataceae, Aizoaceae, Portulacaceae-clade, Caryophyllaceae, Molluginaceae’. Considering the reconstructions provided by Ronse De Craene (2008), the difference in our respective estimations of perianth differentiation can be attributed to several factors. Most significantly, coding and definition of the perianth differs in our studies; e.g. Nyctaginaceae and the portulacaceous cohort are coded as ‘petals absent’ (Ronse De Craene, 2008, Figure 2-3) but by our definition both *Mirabilis jalapa* (Nyctaginaceae) and the portulacaceous cohort have a differentiated perianth and are listed as polymorphic and differentiated, respectively. Similarly, *Glinus* is a member of the Molluginaceae that possesses putatively staminodial ‘petals’ (Hofmann, 1994; pp. 137, 141) but is coded as ‘petals absent’ by Ronse De Craene (2008). In our analysis, Molluginaceae are coded as polymorphic, exhibiting both taxa with a uniseriate, undifferentiated perianth and taxa with differentiated perianth. A different tree topology may also be a factor contributing to the different results, e.g. *Rhabdodendron* is sister to the core Caryophyllales (this study), and the placement of *Corbichonia* and *Glinus* as successive sisters to the ‘globuloid’ clade by Ronse De Craene (2008) is erroneous based on current understanding; *Corbichonia* is most likely sister to the ‘raphide’ clade (Cuénoud et al. 2002), and *Glinus* (Molluginaceae) is sister to the portulacaceous cohort (70% BS according to Cuénoud et al., 2002 and 100% BS in this study). Finally, due to the broader scope of the study by Ronse De Craene (2008) (i.e. all eudicots), lineages of core Caryophyllales with differentiated perianth are also under-sampled, with both *Asteropeia* and *Limeum* excluded from his study. Consequently, differences in emphasis, sampling, coding, and

tree topology may all have contributed to the differences between Ronse De Craene's 2008 results and those we report here.

Despite these differences, the five independent origins of 'petals' described by Ronse De Craene (2008) are included in the nine independent derivations of differentiated perianth inferred in our study. These nine origins occur in: Asteropeiaceae; Caryophyllaceae (although several genera do not have differentiated perianth); Stegnospermataceae; some species of *Limeum*; *Corbichonia* (not sequenced in this study); the subfamilies Mesembryanthemoideae and Ruschioideae within Aizoaceae; *Mirabilis* in Nyctaginaceae; *Glinus* in Molluginaceae; the portulacaceous cohort (Portulacaceae, Didiereaceae, Basellaceae) including Cactaceae. The number of origins of differentiated perianth could well increase depending on the final placement of the enigmatic *Macarthuria* and increased resolution of phylogenetic relationships within Caryophyllaceae. Developmental evidence (where available) is consistent with these independent origins of differentiated perianth indicated by character reconstruction analyses. Below, we discuss the developmental evidence for perianth differentiation by different mechanisms in these nine lineages: through differentiation of putatively homologous organs and through the recruitment of floral structures derived either from the androecium or preceding bract.

Recruitment of Preceding Bracts

The secondary recruitment of preceding bracts to from perianth parts has occurred twice within the 'globular inclusion' clade, once in Nyctaginaceae and again in the portulacaceous cohort (Figure 2-3). Developmental studies suggest that the mechanism underlying the recruitment of preceding bracts is different in these distinct lineages. Within Nyctaginaceae, an involucre may have evolved more than once, occurring also in *Abronia*, *Allionia*, *Boerhavia*, *Bougainvillea*, *Mirabilis*, *Nyctaginia* and *Tripterocalyx* (Douglas and Manos, 2007). In *Boerhavia* Sharma (1963) describes an involucre surrounding five lateral flowers and one central

flower. In *Mirabilis* however there appears to a tendency to reduction in floral number. In *Mirabilis nyctagineus* only the first three leaves of the involucre produce axillary flowers (Hofmann, 1994). In *Mirabilis jalapa*, each flower has a differentiated perianth with a calyx of five fused parts that has been secondarily derived from an involucre of bracts (Figure 2-4; L). This variation within *Mirabilis* suggests that the apparent bipartite perianth in *M. jalapa* may have been derived through reduction in floral number. Subsequent loss of five lateral flowers is inferred, leaving a single central flower with the involucre appearing as a pseudocalyx (Vanvinckenroye et al., 1993). In Nyctaginaceae, floral loss within an involucre of bracts would appear to result in an apparently differentiated perianth, although the association of the involucre (calyx) with the rest of the flower is weak (Rohweder and Huber, 1974).

Portulacaceae *s.l.*, Didiereaceae and Basellaceae share a distinct floral morphology that emerges following the divergence of Molluginaceae (Figure 2-3). These lineages possess flowers with an involucre which in contrast to *Mirabilis* (Nyctaginaceae) comprises two leafy phyllomes that are inserted below the petaloid members of the perianth. Importantly, their developmental origin is probably different from the involucre found in Nyctaginaceae as Hofmann (1994) comments that axillary products are never formed in the axes of these phyllomes. They are termed involucral phyllomes by Hofmann (1994), reflecting the belief that these organs are ‘additional phyllomes inserted between the bracteoles and the sepals; however, there have been other interpretations as to the nature of these phyllomes. Sharma (1954) (reviewed in Milby, 1980), who examined vascular anatomy in *Portulaca* and *Talinum*, concluded that the flowers are essentially dimerous with the pentamerous petaloid perianth inferred as a derived condition. These alternatives will merit further developmental study as phylogenetic understanding within this group is clarified but it is valuable to consider these different interpretations in light of the

current phylogeny and perianth reconstruction analysis (Figure 2-3). The ancestral floral condition of the portulacaceous cohort is uniseriate pentamery; therefore, Sharma's interpretation (1954) suggests reduction to a dimerous state followed by a reversal to a pentamerous condition. Irrespective of the developmental origin of these two phyllomes, in many species they cover the developing floral meristem very early in development and thus perform the function of a calyx in a differentiated perianth (Hofmann, 1994). Subfunctionalization of perianth roles may have facilitated the high degree of petaloidy in the inner quincuncial perianth members of these families (Figure 2-4; B, I, L): "...the involucreal phyllomes cover the inner bud very early and take over the function of the calyx. Therefore, the sepals [uniseriate pentamers] behave like petals" (Hofmann, 1994).

Within the portulacaceous cohort, a very different floral structure is found in Cactaceae. In contrast to the perianth of Portulacaceae *s.l.*, Didiereaceae and Basellaceae, Cactaceae exhibit a great increase in perianth parts. Increases in floral merism and generally modified floral form make it challenging to determine correspondence between perianth in Cactaceae and its closest relatives – in this study, *Portulaca* and *Talinum*. The perianth parts of Cactaceae are suggested to be bracteal rather than staminodial in their homology (Buxbaum, 1950-55 pp 122-123; Ronse De Craene, 2007; Ronse De Craene, 2008) and are arranged in a spiral phyllotaxy. The perianth may have arisen by inclusion and differentiation of supernumary bracts (Ronse De Craene, 2008) or simply by formation of additional bracts. Differentiation of the perianth occurs, with outer sepaloid parts and highly petaloid inner parts (Figure 2-4; D). This high degree of differentiation together with a spiral phyllotaxy is unusual within the Caryophyllales however Ronse de Crane (2008) highlights that this combination of floral characters (large, spirally arising petals with a multi-staminate androecium) occurs in several derived lineages in the core eudicots. Endress

(2002) suggested that increases in numbers of stamens and/or carpels may result in an increase in size of the flower, greater plasticity, and an irregular petal development. This developmental interpretation is consistent with our reconstruction analyses, which do not argue for an independent origin of differentiated perianth in Cactaceae; rather, an increase in meristem size and merosity of reproductive organs may be in part responsible for the unusual perianth in Cactaceae.

Petaloid Modification of the Androecium

Reconstruction analyses suggest that perianth differentiation through sterilization and petaloid modification of the outer members of a centrifugally initiating androecium has arisen a minimum of three times in Caryophyllales (Figure 2-3): clear examples occur in Aizoaceae (Figure 2-4; C), Molluginaceae and *Corbichonia* (not sampled in this study but shown to be a distinct lineage within the ‘raphide’ clade: Cuénoud et al., 2002). In *Glinus*, *Corbichonia* and Aizoaceae, the petaloid structures can be readily interpreted as differentiated staminodial structures (Ronse De Craene, 2008). For example, within Aizoaceae subfamilies, Ruschioideae and Mesembryanthemoideae, androecial development proceeds centrifugally, and the basipetal members become progressively more sterile and petaloid with intermediates conceptually linking the outermost petals to the inner fertile stamens (Figure 2-4; C). A similar situation has been described in *Glinus* in the Molluginaceae (Hofmann, 1994) and in *Corbichonia* (Ronse De Craene, 2007).

Petaloid members of the differentiated perianth in Caryophyllaceae, *Limeum*, *Stegnosperma* and *Macarthuria* have also been attributed to the androecium (Hofmann, 1973; Ronse De Craene, 2007; 2008). The reconstruction analyses suggest that these differentiated perianths have occurred independently and thus merit further developmental study. The assessment of homology between the petaloid members of the differentiated perianth and the

androecium is complicated by a high degree of variability in androecium organization, processes of reduction and differences in phyllotaxy. However, several lines of evidence suggest an androecial origin of the petals in Caryophyllaceae (Rohweder, 1967) (reviewed in Ronse De Craene 1998, 2007, 2008). Ronse De Craene et al. (1998) review the presence and absence of petals in 52 genera of Caryophyllaceae: nine genera lack petals, 11 genera have both species with petals and species without, while the remaining 32 genera in the survey possess petals. It remains unclear whether the absence of petals is ancestral in Caryophyllaceae or whether instances of petal loss have occurred. The most comprehensive molecular phylogeny of Caryophyllaceae to date (Fior et al., 2006) sampled only two genera with apetalous members (*Paronychia* and *Sagina*), but none of the entirely apetalous genera were sampled.

Differentiation of Homologous Perianth Parts

Despite the high degree of variation in floral structure found in different lineages of Caryophyllales, there are key common elements. Almost all lineages within the order possess five perianth members that are organized in a uniseriate quincuncial arrangement (with the exception of Cactaceae, which is multiseriate). Occasionally, one of the members in this series has been lost to give a tetramerous perianth e.g. in *Tetragonia* and *Mesembryanthemum* in Aizoaceae, Rivinoideae and Didiereaceae, but these cases of tetramery are clearly derived from pentamerous ancestors. These uniseriate quincuncial perianth members are probably homologous, given their constancy, position in the flower and common phyllotaxy. These putatively homologous organs have, however, undergone considerable differentiation in certain lineages, which often correlates with the emergence of a differentiated perianth. For example, in Aizoaceae, members of the early-diverging subfamilies Sesuvioideae and Aizooideae possess a quincuncial uniseriate perianth whose members are petaloid on the adaxial surface and sepaloid on the abaxial side. In the derived subfamilies Mesembryanthemoideae and Ruschioideae, the

androecium is polyandrous, and the outer members of centrifugally initiating stamens are sterile, resulting in a differentiated perianth with androecial-derived petaloid organs. Concomitantly, the outer quincuncial uniseriate perianth loses all petaloid characteristics and resembles only a calyx. In instances where differentiation of the perianth has been achieved through recruitment of involucre bracts and/or bracteoles (Portulacaceae and *Mirabilis*), the involucre organs act as a calyx and the now-inner uniseriate quincuncial perianth members are considerably more showy and petaloid (compare the showy petaloid perianth of the portulacaceous cohort (Figure 2-4; B, D and I) with the diminutive simple perianth of some genera in Molluginaceae. Seemingly homologous perianth parts within Caryophyllales can be either petaloid, e.g. Nyctaginaceae (Figure 2-4; A, L) and Portulacaceae (Figure 2-4; I), or sepaloid e.g. *Limeum*, *Stegnosperma* (Figure 2-4; E), Molluginaceae, Ruschioideae and Mesembryanthemoideae (Figure 2-4; C), Caryophyllaceae (Figure 2-4; J) and *Simmerdsia*, or chimeric, e.g. Sesuvioideae/Aizoioideae (Figure 2-4; F), *Hypertelis* (Figure 2-4; G).

Caryophyllales as a System for Floral Evo-Devo

Nine independent origins of a differentiated perianth, the concomitant independent evolution of petaloid from either androecial or bracteal organs and varying degrees of petaloid differentiation in homologous structures across the order make the Caryophyllales a valuable system for exploring the evolutionary developmental genetics of petaloidy in core eudicots. In the majority of core eudicots whose petal developmental genetics have been examined (e.g. in *Arabidopsis thaliana*, *Antirrhinum majus*, *Solanum lycopersicon*, *Nicotiana tabacum*, *Petunia hybrida*), differentiation of the petals is strongly influenced by MADS-box transcription factors: *APETALA3* (*AP3*) and *PISTILLATA* (*PI*) (in *A. thaliana*) and their orthologues (Irish and Kramer, 1998; Kramer and Irish, 1999). In these core eudicot species, *AP3* and *PI* orthologues are expressed throughout the development of the petal and their ubiquitous expression in the

petal has been shown to be necessary for normal petal development in *A. thaliana* and *A. majus* (Bowman et al., 1989; Sommer et al., 1991; Zachgo et al., 1995). It seems apparent that these genes play a conserved role in petal identity in the core eudicots examined so far, yet core eudicot petals have also traditionally been considered to be homologous, stamen-derived organs: this homology has been invoked to explain such developmental genetic similarities (Irish and Kramer, 1998). More recently, however, the assertion that petals in core eudicots are largely homologous and predominantly stamen-derived has been questioned (Ronse De Craene, 2007). Although in Caryophyllales the homology of the perianth parts to petals in other core eudicots is uncertain, it is clear that many lineages (Sesuvioideae, Nyctaginaceae, Portulacaceae, Cactaceae) possess petaloid organs that are bracteal rather than staminal in origin. Furthermore the occurrences of stamen-derived petals within Caryophyllales (Caryophyllaceae, Aizoaceae, *Glinus* and *Corbichonia*) are phylogenetically, derived, independent events. These independent occurrences are valuable for further study as there are very few examples of petals within core eudicots that are unquestionably stamen-derived (Ronse De Craene, 2007). The pattern of perianth evolution in the Caryophyllales therefore presents a unique opportunity to address long-standing questions regarding differences and/or similarities in the developmental genetics of bracteopetals and andropetals (Ronse De Craene, 2008) - articulated by Ronse De Craene (2008) this question remains highly pertinent in studies of floral diversification.

The improved phylogenetic understanding reported here provides opportunities for comparing bracteopetalous and andropetalous lineages that have arisen more recently than both basal angiosperms (traditionally considered to bear bracteopetals) and the early-diverging eudicot lineages (with their presumed andropetals). The Caryophyllales are a well-defined clade within core eudicots but, in a sense, the patterns of perianth evolution discussed here recapitulate

(on a smaller phylogenetic scale) the evolutionary trends traditionally thought to have taken place across the angiosperms as a whole (Bessey, 1915; Takhtajan, 1991). Therefore, despite uncertainty surrounding the precise correspondence of the caryophyllid perianth with the perianth of other eudicots, evo-devo investigations in the Caryophyllales may have far-reaching implications for our understanding of petal evolution and perianth differentiation. Is there latent developmental genetic homology underlying these derived and oft-seemingly dissimilar occurrences of perianth differentiation in Caryophyllales? What is the involvement of *AP3* and *PI* orthologues in these bracteopetals in Caryophyllales? How do expression and function of *AP3* and *PI* orthologues in caryophyllid bracteopetals compare with expression and function in the derived instances of andropetals? How expression and function of *AP3* and *PI* compare in the different occurrences of andropetals? Evolutionary developmental approaches to these questions are currently underway (Brockington et al., 2007) and may shed light on the evolutionary origins and homology of these diverse perianth forms in relation to other petals in core eudicots.

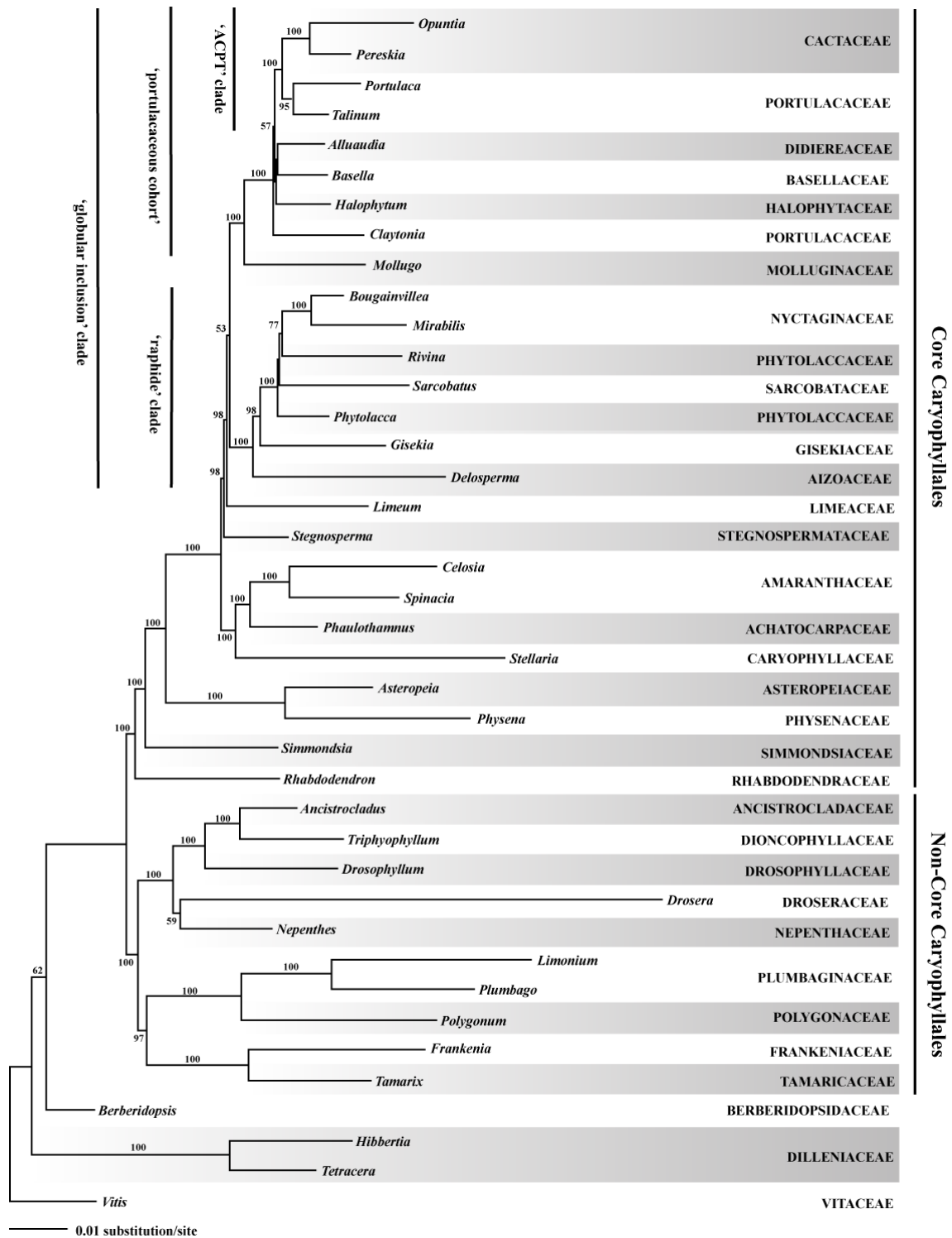


Figure 2-1. Maximum likelihood (ML) tree resulting from GARLI analysis of total evidence data set (2 nuclear genes, 8 plastid genes from the single-copy region, and the Inverted Repeat) for 36 members of the Caryophyllales and 4 outgroups. Numbers above branches are bootstrap values. [-lnL score 210420.96]

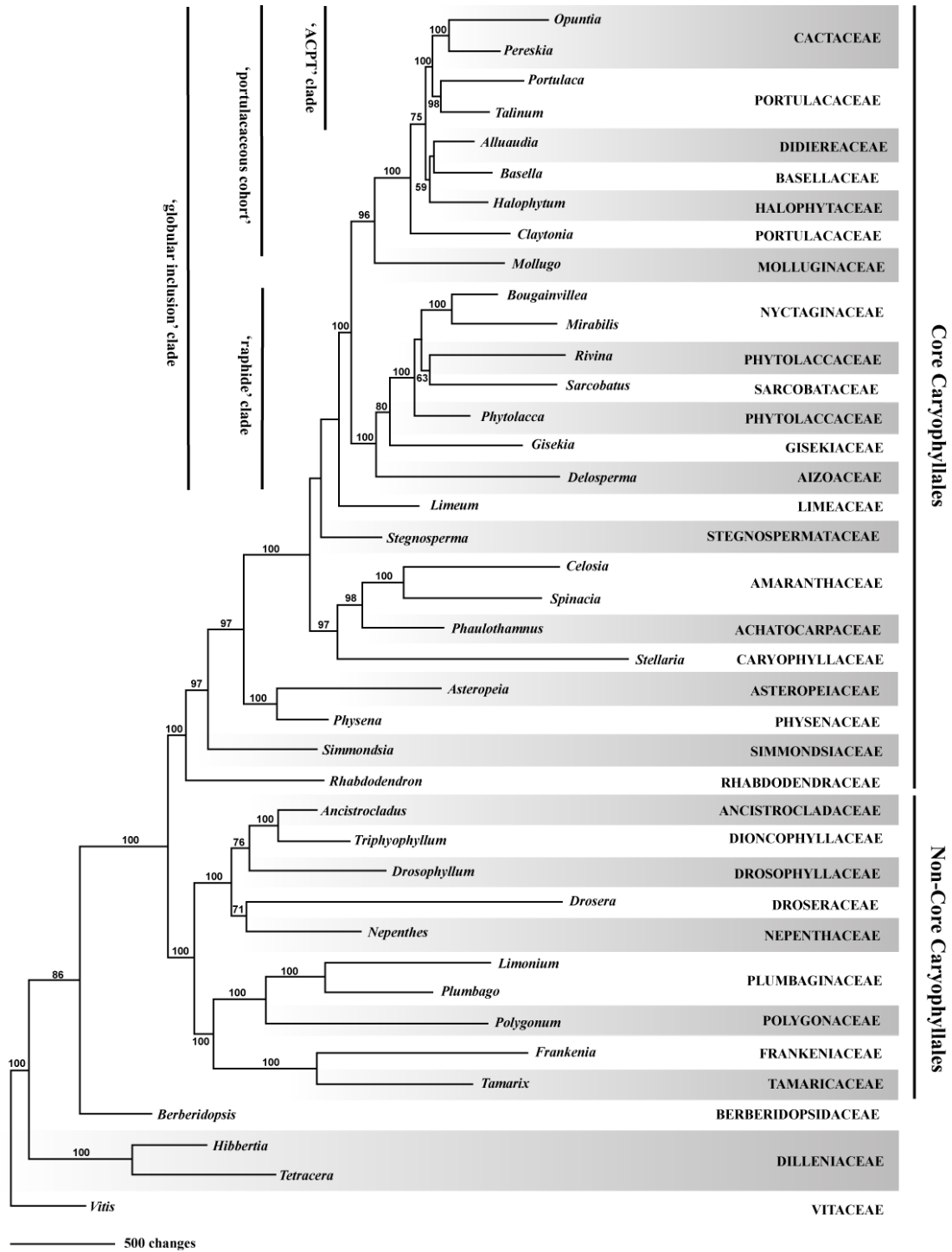


Figure 2-2. Phylogram of single most parsimonious tree based on the total evidence data set (2 nuclear genes, 8 plastid genes from the single-copy region, and the Inverted Repeat) for 36 members of the Caryophyllales and 4 outgroups. Numbers above branches are bootstrap values. [Length 27604, Consistency Index = 0.605, Retention Index = 0.538]

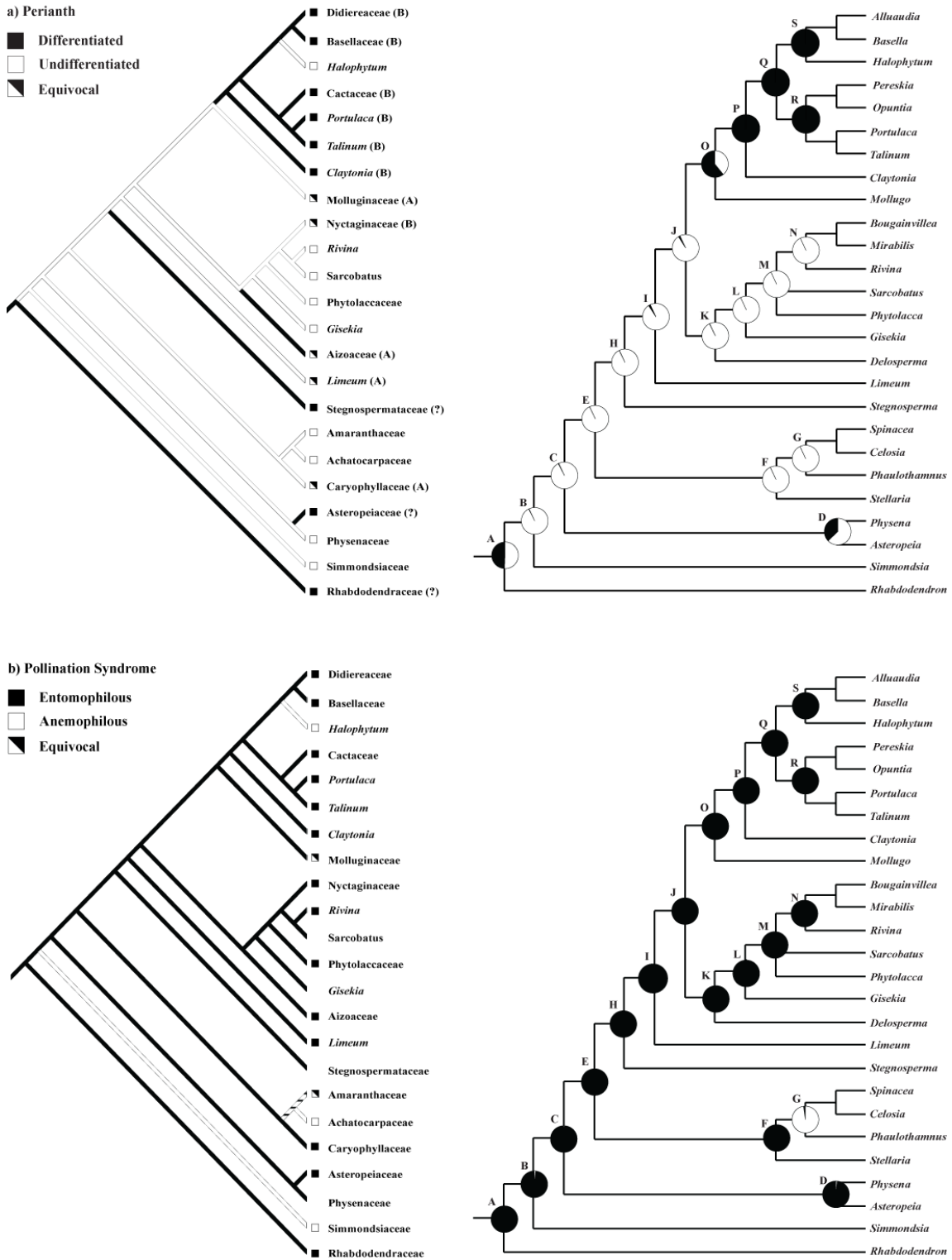


Figure 2-3. Parsimony reconstruction (illustrated on an MP tree) and stochastic character mapping (illustrated on Bayesian consensus tree): A) Reconstruction of perianth evolution; B) Pollination syndromes.

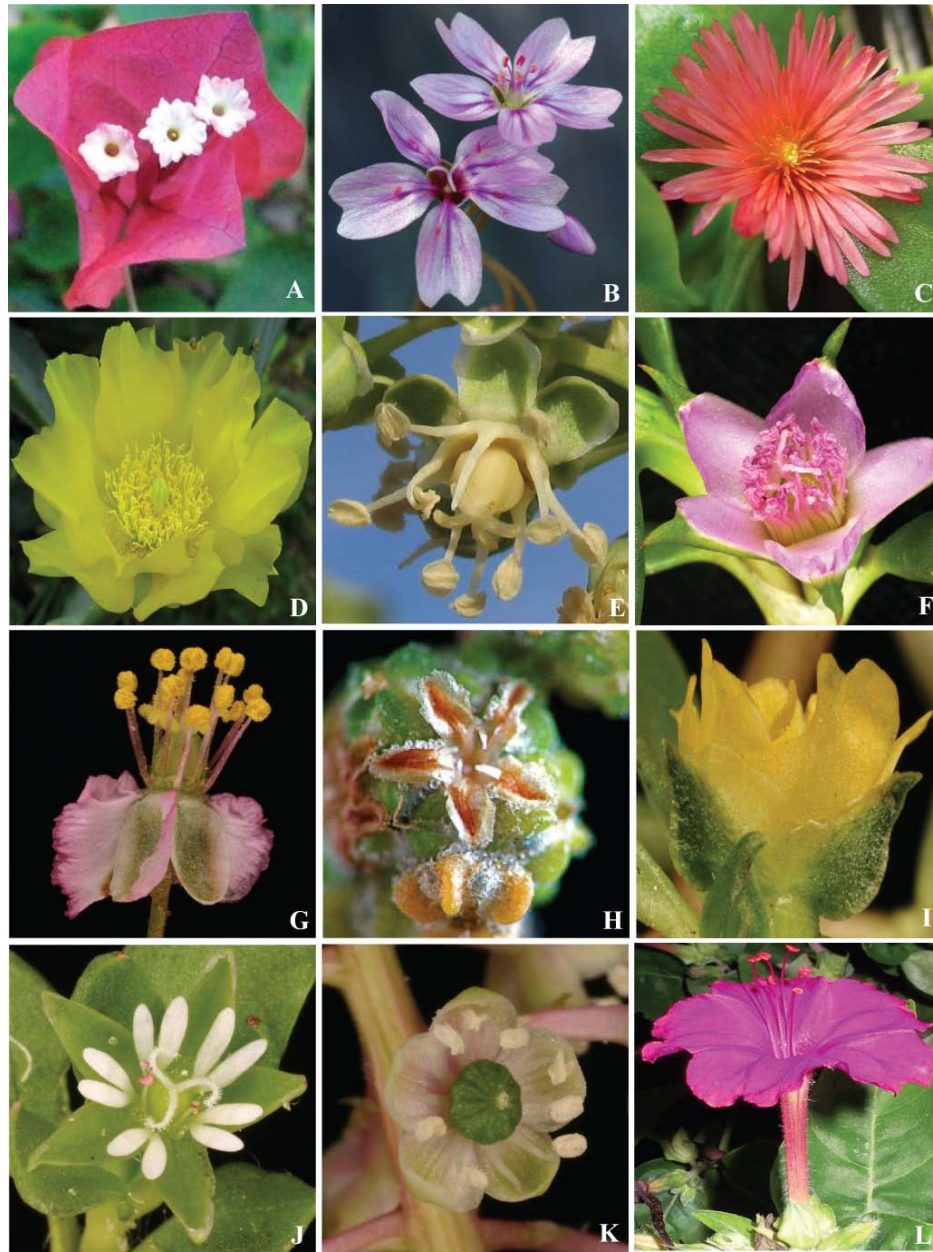


Figure 2-4. The diverse forms of the perianth in the core Caryophyllales. A - *Bougainvillea* sp. (Nyctaginaceae); B - *Claytonia* sp. (© Ron Wolf) (Portulacaceae *s.l.*); C - *Mesembryanthemum cordifolia* (Aizoaceae); D - *Opuntia humifusa* (Cactaceae); E - *Stegnospemataceae* sp. (© Debra Valov) (Stegnospemataceae); F - *Sesuvium portulacastrum* (Aizoaceae); G - *Hypertelis salsoloides* (Molluginaceae); H - *Chenopodium* sp. (© Brian Johnston) (Amaranthaceae); I - *Portulaca oleracea* (© Kurt Neubig) (Portulacaceae); J - *Stellaria media* (© Kurt Neubig) Caryophyllaceae; K - *Phytolacca americana* (© Kurt Neubig) (Phytolaccaceae); L - *Mirabilis jalapa* (© Walter Judd) (Nyctaginaceae).

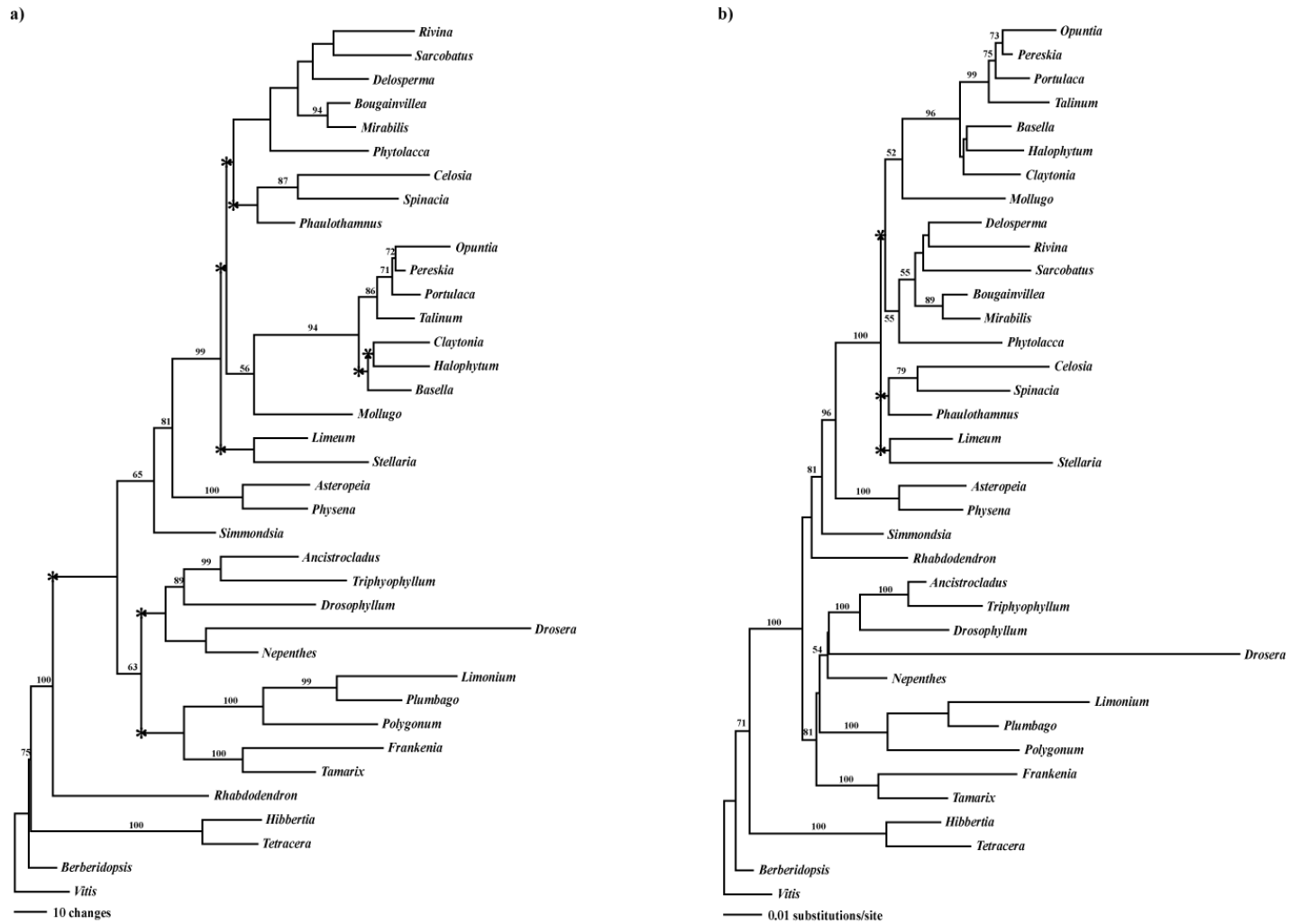


Figure 2-5. Trees derived from analyses of the *atpB* data set (missing taxa: *Gisekia* and *Alluaudia*).a) 1 of 23 MP trees; Numbers above branches are bootstrap support values; starred nodes collapse in strict consensus. [Length 1296, Consistency Index = 0.525, Retention Index = 0.566] b) ML tree resulting from GARLI analysis; Numbers above branches are bootstrap support values; starred nodes collapse in strict consensus. [-lnL score 8854.1973]

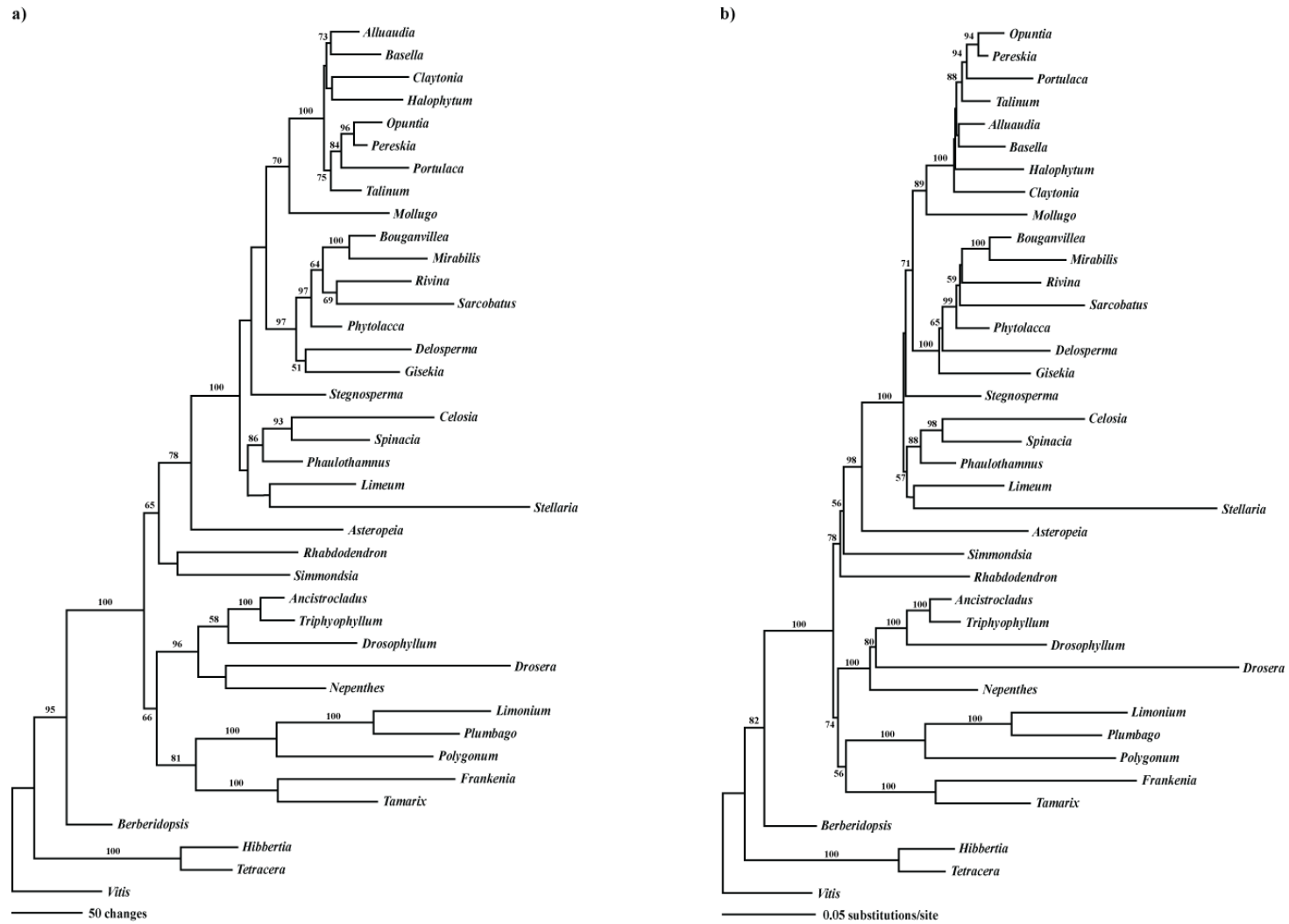


Figure 2-6. Trees derived from analyses of the *matK* data set (missing taxon: *Physena*). a) 1 of 2 MP trees; numbers above branches are bootstrap support values. [Length 3360, Consistency Index = 0.519, Retention Index = 0.522] b) ML tree; numbers above branches are bootstrap support values. [-lnL score 18173.934]

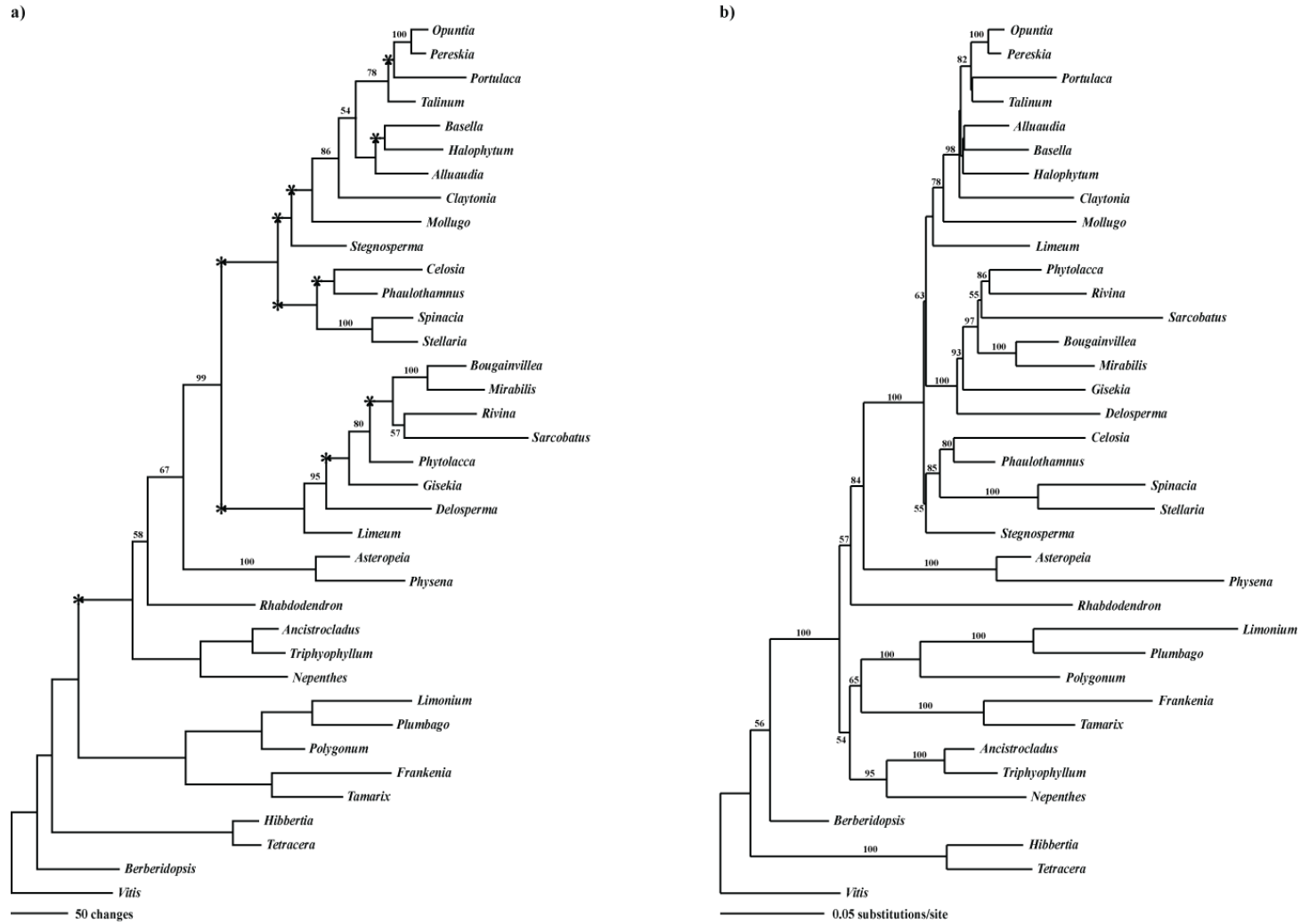


Figure 2-7. Trees derived from analyses of the *ndhF* data set (missing taxa: *Drosera*, *Drosophyllum*, *Simmondsia*). a) 1 of 20 MP trees; numbers above branches are bootstrap support values; starred nodes collapse in strict consensus. [Length 3159, Consistency Index = 0.514, Retention Index = 0.493]. b) ML tree; numbers above branches are bootstrap support values. [-lnL score 17917.229]

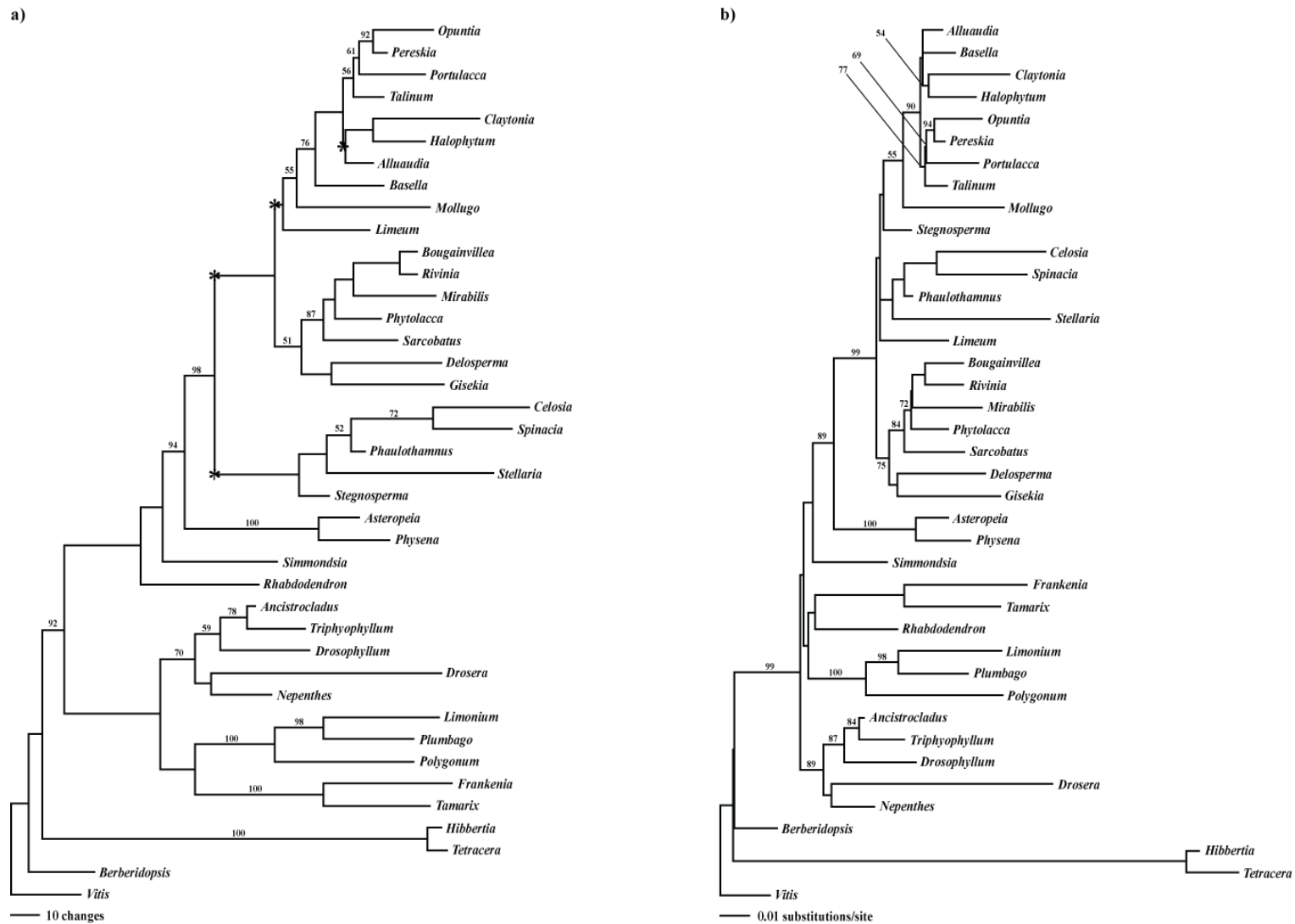


Figure 2-8. Trees derived from analyses of the *psbBTN* data set. a) 1 of 15 MP trees; numbers above branches are bootstrap support values; starred nodes collapse in strict consensus. [Length 1639, Consistency Index = 0.494, Retention Index = 0.541]. b) ML tree; numbers above branches are bootstrap support values. [-lnL score 10692.37]

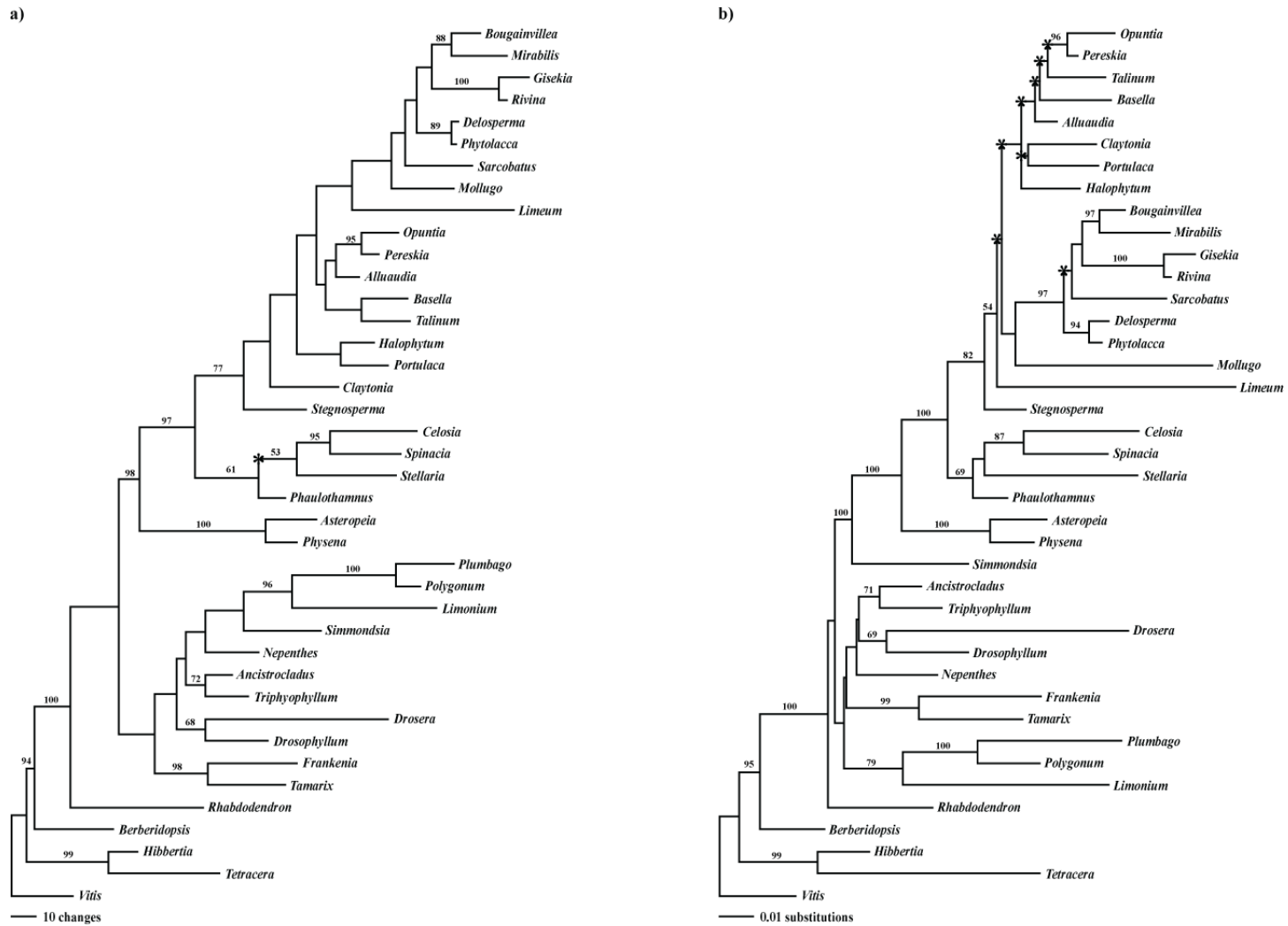


Figure 2-9. Trees derived from analyses of the *rbcL* data set. a) 1 of 73 MP trees; numbers above branches are bootstrap support values; starred nodes collapse in strict consensus. [Length 1451, Consistency Index = 0.522, Retention Index = 0.601]. b) ML tree; numbers above branches are bootstrap support values; starred nodes collapse in strict consensus. [-lnL score 9770.5926]

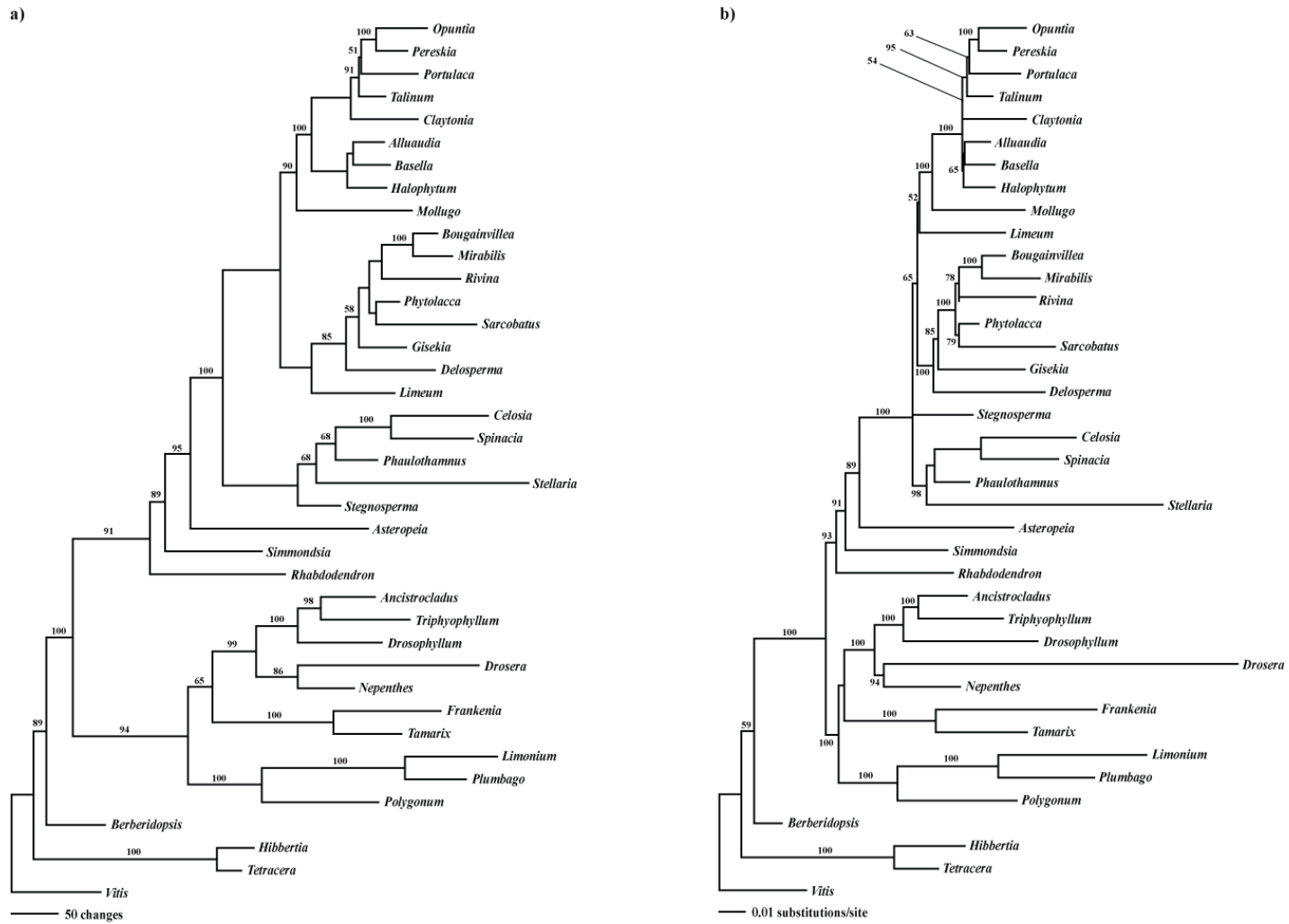


Figure 2-10. Trees derived from analyses of the *rpoC2* data set (missing taxa: *Physena*). a) 1 of 3 MP trees; numbers above branches are bootstrap support values. [Length 4529, Consistency Index = 0.576, Retention Index = 0.567]. b) ML tree; numbers above branches are bootstrap support values. [-lnL score 28139.564]

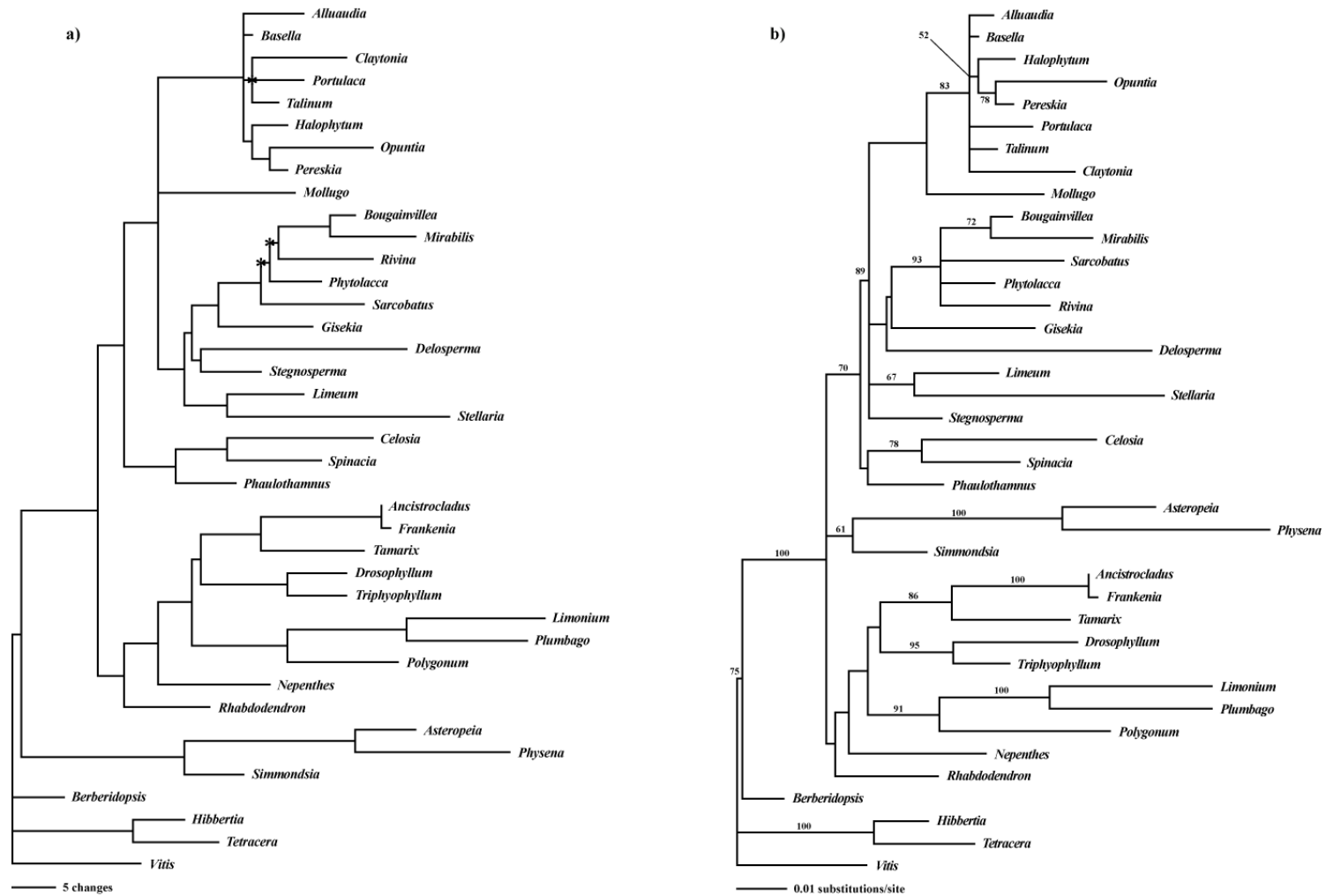


Figure 2-11. Trees derived from analyses of the *rps4* data set (missing taxa: *Drosera*). a) 1 of 122,155 MP trees; numbers above branches are bootstrap support values; starred nodes collapse in strict consensus [Length 545, Consistency Index = 0.646, Retention Index = 0.623]. b) ML tree; numbers above branches are bootstrap support values; starred nodes collapse in strict consensus [-lnL score 3826.098]

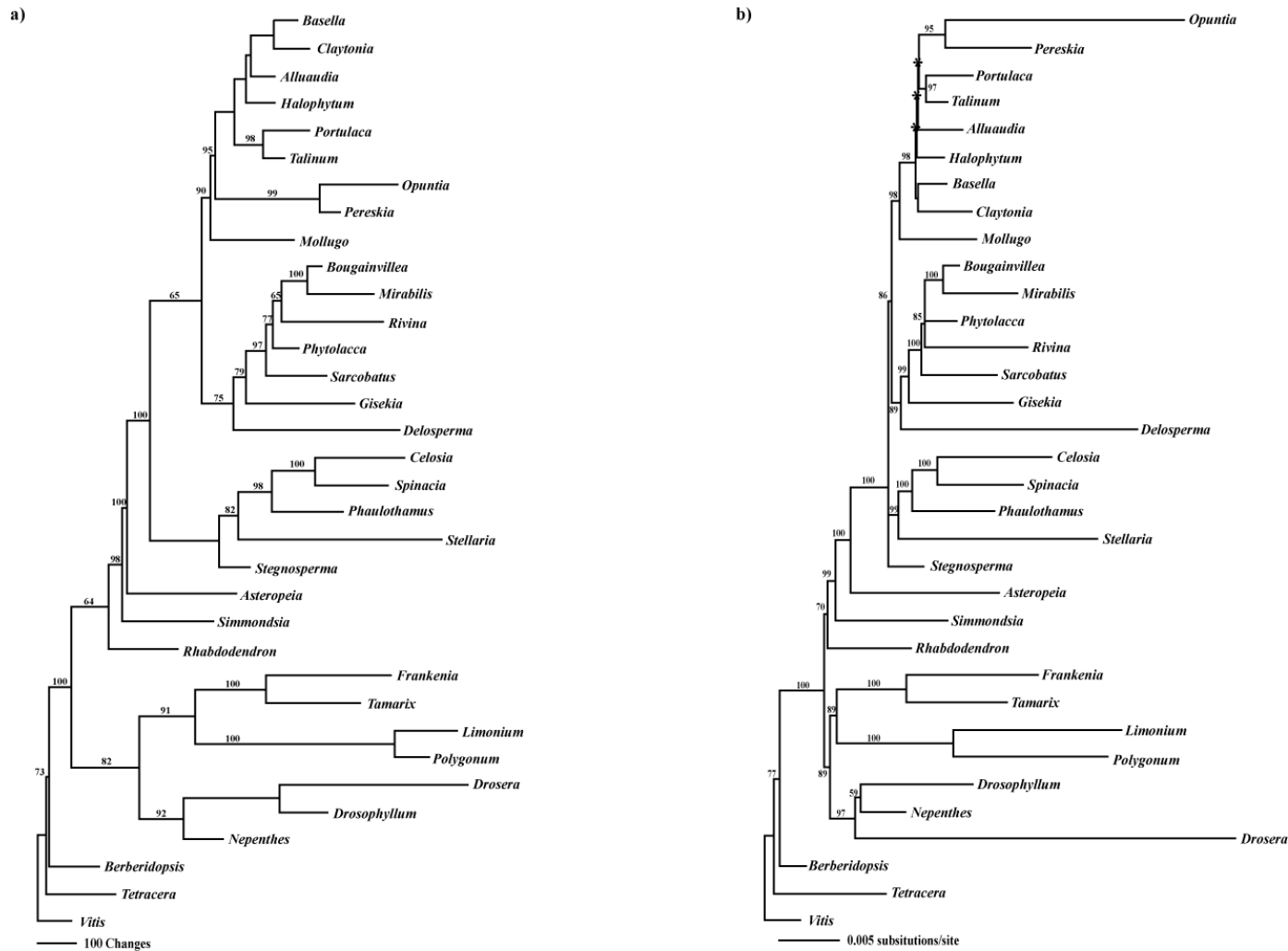


Figure 2-12. Trees derived from analyses of the IR data set (missing taxa: *Limeum*, *Physena*, *Plumbago*). a) Single MP tree; numbers above branches are bootstrap support values; starred nodes collapse in strict consensus. [Length 8649, Consistency Index = 0.781, Retention Index = 0.600]. b) ML tree; numbers above branches are bootstrap support values; starred nodes collapse in strict consensus. [-lnL score 86224.798]

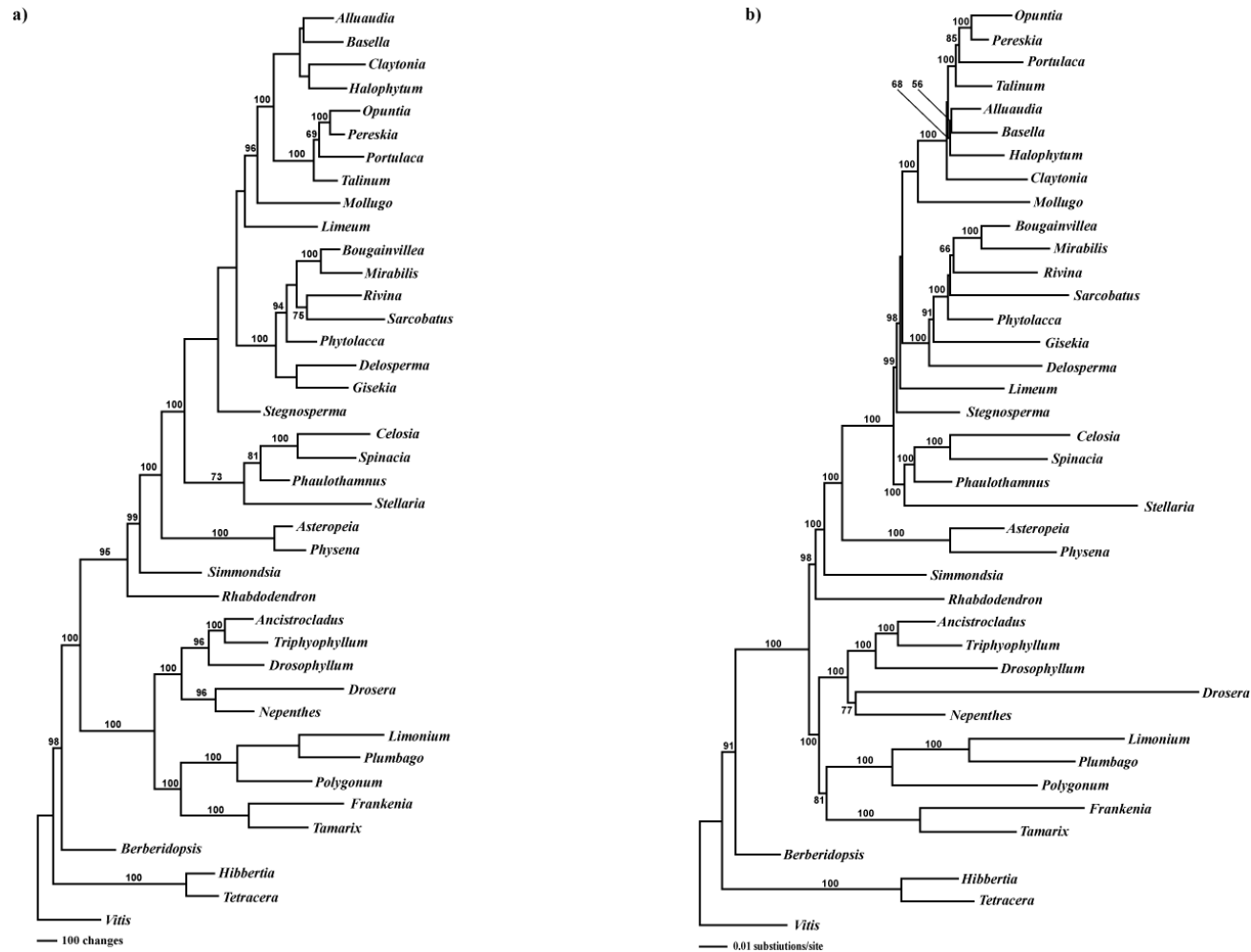


Figure 2-13. Trees derived from analyses of the combined plastid single-copy gene data set. a) Single MP tree; numbers above branches are bootstrap support values; starred nodes collapse in strict consensus. [Length 16158, Consistency Index = 0.530, Retention Index = 0.535] b) ML tree; numbers above branches are bootstrap support values; starred nodes collapse in strict consensus. [-lnL score 99154.419]

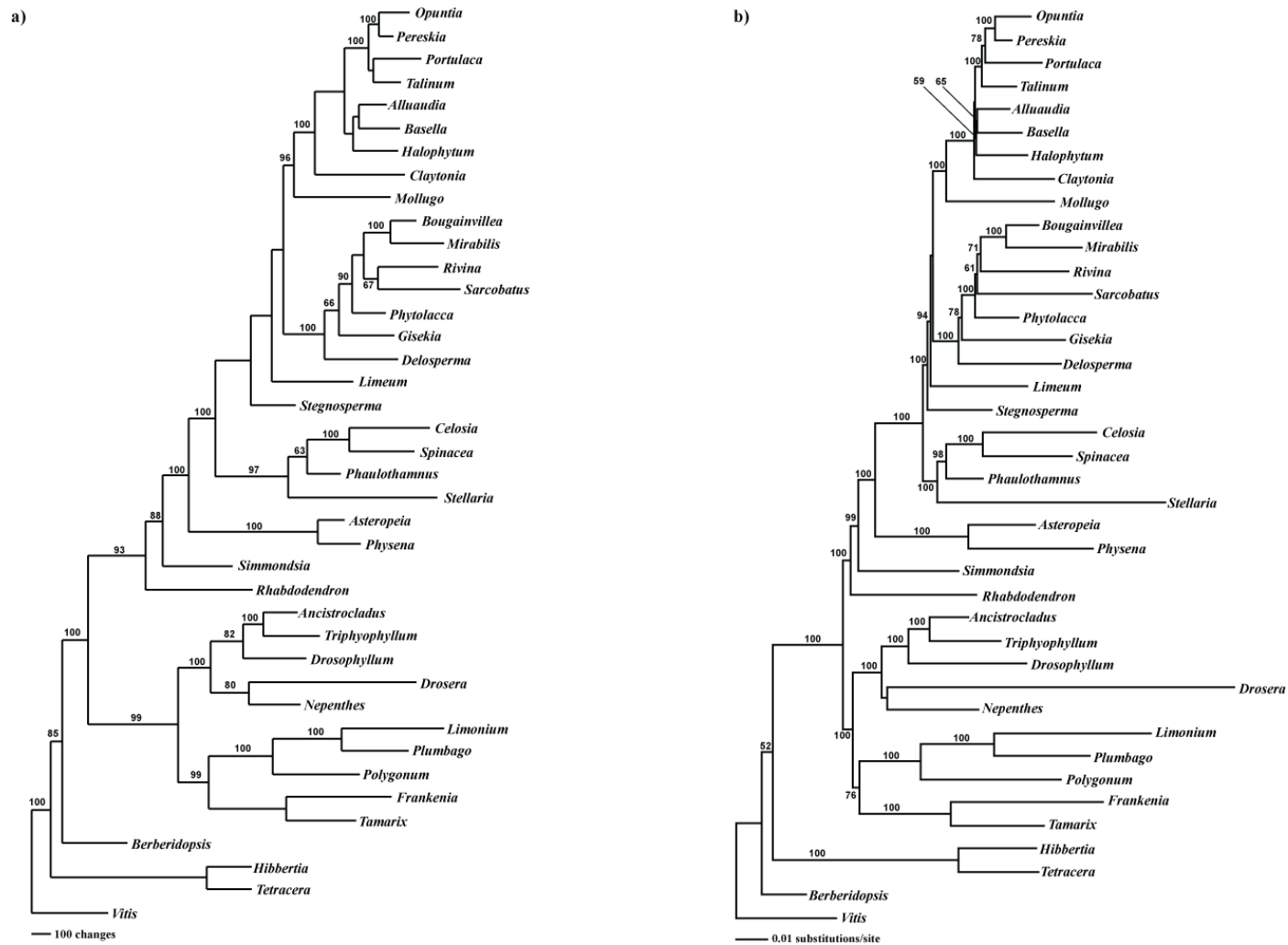


Figure 2-14. Trees derived from analyses of the combined single copy plastid gene and nuclear gene data sets. a) Single MP; numbers above branches are bootstrap support values; starred nodes collapse in strict consensus. [Length 18939, Consistency Index = 0.524, Retention Index = 0.523]. b) ML Tree; numbers above branches are bootstrap support values; starred nodes collapse in strict consensus. [-lnL score 121955.45]

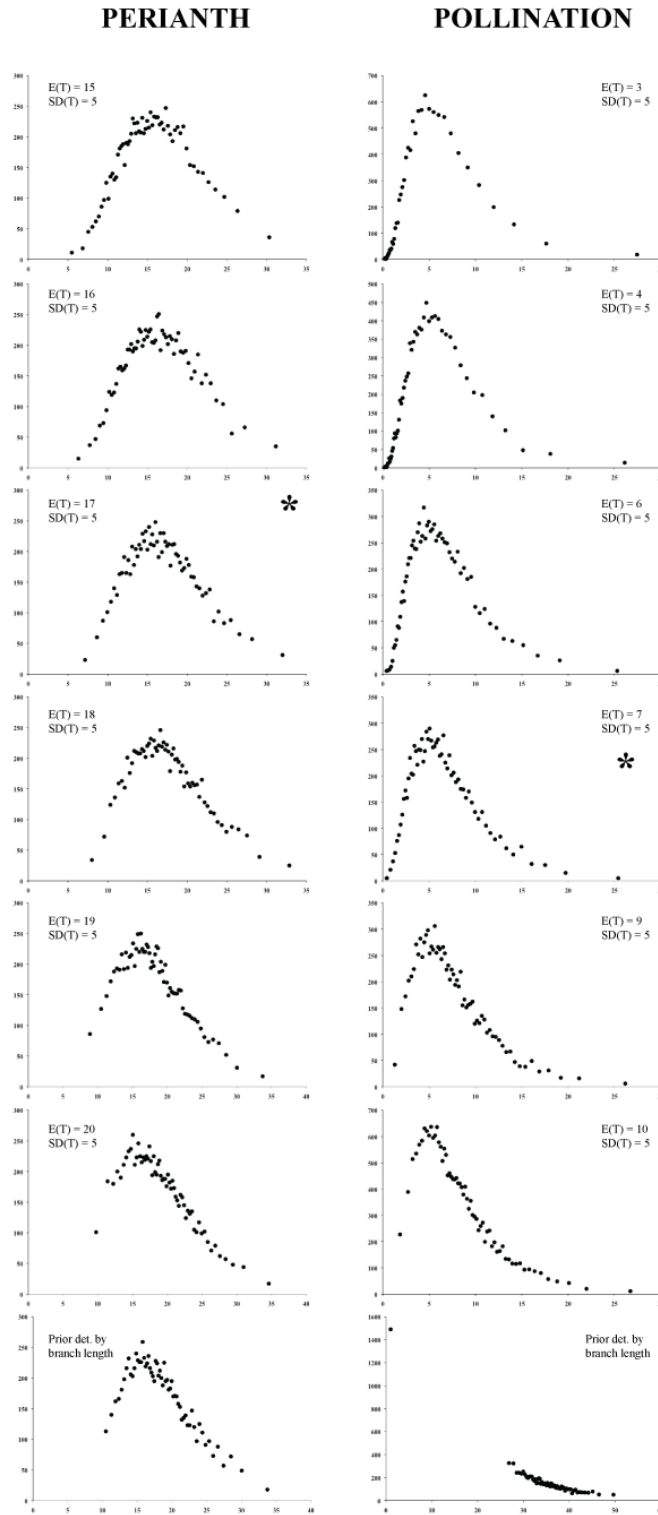


Figure 2-15. Posterior probabilities of each rate category given each combination of $E(T)$ and $SD(T)$ and sampled from the prior with 10,000 realizations.

Table 2-1. Table showing for each data partition: aligned and analysed length of data partitions; No. of MP trees; Length of MP tree; Retention and Consistency Indices; ML score; length of ML tree under parsimony

Data Partition	Total Aligned Length (bp)	Analysed Aligned Length (bp)	No. of MP Trees	Length of MP Tree	Consistency Index of MP Tree	Retention Index of MP Tree	ML Tree Score	ML Tree Length under Parsimony
<i>atpB</i>	1497	1497	23	1296	0.525	0.566	8854.1973	1302
<i>matk</i>	1650	1650	2	3360	0.519	0.522	18173.934	3370
<i>ndhF</i>	2319	2182	20	3159	0.514	0.493	17917.229	3169
<i>psbBTN</i>	1780	1780	15	1639	0.494	0.541	10692.37	1644
<i>rbcL</i>	1449	1449	73	1451	0.522	0.601	9770.5926	1459
<i>rpoC2</i>	3903	3652	3	4529	0.576	0.567	28139.564	4533
<i>rps4</i>	609	609	122,155	545	0.646	0.623	3826.098	564
IR	29410	23966	1	8649	0.781	0.600	86224.798	8654
18S + 26S	5221	5221	14	2713	0.502	0.469	21309.042	2724
SC Plastid	13207	12819	1	16158	0.530	0.535	99154.419	16171
SC Plastid + Nuclear	18428	18040	1	18939	0.524	0.523	121955.45	18962
SC Plastid + Nuclear +IR	47838	42,006	1	27604	0.605	0.538	210420.96	27613

Table 2-2. Voucher, Citation, and GenBank Accession No. for *rbcL*

Family	Species	Voucher	Citation	Embl
Achatocarpaceae	<i>Phaulothamnus spinescens</i>	Manhart and Rettig s.n.	Rettig et al. 1992	M97887
Aizoaceae	<i>Delosperma echinatum</i>	Chase 2539 K	Savolainen et al. 2000	AJ235778
Amaranthaceae	<i>Celosia argentea</i>	Bot. Gard. Mainz (no voucher)	Kadereit et al. 2003	AY270072
Amaranthaceae	<i>Spinacia oleracea</i>	not published	Schmitz-Linne Weber, 2001	AJ400848
Ancistrocladaceae	<i>Ancistrocladus korupensis</i>	Fay s.n.	Fay et al. 1997	Z97636
Asteropeiaceae	<i>Asteropeia micraster</i>	Civeyrel s.n. K	Soltis et al. 2000	AF206737
Basellaceae	<i>Basella alba</i>	Wilson s.n.	Rettig et al. 1992	M62564
Berberidopsidaceae	<i>Berberidopsis sp.</i>	Moore 326	this study	
Cactaceae	<i>Opuntia dillenii</i>	Greuter s.n.	Edwards et al. 2005	AY875233
Cactaceae	<i>Pereskia aculeata</i>	Manhart and Rettig s.n.	Rettig et al. 1992	M97888
Caryophyllaceae	<i>Stellaria media</i>	Mort s.n. WS	Soltis et al. 2000	AF206823
Didiereaceae	<i>Alluaudia procera</i>	Manhart and Rettig s.n.	Rettig et al. 1992	M62563
Dilleniaceae	<i>Hibbertia volubilis</i>	Hoot 9222 UWM	Hoot et al. 1999	AF093721
Dilleniaceae	<i>Tetracera asiatica</i>	Chase 1238 K	Savolainen et al. 2000	AJ235796
Dioncophyllaceae	<i>Triphyophyllum peltatum</i>	Fay s.n.	Fay et al. 1997	Z97637
Droseraceae	<i>Drosera capensis</i>	Williams D1 LVC	Albert et al. 1994	L01909
Drosophyllaceae	<i>Drosophyllum lusitanicum</i>	Williams D100 LVC	Albert et al. 1994	L01907
Frankeniaceae	<i>Frankenia pulverulenta</i>	Collenette 6/93 K	Savolainen et al. 2000	Z97638
Gisekiaceae	<i>Gisekia pharmacioides</i>	Manhart and Rettig s.n.	Rettig et al. 1992	M97890
Halophytaceae	<i>Halophytum ameghinoi</i>	Tortosa, Bartoli, and Chubut s.n.	Savolainen et al. 2000	AJ403024
Molluginaceae	<i>Limeum aethiopicum</i>	not published	unpublished	AF132095
Molluginaceae	<i>Mollugo verticellata</i>	Hershkovitz 37 WS	Soltis et al. 2000	M62566
Nepenthaceae	<i>Nepenthes alata</i>	M.W Chase 145 (NCU)	Albert et al. 1994	L01936
Nyctaginaceae	<i>Bougainvillea glabra</i>	Chase 2485 K	Savolainen et al. 2000	M88340
Nyctaginaceae	<i>Mirabilis jalapa</i>	Hershkovitz 60 WS	Soltis et al. 2000	M62565
Phyсенaceae	<i>Phyсенa madagascariensis</i>	Morton n.s.	Morton et al., 1997	Y13116
Phytolaccaceae	<i>Phytolacca americana</i>	Wells 4366 (1997)	Kress et al. 2005	DQ006112
Phytolaccaceae	<i>Rivinia humulis</i>	Manhart and Rettig s.n.	Rettig et al. 1992	M62569
Plumbaginaceae	<i>Limonium gibertii</i>	not published	Galmes et al. 2005	AJ786659
Plumbaginaceae	<i>Plumbago auriculata</i>	Voucher , UCR	Giannasi et al. 1992	M77701
Polygonaceae	<i>Polygonum sagittatum</i>	not published	Kress et al. 2005	DQ006118
Portulacaceae	<i>Claytonia perfoliata</i>	not published	unpublished	AF132093
Portulacaceae	<i>Portulaca oleracea</i>	Applequist 7, unk, ISC	Edwards et al. 2005	AY875249
Portulacaceae	<i>Talinum paniculatum</i>	Edwards 6, Garden, YU	Edwards et al. 2005	AY875214
Rhabdodendraceae	<i>Rhabdodendron amazonicum</i>	Fay s.n.	Fay et al. 1997	Z97649
Sarcobataceae	<i>Sarcobatus vermiculatus</i>	not published	unpublished	AF132088
Simmondsiaceae	<i>Simmondsia chinensis</i>	S. Boyd et al. 3555 (F)	Hoot et al. 1999	AF093732
Stegnospermataceae	<i>Stegnosperma halmifolium</i>	Miss.Bot. Gar	Rettig et al. 1992	M62571
Tamaricaceae	<i>Tamarix pentandra</i>	Fay s.n.	Fay et al. 1997	Z97650
Vitaceae	<i>Vitis vinifera</i>	not published	Jansen et al., 2006	DQ424856

Table 2-3. Voucher, Citation, and GenBank Accession No. for *rpoC2*

Family	Species	Voucher	Citation	Embl
Achatocarpaceae	<i>Phaulothamnus spinescens</i>	J. Panhart s.n	this study	
Aizoaceae	<i>Delosperma napiforme</i>	Brockington S700	this study	
Amaranthaceae	<i>Celosia cristata</i>	Qiu 94153 IND	this study	
Amaranthaceae	<i>Spinacia oleracea</i>	unpublished	Schmitz-Linneweber, 2001	AJ400848
Ancistrocladaceae	<i>Ancistrocladus korupensis</i>	Gereau et al. 5203 MO	this study	
Asteropeiaceae	<i>Asteropeia micraster</i>	Civeyrel s.n., K	this study	
Basellaceae	<i>Basella alba</i>	Qiu 02055 Univ	this study	
Berberidopsidaceae	<i>Berberidopsis corallina</i>	Moore 326	this study	
Cactaceae	<i>Opuntia microdasys</i>	D. Soltis s.n	this study	
Cactaceae	<i>Pereskia aculeata</i>	D. Soltis 2645	this study	
Caryophyllaceae	<i>Stellaria media</i>	D. Soltis s.n	this study	
Didiereaceae	<i>Alluaudia ascendens</i>	Qiu 97030 IND	this study	
Dilleniaceae	<i>Hibbertia cuneiformis</i>	Qiu 97020 IND	this study	
Dilleniaceae	<i>Tetracera asiatica</i>	Prance 30760 K	this study	
Dioncophyllaceae	<i>Triphyophyllum peltatum</i>	Chase 663 K	this study	
Droseraceae	<i>Drosera capensis</i>	D. Soltis s.n	this study	
Drosophyllaceae	<i>Drosophyllum lusitanicum</i>	J. Cortez s.n, GBG	this study	
Frankeniaceae	<i>Frankenia pulverulenta</i>	Collenette 6/93 K	this study	
Gisekiaceae	<i>Gisekia africana</i>		this study	
Halophytaceae	<i>Halophytum ameghinoi</i>	Tortosa + Bartoli, Chubut, s.n	this study	
Molluginaceae	<i>Limeum africanum</i>	Goldblatt et al. 11512	this study	
Molluginaceae	<i>Mollugo verticellata</i>	Moore 321	this study	
Nepenthaceae	<i>Nepenthes alata</i>	Botany Greenhouse, UF	this study	
Nyctaginaceae	<i>Bougainvillea glabra</i>	Moore 323	this study	
Nyctaginaceae	<i>Mirabilis jalapa</i>	D.Soltis 2638	this study	
Physenaceae	<i>Physena madagascariensis</i>	Miller et al. 8817 MO	this study	
Phytolaccaceae	<i>Phytolacca americana</i>	Brockington s.n	this study	
Phytolaccaceae	<i>Rivinia humilis</i>	D.Soltis 2643	this study	
Plumbaginaceae	<i>Limonium arborescens</i>	Moore 318	this study	
Plumbaginaceae	<i>Plumbago auriculata</i>	Moore 306	this study	
Polygonaceae	<i>Polygonum virginicum</i>	D.Soltis 2656	this study	
Portulacaceae	<i>Claytonia virginica</i>		this study	
Portulacaceae	<i>Portulaca oleracea</i>	Moore 322	this study	
Portulacaceae	<i>Talinum paniculatum</i>	D.Soltis 2646	this study	
Rhabdodendraceae	<i>Rhabdodendron amazonicum</i>	E. Ribéiro 1187 K	this study	
Sarcobataceae	<i>Sarcobatus vermiculatus</i>	King and Garvey, 13892 MO	this study	
Simmondsiaceae	<i>Simmondsia chinensis</i>	Qiu 96120 IND	this study	
Stegnospermataceae	<i>Stegnosperma halmifolium</i>	Martin et al. s.n MO	this study	
Tamaricaceae	<i>Tamarix pentandra</i>	Chase 252 NCU	this study	
Vitaceae	<i>Vitis vinifera</i>	unpublished	Jansen et al., 2006	DQ424856

Table 2-4. Voucher, Citation, and GenBank Accession No. for *atpB*

Family	Species	Voucher	Citation	Embl
Achatocarpaceae	<i>Phaulothamnus spinescens</i>	J. Panhart s.n	This study	
Aizoaceae	<i>Delosperma echinatum</i>	Chase 2539 K	Savolainen et al. 2000	AJ235452
Amaranthaceae	<i>Celosia argentea</i>	no voucher	Soltis et al. 2000	AF209559
Amaranthaceae	<i>Spinacia oleracea</i>	not published	Schmitz-Linneweber, 2001	AF528861
Ancistrocladaceae	<i>Ancistrocladus korupensis</i>	not published	not published	AF209526
Asteropeiaceae	<i>Asteropeia micraster</i>	Civeyrel s.n K	Soltis et al. 2000	AF209533
Basellaceae	<i>Basella alba</i>	Qiu 02055	this study	
Berberidopsidaceae	<i>Berberidopsis sp.</i>	Moore 326	this study	
Cactaceae	<i>Opuntia microdasys</i>	D. Soltis s.n	this study	
Cactaceae	<i>Pereskia aculeata</i>	Soltis and Soltis, s.n	Soltis et al. 2000	AF209648
Caryophyllaceae	<i>Stellaria media</i>	Mort s.n WS	Soltis et al. 2000	AF209680
Didiereaceae	<i>Alluaudia ascendens</i>	Qiu 97030 IND	this study	
Dilleniaceae	<i>Hibbertia volubilis</i>	Hoot 922 UWM	Hoot et al. 1999	AF092120
Dilleniaceae	<i>Tetracera asiatica</i>	Chase 1238 K	Savolainen et al. 2000	AJ235622
Dioncophyllaceae	<i>Triphyphyllum peltatum</i>	Chase 663K	Soltis et al. 2000	AF209693
Droseraceae	<i>Drosera capensis</i>	K.Cameron 2134 NY	Cameron et al. 2002	AY096110
Drosophyllaceae	<i>Drosophyllum lusitanicum</i>	J. Horn s.n	Cameron et al. 2002	AY096113
Frankeniaceae	<i>Frankenia pulverulenta</i>	Collenette 6/93 K	Savolainen et al. 2000	AJ235476
Gisekiaceae	<i>Gisekia africana</i>		this study	
Halophytaceae	<i>Halophytum ameghinoi</i>	Tortosa + Bartoli, Chubut, s.n	this study	
Molluginaceae	<i>Limeum africanum</i>	Goldblatt et al. 11512	Klak et al. 2002	AJ532610
Molluginaceae	<i>Mollugo verticellata</i>	Hershkovitz 37 WS	Soltis et al. 2000	AF209631
Nepenthaceae	<i>Nepenthes alata</i>	M.W Chase 145 NCU	Albert et al. 1994	AJ235542
Nyctaginaceae	<i>Bougainvillea glabra</i>	Chase 2485 K	Savolainen et al. 2000	AJ235415
Nyctaginaceae	<i>Mirabilis jalapa</i>	Hershkovitz 60 WS	Soltis et al. 2000	AJ532611
Physenaceae	<i>Physena madagascariensis</i>	Miller et al. 8817 MO	this study	
Phytolaccaceae	<i>Phytolacca americana</i>	unpublished	Kai et al., 2002	AF528855
Phytolaccaceae	<i>Rivinia humulis</i>	D.Soltis 2643	this study	
Plumbaginaceae	<i>Limonium dendroides</i>	Chase 706 K	Soltis et al. 2000	AF209620
Plumbaginaceae	<i>Plumbago zeylanica</i>	Chase 994 K	Soltis et al. 2000	AJ235565
Polygonaceae	<i>Polygonum sachalinense</i>	Chase 896 K	Soltis et al. 2000	AJ235569
Portulacaceae	<i>Claytonia virginica</i>		this study	
Portulacaceae	<i>Portulaca grandiflora</i>	Soltis s.n WS	Soltis et al. 2000	AF209659
Portulacaceae	<i>Talinum paniculatum</i>	D.Soltis 2646	this study	
Rhabdodendraceae	<i>Rhabdodendron amazonicum</i>	Ribeiro 1187 K	Savolainen et al. 2000	AJ235578
Sarcobataceae	<i>Sarcobatus vermiculatus</i>	King and Garvey, 13892 MO	this study	
Simmondsiaceae	<i>Simmondsia chinensis</i>	S. Boyd et al. 3555 (F)	Hoot et al. 1999	AF093401
Stegnospermataceae	<i>Stegnosperma halmifolium</i>	Martin et al. s.n MO	this study	
Tamaricaceae	<i>Tamarix pentandra</i>	Chase 262 NCU	Soltis et al. 2000	AF209684
Vitaceae	<i>Vitis vinifera</i>	unpublished	Jansen et al., 2006	DQ424856

Table 2-5. Voucher, Citation, and GenBank Accession No. for *psbBTN*

Family	Species	Voucher	Citation	Embl
Achatocarpaceae	<i>Phaulothamnus spinescens</i>	J. Panhart s.n	this study	
Aizoaceae	<i>Delosperma napiforme</i>	Brockington S700	this study	
Amaranthaceae	<i>Celosia cristata</i>	Qiu 94153 IND	this study	
Amaranthaceae	<i>Spinacia oleracea</i>	unpublished	Schmitz-Linneweber, 2001	AJ400848
Ancistrocladaceae	<i>Ancistrocladus korupensis</i>	Gereau et al. 5203 MO	this study	
Asteropeiaceae	<i>Asteropeia micraster</i>	Civeyrel s.n., K	this study	
Basellaceae	<i>Basella alba</i>	Qiu 02055	this study	
Berberidopsidaceae	<i>Berberidopsis corallina</i>	Moore 326	this study	
Cactaceae	<i>Opuntia microdasys</i>	D. Soltis s.n	this study	
Cactaceae	<i>Pereskia aculeata</i>	D. Soltis 2645	this study	
Caryophyllaceae	<i>Stellaria media</i>	D. Soltis s.n	this study	
Didiereaceae	<i>Alluaudia ascendens</i>	Qiu 97030 IND	this study	
Dilleniaceae	<i>Hibbertia cuneiformis</i>	Qiu 97020 IND	this study	
Dilleniaceae	<i>Tetracera asiatica</i>	Prance 30760 K	this study	
Dioncophyllaceae	<i>Triphyophyllum peltatum</i>	Chase 663 K	this study	
Droseraceae	<i>Drosera capensis</i>	D. Soltis s.n	this study	
Drosophyllaceae	<i>Drosophyllum lusitanicum</i>	J. Cortez s.n, GBG	this study	
Frankeniaceae	<i>Frankenia pulverulenta</i>	Collenette 6/93 K	this study	
Gisekiaceae	<i>Gisekia africana</i>		this study	
Halophytaceae	<i>Halophytum ameghinoi</i>	Tortosa + Bartoli, Chubut, s.n	this study	
Molluginaceae	<i>Limeum africanum</i>	Goldblatt et al. 11512	this study	
Molluginaceae	<i>Mollugo verticellata</i>	Moore 321	this study	
Nepenthaceae	<i>Nepenthes alata</i>	Botany Greenhouse, UF	this study	
Nyctaginaceae	<i>Bougainvillea glabra</i>	Moore 323	this study	
Nyctaginaceae	<i>Mirabilis jalapa</i>	D.Soltis 2638	this study	
Physenaceae	<i>Physena madagascariensis</i>	Miller et al. 8817 MO	this study	
Phytolaccaceae	<i>Phytolacca americana</i>	Brockington s.n	this study	
Phytolaccaceae	<i>Rivinia humulis</i>	D.Soltis 2643	this study	
Plumbaginaceae	<i>Limonium arborescens</i>	Moore 318	this study	
Plumbaginaceae	<i>Plumbago auriculata</i>	Moore 306	this study	
Polygonaceae	<i>Polygonum virginicum</i>	D.Soltis 2656	this study	
Portulacaceae	<i>Claytonia virginica</i>		this study	
Portulacaceae	<i>Portulaca oleracea</i>	Moore 322	this study	
Portulacaceae	<i>Talinum paniculatum</i>	D.Soltis 2646	this study	
Rhabdodendraceae	<i>Rhabdodendron amazonicum</i>	E. Ribéiro 1187 K	this study	
Sarcobataceae	<i>Sarcobatus vermiculatus</i>	King and Garvey, 13892 MO	this study	
Simmondsiaceae	<i>Simmondsia chinensis</i>	Qiu 96120 IND	this study	
Stegnospermataceae	<i>Stegnosperma halmifolium</i>	Martin et al. s.n MO	this study	
Tamaricaceae	<i>Tamarix pentandra</i>	Chase 252 NCU	this study	
Vitaceae	<i>Vitis vinifera</i>	unpublished	Jansen et al., 2006	DQ424856

Table 2-6. Voucher, Citation, and GenBank Accession No. for *rps4*

Family	Species	Voucher	Citation	Embl
Achatocarpaceae	<i>Phaulothamnus spinescens</i>	J. Panhart s.n	this study	
Aizoaceae	<i>Delosperma napiforme</i>	Brockington S700	this study	
Amaranthaceae	<i>Celosia cristata</i>	Qiu 94153 IND	this study	
Amaranthaceae	<i>Spinacia oleracea</i>	unpublished	Schmitz-Linneweber, 2001	AJ400848
Ancistrocladaceae	<i>Ancistrocladus korupensis</i>	Gereau et al. 5203 MO	this study	
Asteropeiaceae	<i>Asteropeia micraster</i>	Civeyrel s.n., K	this study	
Basellaceae	<i>Basella alba</i>	Qiu 02055	this study	
Berberidopsidaceae	<i>Berberidopsis corallina</i>	Moore 326	this study	
Cactaceae	<i>Opuntia microdasys</i>	D. Soltis s.n	this study	
Cactaceae	<i>Pereskia aculeata</i>	D. Soltis 2645	this study	
Caryophyllaceae	<i>Stellaria media</i>	D. Soltis s.n	this study	
Didiereaceae	<i>Alluaudia ascendens</i>	Qiu 97030 IND	this study	
Dilleniaceae	<i>Hibbertia cuneiformis</i>	Qiu 97020 IND	this study	
Dilleniaceae	<i>Tetracera asiatica</i>	Prance 30760 K	this study	
Dioncophyllaceae	<i>Triphyophyllum peltatum</i>	Chase 663 K	this study	
Droseraceae	<i>Drosera capensis</i>	D. Soltis s.n	this study	
Drosophyllaceae	<i>Drosophyllum lusitanicum</i>	J. Cortez s.n, GBG	this study	
Frankeniaceae	<i>Frankenia pulverulenta</i>	Collenette 6/93 K	this study	
Gisekiaceae	<i>Gisekia africana</i>		this study	
Halophytaceae	<i>Halophytum ameghinoi</i>	Tortosa + Bartoli, Chubut, s.n	this study	
Molluginaceae	<i>Limeum africanum</i>	Goldblatt et al. 11512	this study	
Molluginaceae	<i>Mollugo verticellata</i>	Moore 321	this study	
Nepenthaceae	<i>Nepenthes alata</i>	Botany Greenhouse, UF	this study	
Nyctaginaceae	<i>Bougainvillea glabra</i>	Moore 323	this study	
Nyctaginaceae	<i>Mirabilis jalapa</i>	D.Soltis 2638	this study	
Physenaceae	<i>Physena madagascariensis</i>	Miller et al. 8817 MO	this study	
Phytolaccaceae	<i>Phytolacca americana</i>	Brockington s.n	this study	
Phytolaccaceae	<i>Rivinia humulis</i>	D.Soltis 2643	this study	
Plumbaginaceae	<i>Limonium arborescens</i>	Moore 318	this study	
Plumbaginaceae	<i>Plumbago auriculata</i>	Moore 306	this study	
Polygonaceae	<i>Polygonum virginicum</i>	D.Soltis 2656	this study	
Portulacaceae	<i>Claytonia virginica</i>		this study	
Portulacaceae	<i>Portulaca oleracea</i>	Moore 322	this study	
Portulacaceae	<i>Talinum paniculatum</i>	D.Soltis 2646	this study	
Rhabdodendraceae	<i>Rhabdodendron amazonicum</i>	E. Ribéiro 1187 K	this study	
Sarcobataceae	<i>Sarcobatus vermiculatus</i>	King and Garvey, 13892 MO	this study	
Simmondsiaceae	<i>Simmondsia chinensis</i>	Qiu 96120 IND	this study	
Stegnospermataceae	<i>Stegnosperma halmifolium</i>	Martin et al. s.n MO	this study	
Tamaricaceae	<i>Tamarix pentandra</i>	Chase 252 NCU	this study	
Vitaceae	<i>Vitis vinifera</i>	unpublished	Jansen et al., 2006	DQ424856

Table 2-7. Voucher, Citation, and GenBank Accession No. for *ndhF*

Family	Species	Voucher	Citation	Embl
Achatocarpaceae	<i>Phaulothamnus spinescens</i>	J. Panhart s.n	this study	
Aizoaceae	<i>Delosperma cooperi</i>			DQ855864.
Amaranthaceae	<i>Celosia argentea</i>			AY959890
Amaranthaceae	<i>Spinacia oleracea</i>	not published	Schmitz-Linneweber, 2001	AY090621
Ancistrocladaceae	<i>Ancistrocladus korupensis</i>	Gereau et al. 5203 MO	this study	
Asteropeiaceae	<i>Asteropeia micraster</i>	Civeyrel s.n., K	this study	
Basellaceae	<i>Basella alba</i>	Qiu 02055	this study	
Berberidopsidaceae	<i>Berberidopsis corallina</i>	Moore 326	this study	
Cactaceae	<i>Opuntia microdasys</i>	D. Soltis s.n	this study	
Cactaceae	<i>Pereskia aculeata</i>	D. Soltis 2645	this study	
Caryophyllaceae	<i>Stellaria media</i>	D. Soltis s.n	this study	
Didiereaceae	<i>Alluaudia ascendens</i>	Qiu 97030 IND	this study	
Dilleniaceae	<i>Hibbertia cuneiformis</i>	Qiu 97020 IND	this study	
Dilleniaceae	<i>Tetracera asiatica</i>			AJ236277
Dioncophyllaceae	<i>Triphyophyllum peltatum</i>	Chase 663 K	this study	
Droseraceae	<i>Drosera capensis</i>	D. Soltis s.n	this study	
Drosophyllaceae	<i>Drosophyllum lusitanicum</i>	J. Cortez s.n, GBG	this study	
Frankeniaceae	<i>Frankenia pulverulenta</i>	Collenette 6/93 K	this study	
Gisekiaceae	<i>Gisekia africana</i>		this study	
Halophytaceae	<i>Halophytum ameghinoi</i>	Tortosa + Bartoli, Chubut, s.n	this study	
Molluginaceae	<i>Limeum africanum</i>	Goldblatt et al. 11512	this study	
Molluginaceae	<i>Mollugo verticellata</i>	Moore 321	this study	
Nepenthaceae	<i>Nepenthes alata</i>	Botany Greenhouse, UF	this study	
Nyctaginaceae	<i>Bougainvillea alba</i>			AF194825
Nyctaginaceae	<i>Mirabilis jalapa</i>	D.Soltis 2638	this study	
Physenaceae	<i>Physena madagascariensis</i>	Miller et al. 8817 MO	this study	
Phytolaccaceae	<i>Phytolacca americana</i>	Brockington s.n	this study	
Phytolaccaceae	<i>Rivinia humulis</i>	D.Soltis 2643	this study	
Plumbaginaceae	<i>Limonium arborescens</i>	Moore 318	this study	
Plumbaginaceae	<i>Plumbago zeylanica</i>			AJ236279
Polygonaceae	<i>Polygonum virginicum</i>	D.Soltis 2656	this study	
Portulacaceae	<i>Claytonia virginica</i>			AF194856
Portulacaceae	<i>Portulaca oleracea</i>	Moore 322	this study	
Portulacaceae	<i>Talinum paniculatum</i>	D.Soltis 2646	this study	
Rhabdodendraceae	<i>Rhabdodendron amazonicum</i>	E. Ribéiro 1187 K	this study	
Sarcobataceae	<i>Sarcobatus vermiculatus</i>	King and Garvey, 13892 MO	this study	
Simmondsiaceae	<i>Simmondsia chinensis</i>	Qiu 96120 IND	this study	
Stegnospermataceae	<i>Stegnosperma halmifolium</i>	Martin et al. s.n MO	this study	
Tamaricaceae	<i>Tamarix pentandra</i>	Chase 252 NCU	this study	
Vitaceae	<i>Vitis vinifera</i>	not published	Jansen et al., 2006	DQ424856

Table 2-8. Voucher, Citation, and GenBank Accession No. for 18S rDNA

Family	Species	Voucher	Citation	Embl
Achatocarpaceae	<i>Phaulothamnus spinescens</i>	Manhart and Rettig s.n.	this study	
Aizoaceae	<i>Delosperma echinatum</i>	Chase 2539 K	this study	
Amaranthaceae	<i>Celosia argentea</i>	Bot. Gard. Mainz (no voucher)	Kadereit et al. 2003	AF206883
Amaranthaceae	<i>Spinacia oleracea</i>	not published	Schmitz-Linne weber, 2001	L24420
Ancistrocladaceae	<i>Ancistrocladus korupensis</i>	Fay s.n	Fay et al. 1997	AF206846
Asteropeiaceae	<i>Asteropeia micraster</i>	Civeyrel s.n K	Soltis et al. 2000	AF206857
Basellaceae	<i>Basella alba</i>	Wilson s.n	this study	
Berberidopsidaceae	<i>Berberidopsis corallina</i>	Moore 326	this study	AF206866
Cactaceae	<i>Opuntia microdasys</i>	D. Soltis s.n	this study	
Cactaceae	<i>Pereskia aculeata</i>	Manhart and Rettig s.n.	Rettig et al.1992	AF206986
Caryophyllaceae	<i>Stellaria media</i>	Mort s.n WS	Soltis et al. 2000	AF207027
Didiereaceae	<i>Alluaudia procera</i>	Manhart and Rettig s.n.	this study	
Dilleniaceae	<i>Hibbertia volubilis</i>	Hoot 9222 UWM	Hoot et al. 1999	AF094542
Dilleniaceae	<i>Tetracera asiatica</i>	Chase 1238 K	Savolainen et al. 2000	AJ235982
Dioncophyllaceae	<i>Triphyophyllum peltatum</i>	Fay s.n	Fay et al. 1997	AF207049
Droseraceae	<i>Drosera capensis</i>	Williams D1 LVC	Albert et al. 1994	U42532
Drosophyllaceae	<i>Drosophyllum lusitanicum</i>	Williams D100 LVC	Albert et al. 1994	AB072556
Frankeniaceae	<i>Frankenia pulverulenta</i>	Collenette 6/93 K	Savolainen et al. 2000	AF206914
Gisekiaceae	<i>Gisekia pharnacioides</i>	Manhart and Rettig s.n.	this study	
Halophytaceae	<i>Halophytum ameghinoi</i>	Tortosa, Bartoli, and Chubut s.n.	this study	
Molluginaceae	<i>Limnium aethiopicum</i>	not published	unpublished	AF094554
Molluginaceae	<i>Mollugo verticellata</i>	Hershkovitz 37 WS	this study	
Nepenthaceae	<i>Nepenthes alata</i>	M.W Chase 145 (NCU)	Albert et al. 1994	U42787
Nyctaginaceae	<i>Bougainvillea glabra</i>	Chase 2485 K	Savolainen et al. 2000	AF206873
Nyctaginaceae	<i>Mirabilis jalapa</i>	Hershkovitz 60 WS	this study	
Physenaceae	<i>Physena madagascariensis</i>	Morton n.s	this study	
Phytolaccaceae	<i>Phytolacca americana</i>	Wells 4366 (1997)	this study	
Phytolaccaceae	<i>Rivinia humulis</i>	Manhart and Rettig s.n.	this study	
Plumbaginaceae	<i>Limonium gibertii</i>	not published	Galmes et al. 2005	AF206953
Plumbaginaceae	<i>Plumbago auriculata</i>	Voucher , UCR	Giannasi et al. 1992	U42795
Polygonaceae	<i>Polygonum sagittatum</i>	not published	this study	
Portulacaceae	<i>Claytonia perfoliata</i>	not published	this study	
Portulacaceae	<i>Portulaca oleracea</i>	Applequist 7, unk, ISC	this study	
Portulacaceae	<i>Talinum paniculatum</i>	Edwards 6, Garden, YU	this study	
Rhabdodendraceae	<i>Rhabdodendron amazonicum</i>	Fay s.n	Fay et al. 1997	AF207007
Sarcobataceae	<i>Sarcobatus vermiculatus</i>	not published	this study	
Simmondsiaceae	<i>Simmondsia chinensis</i>	S. Boyd et al. 3555 (F)	Hoot et al. 1999	AF094562
Stegnospermataceae	<i>Stegnosperma halmifolium</i>	Miss.Bot. Gar	this study	
Tamaricaceae	<i>Tamarix pentandra</i>	Fay s.n	Fay et al. 1997	AF207033
Vitaceae	<i>Vitis vinifera</i>			AF321271

Table 2-9. Voucher, Citation, and GenBank Accession No. for 26S rDNA

Family	Species	Voucher	Citation	Embl
Achatocarpaceae	<i>Phaulothamnus spinescens</i>	J. Panhart s.n	this study	
Aizoaceae	<i>Delosperma napiforme</i>	Brockington S700	this study	
Amaranthaceae	<i>Celosia cristata</i>	Qiu 94153 IND	this study	
Amaranthaceae	<i>Spinacia oleracea</i>	unpublished	this study	
Ancistrocladaceae	<i>Ancistrocladus korupensis</i>	Gereau et al. 5203 MO	this study	
Asteropeiaceae	<i>Asteropeia micraster</i>	Civeyrel s.n K	Soltis et al. 2000	AF479090
Basellaceae	<i>Basella alba</i>	Qiu 02055		
Berberidopsidaceae	<i>Berberidopsis sp.</i>	Moore 326	this study	AF389242
Cactaceae	<i>Opuntia microdasys</i>	D. Soltis s.n	this study	
Cactaceae	<i>Pereskia aculeata</i>	Manhart and Rettig s.n.	Rettig et al. 1992	AF479092
Caryophyllaceae	<i>Stellaria media</i>	Mort s.n WS	Soltis et al. 2000	AF479084
Didiereaceae	<i>Alluaudia ascendens</i>	Qiu 97030 IND	this study	
Dilleniaceae	<i>Hibbertia cuneiformis</i>	Qiu 97020 IND	this study	
Dilleniaceae	<i>Tetracera asiatica</i>	Chase 1238 K	Savolainen et al. 2000	AF479097
Dioncophyllaceae	<i>Triphyophyllum peltatum</i>	Fay s.n	Fay et al. 1997	AF479091
Droseraceae	<i>Drosera capensis</i>	Williams D1 LVC	Albert et al. 1994	AF389248
Drosophyllaceae	<i>Drosophyllum lusitanicum</i>	J. Cortez s.n, GBG	this study	
Frankeniaceae	<i>Frankenia pulverulenta</i>	Collenette 6/93 K	this study	
Gisekiaceae	<i>Gisekia africana</i>		this study	
Halophytaceae	<i>Halophytum ameghinoi</i>	Tortosa + Bartoli, Chubut, s.n	this study	
Molluginaceae	<i>Limeum africanum</i>	Goldblatt et al. 11512	this study	
Molluginaceae	<i>Mollugo verticellata</i>	Moore 321	this study	
Nepenthaceae	<i>Nepenthes alata</i>	M.W Chase 145 (NCU)	Albert et al. 1994	AF389260
Nyctaginaceae	<i>Bougainvillea glabra</i>	Moore 323	this study	
Nyctaginaceae	<i>Mirabilis jalapa</i>	D.Soltis 2638	this study	
Physenaceae	<i>Physena madagascariensis</i>	Miller et al. 8817 MO	this study	
Phytolaccaceae	<i>Phytolacca americana</i>	Brockington s.n	this study	
Phytolaccaceae	<i>Rivinia humulis</i>	D.Soltis 2643	this study	
Plumbaginaceae	<i>Limonium arborescens</i>	Moore 318	this study	
Plumbaginaceae	<i>Plumbago auriculata</i>	Voucher , UCR	Giannasi et al. 1992	AF036492
Polygonaceae	<i>Polygonum sagittatum</i>	not published	Kress et al. 2005	AF479085
Portulacaceae	<i>Claytonia virginica</i>		this study	
Portulacaceae	<i>Portulaca oleracea</i>	Applequist 7, unk, ISC	Edwards et al. 2005	AF479093
Portulacaceae	<i>Talinum paniculatum</i>	D.Soltis 2646	this study	
Rhabdodendraceae	<i>Rhabdodendron amazonicum</i>	E. Ribéiro 1187 K	this study	
Sarcobataceae	<i>Sarcobatus vermiculatus</i>	King and Garvey, 13892 MO	this study	
Simmondsiaceae	<i>Simmondsia chinensis</i>	Qiu 96120 IND	this study	
Stegnospermataceae	<i>Stegnosperma halmifolium</i>	Martin et al. s.n MO	this study	
Tamaricaceae	<i>Tamarix pentandra</i>	Chase 252 NCU	this study	AF479083
Vitaceae	<i>Vitis vinifera</i>	unpublished	this study	AF479207

Table 2-10. Voucher, Citation, and GenBank Accession No. for IR

Family	Species	Voucher	Citation	Embl
Achatocarpaceae	<i>Phaulothamnus spinescens</i>	J. Panhart s.n	this study	
Aizoaceae	<i>Delosperma napiforme</i>	Brockington S700	this study	
Amaranthaceae	<i>Celosia cristata</i>	Qiu 94153 IND	this study	
Amaranthaceae	<i>Spinacia oleracea</i>	unpublished	Schmitz-Linneweber, 2001	AJ400848
Ancistrocladaceae	<i>Ancistrocladus korupensis</i>	Gereau et al. 5203 MO	this study	
Asteropeiaceae	<i>Asteropeia micraster</i>	Civeyrel s.n., K	this study	
Basellaceae	<i>Basella alba</i>	Qiu 02055	this study	
Berberidopsidaceae	<i>Berberidopsis corallina</i>	Moore 326	this study	
Cactaceae	<i>Opuntia microdasys</i>	D. Soltis s.n	this study	
Cactaceae	<i>Pereskia aculeata</i>	D. Soltis 2645	this study	
Caryophyllaceae	<i>Stellaria media</i>	D. Soltis s.n	this study	
Didiereaceae	<i>Alluaudia ascendens</i>	Qiu 97030 IND	this study	
Dilleniaceae	<i>Hibbertia cuneiformis</i>	Qiu 97020 IND	this study	
Dilleniaceae	<i>Tetracera asiatica</i>	Prance 30760 K	this study	
Dioncophyllaceae	<i>Triphyophyllum peltatum</i>	Chase 663 K	this study	
Droseraceae	<i>Drosera capensis</i>	D. Soltis s.n	this study	
Drosophyllaceae	<i>Drosophyllum lusitanicum</i>	J. Cortez s.n, GBG	this study	
Frankeniaceae	<i>Frankenia pulverulenta</i>	Collenette 6/93 K	this study	
Gisekiaceae	<i>Gisekia africana</i>		this study	
Halophytaceae	<i>Halophytum ameghinoi</i>	Tortosa + Bartoli, Chubut, s.n	this study	
Molluginaceae	<i>Limeum africanum</i>	Goldblatt et al. 11512	this study	
Molluginaceae	<i>Mollugo verticellata</i>	Moore 321	this study	
Nepenthaceae	<i>Nepenthes alata</i>	Botany Greenhouse, UF	this study	
Nyctaginaceae	<i>Bougainvillea glabra</i>	Moore 323	this study	
Nyctaginaceae	<i>Mirabilis jalapa</i>	D.Soltis 2638	this study	
Physenaceae	<i>Physena madagascariensis</i>	Miller et al. 8817 MO	this study	
Phytolaccaceae	<i>Phytolacca americana</i>	Brockington s.n	this study	
Phytolaccaceae	<i>Rivinia humilis</i>	D.Soltis 2643	this study	
Plumbaginaceae	<i>Limonium arborescens</i>	Moore 318	this study	
Plumbaginaceae	<i>Plumbago auriculata</i>	Moore 306	this study	
Polygonaceae	<i>Polygonum virginicum</i>	D.Soltis 2656	this study	
Portulacaceae	<i>Claytonia virginica</i>		this study	
Portulacaceae	<i>Portulaca oleracea</i>	Moore 322	this study	
Portulacaceae	<i>Talinum paniculatum</i>	D.Soltis 2646	this study	
Rhabdodendraceae	<i>Rhabdodendron amazonicum</i>	E. Ribéiro 1187 K	this study	
Sarcobataceae	<i>Sarcobatus vermiculatus</i>	King and Garvey, 13892 MO	this study	
Simmondsiaceae	<i>Simmondsia chinensis</i>	Qiu 96120 IND	this study	
Stegnospermataceae	<i>Stegnosperma halmifolium</i>	Martin et al. s.n MO	this study	
Tamaricaceae	<i>Tamarix pentandra</i>	Chase 252 NCU	this study	
Vitaceae	<i>Vitis vinifera</i>	unpublished	Jansen et al., 2006	DQ424856

Table 2-11. Primers used for PCR and Sequencing

<i>rpoC2</i> Primers		26S Primers	
rpoC2.80F	TAGATCACTTCGGAATGGC	26S.N.nc.S1	CGACCCCAGGTCAGGCG
rpoC2.750F	GGTCGTGTATTAGCRGACG	26S.N.nc.S3	AGGGAAGCGGATGGGGGC
rpoC2.1000F	GGTATTATTGCGGGTCAATC	26S.N.nc.S5	CGTGCAAATCGTTCTGCT
rpoC2.1000R	GATTGACCCGCAATAATACC	26S.N.nc.S7	GATGAGTAGGAGGGCGCG
rpoC2.1400F	AGGGRGARATGGCAATGGAG	26S.N.nc.S9	AATGTAGGCAAGGGAAGT
rpoC2.1400R	CTCCARTGCCATYTCYCCCT	26S.N.nc.S11	AATCAGCGGGGAAAGAAG
rpoC2.1950F	GATCCTCGATACAGAAGAAAGAGTTC	26S.N.nc.S13	CCTATCATTGTGAAGCAG
rpoC2.1950R	GAACCTTTCTTCTGTATCGAGGATC	26S.N.nc.S14	TTATGACTGAACGCCTCT
rpoC2.2100F	TCATTCCCGAGGAAGTRCAT	26S.268rev	GCATTCCCAAACAACCCGAC
rpoC2.2100R	ATGYACTTCCTCGGGAATGA	26S.541rev	GCATTCCCAAACAAGCCGAC
rpoC2.2300F	GTGGCATCTTGATACCRCCAG	26S.950rev	GCTATCCTGAGGAAACTTC
rpoC2.2300R	CTGGRGGTATC AAGATGCCAC	26S.1499rev	ACCCATGTGCAAGTGCCGTT
rpoC2.2600F	CAAGTATTC AATTAGTTCGGACTTG	26S.1839rev	TTCACCTTGGAGACCTGATG
rpoC2.2600R	CAAGTCCGAAC TAATTGAATACTTG	26S.2426rev	MCTACACCTCTCAAGTCAT
rpoC2.3000F	CATCTAATTGTTTTCGAATGGGTCC	26S.2782rev	GGTAACTTTTCTGACACCTC
rpoC2.3000R	GGACCCATTCGAAAACAATTAGATG	26S.3058rev	TTCGCGCCACTGGCTTTTCA
rpoC2.3400F	CATTYAATTGTAATTGGTATTTTCTSC	26S.950rev	GCTATCCTGAGGAAACTTC
rpoC2.3400R	GGAGAAAATACCAATTC AAATTYAATG	26S.1499rev	ACCCATGTGCAAGTGCCGTT
rpoC2.3700R	ATGYACTTCCTCGGGAATGA	26S.1839rev	TTCACCTTGGAGACCTGATG
rpoC2.4200R	TTTAGGCC TTTYARCCARTC	26S.2426rev	MCTACACCTCTCAAGTCAT
	<i>rps4</i> Primers	26S.2782rev	GGTAACTTTTCTGACACCTC
rps4.1F	ATG TCR CGT TAC CGA GGG	26S.3058rev	TTCGCGCCACTGGCTTTTCA
rps4.8F	GTT ACC GAG GRC CTC GTT TC	26S.3331rev	ATCTCAGTGGATCGTGCCAG
rps4.48F	GGT TTT ACC RGG ACT AAC		
rps4.124F	TCTCAATATCGTATTTCGTYTAGAAG	18S.C18L	CGACTTCTCCTTCTCTC
trnsR	TACCGAGGGTTCGAATC	18S.NS1	GTAGTCATATGCTTGTCTC
	<i>ndhF</i> Primers	18S.42F	GATTAAGCCATGCATGTGTAAGTATGAAC
ndhF.1F	ATGGAACAACATATAATATGC	18S.1706R	CGGTGTGTACAAAGGGCAGGGACGTAGTC
ndhF.73F	CCCTTCATTCRCTTCCAGTTCTT	18S.1740R	CGCACCATTCAATCGGTAGGAGCGAC
ndhF.95F	CTTTRTTAATAGGARYVGGACTTC		
ndhF.142F	AATYTTCGDCGYATMTGGGCTT	atpB.S2	TATGAGAATCAATCCTACTACTTCT
ndhF.274F	CTTACTTCTATTATGTCAATATTAAT	atpB.S1494R	CAGTACACAAAGATTTAAGGTCAT
ndhF.536F	TTG TAA CTA ATC GTG TAG GGG A		
ndhF.536R	TCCCCTACACGATTAGTTACAA	rbcL.Z1	ATGTCACCACAAACAGAACTAAAGCAAGT
ndhF.803F	CTATGGTAGCGCGGGAATTTTTT	rbcL.3'	CTCGGAGCTCCTTTTAGTAAAAGATTGGGCCGA
ndhF.803R	GAAAAATTCCCGCCGCTACCATAG		
ndhF.972F	GTCTCAATTGGGTTATATGATG	psbBNTH.60F	ATGGGTTTGCCTTGGTATCGTGTTCATAC
ndhF.972R	CATCATATAACCAATTGAGAC	psbBNTH.B60F	CATACAGCTCTAGTTKCTGGTTGG
ndhF.1006F	CCCARTTGAGACATTGTMGAATARGC	psbBNTH.66R	CCAAAAGTRAACCAACCCCTTGGAC
ndhF.1318F	GGATTAACGCATTTTATATGTTTCG	psbBNTH.B66R	CCCCTTGGACTRCTACGAAAAAACC
ndhF.1318R	CGAAACATATAAAATGCGTTAATCC	psbBNTH.65F	TGCCTACTTTTTTTGAAAACATTTCC
ndhF.1603R	GCATAGTATTGTCCGATTCATRAGG	psbBNTH.71R	CCCATMAAAGGAGTAGTYCCCC
ndhF.2110R	CCCCCTAYATATTTGATACCTTCTCC	psbBNTH.B71R	CCAGGAGCTACTTTACCATATTC
ndhF.2153R	GGAATTCATCAATKATCGTYTATC		
			<i>psbBTNH</i> Primers

Table 2-12. Coding of Perianth for Parsimony Reconstruction and Stochastic Character Mapping, with references used to code taxa

Taxa	Parsimony Character Mapping	Stochastic Character Mapping	Literature Cited
<i>Alluaudia</i>	1	1	(Hofmann 1994)
<i>Ancistrocladus</i>	3	3	(Porembski S 2003)
<i>Asteropeia</i>	3	3	(Kubitzki K 2003)
<i>Basella</i>	1	1	(Hofmann 1994)
<i>Berberidopsis</i>	3	3	(Kubitzki K 2007)
<i>Bougainvillea</i>	0	0	(Vanvinckenroye et al. 1993)
<i>Celosia</i>	0	0	(Townsend 1993)
<i>Claytonia</i>	1	1	(Hofmann 1994)
<i>Delosperma</i>	0	0	(Hartmann 1993)
<i>Drosera</i>	3	3	(Kubitzki 2003a)
<i>Drosophyllum</i>	3	3	(Kubitzki 2003b)
<i>Frankenia</i>	3	3	(Kubitzki 2003c)
<i>Gisekia</i>	0	0	(Stevens 2001 onwards)
<i>Halophytum</i>	0	0	(Pozner and Cocucci 2006)
<i>Hibbertia</i>	3	3	(Horn 2007)
<i>Limeum</i>	0/2	?	(Hofmann 1994)
<i>Limonium</i>	3	3	(Kubitzki 1993)
<i>Mirabilis</i>	1	1	(Bittrich and Kuhn 1993)
<i>Mollugo</i>	0	0	(Endress and Bittrich 1993)
<i>Nepenthes</i>	0	0	(Kubitzki 2003d)
<i>Opuntia</i>	3	3	(Buxbaum 1950-55)
<i>Pereskia</i>	3	3	(Buxbaum 1950-55)
<i>Phaulothamnus</i>	0	0	(Bittrich 1993a)
<i>Physena</i>	0	0	(Dickison 2003)
<i>Phytolacca</i>	0	0	(Rohwer 1993)
<i>Plumbago</i>	3	3	(Kubitzki 1993)
<i>Polygonum</i>	0	0	(Brandbyge 1993)
<i>Portulaca</i>	1	1	(Hofmann 1994)
<i>Rhabdodendron</i>	3	3	(Prance 2003)
<i>Rivina</i>	0	0	(Rohwer 1993)
<i>Sarcobatus</i>	0	0	(Stevens 2001 onwards)
<i>Simmondsia</i>	0	0	(Schmid 1978)
<i>Spinacea</i>	0	0	(Townsend 1993)
<i>Stegnosperma</i>	2	2	(Hofmann 1994)
<i>Stellaria</i>	0/2	?	(Ronse De Craene et al. 1998)
<i>Talinum</i>	1	1	(Vanvinckenroye and Smets 1996)
<i>Tamarix</i>	3	3	(Gaskin 2003)
<i>Tetracera</i>	3	3	(Horn 2007)
<i>Triphyophyllum</i>	3	3	(Porembski and Barthlott 2003)
<i>Vitis</i>	3	3	(Wen 2007)

Table 2-13. Coding of Pollination for Parsimony Reconstruction and Stochastic Character Mapping, with references used to code taxa.

Taxa	Parsimony Character Mapping	Stochastic Character Mapping	Source of coding Information
<i>Alluaudia</i>	1	1	(Kubitzki K 1993)
<i>Ancistrocladus</i>	?	?	(Porembski S 2003)
<i>Asteropeia</i>	1	1	(Birkinshaw et al. 2004)
<i>Basella</i>	1	1	(Sperling and Bittrich 1993)
<i>Berberidopsis</i>	?	?	(Kubitzki K 2007)
<i>Bougainvillea</i>	1	1	(Bittrich and Kuhn 1993)
<i>Celosia</i>	0/1	?	(Townsend 1993)
<i>Claytonia</i>	1	1	(Carolin 1993)
<i>Delosperma</i>	1	1	(Hartmann 1993)
<i>Drosera</i>	1	1	(Kubitzki 2003a)
<i>Drosophyllum</i>	1	1	(Kubitzki 2003b)
<i>Frankenia</i>	1	1	(Kubitzki 2003c)
<i>Gisekia</i>	?	?	-
<i>Halophytum</i>	0	0	(Pozner and Cocucci 2006)
<i>Hibbertia</i>	1	1	(Horn 2007)
<i>Limeum</i>	1	1	(Endress and Bittrich 1993)
<i>Limonium</i>	1	1	(Kubitzki 1993)
<i>Mirabilis</i>	1	1	(Bittrich and Kuhn 1993)
<i>Mollugo</i>	0/1	?	(Endress and Bittrich 1993)
<i>Nepenthes</i>	1	1	(Kubitzki 2003d)
<i>Opuntia</i>	1	1	(Barthlott and Hunt 1993)
<i>Pereskia</i>	1	1	(Barthlott and Hunt 1993)
<i>Phaulothamnus</i>	0	0	(Bittrich 1993a)
<i>Physena</i>	?	?	(Dickison 2003)
<i>Phytolacca</i>	1	1	(Rohwer 1993)
<i>Plumbago</i>	1	1	(Kubitzki 1993)
<i>Polygonum</i>	0/1	?	(Brandbyge 1993)
<i>Portulaca</i>	1	1	(Carolin 1993)
<i>Rhabdodendron</i>	1	1	(Prance 2003)
<i>Rivina</i>	1	1	(Rohwer 1993)
<i>Sarcobatus</i>	?	?	-
<i>Simmondsia</i>	0	0	(Kohler 2003)
<i>Spinacea</i>	0/1	?	(Kuhn 1993)
<i>Stegnosperma</i>	?	?	-
<i>Stellaria</i>	1	1	(Bittrich 1993b)
<i>Talinum</i>	1	1	(Carolin 1993)
<i>Tamarix</i>	0/1	?	(Gaskin 2003)
<i>Tetracera</i>	1	1	(Horn 2007)
<i>Triphyophyllum</i>	?	?	(Porembski and Barthlott 2003)
<i>Vitis</i>	1	1	(Wen 2007)

Table 2-14. Estimations of the posterior probability of ancestral perianth character states at each node. Coding Strategy for Perianth: 0= Uniseriate Undifferentiated Perianth, 1 = Differentiated Perianth with involucre derived outer whorl 2 = Differentiated Perianth with stamen-derived petaloid organs 3 = Differentiated perianth of uncertain affinity

Name	Freq	Character 0	Character 1	Character 2	Character 3
Node A	1	0.5059	0.0006	0.0005	0.493
Node B	1	0.9956	0.0003	0.0003	0.0039
Node C	1	0.9936	0.0009	0.0009	0.0046
Node D	1	0.6279	0.0211	0.0209	0.3301
Node E	1	0.9981	0.0005	0.0001	0.0012
Node F	1	0.9989	0.0004	0.0003	0.0004
Node G	1	0.9995	0.0002	0.0002	0.0002
Node H	1	0.9968	0.0012	0.0001	0.0019
Node I	1	0.9761	0.0217	0.0004	0.0018
Node J	0.622	0.9788	0.0209	0.0002	0.0001
Node K	1	0.9965	0.0015	0.0017	0.0003
Node L	1	0.9998	0	0.0001	0
Node M	1	1	0	0	0
Node N	0.9973	0.9996	0.0003	0	0
Node O	1	0.3924	0.6039	0.002	0.0017
Node P	1	0.0001	0.9999	0	0
Node Q	0.9884	0	1	0	0
Node R	1	0.0001	0.9982	0	0.0017
Node S	0.9994	0.0002	0.9998	0	0

Table 2-15. Estimations of the posterior probability of ancestral pollination character states at each node. Coding Strategy for Pollination: Anemophilous = 0, Entomophilous = 1

Name	Freq	Character 0	Character 1
Node A	1	0.0007	0.9993
Node B	1	0.017	0.983
Node C	1	0.007	0.993
Node D	1	0.0148	0.9852
Node E	1	0.0023	0.9977
Node F	1	0.1052	0.8948
Node G	1	0.9781	0.0219
Node H	1	0.0002	0.9998
Node I	1	0	1
Node J	0.622	0	1
Node K	1	0.0002	0.9998
Node L	1	0.0004	0.9996
Node M	1	0.0001	0.9999
Node N	0.9973	0.0001	0.9999
Node O	1	0.0007	0.9993
Node P	1	0	1
Node Q	0.9884	0	1
Node R	1	0	1
Node S	0.9994	0.0002	0.9998

CHAPTER 3 LABILE EVOLUTION OF PIGMENTATION IN THE CORE CARYOPHYLLALES

Flavonoids, anthocyanins and carotenoids are the predominant pigments in flowering plants and play critical roles in floral and fruit coloration. However, in certain families within the core Caryophyllales (a major clade within the core eudicots) pigments known as betalains, which are structurally and biosynthetically distinct from flavonoids and anthocyanins, replace the latter in providing red to yellow pigmentation. The isolated occurrence of betalains in the core Caryophyllales has stimulated over half a century of speculation, debate and experimentation. Anthocyanins and betalains are mutually exclusive with two families of core Caryophyllales (Caryophyllaceae and Molluginaceae) producing anthocyanins and the remaining families producing betalains. The extensive phylogenetic analysis reported here demonstrates that the anthocyanic Molluginaceae are polyphyletic such that *Hypertelis* and *Macarthuria* should be excluded from Molluginaceae *s.s.* (comprising nine genera, *Adenogramma*, *Polpoda*, *Psammotropha*, *Coelanthum*, *Pharnaceum*, *Suessenguthiella*, *Glinus*, *Glischrothamnus* and *Mollugo*). As a result, reconstructions indicate that four (as opposed to two) anthocyanic lineages occur within the core Caryophyllales. *Hypertelis* arises toward the base of the ‘raphide’ clade while *Macarthuria* constitutes a distinct lineage following divergence of Asteropeiaceae and Physenaceae. The ancestral pigment status of Molluginaceae *s.s.* becomes uncertain due to lack of published pigment data in genera of this now narrowly defined family. We explore the effect of this altered topology on inferences of pigment evolution in the core Caryophyllales. Data for Caryophyllaceae and *Macarthuria* imply that the early-diverging lineages of core Caryophyllales may have been anthocyanic although their pigment status is unknown, and analyses suggest a minimum of two reversals to anthocyanin pigmentation with the core Caryophyllales. Although the biochemical switch to betalains has traditionally been considered to have had only one origin,

seven out of eight character-state reconstruction analyses suggest multiple origins of betalain pigmentation within the clade. Consequently, we discuss molecular and biochemical evidence that might support this finding.

Introduction

Pigments perform critical roles in the biology of angiosperms, acting as visible signals to attract insects, birds and mammals for pollination and seed dispersal, and to protect plants from damage caused by UV or visible light. Flavonoids, especially anthocyanins, are widely distributed across angiosperms where they are responsible for the yellow to blue coloration found in flowers, leaves, fruit and seed (Tanaka et al. 2008). Betalains are yellow, orange to red pigments that are structurally and biosynthetically distinct from flavonoids and anthocyanins and in flowering plants are found only in certain families within the core Caryophyllales (Bischoff 1876; reviewed in Mabry 1964), a clade of ~ 29 families and ~ 9000 species (APG II, 2003). In these betalain-producing families, a diversity of flavonoids, including the immediate anthocyanin precursors, leucoanthocyanidins, have been detected, and yet anthocyanins are not present (Bate-Smith 1962; Bittrich and Amaral 1991); thus in the Caryophyllales, the production of betalains apparently substitutes for the otherwise ubiquitous anthocyanins. However, two families in the core Caryophyllales, Molluginaceae and Caryophyllaceae, produce only anthocyanins and not betalains, suggesting that the presence of anthocyanins or betalains is mutually exclusive (Mabry 1964). The novel nature of this chemosystematic character has engendered considerable debate (e.g. Cronquist and Thorne 1994). Some early taxonomic treatments, influenced by this mutual exclusion, placed the Molluginaceae and Caryophyllaceae together (Caryophyllinae), separated from the betalain-producing lineages (Chenopodiinae) (Mabry 1976; Cronquist and Thorne 1994).

Subsequent molecular phylogenetic analyses, however, determined that Molluginaceae and Caryophyllaceae form disparate lineages within Caryophyllales (Rettig et al. 1992; Manhart and Rettig 1994), each allied to derived clades containing betalain-producing families (Cuénoud et al. 2002). Molluginaceae are sister to a large clade of betalain-producing succulent plant families including Cactaceae, while Caryophyllaceae are sister to both Achatocarpaceae, which apparently lack pigments (Clement et al. 1994), and Amaranthaceae, which produce betalains. Molluginaceae occupy a derived position within the core Caryophyllales, following the divergence of betalain-producing lineages (Cuénoud et al. 2002), suggesting the possibility of at least one reversal from betalain pigmentation to anthocyanin pigmentation.

Many evolutionary scenarios have been suggested to explain this complex distribution of pigment types, and yet hypotheses concerning the evolution of pigmentation in the core Caryophyllales must be able to account for the following: 1) the unique presence of betalain pigmentation in the core Caryophyllales; 2) the intercalation of anthocyanin-pigmented taxa with betalain-pigmented lineages; and 3) the mutual exclusivity of the two pigment types. Although many of the hypotheses that have been advanced to date are not mutually exclusive, none of them alone easily explains these phenomena (as summarized in table 3-1 and discussed below).

The Unique Origin of Betalains

Ehrendorfer (1976) argued that the unique presence of betalains in the Caryophyllales was the consequence of an unusual evolutionary history, in which the ancestor to the Caryophyllales evolved in arid to semi-arid conditions prior to the radiation of major pollinator lineages. In this open, pollinator-deprived environment, wind pollination may have prevailed, and anthocyanic pigmentation was lost due to lack of need. Subsequently, following the radiation of pollinator lineages and colonization of less marginal habitats, reversion to zoophily engendered a return to pigmentation in the form of betalains rather than anthocyanins (Ehrendorfer 1976). This

hypothesis is difficult to evaluate (Clement and Mabry 1996), and the concept of the Caryophyllales has changed considerably since Ehrendorfer (1976). Many morphological features of extant Caryophyllales are consistent with a wind-pollinated ancestor, including the predominant uniovular condition (Friedman and Barrett 2008) and an ancestrally uniseriate undifferentiated flower (i.e., a perianth of one organ type rather than differentiated sepals and petals). However several recently identified early-diverging lineages are probably entomophilous (Rhabdodendraceae and Asteropeiaceae) (Brockington et al. in press). Furthermore, anthocyanins and betalains accumulate in both vegetative and reproductive tissues, and their presence in vegetative organs is inconsistent with their evolutionary loss or gain due to absence or presence of pollinators alone.

The Intercalation of Betalain and Anthocyanin Lineages

In an attempt to explain the intercalation of betalain and anthocyanin lineages, Clement and Mabry (1996) suggested that the two classes of compounds might have co-occurred in an ancestor to the core Caryophyllales. The two pigments might have been selectively maintained in ancestors of extant Caryophyllales, with the subsequent loss of one or the other of the pigments in extant lineages. Clement and Mabry (1996) did not identify the nature of the selection maintaining this co-occurrence, or its loss, but Cronquist (1977) proposed that betalains evolved due to their repellent (and fungicidal) properties (Mabry 1980; Piatelli 1981) rather than pigmentation and thus the two pigments could have co-existed due to complementary functions. The most significant objection to this hypothesis is that to date no extant taxa have been identified that possess both anthocyanins and betalains - a surprising observation if they were complementary in function. It is important to note, however, that no pigment data exist for the four earliest-diverging lineages of core Caryophyllales (*Rhabdodendron*, *Simmondsia*, *Asteropeia* and *Physena*) as in general these are hard-to-obtain taxa from remote geographical

areas. It remains possible that the two pigment types coexist in these unexplored taxa however the maintenance of both pigments in an early ancestor does not provide mechanisms for their ultimate mutual exclusion. Clement and Mabry (1996) referred to the ‘stochastic loss’ of one or the other pigment in extant lineages, and yet the use of the term ‘stochastic’ circumvents specific mechanisms to explain loss of a pigment.

Mutual Exclusion of Anthocyanins and Betalains

Additional hypotheses are needed to explain the mutual exclusion of these pigment types and/or the replacement of one pigment type with another. Clement and Mabry (1996) explored the relative metabolic cost of betalain and anthocyanin synthesis but reached no clear conclusions in part because the full physiological roles of anthocyanins and betalains are not thoroughly understood and in part because true metabolic costs are not easily assessed. The relative effectiveness of the pigments have also been discussed in terms of molar absorptivity, with the suggestion that much smaller amounts of betacyanin are needed to absorb equivalent amounts of visible light relative to their anthocyanic counterparts, and betacyanins are thus more ‘cost-effective’ (Clement and Mabry 1996). This precludes the significant absorption of UV wavelengths by anthocyanins. The recent discovery that yellow betaxanthins are fluorescent (Gandia-Herrero et al. 2005) and the increasingly recognized importance of fluorescence for biological signaling (Arnold et al. 2002; Mazel et al. 2004) highlight a further asset that betalains may possess over anthocyanins and complicates analyses of the ‘cost effectiveness’ of pigments.

Biosynthetic Inhibition

Stafford (1994), taking a different line of reasoning, proposed that the remarkably similar patterns in accumulation of betalains and anthocyanins in both vegetative and floral tissues are indicative of a common regulatory system. In this situation, should the ultimate step in anthocyanin synthesis be in some way inhibited by an end-product of betalain synthesis

(Stafford, 1994), then anthocyanin accumulation might be repressed and replaced entirely by betalain pigmentation. To invoke repression of anthocyanin pigmentation by betalain synthesis is problematic, however, when explaining the occurrence of anthocyanins in lineages diverging after the inferred origin of betalain pigmentation.

Confidence in the phylogeny of the core Caryophyllales is fundamental to consideration of this complex, and sometimes contradictory, set of hypotheses. The anthocyanic Molluginaceae have been thought to be polyphyletic with the doubtful inclusion of *Polpoda* (due to lack of sympodial growth; Endress and Bittrich 1993) and *Macarthuria* (due to the angular inclusion in P-plastids; Cuénoud et al. 2002). Resolution of this putative polyphyly might be expected to clarify patterns of pigment evolution. To elucidate the full extent of the anthocyanin-producing lineages and their phylogenetic pattern in relation to betalain-producing lineages, we performed a phylogenetic analysis on genera within the Molluginaceae using multiple genetic markers. No attempt has been made to rigorously evaluate hypotheses of pigment evolution since the advent of DNA-based phylogenies for the core Caryophyllales (Clement and Mabry 1996) other than simple reconstructions in Soltis et al. (2005) and Cuénoud (2006). Furthermore, the significance of apparently ‘pigment-less lineages’ (lacking anthocyanins and betalains) for understanding pigment evolution has been largely ignored (with the exception of Cuénoud et al. 2002), despite their frequent occurrence (e.g., Achatocarpaceae, *Limeum*, and members of Molluginaceae, according to Clement and Mabry, 1996). In this study we: (1) conduct a phylogenetic analysis of all genera within Molluginaceae in the context of the core Caryophyllales, (2) explore concepts of pigment evolution in light of a revised molecular phylogeny using a variety of character-state reconstruction methods and character-coding strategies and (3) assess the implications of a polyphyletic Molluginaceae for inferring pigment evolution.

Materials And Methods

Taxon Sampling and Data Assembly

All 11 genera currently assigned to Molluginaceae were sampled (presented tables 3-4 and 3-5). The plastid genes *matK* and *rbcL* were targeted for amplification. Amplification and sequencing protocols are previously described (Brockington et al. 2008). Sequences generated in this study were combined with previously published sequences for 35 additional genera representing all major lineages within the core Caryophyllales and four outgroups (*Hibbertia*, *Tetracera*, *Vitis* and *Berberidopsis*). In some instances sequence data were combined from multiple species to represent a family; in 10 of 11 cases the species that were combined are congeneric. This approach was judged not to significantly affect the primarily family-level analysis performed in this study, but the instances are listed here: Aizoaceae (*Delosperma napiforme* and *Delosperma echinatum*); Amaranthaceae (*Celosia argentea* and *Celosia trigyna*); Cactaceae (*Opuntia quimilo* and *Opuntia stricta*); Didiereaceae (*Alluaudia ascendens* and *Alluaudia procera*); Dilleniaceae (*Hibbertia volubilis* and *Dillenia indica*); Gisekiaceae (*Gisekia africana* and *Gisekia pharnacioides*); Molluginaceae (*Limeum africanum* and *Limeum aetheopicum*); Plumbaginaceae (*Limonium gibertii* and *Limonium latifolium*); Polygonaceae (*Polygonum sagittatum* and *Polygonum cespitosum*); Portulacaceae (*Claytonia magarhiza* and *Claytonia perfoliata*); Tamaricaceae (*Tamarix pentandra* and *Tamarix canariensis*).

Phylogenetic Analyses

Sequences were automatically aligned using Clustal X (Thompson et al., 1997) and then manually adjusted. Coding regions were aligned by predicted amino acid sequence. Regions at the beginnings and ends of genes for which sequences were incomplete, together with regions that were difficult to align, were excluded from the analysis. The *matK* and *rbcL* data sets were combined into a single data partition. This partition was subject to phylogenetic analyses using

three optimality criteria: maximum parsimony (MP), maximum likelihood (ML) and Bayesian posterior probability.

MP analyses were implemented in PAUP*4.0 (Swofford 2000). Shortest trees were obtained using a heuristic search with 1,000 replicates of random taxon addition with tree-bisection-reconnection (TBR) branch swapping, saving all shortest trees per replicate. Bootstrap support (BS) for relationships was estimated from 1,000 bootstrap replicates using 10 random taxon additions per replicate, with TBR branch swapping, saving all trees.

For ML analyses we employed GARLI (Genetic Algorithm for Rapid Likelihood Inference; version 0.942, Zwickl, 2006), which performs maximum likelihood heuristic phylogenetic searches under the GTR model of nucleotide substitution, in addition to models that incorporate among-site rate variation, either assuming a gamma distribution (Γ) or a proportion of invariable sites (I), or both. Models of nucleotide substitution were determined using MrModeltest (Nylander 2004). The Akaike information criterion (AIC) was used to select GTR+I+G as an appropriate model based on the relative informational distance between the ranked models. Analyses were run with default options, except that the “significant top change” parameter was reduced to 0.01 to make searches more stringent. Five replicate analyses were performed in GARLI. ML bootstrap analyses were conducted in GARLI with the default parameters and 100 replicates.

Bayesian analyses were implemented in MrBayes, version 3.1.2 (Huelsenbeck and Ronquist 2001; Ronquist and Huelsenbeck 2003). Two independent analyses each ran for 5 million generations, using four Markov chains, and with all other parameters at default values; trees were sampled every thousandth generation, with a burn-in of 20,000 generations. Stationarity of the Markov chain Monte Carlo was determined by the average standard deviation

of split frequencies between runs (after 5 million generations the average standard deviation was 0.004%) and by examination of the posterior in Tracer, version 1.3 (Rambaut and Drummond 2003). All trees from the two runs were combined in a majority-rule consensus tree generated in PAUP*4.0 (Swofford 2000), using the posterior distribution of the trees.

Character Coding

Pigment type was coded as a multistate character: ‘betalain pigmented’, ‘anthocyanin pigmented’, or ‘pigment-less’. Due to the apparent mutual exclusion of these two types of pigments, no terminals were coded as equivocal; where data were unavailable or uncertain, taxa were coded as unknown. Coding matrices and sources of information on coding are given in table 3-6. To allow for different hypotheses of pigment evolution, two alternative coding strategies were employed: unordered and ordered. The unordered strategy permitted direct transitions between all character states, allowing direct transitions to occur between anthocyanin and betalain pigmentation. The ordered strategy allowed transitions between betalain and anthocyanin pigmentation to occur only through an intervening ‘unpigmented’ state. These two coding strategies represent alternative traditional hypotheses concerning the evolutionary history and biology of pigmentation within the core Caryophyllales. An ordered coding strategy in which betalains and anthocyanins can arise only via a pigment-less condition is consistent with the hypothesis of Ehrendorfer (1976). The unordered coding strategy, in which transitions directly occur between betalains and anthocyanins, is more consistent with hypotheses suggesting selective advantage of betalains (Clement and Mabry 1996) or regulatory inhibition of the anthocyanin pathway by betalains (Stafford, 1994).

Character-state Reconstruction

Parsimony-based character-state reconstructions on both ordered and unordered characters were performed in Mesquite (Maddison and Maddison 2008) using the ML tree topology with

the highest likelihood score (Figure 3-2). The ML topology was chosen to best represent the phylogeny of the Caryophyllales because of the high degree of rate heterogeneity detected among lineages (see below). Characters were mapped under ACCTRAN and DELTRAN resolving options, and the all most parsimonious states option. The number of state-to state transformations is listed in table 3-2.

Stochastic Mapping

Changes in pigmentation were further modeled by means of stochastic mapping techniques as described by Huelsenbeck et al. (2003) and implemented in SIMMAP (Bollback 2006). This approach estimates the rates at which a discrete character undergoes state changes as it evolves through time. Bayesian estimation has some advantages over traditional parsimony-based reconstruction (Huelsenbeck et al. 2003). First, it allows one to average over equally likely topologies, which is valuable as the position of *Hypertelis* within the ‘raphide’ clade is unresolved or poorly supported and the position of *Macarthuria* is weakly supported in some analyses. Second, it allows more than one character change per branch and is therefore a useful methodology for character-state reconstruction in the Caryophyllales - a clade in which long branches are common.

Prior Specification

Posterior mapping requires the specification of prior values. The prior on the bias parameter was fixed at $1/k$, where k is the number of states (this being the recommended approach in SIMMAP (Bollback 2006) for characters of more than two states; Renner et al. 2007); the bias parameter is therefore 0.333 (3 states: betalain-pigmented, anthocyanin-pigmented and unpigmented). We applied an empirical Bayesian approach in choosing appropriate priors for the substitution rate parameters (Couvreur et al. 2008a, 2008b). The gamma distribution of the substitution rate is governed by two hyperparameters defining the

mean $E(T)$ and the standard deviation $SD(T)$. The values of these hyperparameters for the prior gamma distribution were selected independently for each character-coding strategy (ordered vs. unordered) by using the ‘number of realizations sampled from priors’ function in SIMMAP with 10,000 draws. A series of trials was performed (10,000 realizations in each) that systematically sampled for values of $E(T)$ between 1 and 30, in combination with $SD(T)$ values of either 1 or 5. The posterior distribution of these combinations was visualized in Tracer v. 1.3 and further plotted as graphs of frequency against rate (Figures 3-4 and 3-5). The posterior distribution curves derived from these trials allowed the selection of values of $E(T)$ that gave highest sampling and allowed optimization of the $E(T)$ value (Couvreur et al., 2008a, 2008b). A trial was also performed without specifying priors and allowing rates to be determined by branch lengths (as performed by Renner et al. 2007); however, the posterior distribution curves were generally highly skewed, and this form of prior selection was not employed in subsequent analyses. For the unordered coding strategy, the chosen prior mean rate $E(T)$ was 14 (Figure 3-4), and for the ordered coding strategy, the chosen prior mean rate $E(T)$ was 25 (Figure 3-5). For both of these values, an $SD(T)$ value of 5 was applied in subsequent analyses, allowing a large standard deviation to accommodate uncertainty in the mean rate of character substitution e (Couvreur et al., 2008a, 2008b).

Rates of Transformation and Ancestral State Reconstruction

Following specification of priors, the rate and number of state transformations were estimated by 100 realizations on the 4800 post burn-in trees (with branch lengths) from the Bayesian analyses. As recommended, branch lengths were rescaled so that the total tree length was 1 but the branch length proportions were maintained. The total number of transformations and average number of state-to-state transformations were recorded for each coding strategy (recorded in tables 3-2, and 3-3). The ancestral state at different nodes was assessed using a

hierarchical Bayesian ancestral state reconstruction method implemented in the ‘posterior ancestral states’ function of SIMMAP. The nodes for which ancestral states were estimated are labeled in Figure 3-3. The estimations of the posterior probability of ancestral character states for the ordered and unordered evolution of pigments are listed in table 3-7 and presented graphically on the nodes in Figure 3-3. The effect of missing data (i.e., unknown pigmentation character states at terminals) on the stochastic mapping analyses was examined by pruning unknown taxa from the Bayesian-derived trees. Analyses were then re-run on these pruned trees to assess the effect of pruning unknown taxa on estimations of state-to-state transformations.

Results

Phylogenetic Relationships

Maximum parsimony analysis of the combined *matK* and *rbcL* data set yielded 12 trees. Nine of the Molluginaceae genera (*Glinus*, *Glischrothamnus*, *Mollugo*, *Adenogramma*, *Polpoda*, *Psammotropha*, *Suessenguthiella*, *Coelanthum* and *Pharnaceum*) constitute a strongly supported monophyletic clade (BS = 98%), hereafter, Molluginaceae *sensu stricto s.s.*, sister to the ‘portulacaceous cohort’ (Figure 3-1). These nine genera form three subclades: the clade containing *Glinus*, *Glischrothamnus* and *Mollugo* is sister to a clade comprising (1) *Adenogramma*, *Polpoda* and *Psammotropha*, and (2) a clade comprising *Suessenguthiella*, *Coelanthum* and *Pharnaceum*. The strict consensus tree derived from the replicates of the ML analysis and the consensus tree derived from the Bayesian analyses are almost identical to the MP strict consensus tree with respect to the placement of the genera within Molluginaceae *s.s.* The sole exception is the relative position of *Adenogramma*, *Polpoda* and *Psammotropha*; however, internal relationships within this clade are unresolved in the strict MP consensus tree and unsupported in the GARLI bootstrap analysis (Figure 3-1). Two of the sampled taxa, *Hypertelis* and *Macarthuria*, are not placed in monophyly with the rest of the Molluginaceae.

Macarthuria is resolved as sister to the rest of the core Caryophyllales following the divergence of *Rhabdodendron*, *Simmondsia*, *Asteropeia* and *Physena*. *Hypertelis* is placed as sister to members of the ‘raphide clade’ following the divergence of *Corbichonia* (Figure 3-1 and 3-2). The placements of *Hypertelis* and *Macarthuria* are identical in both the MP and ML trees.

Character Mapping with Unordered Coding

Using parsimony, anthocyanin pigmentation is recovered for the most basal nodes in the core Caryophyllales (Figure 3-3 and Figure 6-3). However, following the divergence of *Macarthuria*, reconstruction of pigment evolution varies depending on whether ACCTRAN or DELTRAN optimization is used. With the ACCTRAN option, following the divergence of *Macarthuria*, node G (Figure 3-3 and Figure 6-3) is reconstructed as betalain-pigmented; thus, a single origin of betalain pigmentation is inferred, with three subsequent reversals to anthocyanin pigmentation in Caryophyllaceae, *Hypertelis*, and Molluginaceae *s.s.* Furthermore, three instances of pigmentation loss are inferred: in Achatocarpaceae, *Limeum* and, via anthocyanin pigmentation, the subclade containing *Adenogramma*, *Psammotropha* and *Polpoda* within Molluginaceae *s.s.* With the DELTRAN option, node G is recovered as anthocyanin-pigmented (Figure 3-3 and Figure 6-3), with two origins of betalain pigmentation, one following the divergence of the clade comprising Caryophyllaceae, Achatocarpaceae and Amaranthaceae (the ‘CAA’ clade) and one within this same clade, in the Amaranthaceae. Following the origin of betalain pigmentation, there are two subsequent reversals to anthocyanin pigmentation (rather than the three under ACCTRAN): in *Hypertelis* and Molluginaceae *s.s.* The same instances of pigmentation loss are inferred under DELTRAN as in ACCTRAN.

Using the stochastic mapping approach, the total mean number of pigment transformations using unordered coding was 15.60 (see table 3-2). The mean number of transitions to betalain pigmentation was 3.43 (anthocyanin to betalain = 2.1147, non-pigmented to betalain = 1.3162).

Pruning of early-diverging taxa of unknown pigment status reduced the mean number of transitions to betalain pigmentation to 3.23. Pruning all taxa of unknown pigment status reduced the mean number of transitions to betalain pigmentation to 2.39. Transitions between other pigment states are shown in table 3-2. The reconstruction of ancestral states derived from the stochastic mapping approach is shown in Figure 3-3b).

Character Mapping with Ordered Coding

Using parsimony reconstruction with ordered coding, anthocyanin pigmentation is again recovered for the most basal nodes in the core Caryophyllales (nodes C, D, E, F), but again, following the divergence of *Macarthuria*, reconstruction of pigment evolution varies dramatically depending on whether ACCTAN or DELTRAN optimization is used. With ACCTAN optimization, node G (Figure 3-3 and Figure 3-6) is inferred to be ancestrally lacking in pigment, with one reversal to betalain pigmentation in Amaranthaceae and a reversal to anthocyanin pigmentation in Caryophyllaceae. Following the divergence of the ‘CAA’ clade, an origin of betalain pigmentation is inferred on the branch leading to the rest of the core Caryophyllales, with two reversals to anthocyanin pigmentation in *Hypertelis* and Molluginaceae *s.s.* Complete loss of pigmentation is inferred to have occurred three times, once following the divergence of *Macarthuria*, once in *Limeum* and again in a subclade of Molluginaceae *s.s.* (*Adenogramma*). The DELTRAN optimization differs considerably from ACCTAN in its reconstruction of ancestral states (Figure 3-6). The basalmost nodes and the node giving rise to the ‘CAA’ clade are reconstructed as anthocyanic. Within the ‘CAA’ clade, pigment is inferred as lost on the branch leading to Achatocarpaceae and Amaranthaceae but subsequently regained in Amaranthaceae. Following the divergence of the ‘CAA’ clade, pigmentation is inferred as lost on the branch leading to the rest of the core Caryophyllales. From this unpigmented condition, four separate origins of betalain pigmentation and three origins of anthocyanin pigmentation are

inferred. The instances of derived betalain pigmentation are inferred in Stegnospermataceae, *Corbichonia*, the ‘raphide’ clade following divergence of *Hypertelis*, and on the branch leading to the ‘portulacaceous clade’. The three instances of anthocyanin pigmentation are inferred to have occurred in *Mollugo*, *Pharnaceum* and *Hypertelis*.

Using the stochastic mapping approach, the total mean number of pigment transformations using ordered coding was 24.74 (table 3-3). The mean number of transitions to betalain pigmentation was 4.76. Pruning of early-diverging taxa of unknown pigment status reduced the mean number of transitions to betalain pigmentation to 3.7. Pruning of all taxa of unknown pigment status reduced the mean number of transitions to betalain pigmentation to 3.2. Transitions between other pigment states are shown in table 3-3. The reconstruction of ancestral states derived from the stochastic mapping approach is shown in Figure 3-3d).

Discussion

Polyphyletic Molluginaceae

Our analyses demonstrate that the anthocyanic lineage Molluginaceae is polyphyletic such that two genera originally assigned to the Molluginaceae (*Hypertelis* and *Macarthuria*) now form distinct lineages (Figure 3-1 and 3-2). *Limeum* and *Corbichonia* also previously belonging to the Molluginaceae have previously been shown to form distinct lineages. Molluginaceae s.s. are re-defined as comprising nine genera: *Adenogramma*, *Polpoda*, *Psammotropha*, *Coelanthum*, *Pharnaceum*, *Suessenguthiella*, *Glinus*, *Glischrothamnus* and *Mollugo*. The anthocyanic genus *Hypertelis* is placed as sister to all of the ‘raphide’ clade except *Corbichonia* and the anthocyanic *Macarthuria* is assigned to a grade of early-diverging core Caryophyllales. Given this polyphyly, the number of anthocyanic lineages within the core Caryophyllales has increased from two to four, with each major betalain-pigmented clade (the ‘portulacaceous’ clade, ‘raphide’ clade and ‘CAA’ clade) subtended completely or in part by an anthocyanin-pigmented lineage (Figure 3-1,

3-2 and 3-3). Furthermore, the anthocyanic genus *Macarthuria* is placed prior to the divergence of any known betalain-pigmented taxa. The presence of an angular protein inclusion in the P-plastid of *Macarthuria* (Behnke 1994) is consistent with its position outside of the ‘globular inclusion’ clade (Brockington et al. in press; Cuénoud et al. 2002).

We conducted several types of character-state reconstruction analyses to evaluate the effect of this new topology on concepts of pigment evolution within the Caryophyllales. These analyses do not provide a consistent impression of the evolution of pigmentation. While we recognize that these character-state reconstructions cannot solve the complexity of pigment evolution in the core Caryophyllales, the phylogenetic topology provided here, together with these analyses, highlights some key questions and uncertainties. Here we discuss the salient similarities and differences in our reconstruction analyses with the aim of defining themes and questions for future research.

Early-Diverging Anthocyanic Lineages

Caryophyllaceae, represented in our analyses by *Stellaria* are the most species-rich and best-studied of the anthocyanic lineages within the core Caryophyllales; with 10 genera analyzed, only anthocyanins have been detected (Clement et al. 1994). Due to the early divergence of Caryophyllaceae, within the core Caryophyllales (Figure 3-1 and 3-2), it is uncertain whether the presence of anthocyanins is a derived state or the plesiomorphic condition. At the level of ancestral character-state reconstruction, distinguishing between these two alternatives depends on the pigment status of the early-diverging grade, which, with the exception of *Macarthuria*, is unknown. In parsimony reconstruction, the early-diverging lineages are always recovered as anthocyanic (Figure 3-4). However, this result is influenced by the position of Caryophyllaceae and the position of the anthocyanic *Macarthuria*, identified by this study as a member of the early-diverging grade. Thus, although the pigment status of the other

early-diverging lineages is unknown, the position of anthocyanic *Macarthuria*, together with the parsimony reconstruction analyses, suggests they could also be anthocyanic. The stochastic mapping analyses, however are less supportive for the anthocyanic condition of the unknown early-diverging lineages (Figure 3-3).

If the occurrence of anthocyanins is plesiomorphic within Caryophyllales, then the presence of anthocyanins in Caryophyllaceae could represent a retention of this plesiomorphic condition (parsimony; DELTRAN; Figure 3-6) rather than a derivation from a pigment-less or betalain condition (ACCTRAN; Figure 3-6: stochastic mapping analyses; Figure 3-3). Clearly, determining the pigment status of recently identified early-diverging lineages (*Rhabdodendron*, *Simmondsia*, *Physena* and *Asteropeia*) is crucial for clarifying the early evolution of pigmentation, yet the geographical isolation of these often rare endemics makes this challenging.

Derived Anthocyanic Lineages

Molluginaceae *s.s.* occupies a more derived position than the Caryophyllaceae, and consequently in all reconstruction analyses, the origin of anthocyanins within this clade is invariably inferred as derived, either from a lack of pigments or from betalains. Although Molluginaceae are widely cited as an anthocyanic family, this claim is based on limited data, partly as a result of the restricted circumscription presented in this study. Of the nine genera that now constitute Molluginaceae as defined in this study, only three have been examined for the presence of pigments: *Adenogramma*, *Pharnaceum* and *Mollugo*. Of these, presence of anthocyanin in *Mollugo* was reported with no reference to experimental data (Mears 1976), and anthocyanins in *Pharnaceum* have been reported only as unpublished data (Clement et al. 1994). Due to the resolved polyphyly presented in this study, there are currently no genera within Molluginaceae that have published data to support an anthocyanic status for the family. The absence of pigments reported in *Adenogramma* might be due to the fact that only dried stems

were analyzed (Cuénoud et al. 2002). Presence of pigments in vegetative tissue is more likely to be dependent on environmental conditions, unlike floral tissue, which tends to be ‘constitutively’ pigmented (Stafford 1994). Clement et al. (1994) reported that most genera in Molluginaceae lack detectable pigments (again without reference to experimental data); if this is accurate, pigments might have been secondarily lost in an ancestor to Molluginaceae with the presence of anthocyanins in *Pharnaceum* and *Mollugo* a further derivation (DELTRAN; Figure 3-6 and stochastic mapping; ordered coding; Figure 3-6).

The isolated status of anthocyanic *Hypertelis* towards the base of the raphide clade is surprising from the point of view of pigment evolution. Although *Hypertelis* was determined to be anthocyanic (Beck et al. 1962), Clement et al. (1994) cast doubt on this finding (but later cite *Hypertelis* as anthocyanic in Clement and Mabry, 1996). In light of its current phylogenetic position, the presence of anthocyanins in *Hypertelis* should be re-evaluated.

Evidence for Reversals to Anthocyanin Pigmentation

Due to the derived position of Molluginaceae and *Hypertelis*, all reconstruction analyses suggest reversals to anthocyanins within the core Caryophyllales (tables 3-1 and 3-2, Figure 3-3 and Figure 6-3), however, historically, reversals to anthocyanins have not been discussed. Elements of the anthocyanin synthesis pathway must be conserved in betalain-pigmented plants due to the presence and accumulation of various precursors such as flavonols, leucoanthocyanidins and proanthocyanidins (Clement and Mabry 1996). This inference has been confirmed by recent studies demonstrating the presence of genes encoding enzymes of the anthocyanin synthetic pathway within betalain-pigmented taxa (Shimada et al. 2005; 2007). Interestingly, the betalain-pigmented *Phytolacca americana* and *Spinacia oleracea* possess fully functioning enzymes for the penultimate stages of the anthocyanin pathway – dihydroflavonol reductase (DFR) and anthocyanidin synthase (ANS) (Shimada et al. 2005). The genes encoding

DFR and ANS are transcribed in the seeds in correlation with production of proanthocyanidins and yet are not transcribed in other parts of the plant. It is probable, therefore, that the absence of anthocyanic pigments is due to altered transcriptional regulation rather than loss of enzymatic genes. This finding is important because if the enzymatic and regulatory machinery are maintained in the betalain-pigmented or unpigmented taxa, then 'reactivated' transcriptional regulation provides a simple mechanism for the reappearance of anthocyanic lineages. Identifying the primary cause for a switch from betalain to anthocyanin production, however, remains problematic.

Effect of Ordered Character Coding - Support for Ehrendorfer (1976).

In this study, different forms of character coding were employed to reflect alternative interpretations of evolutionary, developmental and biosynthetic evidence: and the different coding strategies have a significant effect on the reconstruction of pigment evolution (table 3-2 and 3-3, Figure 3-3). Use of ordered coding, which only allows pigments to arise from an unpigmented state, increased the total number of transformations from seven (unordered analyses) to as many as ten, in the parsimony reconstruction analyses, and from 15 transformations (unordered analyses) to 24 in the stochastic mapping analyses (tables 3-1 and 3-2). These increases were anticipated, as a single transition between pigments in the ordered character coding analyses would automatically be doubled due to the intervening unpigmented stage. In stochastic mapping analyses, as expected, ordered coding also resulted in an increase in unpigmented 'dwell time' which is a measure of the amount of branch length that is occupied by the unpigmented state (tables 3-1 and 3-2). There are, however, more subtle consequences of ordered coding. The intercalation of betalain and anthocyanic lineages is such that ordered character-state parsimony reconstruction with DELTRAN optimality reconstructs the backbone of the tree as lacking pigment, with seven separate origins of betalains and anthocyanins arising

from this unpigmented condition (Figure 6-3). The ordered stochastic mapping analysis also reconstructs the early backbone of the tree as unpigmented (Figure 3-2). Therefore, the pattern of distribution of pigment types across the core Caryophyllales can be somewhat consistent with the Ehrendorfer hypothesis (1976) of ancestral lack of pigments, if the assumption is made that no direct transitions can occur between betalains and anthocyanins.

The Occurrence of Unpigmented Lineages

The presence of derived unpigmented lineages is, in general, difficult to explain. Above we highlighted the possibility that, in concordance with Ehrendorfer (1976), these lineages might have retained the plesiomorphic, unpigmented state. Only one analysis (DELTRAN; Figure 3-6) was able to reconstruct this scenario with the consequence that eight origins of pigment are also inferred. However, in all other analyses, at least three losses of pigment are always inferred. Biological explanations for these instances of pigment loss are lacking, with the exception of Achatocarpaceae, which exhibits a wind-pollination syndrome. *Limeum* is suggested to be unpigmented, and yet some species of *Limeum* possess a differentiated perianth with five small whitish petaloid structures (Endress and Bittrich 1993), clearly adapted for entomophily. In Molluginaceae *s.s.*, although the flowers are often diminutive, many genera (*Psammotropha*, *Glinus*, *Pharnaceum* and *Coelanthum*) have nectariferous secretory tissue (Endress and Bittrich 1993), and flowers of *Glinus* possess staminodial petals, all indicative of entomophily. Complete loss of pigment in these entomophilous taxa would be surprising. Again, the appearance and possible function of pigments in vegetative tissue ensures that the above explanations based solely on floral biology remain unsatisfactory.

As emphasized by our character-state reconstruction analyses, the presence and coding of these derived unpigmented taxa have significant effects on reconstructions of pigment evolution, and therefore it is important to resolve these uncertainties. Are these taxa truly unpigmented or

are the pigment levels just low? To what extent are the structural genes for anthocyanin and betalain synthesis present in these unpigmented taxa? Due to the lack of published experimental data, it is unclear if analyses of these unpigmented taxa were conducted using fresh material, or on dried material in which pigments can degrade. These uncertainties may be resolved by the use of fresh floral material, application of sensitive methods for pigment detection such as HPLC, and possibly use of semi-quantitative RT-PCR to assess the transcription of key pigment synthesis genes such as anthocyanin synthase.

Multiple Origins of Betalain Pigmentation

The distribution of anthocyanic taxa at or towards the base of three predominantly betalain-pigmented clades (Molluginaceae sister to the portulacaceous cohort; *Hypertelis* within the ‘raphide’ clade; Caryophyllaceae sister to the Achatocarpaceae and Amaranthaceae) is provocative. Together with the early divergence of two of the anthocyanic taxa (*Macarthuria* and Caryophyllaceae), it suggests the possibility that the core Caryophyllales were ancestrally anthocyanic, with subsequent multiple origins of betalains (Figure 3-3 and Figure 3-6). Multiple origins of betalains is supported by seven out of eight of the reconstruction analyses, which recover at least two transformations to betalains from either anthocyanins or from the unpigmented state (tables 3-1 and 3-2). In stochastic mapping analyses, we observed higher rates of character transformation along branches leading to terminals of unknown pigment status because transformations along these branches are not forced to culminate at a pigment type in ‘unknown’ terminals. Inclusion of terminals of unknown pigment status could consequently inflate estimations of character transformation. We therefore pruned out all branches to unknown terminals in SIMMAP and demonstrated that multiple origins of betalains were recovered even when taxa of unknown pigment status were excluded from the analysis. The possibility of multiple origins of betalain pigmentation has been raised by Soltis et al. (2005) and Cuénoud

(2006) but has not been discussed in the literature. The betalain pathway is unique to this clade, and with a complex pathway, would seem unlikely to have evolved more than once. Therefore, here we consider additional evidence that may be consistent with this ‘multiple origins’ scenario.

Betalain biosynthesis has only been partly characterized in a limited number of species and certain key enzymes have not yet been isolated. All of the enzymes that have been characterized (i.e DOPA 4, 5-dioxygenase, betanidin 5-*O*-glucosyl-transferase and betanidin 6-*O*-glucosyl-transferase) have homologues in non-betalain-synthesizing plants (Tanaka et al. 2008). DOPA 4, 5-dioxygenase converts dihydroxyphenylalanine (DOPA) into betalamic acid – a precursor for both betaxanthins and betacyanins. The DOPA 4, 5-dioxygenase orthologues from anthocyanic plants have been shown to have DOPA 4, 5-dioxygenase catalytic activity *in vitro* (Tanaka et al. 2008). This suggests that key enzymes in betalain synthesis may be derived from orthologues in anthocyanic plants (Sasaki et al. 2005). Betanidin 5-*O*-glucosyl-transferase and betanidin 6-*O*-glucosyl-transferase convert the precursor betanidin to betanin. These enzymes indiscriminately catalyze *in vitro* the transfer of glucose from UDP-glucose to hydroxyl groups of not just betanidin but also flavonols, anthocyanidins and flavones (Vogt et al. 1997); this indiscriminate catalysis highlights the possibility that certain enzymatic steps in the betalain biosynthetic pathway could be performed by enzymes with broad substrate specificity. This broad substrate specificity may have existed prior to the origin of betalain synthesis and might have facilitated the co-option of these enzymes to the betalain biosynthetic pathway.

The two glucosyl transferases (betanidin 5-*O*-glucosyl-transferase and betanidin 6-*O*-glucosyl-transferase) only share 15% amino acid identity and belong to different lineages of glucosyl transferases; in each lineage the betanidin glucosyl transferases are sister to glucosyl transferases involved in flavonoid or anthocyanin pathways (Vogt 2002). The existence of

betanidin glucosyl transferases derived from distinct lineages emphasizes that recruitment of genes to the betalain biosynthetic pathway may have occurred independently from distinct gene lineages. Evidence of such independent gene recruitment encourages speculation that betalain pigmentation in distinct organismal lineages may also be the consequence of independent co-option of ancestral homologues.

Biochemical and molecular investigations in a range of caryophyllid taxa have suggested several semi-independent pathways in the synthesis of betalains, as discussed by Tanaka et al. (2008). Betaxanthins can be derived from betalamic acid and amino acids conjugates. Some betalains may be synthesized by tyrosinase or polyphenol oxidase after the condensation of betalamic acid and amino acid (Gandia-Herrero et al. 2005). Additionally, betalains can be synthesized by two semi-independent pathways from the intermediate dihydroxyphenylalanine via the betalamic biosynthetic pathway or the via cyclo-dihydroxyphenylalanine glycoside pathway (Tanaka et al. 2008). Our study asks whether this variability in betalain synthesis pathways in different taxa could be in part a reflection of independent origins of betalain pigmentation: a hypothesis that deserves further consideration.

Conclusion

The reds, blues and violet colors of the plant world are typically due to anthocyanins with the exception of one clade of angiosperms (the core Caryophyllales) in which anthocyanins are inexplicably replaced by betalains in most members of the clade. The betalain pathway has traditionally been considered to have had a single origin but our phylogenetic analyses of the core Caryophyllales (including the polyphyletic Molluginaceae), coupled with multiple methods of character reconstruction indicate a likely minimum of two origins of betalain pigmentation in this clade, as well as possible reversals to anthocyanin pigmentation. Additionally we highlight the unknown pigment status of recently identified, early-diverging lineages and the now-

uncertain pigment status of Molluginaceae *s.s.* We provide a robust phylogenetic framework with which to further explore the biology of betalain synthesis and to address the complex and labile evolution of betalains and anthocyanins within the core Caryophyllales.

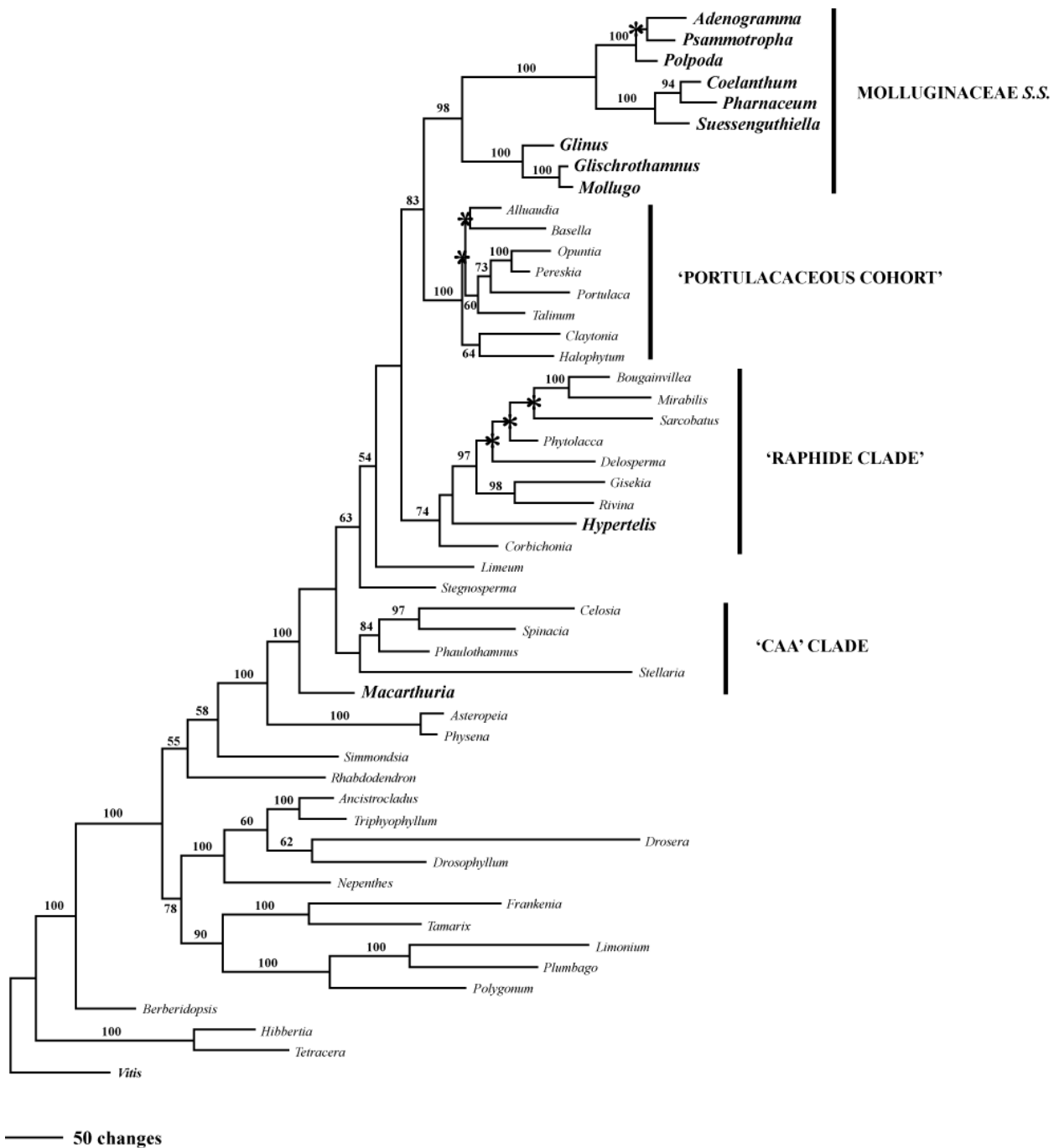


Figure 3-1. Phylogram of one of twelve most parsimonious trees based on the *matK* and *rbcl* data set for 11 genera of Molluginaceae, 35 members of the Caryophyllales and four outgroups. All taxa newly sequenced in this study and previously assigned to Molluginaceae are marked in bold. Numbers above branches are bootstrap values. Starred nodes collapse in strict consensus.

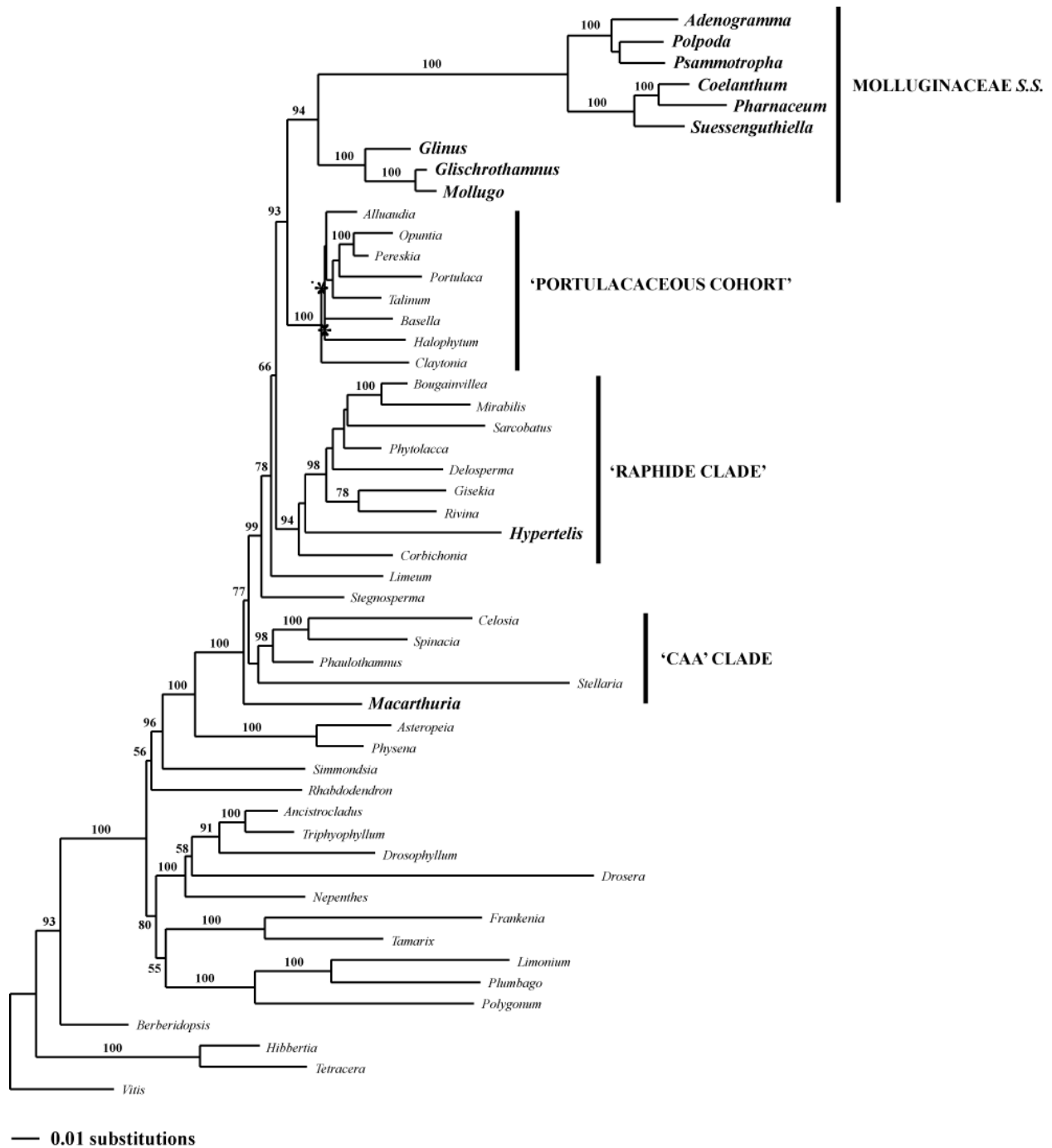


Figure 3-2. Maximum likelihood (ML) tree resulting from GARLI analysis of *matK* and *rbcL* data set for 11 genera of Molluginaceae, 35 members of the Caryophyllales and four outgroups. All taxa newly sequenced in this study and previously assigned to Molluginaceae are marked in bold. Numbers above branches are bootstrap values. Starred nodes collapse in strict consensus of 5 replicate GARLI trees.

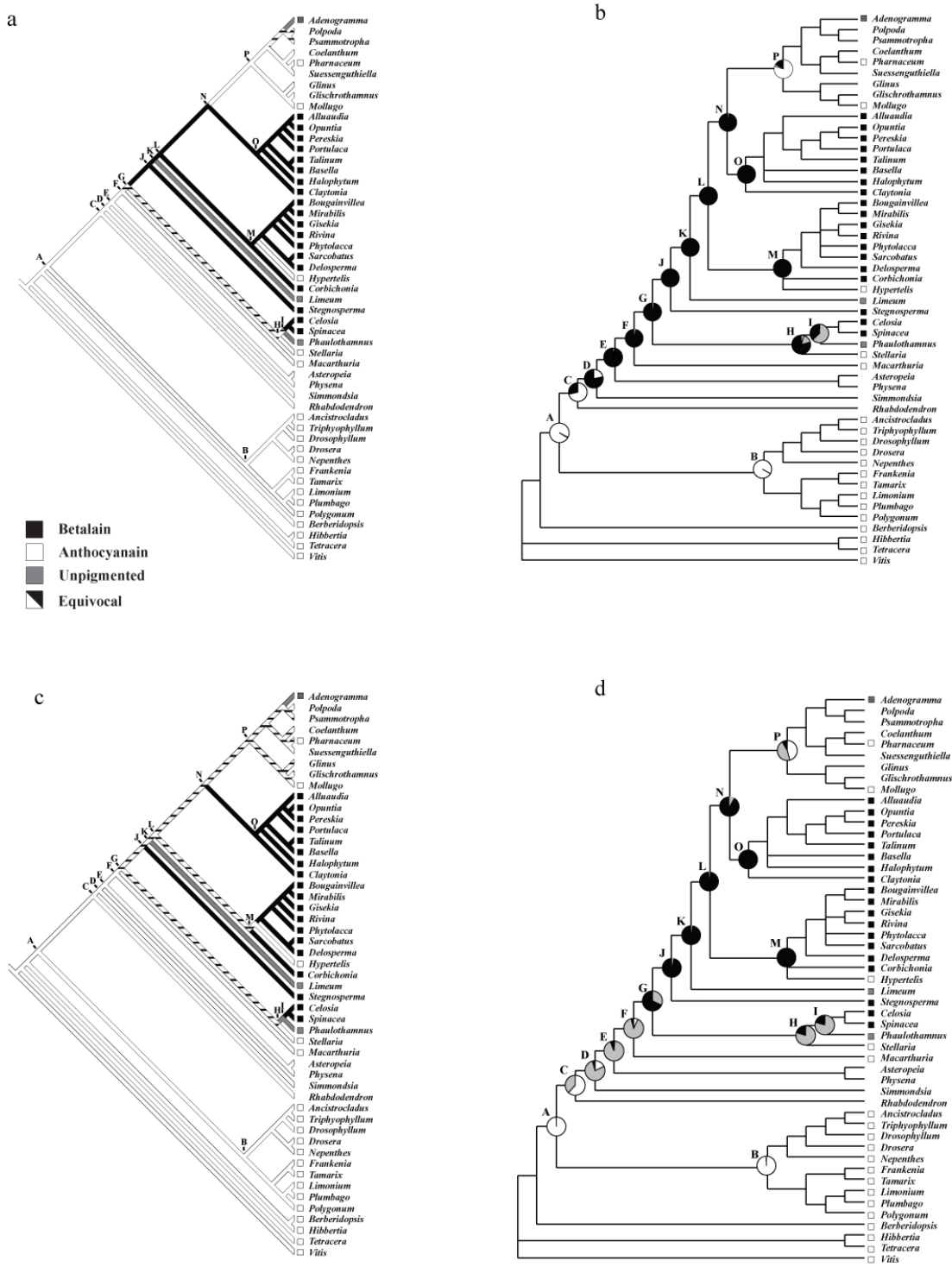


Figure 3-3. Reconstruction of pigment evolution: a) parsimony reconstruction over MP tree with unordered data set; b) Stochastic mapping reconstruction of pigment evolution on a Bayesian consensus tree using unordered dataset; c) parsimony reconstruction over MP tree with ordered data set d) stochastic mapping reconstruction of pigment evolution on a Bayesian consensus tree using ordered data set.

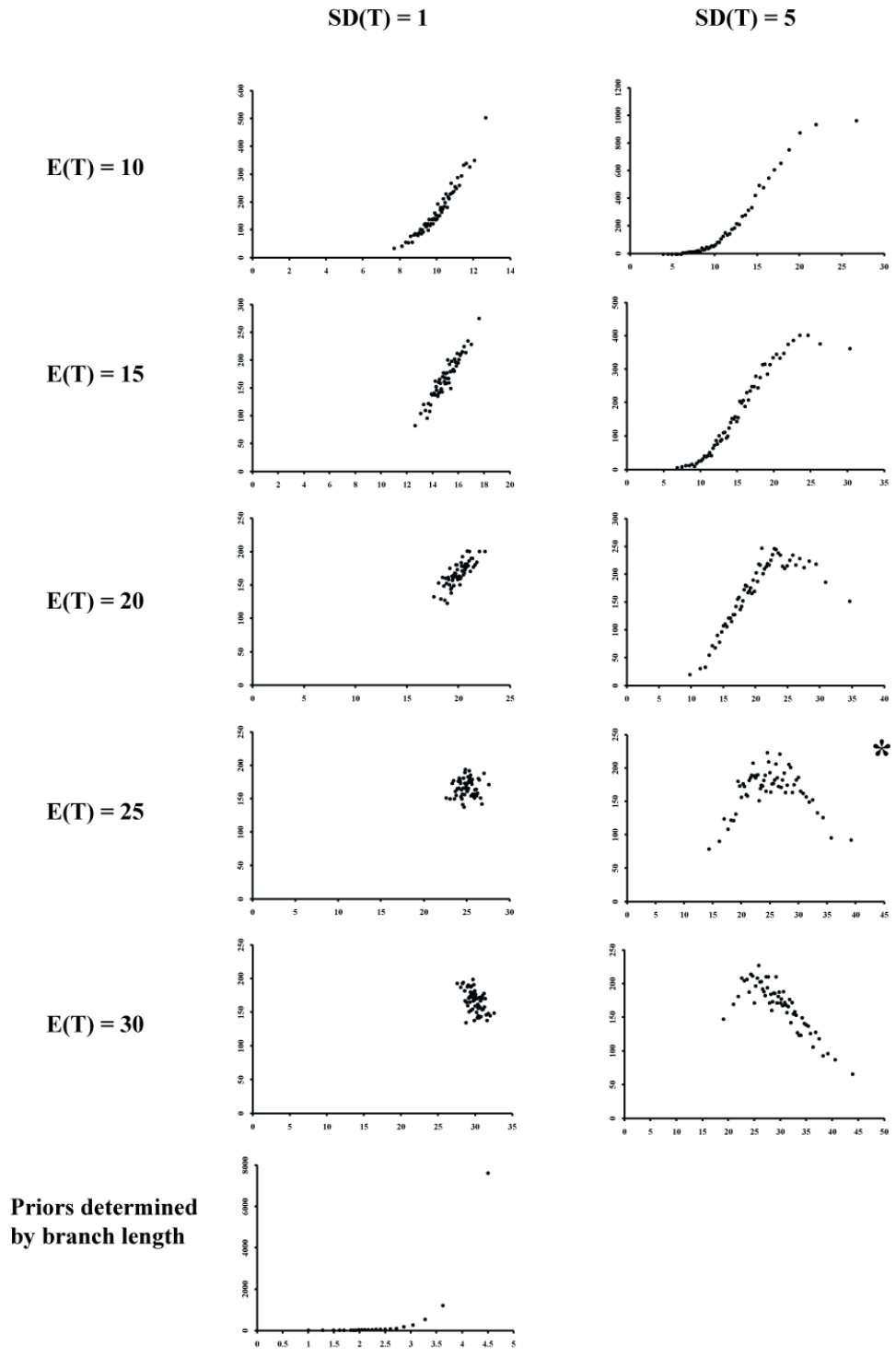


Figure 3-4. Prior simulations for ordered data set. Posterior probabilities of each rate category given each combination of E(T) and SD(T) and sampled from the prior with 10,000 realizations. X axis: rate of substitution. Y axis: sampling frequency of each discrete category.

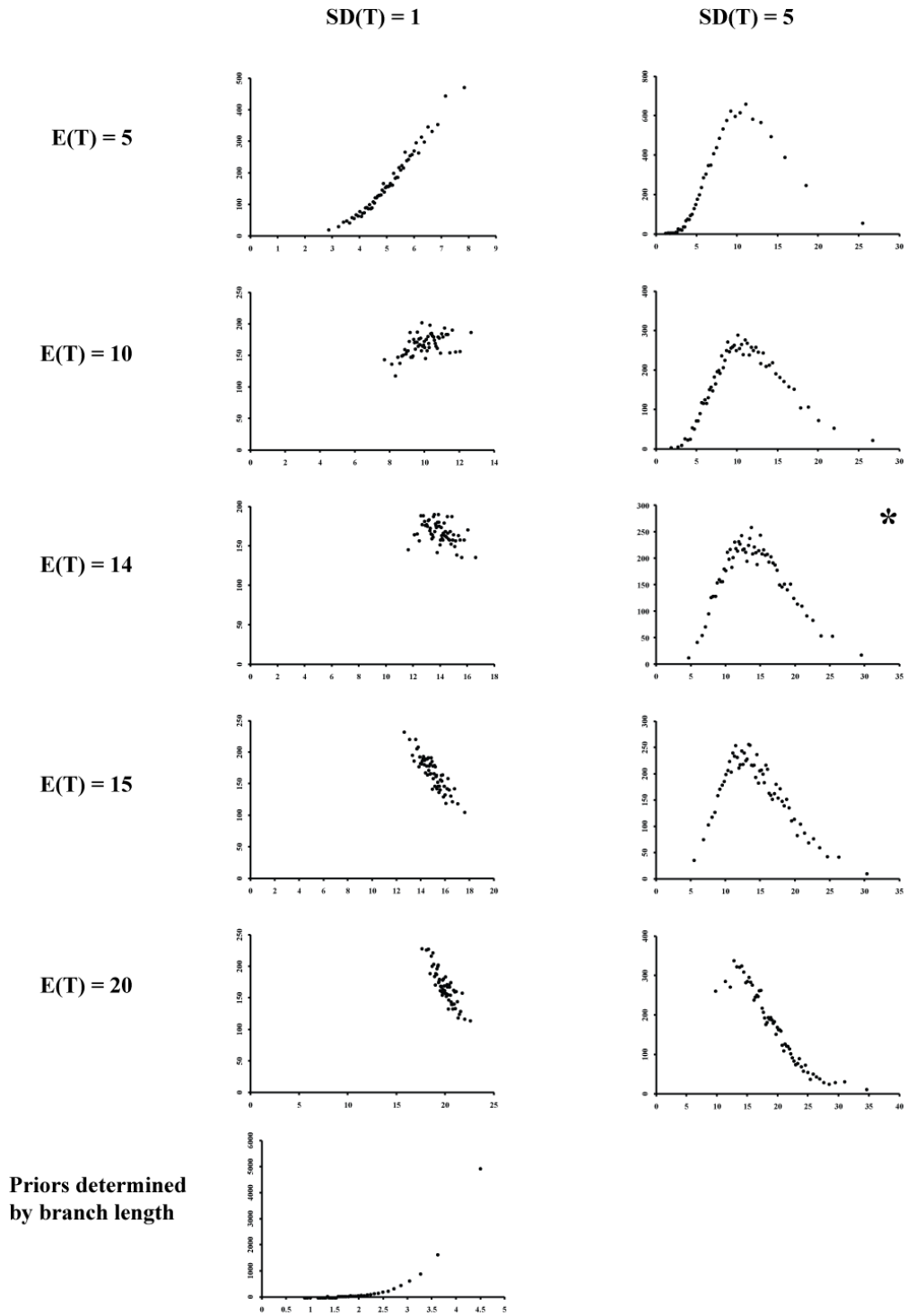


Figure 3-5. Prior simulations for unordered data set. Posterior probabilities of each rate category given each combination of $E(T)$ and $SD(T)$ and sampled from the prior with 10,000 realizations. X axis: rate of substitution. Y axis: sampling frequency of each discrete category.

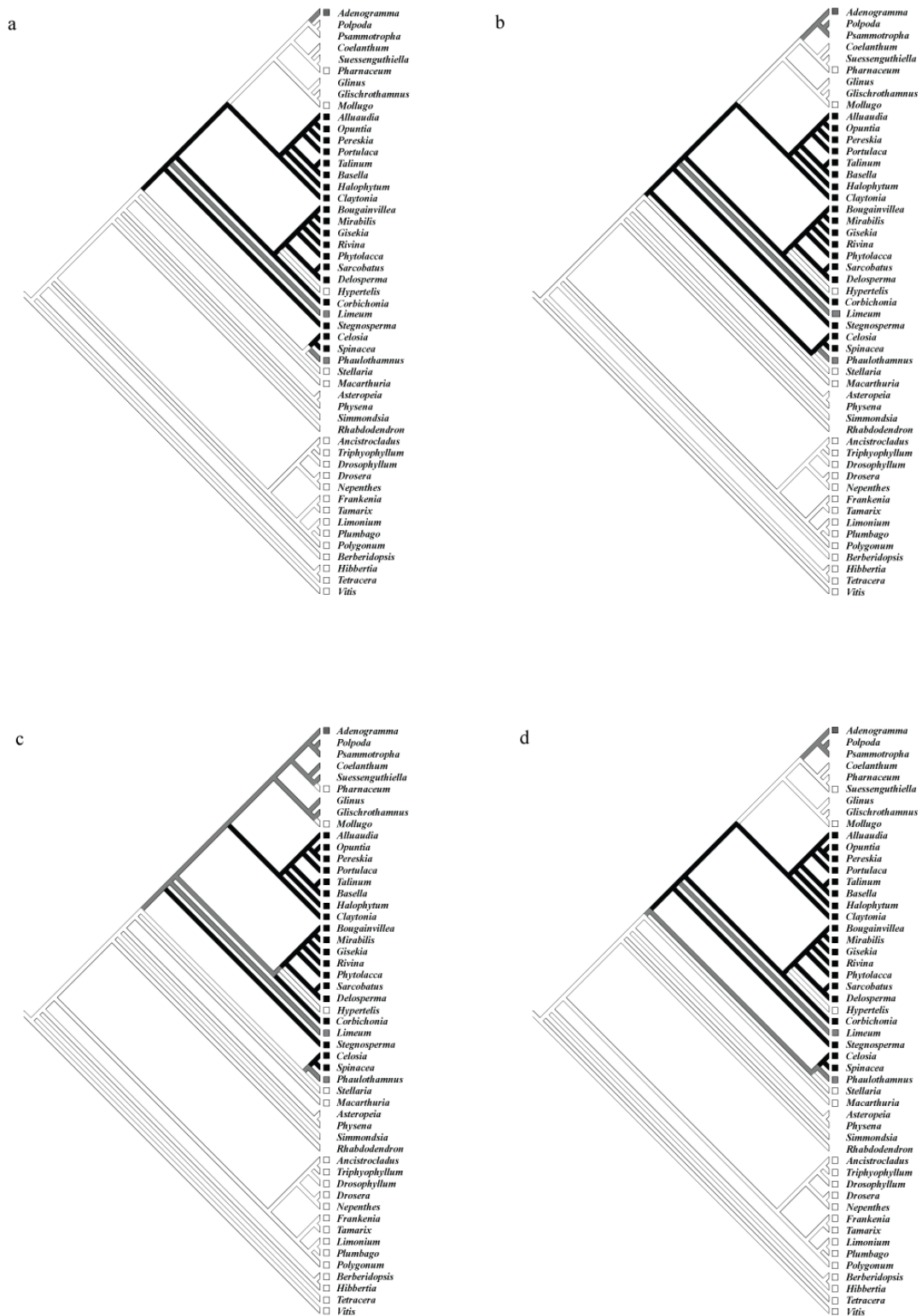


Figure 3-6. Parsimony reconstruction of pigment evolution using unordered data sets and ordered data sets: a) unordered: DELTRAN; b) unordered: ACCTRAN; c) ordered: DELTRAN; d) unordered: ACCTRAN.

Table 3-1. Summary of hypotheses historically proposed to explain the evolution of pigmentation in the Caryophyllales, with limitations of each.

Hypotheses	Proposes to Explain	Limitations
Loss of pigmentation through anemophily (Ehrendorfer, 1976)	<ul style="list-style-type: none"> ▪ Origin of betalains. ▪ Mutual exclusivity of anthocyanins and betalains. 	<ul style="list-style-type: none"> ▪ In current molecular phylogeny anthocyanic and betalain lineages are intercalated. ▪ Pigments occur in vegetative parts. ▪ Little evidence for anemophily in early diverging lineages.
Selective advantage of betalains over anthocyanins (Clement and Mabry, 1994)	<ul style="list-style-type: none"> ▪ Origin of betalains. ▪ Mutual exclusivity of anthocyanins and betalains. 	<ul style="list-style-type: none"> ▪ Little evidence for selective advantage of either betalains or anthocyanins.
Functional equivalency between pigments followed by stochastic loss (Clement and Mabry, 1994)	<ul style="list-style-type: none"> ▪ Intercalation of anthocyanic and betalain-pigmented lineages. 	<ul style="list-style-type: none"> ▪ Mutual exclusion argues against functional equivalency. ▪ Reason for stochastic loss unclear.
Inhibition of anthocyanin pathway by betalains (Stafford, 1994)	<ul style="list-style-type: none"> ▪ The mutual exclusivity of anthocyanins and betalains. 	<ul style="list-style-type: none"> ▪ Little evidence for inhibition. ▪ Hard to explain possible reversals to anthocyanin following origin of betalains.

Table 3-2. Frequencies of each transformation for four alternative reconstructions employing unordered character coding (parsimony with ACCTRAN and DELTRAN optimality, stochastic mapping with all taxa included, and stochastic mapping with taxa of unknown pigment status pruned). Transformations to betalains marked in bold.

Transformation Type	Parsimony: ACCTRAN	Parsimony: DELTRAN	Stochastic Mapping (total)	Stochastic Mapping (unknown terminals pruned)
Anthocyanin to Pigment-less	1	2	1.86	1.38
Pigment-less to Anthocyanin	0	0	1.89	1.42
Betalain to Pigment-less	2	1	3.4	2.4
Pigment-less to Betalain	0	0	1.3	0.94
Anthocyanin to Betalain	1	2	2.1	1.45
Betalain to Anthocyanin	3	2	5	2.4
Total Transformations	7	7	15.603	11.33
Total Transformations to Anthocyanin	3	2	6.89	3.82
Total Transformations to Pigment-less	3	3	5.26	3.78
Total Transformations to Betalain	1	2	3.4	2.39
Anthocyanin Dwell Time	n/a	n/a	0.548	0.5753
Pigment-less Dwell Time	n/a	n/a	0.082	0.0647
Betalain Dwell Time	n/a	n/a	0.3722	0.36

Table 3-3. Frequencies of each transformation for four alternative reconstructions employing ordered character coding (parsimony with ACCTRAN and DELTRAN optimality, stochastic mapping with all taxa included, and stochastic mapping with taxa of unknown pigment status pruned). Transformations to betalains marked in bold.

Transformation Type	Parsimony: ACCTRAN	Parsimony: DELTRAN	Stochastic Mapping (total)	Stochastic Mapping (unknown terminals pruned)
Anthocyanin to Pigment-less	2	2	4.7985	3.86
Pigment-less to Anthocyanin	1	3	8.5503	6.95
Betalain to Pigment-less	1	0	6.6034	5.14
Pigment-less to Betalain	2	5	4.7597	3.16
Anthocyanin to Betalain	0	0	0	0
Betalain to Anthocyanin	2	0	0	0
Total Transformations	8	10	24.81	19.13
Total Transformations to Anthocyanin	3	3	8.56	6.95
Total Transformations to Pigment-less	3	2	11.40	9.0
Total Transformations to Betalain	2	5	4.7597	3.16
Anthocyanin Dwell Time	n/a	n/a	0.5165	0.54
Pigment-less Dwell Time	n/a	n/a	0.1736	1.339
Betalain Dwell Time	n/a	n/a	0.3099	0.3229

Table 3-4. Voucher, citation, and GenBank accession No. for *rbcL* (Voucher information not shown for previously published sequences).

Family	Species	Voucher	Citation	Embl
Molluginaceae	<i>Adenogramma</i> sp.	Unvouchered, 11501 (K)	This Study	
Didieraceae	<i>Alluaudia ascendens</i>	-	Cuénoud et al, 2002	AY0425
Ancistrocladac	<i>Ancistrocladus korupensis</i>	-	Meimberg et al. 2001	AF31593
Asteropeiaceae	<i>Asteropeia micraster</i>	-	Cuénoud et al, 2002	AY0425
Basellaceae	<i>Basella alba</i>	-	Crawley et al, unpublished	
Berberidopsida	<i>Berberidopsis corralina</i>	-	Cuénoud et al, 2002	A042554
Nyctaginaceae	<i>Bougainvillea glabra</i>	-	Crawley et al, unpublished	
Amaranthaceae	<i>Celosia trigyna</i>	-	Muller and Borsch, 2005	AY5148
Portulacaceae	<i>Claytonia megarhiza</i>	-	O'Quinn and Hufford 2005	AY7641
Molluginaceae	<i>Coelanthum grandiflorum</i>	Thompson and Le Roux,	This Study	
Lophiocarpaceae	<i>Corbichonia decumbens</i>	-	Cuénoud et al, 2002	AY0425
Aizoaceae	<i>Delosperma cooperi</i>	-	Nyffeler 2007	DQ5584
Droseraceae	<i>Dillenia indica</i>	-	Crawley et al, unpublished	
Drosophyllaceae	<i>Drosera capensis</i>	-	Cameron et al, 2002	
Frankeniaceae	<i>Drosophyllum lusitanicum</i>	-	Muller and Borsch, 2005	AY5148
Gisekiaceae	<i>Frankenia pulverulenta</i>	-	Muller and Borsch, 2005	AY5148
Molluginaceae	<i>Gisekia africana</i>	JR Clarkson, 5499 (K)	Cuénoud et al, 2002	AY0425
Molluginaceae	<i>Glinus lotoides</i>	RM Harley, 19007 (K)	Cuénoud et al, 2002	
Halophytaceae	<i>Glischrothamnus ulei</i>	-	Cuénoud et al, 2002	AY0425
Dilleniaceae	<i>Halophytum ameghinoi</i>	-	Muller and Borsch, 2005	AY5148
Molluginaceae	<i>Hypertelis salsoloides</i>	Brockington SF, Moll 01	This study	
Limeaceae	<i>Limeum africanum</i>	-	Crawley et al, unpublished	
Plumbaginaceae	<i>Limonium latifolium</i>	-	Muller and Borsch 2005	AY5148
Nyctaginaceae	<i>Mirabilis jalapa</i>	-	Cuénoud et al, 2002	AY0426
Molluginaceae	<i>Macarthuria</i> sp.	N Bymes, 2701 (K)	This study	
Molluginaceae	<i>Mollugo verticellata</i>	-	Crawley et al, unpublished	
Nepenthaceae	<i>Nepenthes alata</i>	-	Meimberg et al. 2001	AF31589
Cactaceae	<i>Opuntia quimilo</i>	-	Nyffeler, 2002	AY0152
Cactaceae	<i>Pereskia aculeata</i>	-	Edwards, 2005	AY8753
Molluginaceae	<i>Pharnaceum</i> sp.	Unvouchered, 11503 (K)	Cuénoud et al, 2002	AY0426
Achatocarpaceae	<i>Phaulothamnus spinescens</i>	-	Muller and Borsch, 2005	AY5148
Phytolaccaceae	<i>Phytolacca americana</i>	-	Crawley et al, unpublished	
Plumbaginaceae	<i>Plumbago auriculata</i>	-	Crawley et al, unpublished	
Molluginaceae	<i>Polpoda capesis</i>	-	This study	
Polygonaceae	<i>Polygonum cespitosum</i>	J P H Acocks, 17405 (K)	Crawley et al, unpublished	
Portulacaceae	<i>Portulaca oleracea</i>	-	Edwards et al, 2005	AY8753
Molluginaceae	<i>Psammotropha myriantha</i>	-	This study	
Rhabdodendrac	<i>Rhabdodendron amazonicum</i>	Bidgood et al, 2142 (K)	Crawley et al, unpublished	
Phytolaccaceae	<i>Rivinia humulis</i>	-	Muller and Borsch 2005	AY5148
Sarcobataceae	<i>Sarcobatus vermiculatus</i>	-	Cuénoud et al. 2002	AY0426
Simmondsiaceae	<i>Simmondsia chinensis</i>	-	Muller and Borsch 2005	AY5148
Amaranthaceae	<i>Spinacia oleracea</i>	-	Schmitz-Linneweber et al.	AJ40084
Stegnospermata	<i>Stegnosperma halmifolium</i>	-	Crawley et al, unpublished	
Caryophyllaceae	<i>Stellaria media</i>	-	Fior et al. 2006	AY9326
Molluginaceae	<i>Suessenguthiella scleranthoides</i>	-	Cuénoud et al 2002	AY0426
Portulacaceae	<i>Talinum paniculatum</i>	Merxmüller and Giess,	Nyffeler 2002	AY0152
Tamaricaceae	<i>Tamarix canariensis</i>	-	Cuénoud et al 2002	AY0426
Dilleniaceae	<i>Tetracera asiatica</i>	-	Cuénoud et al. 2002	AY0426
Dioncophyllaceae	<i>Triphyphyllum peltatum</i>	-	Meimberg et al. 2001	AF31594
Vitaceae	<i>Vitis aestivalis</i>	-	Fishbein et al. 2001	AF27463

Table 3-5. Voucher, citation, and GenBank accession No. for *matK* (voucher information not shown for previously published sequences)

Family	Species	Voucher	Citation	Embl
Molluginaceae	<i>Adenogramma sp.</i>	Unvouchered, 11501 (K)	This Study	
Didieraceae	<i>Alluaudia ascendens</i>	-	Cuenoud et al, 2002	AY0425
Ancistrocladac	<i>Ancistrocladus korupensis</i>	-	Meimberg et al. 2001	AF31593
Asteropeiaceae	<i>Asteropeia micraster</i>	-	Cuenoud et al, 2002	AY0425
Basellaceae	<i>Basella alba</i>	-	Crawley et al, unpublished	
Berberidopsida	<i>Berberidopsis corralina</i>	-	Cuenoud et al, 2002	A042554
Nyctaginaceae	<i>Bougainvillea glabra</i>	-	Crawley et al, unpublished	
Amaranthaceae	<i>Celosia trigyna</i>	-	Muller and Borsch, 2005	AY5148
Portulacaceae	<i>Claytonia megarhiza</i>	-	O' Quinn and Hufford 2005	AY7641
Molluginaceae	<i>Coelanthum grandiflorum</i>	Thomspson and Le Roux,	This Study	
Lophiocarpacea	<i>Corbichonia decumbens</i>	-	Cuenoud et al, 2002	AY0425
Aizoaceae	<i>Delosperma cooperi</i>	-	Nyffeler 2007	DQ5584
Droseraceae	<i>Dillenia indica</i>	-	Crawley et al, unpublished	
Drosophyllaceae	<i>Drosophyllum capensis</i>	-	Cameron et al, 2002	
Frankeniaceae	<i>Drosophyllum lusitanicum</i>	-	Muller and Borsch, 2005	AY5148
Gisekiaceae	<i>Frankenia pulverulenta</i>	-	Muller and Borsch, 2005	AY5148
Molluginaceae	<i>Gisekia africana</i>	JR Clarkson, 5499 (K)	Cuenoud et al, 2002	AY0425
Molluginaceae	<i>Glinus lotoides</i>	RM Harley, 19007 (K)	Cuenoud et al, 2002	
Halophytaceae	<i>Glischrothamnus ulei</i>	-	Cuenoud et al, 2002	AY0425
Dilleniaceae	<i>Halophytum ameghinoi</i>	-	Muller and Borsch, 2005	AY5148
Molluginaceae	<i>Hypertelis salsoloides</i>	Brockington SF, Moll 01	This study	
Limeaceae	<i>Limeum africanum</i>	-	Crawley et al, unpublished	
Plumbaginacea	<i>Limonium latifolium</i>	-	Muller and Borsch 2005	AY5148
Nyctaginaceae	<i>Mirabilis jalapa</i>	-	Cuenoud et al, 2002	AY0426
Molluginaceae	<i>Macarthuria sp.</i>	N Byrnes, 2701 (K)	This study	
Molluginaceae	<i>Mollugo verticellata</i>	-	Crawley et al, unpublished	
Nepenthaceae	<i>Nepenthes alata</i>	-	Meimberg et al. 2001	AF31589
Cactaceae	<i>Opuntia quimilo</i>	-	Nyffeler, 2002	AY0152
Cactaceae	<i>Pereskia aculeata</i>	-	Edwards, 2005	AY8753
Molluginaceae	<i>Pharnaceum sp.</i>	Unvouchered, 11503 (K)	Cuenoud et al, 2002	AY0426
Achatocarpaceae	<i>Phaulothamnus spinescens</i>	-	Muller and Borsch, 2005	AY5148
Phytolaccaceae	<i>Phytolacca americana</i>	-	Crawley et al, unpublished	
Plumbaginacea	<i>Plumbago auriculata</i>	-	Crawley et al, unpublished	
Molluginaceae	<i>Polpoda capensis</i>	-	This study	
Polygonaceae	<i>Polygonum cespitosum</i>	J P H Acocks, 17405 (K)	Crawley et al, unpublished	
Portulacaceae	<i>Portulaca oleracea</i>	-	Edwards et al, 2005	AY8753
Molluginaceae	<i>Psammotropha myriantha</i>	-	This study	
Rhabdodendrac	<i>Rhabdodendron amazonicum</i>	Bidgood et al, 2142 (K)	Crawley et al, unpublished	
Phytolaccaceae	<i>Rivinia humulis</i>	-	Muller and Borsch 2005	AY5148
Sarcobataceae	<i>Sarcobatus vermiculatus</i>	-	Cuenoud et al. 2002	AY0426
Simmondsiaceae	<i>Simmondsia chinensis</i>	-	Muller and Borsch 2005	AY5148
Amaranthaceae	<i>Spinacia oleracea</i>	-	Schmitz-Linneweber et al.	AJ40084
Stegnospermata	<i>Stegnosperma halmifolium</i>	-	Crawley et al, unpublished	
Caryophyllaceae	<i>Stellaria media</i>	-	Fior et al. 2006	AY9326
Molluginaceae	<i>Suessenguthiella scleranthoides</i>	-	Cuenoud et al 2002	AY0426
Portulacaceae	<i>Talinum paniculatum</i>	Merxmuller and Giess,	Nyffeler 2002	AY0152
Tamaricaceae	<i>Tamarix canariensis</i>	-	Cuenoud et al 2002	AY0426
Dilleniaceae	<i>Tetracera asiatica</i>	-	Cuenoud et al. 2002	AY0426
Dioncophyllaceae	<i>Triphyophyllum peltatum</i>	-	Meimberg et al. 2001	AF31594
Vitaceae	<i>Vitis aestivalis</i>	-	Fishbein et al. 2001	AF27463

Table 3-6. The estimations of the posterior probability of ancestral characters for the ordered and unordered evolution of pigments for all nodes presented graphically in Fig. 3.

Node	Clade Description	Frequency of Clade	Un-ordered			Ordered		
			Anthocyanin	Pigment-less	Betalain	Anthocyanin	Pigment-less	Betalain
A	Caryophyllales s.l	1.0000	0.9918	0.0012	0.007	0.9953	0.0047	0
B	non-core Caryophyllales	1.0000	0.9999	0	0.0001	0.9999	0.0001	0
C	core Caryophyllales	0.7029	0.7143	0.0085	0.2772	0.6176	0.3819	0.0005
D	<i>Simmondsia</i> + core Caryophyllales	1.000	0.2162	0.0177	0.766	0.1781	0.782	0.0438
E	Asteropeiaceae/Physenaceae + core Caryophyllales	1.0000	0.0279	0.0153	0.9567	0.0125	0.9289	0.0586
F	<i>Macarthuria</i> + core Caryophyllales	1.0000	0.0163	0.0056	0.978	0.074	0.9454	0.0473
G	'CAA' clade + core Caryophyllales	0.6575	0.0006	0.017	0.9977	0.002	0.3165	0.6834
H	'CAA' clade	0.9609	0.046	0.1632	0.7908	0.0115	0.611	0.3776
I	Amaranthaceae/Achatocarpaceae	0.9998	0.0069	0.6231	0.37	0.0014	0.7947	0.2038
J	<i>Stegnosperma</i> + core Caryophyllales	1.0000	0.0001	0.0004	0.9995	0	0.0313	0.9687
K	<i>Limeum</i> + 'globuloid inclusion' clade	0.9992	0.0003	0.0014	0.9983	0	0.0222	0.9778
L	'globuloid inclusion' clade	0.9255	0.0004	0.0002	0.9994	0	0.0207	0.9793
M	'raphide' clade	1.0000	0.0006	0.0001	0.9993	0	0.0093	0.9907
N	Molluginaceae + 'succulent' clade	1.0000	0.013	0.0025	0.9845	0.0008	0.0805	0.9188
O	'succulent' clade	1.0000	0.0001	0	0.9999	0	0.0012	0.9988
P	Molluginaceae s.s.	1.0000	0.7974	0.0348	0.1678	0.4472	0.4459	0.0819

Table 3-7 Pigment coding for each terminal and sources of information used to designate characters states. Coding Strategy: Anthocyanin (0), Unpigmented (1), Betalain (2), Unknown (?).

Taxa	Character Mapping	Literature Cited
<i>Adenogramma</i>	1	Cuenound et al., 2002
<i>Alluaudia</i>	2	Clement et al., 1994
<i>Ancistrocladus</i>	?	-
<i>Asteropeia</i>	?	-
<i>Basella</i>	2	Clement et al., 1994
<i>Berberidopsis</i>	?	-
<i>Bougainvillea</i>	2	Clement et al., 1994
<i>Celosia</i>	2	Clement et al., 1994
<i>Claytonia</i>	2	Clement et al., 1994
<i>Coelanthum</i>	?	-
<i>Corbichonia</i>	2	Cuenound et al., 2002
<i>Delosperma</i>	2	Clement et al., 1994
<i>Drosera</i>	0	(Di Gregorio and Dipalma 1966)
<i>Drosophyllum</i>	?	-
<i>Frankenia</i>	0	(Beale et al. 1941)
<i>Gisekia</i>	2	Clement et al., 1994
<i>Glinus</i>	?	-
<i>Glischrothamnus</i>	?	-
<i>Halophytum</i>	2	Clement et al., 1994
<i>Hibbertia</i>	0	(Price and Sturgess 1938)
<i>Hypertelis</i>	0	Clement et al., 1994
<i>Limeum</i>	1	Clement et al., 1994
<i>Limonium</i>	0	(Price and Sturgess 1938)
<i>Macarthuria</i>	0	Clement et al., 1994
<i>Mirabilis</i>	2	Clement et al., 1994
<i>Mollugo</i>	0	Clement et al., 1994
<i>Nepenthes</i>	0	(Schaefer and Ruxton 2008)
<i>Opuntia</i>	2	Clement et al., 1994
<i>Pereskia</i>	2	Clement et al., 1994
<i>Pharnaceum</i>	0	Clement et al., 1994
<i>Phaulothamnus</i>	1	Clement et al., 1994
<i>Physena</i>	?	-
<i>Phytolacca</i>	2	Clement et al., 1994
<i>Plumbago</i>	0	(Price and Sturgess 1938)
<i>Polpoda</i>	?	Clement et al., 1994
<i>Polygonum</i>	0	(Price and Sturgess 1938)
<i>Portulaca</i>	2	Clement et al., 1994
<i>Psammotropha</i>	?	-
<i>Rhabdodendron</i>	?	-
<i>Rivina</i>	2	Clement et al., 1994
<i>Sarcobatus</i>	2	Cuenound et al., 2002
<i>Simmondsia</i>	?	-
<i>Spinacea</i>	2	Clement et al., 1994
<i>Stegnosperma</i>	2	Clement et al., 1994
<i>Stellaria</i>	0	Clement et al., 1994
<i>Talinum</i>	2	Clement et al., 1994
<i>Tamarix</i>	2	(Beale et al. 1941)
<i>Tetracera</i>	0	(Price and Sturgess 1938)
<i>Triphyophyllum</i>	?	-
<i>Vitis</i>	0	(Robinson and Robinson 1933)

CHAPTER 4

KEEP THE DNA ROLLING: MULTIPLE DISPLACEMENT AMPLIFICATION OF ARCHIVAL PLANT DNA EXTRACTS

Insufficient reserves of genomic DNA can hamper molecular phylogenetic analysis. High-throughput genetic techniques that require relatively large amounts of DNA, the difficulty in obtaining samples of taxa from remote regions, and re-sampling of limited archival DNA by repeated phylogenetic surveys can often limit the DNA available for study. To provide a possible solution to this problem, we applied Multiple Displacement Amplification (MDA) to eight archival genomic DNA extracts. The performance of MDA-treated DNA versus untreated genomic extract was evaluated by PCR amplification of three common phylogenetic markers (*psbB*, *nad7*, and ITS) across a dilution series. Generally, amplification of all three genetic markers from the MDA-treated DNA dilutions was greater than from equivalent dilutions of untreated genomic template. These results indicate that genes from all three plant genomes were amplified and that copies of the target genes *psbB*, *nad7*, and ITS were substantially increased during the MDA procedure. Sequencing of the *psbB*, *nad7*, and ITS PCR products from both the MDA-treated DNA and the untreated template was used to assess the fidelity of the MDA procedure. Sequences from the MDA-treated DNA and the untreated genomic template differed by 1.2×10^{-4} %, which is within the margin of *Taq* error. These findings emphasize the significance of Multiple Displacement Amplification for optimization of weak PCR, maintenance of depleted genetic stocks, increasing density of taxon sampling, and improving consistency between different phylogenetic analyses.

Introduction

Many plant systematists work with taxa that are rare or difficult to collect, making it difficult or impossible to obtain samples for DNA isolation. Small fragments of silica-dried material may be the only source of material for hard-to-obtain taxa. Herbarium collections and

DNA banks are therefore an invaluable source of material for phylogenetic studies and are increasingly important as a source of DNA for molecular analyses (Drabkova et al., 2002). The success of these molecular studies depends on DNA of adequate quantity and quality and yet extraction of sufficient amounts of high-quality DNA from herbarium specimens or silica-dried material can be challenging. Herbaria may limit destructive sampling of specimens in order to preserve collections relatively intact, specimens may be rare and unavailable for sampling, and the DNA of herbarium specimens may have degraded because of age or poor preservation, yielding low quantities of DNA. Furthermore, the DNA of hard-to-obtain samples is often used repeatedly in phylogenetic surveys (Chase et al., 1993; Soltis et al., 2000) and is ultimately depleted.

In recent years a number of methods have been developed for whole genome amplification that generate considerable amounts of DNA from minute quantities of starting material (Pinard et al., 2006). Rolling Circle Amplification (RCA), also known as Multiple Displacement Amplification (MDA), is a widely used method for whole genome amplification that employs a bacteriophage ϕ 29 DNA polymerase together with exonuclease-resistant degenerate primers to amplify genomic DNA isothermally at 30°C (Dean et al., 2002; Lage et al., 2003). MDA has a number of advantages over PCR-based methods of genome amplification. These include a less biased amplification of the genome, greater yields of DNA, and higher fidelity to the template DNA (Pinard et al., 2006).

The importance of genomic data in biological sciences often places considerable demand on supplies of DNA; therefore, there is interest in the use of MDA to augment stocks of low-abundance DNA (Lasken and Egholm, 2003). Several studies from a range of biological disciplines have already demonstrated the utility of MDA in the molecular analysis of rare

biological material. Examples of low-abundance biological samples that have been successfully amplified using MDA include: limited medical samples such as buccal swabs and single cell samples generated by laser capture microscopy (Lasken and Egholm, 2003), single microorganisms (Raghunathan et al., 2005), and single spores of arbuscular mycorrhizal fungi (Gadkar and Rillig, 2005). Despite these successful applications of MDA, the technique does not seem to have been widely adopted by plant systematists, although supplies of DNA may often be limited.

The aim of this study was to assess the efficacy of MDA for amplification of plant DNA extractions by amplifying and sequencing common phylogenetic markers from MDA-treated DNA. We amplified genes from each of the three plant genomes: *psbB* (plastid genome), *nad7* (mitochondrial genome), and ITS (nuclear genome) with the goal of investigating the PCR performance of MDA-treated DNA over its untreated template.

Materials and Methods

DNA Extractions from Herbarium Specimens

DNA from eight different species (table 4-1) belonging to the angiosperm order Caryophyllales was used as template for MDA. These DNA samples were extracted from materials of varying age and condition, which was reflected in the variable quality and quantity of the DNA extracted (Figure 4-1).

Multiple Displacement Amplification

DNA extracts from the eight species were amplified using the Genomiphi kit (Amersham, Piscataway, NJ, USA) according to the manufacturer's instructions. Reactions were performed using crude DNA extract. In each case, 1 μ l of crude DNA extract was combined with 9 μ l of sample buffer, heated to 95°C for 3 min, and then chilled to 4°C. To each tube, 9 μ l of reaction buffer and 1 μ l of Genomiphi enzyme mix were added, and the reactions incubated at 30°C for

16 hrs. A negative control was performed in which no input DNA was added. On completion of the MDA amplification, a 1 µl aliquot of the reaction was fractionated by electrophoresis on a 1.5% agarose gel, stained with ethidium bromide, and visualized under UV light. For comparison a 1 µl aliquot of the untreated DNA extraction was run along with its respective MDA-treated DNA.

PCR

Untreated DNA extract and MDA-treated DNA were both serially diluted: 1:5, 1:10, 1:100, and 1:200. To assess the value of MDA-treated DNA versus untreated DNA extract, PCR was performed across this dilution series. Gene regions from the three plant genomes were amplified: *psbB*, *nad7*, and ITS. Amplification and sequencing was performed in accordance with previously published protocols (Soltis et al., 2000). *psbB* was amplified according to previously published protocols (Soltis et al., 2000) (95°C for 3min, followed by 30-35 cycles of 94°C for 30 sec, 50°C for 30 sec, and 72°C for 1 min with a final extension time of 7 min at 72°C) using primers 60F (ATG GGT TTG CCT TGG TAT CGT GTT CAT AC] and 66R (CCA AAA GTR AAC CAA CCC CTT GGA C) (Graham and Olmstead, 2000), which amplify 1362 bp between positions 1 and 1362 (inclusive) of *psbB*. *nad7* was amplified (95°C for 2 min, followed by 30 cycles of 94°C for 30 sec, 50°C for 30 sec, and 72°C for 1 min with a final extension time of 7 min at 72°C) using primers nad7/2 (GCT TTA CCT TAT TCT GAT CG) and nad7/3 (TGT TCT TGG GCC ATC ATA GA) (Duminil et al., 2002) which amplify ~ 1000 bp product. ITS was amplified (95°C for 2 min, followed by 5 cycles of 94°C for 30sec, 53°C for 30 sec, and 72°C for 1 min with a step down to 28 cycles of 94°C for 30 sec, 48°C for 30 sec, and 72°C for 1 min) using primers ITSA (GGA AGG AGA AGT CGT AAC AAG G) and ITSB (CTT TTC CTC CGC TTA TTG ATA TG) (Blattner, 1999) which amplify a 650-700 bp

product. The PCR products were fractionated by electrophoresis on a 1.5% agarose gel, stained with ethidium bromide, and visualized under UV light.

PCR Cleanup and Sequencing

To remove unused primers and nucleotides, PCR product was treated with ExoSAP-IT (USB Corporation, Cleveland, OH). All PCR products were sequenced using the same primers as for the PCR with the exception of the *psbB* products, which were sequenced using nested primers B60F (CAT ACA GCT CTA GTT KCT GGT TGG) and B66R (CCC CTT GGA CTR CTA CGA AAA ACA CC) (Graham and Olmstead, 2000). Sequencing was performed on the Applied Biosystems 3730xl capillary DNA sequencer. Raw data signals were automatically base-called and subsequently manually checked using Sequencher 4.2 (Gene Codes Corporation, Ann Arbor, MI, USA). Sequences were aligned using Se-Al (Department of Zoology, Oxford, UK). The sequences generated by this study have been submitted to Genbank: EU410352-EU410375

Results

Multiple Displacement Amplification

MDA on all eight DNA extracts resulted in an increase in high-molecular-weight DNA (10-11Kb) relative to the template DNA (Figure 4-1). This increase in high-molecular-weight DNA is especially apparent for *Mollugo verticillata* and *Mirabilis jalapa* from which either very little or highly degraded DNA was initially extracted. An amplification product also occurs in the negative control. This is expected when using the Genomiphi kit and is most likely due to the non-specific amplification of degenerate hexamer primers rather than to DNA contamination (Amersham Biosciences, Protocol 74004229). The presence of this amplification product in the no-template control, however, prevents immediate evaluation of the success of MDA in specifically amplifying herbarium DNA. PCR was therefore performed to evaluate the utility of the MDA-treated DNA.

PCR

Amplification of *psbB* gene was initially performed on a 1:25 dilution of the MDA-treated DNA. All 8 MDA-treated DNAs generated a strong amplification product of the expected size (results not shown). PCR performed on the no-template MDA control product did not generate the expected amplification product, demonstrating that the amplification products from PCR of MDA-treated DNA were not due to spurious amplification during the MDA procedure.

To assess the effectiveness of the MDA-treated DNA versus the original DNA template, amplification of *psbB*, *nad7*, and ITS was performed across a dilution series. Reactions contained 0.2, 0.1, 0.01, or 0.005 μ l of either the untreated genomic template or its MDA-treated equivalent. As a general trend, for all species and at all dilutions, the MDA-treated product generated a similar or stronger PCR amplification than the corresponding genomic template (Figure 4-2). This is particularly apparent for the amplification of *psbB*, *nad7* and ITS from *M. verticillata* and *M. jalapa* (Figure 4-2). Differences between dilutions for the amplification of ITS are less striking but still discernable. For all DNA regions however, it is most informative to compare the 1:5 and 1:10 MDA-treated dilution with the respective 1:100 and 1:200 dilutions of the untreated genomic template. This is an appropriate comparison because the MDA procedure effectively dilutes the initial genomic template by 1:20 (1 μ l of template in a 20 μ l MDA reaction) and thus following further dilution, the 1:5 (M1) and 1:100 (G3), and 1:10 (M2) and 1:200 (G4) represent equivalent dilutions of the initial genomic stock. Amplifications from the 1:5 and 1:10 dilutions of MDA-treated DNA are without exception considerably stronger than their respective 1:100 and 1:200 dilutions of genomic DNA across all 8 species for all three genes (for example see Figure 4-2)).

Sequencing

PCR products from the untreated DNA and corresponding MDA-treated DNA were sequenced to ensure that the amplifications were not due to spurious DNA amplified during the MDA procedure. In all cases, the sequences from untreated and MDA-treated DNA were nearly identical with a difference of only 1.2×10^{-4} %. These differences are within the margin of *Taq* error, demonstrating that no contamination had occurred during the MDA procedure and that replication of DNA in the MDA treatment had been of high fidelity.

Discussion

Phylogenetic studies of plants are based on ever-increasing portions of the nuclear, mitochondrial, and plastid genomes and utilize high-throughput sequencing technology that can often exhaust reserves of DNA. Archived collections of DNA can gradually degrade with use and age and may be difficult to replenish or restore. Collaborative projects rely on the same samples for genetic analysis, yet limited stocks of archival DNA force participating laboratories to exchange minute quantities of DNA. Increased taxon sampling in molecular phylogenetics has created a demand for DNA from difficult-to-obtain species and DNA from these hard-to-obtain species is often available in only limited amounts. For these reasons, DNA is often a limiting resource in molecular phylogenetic analyses.

Strong initial amplification of the *psbB* gene from MDA-treated DNA suggested that template DNA was successfully replicated during the MDA procedure. Comparisons of *psbB*, *nad7*, and ITS amplification across dilutions of untreated and MDA-treated DNA confirmed that amplification was generally greater from MDA-treated DNA than from the original template (Figure 4-2). This was particularly apparent in the amplification of the *psbB* and *nad7* genes; however, differences in the amplification of ITS from MDA-treated DNA versus genomic DNA, though present, were less distinct. This might be due to the efficiency of the ITS amplification

protocol and to the high abundance of the 18S rDNA template in the genomic extract.

Nonetheless, the generally increased amplification from MDA-treated DNA indicates that copies of the target genes *psbB*, *nad7*, and ITS were substantially increased during the MDA reaction as all three genomes were amplified during the MDA procedure. This enhanced amplification suggests that MDA could be a rapid and efficient procedure for the optimization of PCR for genes that weakly amplify from the original template. The comparisons of 1:5 (MDA-treated) with 1:100 (untreated genomic), and 1:10 (MDA-treated) with 1:200 (untreated genomic) dilutions revealed dramatic increases in amplification from MDA-treated DNA. A relatively small investment of 1 μ l of genomic DNA generates 20 μ l of MDA-treated DNA, and improved subsequent PCR of the genes of interest. This illustrates the value of MDA for the augmentation of depleted DNA stocks. Sequencing of the PCR products confirmed that MDA replicated the genomic template with a high degree of fidelity as expected from previous studies that have more rigorously assessed the fidelity of the ϕ 29 DNA polymerase (Pinard et al., 2006).

These findings demonstrate that Multiple Displacement Amplification is a useful procedure for pre-amplification of precious archival DNA prior to subsequent genetic analysis. Pretreatment by MDA enhanced amplification of all three molecular markers from the three plant genomes, while maintaining fidelity to the original template sequence. MDA therefore offers a way to alleviate problems of depleted DNA stocks and help to maintain DNA “standards” to ensure sampling consistency among phylogenetic studies. Multiple rounds of MDA may even be feasible ensuring almost “infinite” supplies of DNA (Sato et al., 2005).

It is important to note that all the DNA extracts utilized in this study studies were of sufficient quality to amplify the phylogenetic markers from the genomic extract prior to MDA treatment. Successful MDA requires the input of good quality DNA and thus it is not clear that

this procedure would permit the augmentation of severely degraded DNA stocks. In our experience, poor quality DNA derived from very old or poorly preserved herbarium material may not be an appropriate substrate for MDA (data not shown). Furthermore, MDA enzymes, as in PCR, may be susceptible to inhibitory substances that can be present in extracted DNA. These limitations mean that the usefulness of MDA must be determined empirically, taking into account the quality of the extracted DNA and its performance in PCR prior to MDA treatment. We have observed that if successful PCR has been performed on a DNA extract, MDA is also likely to perform well. Despite these final cautionary comments, this approach still provides a cheap and efficient method for enhancing and maintaining minute DNA stocks from numerous invaluable museum collections worldwide.

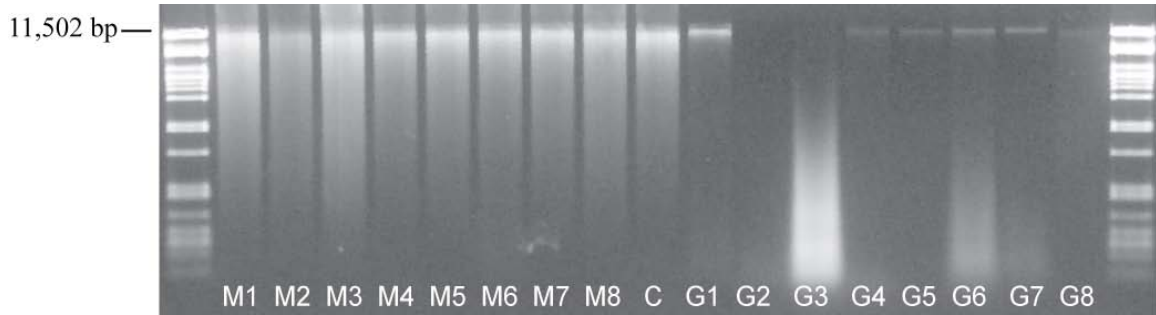


Figure 4-1. MDA-treated reaction products (M1-8) and corresponding untreated genomic equivalent (G1-8). M1 & G1: *H. ameghinoi*; M2 & G2: *M. verticillata*; M3 & G3 : *M. jalapa*; M4 & G4: *D. capensis*; M5 & G5: *L. arborescens*; M6 & G6: *T.paniculatum*; M7 & G7: *P.virginianum*; M8 & G8: *R. amazonicum*. C: the control MDA reaction to which no genomic template was added. L: 1 DNA/ Pst1 (MBI Fermentas Inc, Hanover, NH, USA)

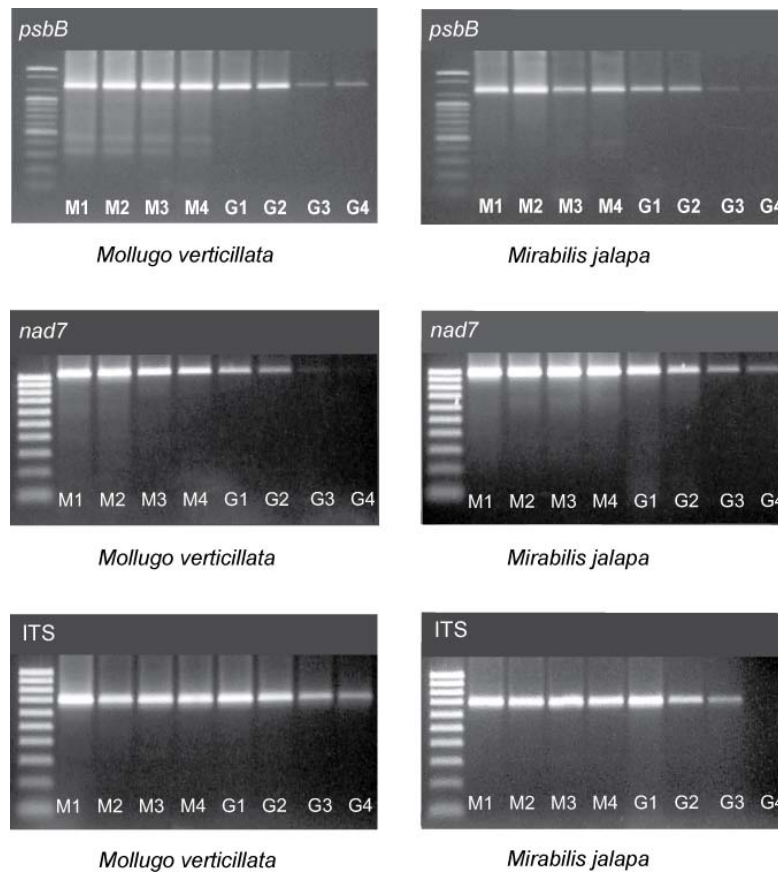


Figure 4-2. Amplification of 1363 bp fragment of *psbB*, fragment of *nad7* gene, fragment of ITS for two of the eight species, *Mollugo verticillata* and *Mirabilis jalapa*. Amplifications across dilution gradient of MDA-treated template (1:5; M1, 1:10; M2, 1:100; M3, 1:200; M4) and untreated genomic template (1:5; G1, 1:10; G2, 1:100; G3, 1:200; G4). 100bp ladder (Bioneer, Alameda, CA, USA).

Table 4-1. Species of Caryophyllales used in this study: family, source, collection date, accession number and DNA extraction method.

Species	Family	Voucher	Date of Collection	Extraction Method
<i>Halophytum ameghinoi</i>	Halophytaceae	Tortosa et al. s.n K	1997	CTAB
<i>Mollugo verticillata</i>	Molluginaceae	Moore 321 FLAS	2006	DNAeasy
<i>Mirabilis jalapa</i>	Nyctaginaceae	Soltis 2638 FLAS	2004	CTAB
<i>Drosera capensis</i>	Droseraceae	Moore 267 FLAS	2006	DNAeasy
<i>Limmonium arborescens</i>	Plumbaginaceae	Chase 1649 K	Uncertain	CTAB
<i>Talinum paniculatum</i>	Portulaccaceae	Soltis 2646 FLAS	2004	CTAB
<i>Polygonum virginicum</i>	Polygonaceae	Soltis 2656 FLAS	2005	DNAeasy
<i>Rhabdodendron amazonicum</i>	Rhabdodendraceae	E. Ribéiro 1187 K	1993	CTAB

CHAPTER 5
PHYLOGENY OF MADS-BOX GENE LINEAGES IN AIZOACEAE (CARYOPHYLLALES)

Introduction

The family of MADS-box genes (for *MCMI*, *AGAMOUS*, *DEFICIENS* and *SRF*; Sommer et al., 1990) encodes transcription factors that play important roles in developmental processes across eukaryotes (Theissen et al., 2000). MADS-box genes have been the focus of particular interest in plants because of notable gene diversification together with the involvement of MADS-box genes in the development of evolutionarily significant traits, particularly in the context of the flower. Describing the diversification of MADS-box genes (in particular the MIKC-type lineage; Alvarez-Buylla et al., 2000) in relation to the radiation and morphological evolution of land plants is a major theme in the field of plant evolutionary development (Becker and Theissen, 2003; Theissen et al., 2000).

The MIKC lineage of MADS-box genes is characterized by the presence of four distinct protein domains: M - MADS; I - Intervening; K- Keratin-like; and C - C-terminus (Alvarez-Buylla et al., 2000). The highly conserved MADS domain at the N-terminus contains the CArG elements that are essential for DNA binding and plays a role in protein dimerization (Norman et al., 1988; Pollock and Treisman, 1991). The Intervening and Keratin-like domains are important in mediating dimerization and influence the specificity of interaction between MADS-box proteins (Krizek and Meyerowitz, 1996; Pnueli et al., 1991; Riechmann et al., 1996). The C-terminus is highly variable at the sequence level but short, conserved and lineage-specific motifs have been identified in the C-termini of many clades of MADS-box genes. Recent evidence suggests that the C-terminus may contribute to the formation of higher-order protein complexes between dimers of MIKC-type proteins (Egea-Cortines et al., 1999).

MIKC Genes and ABCDE Functions in Floral Organ Identity

The MIKC-type genes have become a focus for studies in evolution of development largely due to their role in specifying floral organ identity, underpinning the conceptual framework of the ABC model. On the basis of floral homeotic mutants (Bowman et al., 1989; Carpenter and Coen, 1990; Komaki et al., 1988), the ABC model proposed that the identity of the four concentric whorls of floral organs in *Arabidopsis thaliana* is determined by the combinatorial activity of three functional classes of gene activity (Bowman et al., 1991; Coen and Meyerowitz, 1991; Meyerowitz et al., 1991). A-function alone specifies sepal identity; A-function in combination with B-function specifies petal identity; B-function together with C-function specifies stamen identity; and C-function alone specifies Carpel identity (Coen and Meyerowitz, 1991). MIKC genes were identified as the key genetic components underlying homeotic mutant phenotypes and defining the A, B, and C functional classes of gene activity. For example in *Arabidopsis thaliana*, the *APETALA1* (*API*) locus is involved in determining sepal identity (A-function) (Irish and Sussex, 1990), the paralogous loci *PISTILLATA* (*PI*) and *APETALA3* (*AP3*) are involved in petal and stamen identity (B-function) (Goto and Meyerowitz, 1994; Jack et al., 1992; Jack et al., 1994) and the *AGAMOUS* (*AG*) locus is involved in determining stamen and carpel identity (C-function) (Mizukami and Ma, 1992; Yanofsky et al., 1990). Parallel studies in *Antirrhinum majus* demonstrated that *DEFICIENS* (*DEF*) and *GLOBOSA* (*GLO*) (orthologs of *PI* and *AP3*) specify B-function (Sommer et al., 1990; Trobner et al., 1992); additionally a paralog of *AGAMOUS*, the *PLENA* (*PLE*) locus, specifies C-function in *A. majus* (Bradley et al., 1993). Subsequent studies in *A. thaliana* identified MIKC-type genes such as *SEEDSTICK* (*STK*) together with homologs in other organisms (e.g. *FLORAL BINDING PROTEIN 7* and *11* in *Petunia hybrida*) that are involved in specifying ovule identity (D-function) (Angenent et al., 1995; Favaro et al., 2003; Pinyopich et al., 2003). A fifth functional

class (E-function) is represented in *A. thaliana* by the *AGL2*, 3, 4, 9 genes (also referred to as *SEPALLATA* genes), which are required for specification of all floral organ identities (Pelaz et al., 2000); a similar function for *SEPALLATA* homologs has been demonstrated in *P. hybrida* (Vandenbussche et al., 2003).

Functional analyses of MIKC-type genes in a broad range angiosperm taxa (e.g. *Arabidopsis*, *Antirrhinum*, *Petunia*, *Gerbera*, *Lycopersicon*, *Papaver* and *Oryza*), together with expression-based studies in basal eudicots (Ranunculales), magnoliids, and early-diverging angiosperms (the ANITA grade) have established that homologs of the above ABCDE function MIKC-type genes play an important and conserved role in floral development across all angiosperms (reviewed in Irish, 2003; Ng and Yanofsky, 2001; Theissen et al., 2000; Irish and Kramer, 1998).

Phylogenetic Analyses Reveal the Evolutionary History of MIKC-type Genes

The evolutionary history of the MIKC-type genes is characterized by repeated duplications and divergence that have occurred throughout the evolution of angiosperms. The pervasive nature of these events ensures that comparative studies of MADS-box gene expression and function in relation to the evolution of morphological structures in different organisms require a comprehensive phylogenetic understanding of the MIKC-type gene family (Becker and Theissen, 2003; Jaramillo and Kramer, 2007; Litt and Irish, 2003). Phylogenetic analysis is used to identify clades of MIKC-type genes and identify orthology (homology through speciation) vs paralogy (homology through duplication) of MIKC-type genes isolated from different organismal lineages.

To date, numerous phylogenetic analyses have been conducted on those MIKC-type gene lineages containing homologs of genes that have been assigned to the ABCDE functions of floral organ identity in *Arabidopsis thaliana* and *Antirrhinum majus*. Here the main findings of these

studies are summarized largely to define expectations of the MIKC gene complement in the core eudicot lineage Caryophyllales, but also to highlight the potential role of gene duplication in the evolution of morphological variation. In summarizing these phylogenetic studies the MIKC-type gene complement and nomenclature of model organism *A. thaliana* is employed as a reference.

Phylogeny of A-Function MIKC-type Genes

The *API* (A-function) gene has three closely related genes in *A. thaliana*: *AGAMOUS-LIKE 79* (*AGL79*), *FRUITFUL* (*FUL*) and *CAULIFLOWER* (*CAL*). *CAL* and *API* have been shown to be the product of a recent Brassicaceae-specific duplication (Litt and Irish, 2003); however, *AGL79*, *FUL* and the inferred ancestor of *API* and *CAL* are representatives of ancient duplications that occurred prior to the origin of core eudicots (Litt and Irish, 2003; Shan et al., 2007). Phylogenetic analyses of homologs isolated across angiosperms indicate that, as a whole, early-diverging lineages of angiosperms possessed a single *API* homolog (excluding lineage-specific duplications in e.g. *Magnolia* and *Peperomia*), however these genes have been termed ‘*FUL*-like’ due to their sequence similarity with the *FUL* locus in *A. thaliana* (Litt and Irish, 2003). The ancestral *FUL*-like lineage has undergone several duplication events associated with the radiation of major angiosperm lineages: a single duplication within the Ranunculales (Litt and Irish, 2003); one duplication within the monocots and one duplication at the base of the monocots (Preston and Kellogg, 2006); and two duplications at the base of the core eudicots (Litt and Irish, 2003; Shan et al., 2007). As a result of these last eudicot-specific two duplications, core eudicots tend to exhibit three paralogs of the original *FUL*-like lineage: the euAP1 lineage (containing the *API* locus), the euFUL lineage (containing the *FUL* locus) and the euFUL-like or *AGL79* lineage (containing the *AGL79* locus) (Litt and Irish, 2003; Shan et al., 2007).

B-Function MIKC-type Genes

Kramer et al. (1998) was the first phylogenetic analysis to clearly demonstrate the complexity of MIKC gene evolution in angiosperms. In *A. thaliana* two MIKC genes, *AP3* and *PI*, have been ascribed to B-function. However isolation and phylogenetic isolation of homologs from a range of eudicot, magnoliid, and basal angiosperm taxa has revealed a complicated history of gene duplication, together with gene loss (Kim et al., 2004; Kramer et al., 1998). The *AP3* and *PI* paralogs are probably present in all extant angiosperms and are representatives of an ancient duplication that preceded the emergence of the earliest extant angiosperm *Amborella* (Kim et al., 2004). The *PI* lineage has also undergone additional duplication events for example the many recent duplications in Ranunculaceae (Kramer et al., 2003) The *AP3* lineage has undergone numerous further duplications; again in the Ranunculales (giving rise to three paralogous lineages (Kramer et al., 2003) but also at the base of the core eudicots giving rise to two paralogous lineages, termed eu*AP3* (containing the *AP3* locus) and *TM6* (named after the *TM6* locus in *Lycopersicon*, Kramer et al., 1998). The *TM6* paralog appears to have been lost in the model organisms *A. thaliana* and *A. majus* but is present in many core eudicots and thus constitutes a major eudicot gene lineage. The eudicot-specific duplications in the *AP3* lineage ensure that three major paralogous B-function gene lineages are present in core eudicots: the eu*AP3* lineage, the *PI* lineage and the *TM6* lineage (Kramer et al., 1998).

C and D-Function MIKC-type Genes

In *Arabidopsis* the *AGAMOUS* subfamily of MIKC-type genes is represented by four paralogs *AGAMOUS* (*AG*), *SHATTERPROOF 1* and *2* (*SHP 1* and *2*), and *SEEDSTICK* (*STK*). *AG* and *STK* are representatives of an ancient duplication that preceded the last common ancestor of the angiosperms (Kramer et al., 2004; Zahn et al., 2006). This duplication led to two major lineages of *AGAMOUS* genes in angiosperms termed the *AG* lineage and the *AGL11* lineage (a

synonym of *STK*) (Zahn et al., 2006). The *AG* lineage is largely involved in specifying C-function while the *AG11* lineage tends to be restricted to ovule development (D-function) (Kramer et al., 2004; Zahn et al., 2006). Within the *AG* lineage, further duplications have occurred within the monocots, the Ranunculaceae and within the eudicots. The *AG* lineage duplication within or at the base of the eudicots has generated two subsequent lineages, the eu*AG* lineage and eu*PLENA* (*PLE*) lineage (named after the *PLENA* locus in *A. majus*). Due to uncertainty over deep level relationships within the core eudicots and poor taxon sampling of the *AGAMOUS* lineages, it is currently not clear where this duplication took place. This duplication may have arisen at the base of the rosid and asterid clades as only members of the rosid and asterid lineages possess both homologs of the *AG* and *PLE* lineages (Kramer et al., 2004; Zahn et al., 2006). However, Kramer EM reports a possible *PLE* homolog in *Gunnera* suggesting that this duplication may have arisen earlier at the base of the core eudicots (pers.comm). *SHPI* and *SHPI2* from *A. thaliana* belong to the *PLE* lineage but the presence of two loci in *A. thaliana* suggests a recent duplication perhaps specific to *Arabidopsis* (Kramer et al., 2004; Zahn et al., 2006). Core eudicots may be expected to have a minimum of two *AG* paralogs belonging to the eu*AG* lineage (containing the *AG* lineage) and the *AGL11* (containing the *STK* locus). Depending on the precise timing of the eu*AG*/eu*PLE* duplication, core eudicots may be expected to possess a third paralog from the *PLE* lineage (containing the *SHPI* and 2 loci).

E-function MIKC-type Genes

In *A. thaliana* the *SEPALLATA* (*SEP*) subfamily of MIKC-type genes is represented by four loci, *AGAMOUS*-like (*AGL*) 2, 3, 4, and 9 (also named *SEPALLATA* 1, 4, 2, and 3 respectively) (Ditta et al., 2004; Pelaz et al., 2000). These four paralogs are representatives of several duplication events (Zahn et al., 2005). The first duplication prior to the emergence of extant angiosperms gave rise to two distinct lineages, the *AGL9* and *AGL2/3/4* lineages (Zahn et

al., 2005). These lineages have subsequently undergone additional duplication in association with the radiation of major angiosperm lineages. The *AGL2/3/4* lineage has undergone two major duplications in monocot lineages (Malcomber and Kellogg, 2005) with a further two duplications within the core eudicots (Zahn et al., 2005). The core eudicot-specific duplications of the *AGL2/3/4* lineage have given rise to three lineages: the *AGL2* lineage (containing the *AGL2* and *AGL4* loci); the *FBP9* lineage (named after the representative locus isolated from *Petunia hybrida* - the *FBP9* paralog appears to have been lost in *A. thaliana*); and the *AGL3* lineage (containing the *AGL3* locus). The *AGL9* lineage has undergone duplication within the monocots (Malcomber and Kellogg, 2005) and a further possible duplication within the core eudicots, although both paralogs from this putative core eudicot duplication have been isolated only from asterid lineages. Core eudicots can be expected to possess representatives of up to five paralogous *SEP* gene lineages including three homologs of the *AGL2*-, *FBP9*-, *AGL3* lineage, and up to two homologs from the *AGL9* lineage (Zahn et al., 2006).

Duplications in Association with Morphological Variation and Novelty

Gene duplication is an important phenomenon for studies in evolutionary development due to the potential of paralogs to acquire altered gene functions that might contribute to altered or novel morphology. Three basic models have been proposed to account for the potential consequences of a gene duplication event. The ‘pseudogenization’ model argues that if paralogs remain completely redundant in function, they will not be selectively maintained over evolutionary time, and thus one paralog will rapidly accumulate deleterious mutations and subsequently be lost. The second model, ‘sub-functionalization’, argues that given the often-modular nature of protein structure and/or function, paralogs could be selectively maintained if the various functions of the ancestral homolog were parsed out between its descendent paralogs. In the third model, ‘neofunctionalization’, one of the two paralogs derived from a duplication

event would retain the function of the ancestral homolog while the second would acquire a novel function, again resulting in the selective maintenance of both copies. Although there is evidence for all these potentialities with respect to the evolution of MIKC-type genes, here, a case study of potential neo-functionalization in the Ranunculales is briefly reviewed.

As previously highlighted, there have been several duplications in the *AP3* and *PI* lineages within the Ranunculales (Kramer et al., 2003). Kramer et al. (2007) investigated the evolution of three *AP3* (*AqvAP3-1*, *-2* and *-3*) paralogs and the *AqvPI* homolog in connection to the evolution of novel staminodial organs in *Aquilegia*. The staminodia in *Aquilegia* are considered derived from stamens on the basis of their early ontogeny and their positional homology to stamens in other genera of Ranunculales. The stamens and staminodia in *Aquilegia* share similar expression patterns of *AqvAP3-1*, *AqvAP3-2*, and *AqvPI* early in development, perhaps reflecting the derivation of the staminodia from stamens. Subsequently, however, different *AP3* paralogs are expressed in the stamens and staminodia, with *AqvAP3-2* maintained in the stamens and *AqvAP3-1* in staminodia (Kramer et al., 2007). This partitioning of expression of *AP3* paralogs in association with the evolution of a novel floral organ may signify a neofunctionalization event in which the *AqvAP3-1* paralog has evolved to specify an alternative floral morphology.

This case study from the Ranunculales sets a precedent for investigating instances of perianth differentiation in the core Caryophyllales. In Chapter 2 several instances of perianth differentiation derived from a uniseriate undifferentiated condition were identified in the core Caryophyllales. Several of these differentiated perianths are inferred to have evolved through the recruitment and modification of androecial organs (Caryophyllaceae, *Glinus*, *Corbichonia*, and Aizoaceae) to generate novel floral organs in similar manner to that envisaged in Ranunculales. Given the similar pattern of modification of androecial-derived organs it is reasonable to ask

whether the emergence of these novel structures is associated with similar gene duplication events in the MIKC-type homologs that are implicated in the ABCDE functions of floral development.

Here, the evolution of MIKC-type homologs is investigated in the lineage Aizoaceae, a lineage of Caryophyllales, in which petaloid organs are thought to have arisen through sterilization and modification of stamens. The two early-diverging subfamilies within Aizoaceae, Sesuvioideae and Tetragonoideae, lack petaloid staminodes and form a grade leading to a monophyletic clade containing the subfamilies Mesembryanthemoideae and Ruschoideae, both of which possess petaloid staminodes. Our hypothesis is that, if duplication in ABCDE MIKC-type genes is involved in the emergence of petaloid staminodes, these duplication events should coincide with the origin of the Ruschoideae and Mesembryanthemoideae lineages. These duplication events would be detectable by an increase in the MIKC-type gene complement in these derived sub-families, with the presence of additional paralogs. The focus here is primarily the evolution of those MIKC-type genes that contribute to the ABC functions of floral organ identity although the methodology used ensures that homologs underlying D and E functions are also recovered, as are MIKC-type genes from a wide range of additional gene families.

Methods

Taxon Sampling

The species sampled included five species of Aizoaceae (core Caryophyllales) representing the four sub families in Aizoaceae: *Sesuvium portulacastrum* (Sesuvioideae), *Tetragonia teragonoides* (Aizooideae), *Mesembryanthemum crystallinum* and *Mesembryanthemum cordifolia* (Mesembryanthemoideae) and *Delosperma napiforme* (Ruschoideae). Two additional species of Caryophyllales were also included: *Antigonon leptopus* (Polygonaceae: non-core Caryophyllales) and *Portulaca grandiflora* (Portulacaceae: core Caryophyllales).

RNA Isolation and Gene Amplification

Total RNA was extracted from floral buds of various stages of development using the RNeasy extraction kit (Qiagen, Carlsbad, California, USA). cDNA was synthesized using Superscript II (Invitrogen, Carlsbad, USA) according to the manufacturer's instructions. Amplification of target genes was carried out using degenerate primers from previously published studies (A-function MIKC: Litt and Irish, 2003), B-function MIKC: Kramer et al., 1998), C-function MIKC: Stellari et al., 2004), using degenerate PCR thermocycling conditions. PCR bands over 500 bp in size were excised from the agarose gel and purified using the GeneClean II Kit (Q-Bio Gene, Carlsbad, California, USA). Purified DNAs were cloned using the TOPO TA Cloning Kit (Invitrogen). Plasmid DNAs were amplified using the TempliPhi Cycle (Amersham, Piscataway, NJ, USA) and sequences were generated on an ABI 3730 XL DNA sequencer (Applied Biosystems, Inc., Fullerton, CA, USA) following the manufacturer's protocol.

Alignments

Newly isolated genes were identified by distinctive C-terminal motifs or subject to a BLAST search to preliminarily assign them to a given clade within the MADS-box gene family. New sequences were then automatically aligned by predicted amino acid sequence using Clustal X (Thompson et al., 1997) with previously published sequences representing all major clades of MIKC genes. RevTrans 1.4 (<http://www.cbs.dtu.dk/services/RevTrans/>) was employed to generate a corresponding codon-aligned DNA alignment. This codon-aligned DNA dataset was analysed under the maximum likelihood (ML) criterion (see method section - phylogenetic analyses).

On the basis of this preliminary phylogenetic analysis distinct clades or monophyletic groups of clades that contained newly isolated sequences were separated into different

alignments to be further analyzed separately. Additional previously published sequences that shared affinity to these clades (based on BLAST results and previously published phylogenetic analyses) were added to increase taxon sampling in each separate alignment. Within each group, sequences were automatically aligned by predicted amino acid sequence using Clustal X (Thompson et al., 1997). RevTrans 1.4 was employed to generate a corresponding codon-aligned DNA alignment.

These separate alignments with their included gene lineages were as follows: A-function (*APETALA1*, *FRUITFUL* and *FRUITFUL*-like homologs); B function (*APETALA3*, *TM6*, *PISTILLATA* and B-sister lineages), C- and D-function (*AGAMOUS* and *AGAMOUS-like 11* lineages); E-function (*SEPALLATA* gene lineages). For each group the DNA partition was subjected to phylogenetic reconstruction by maximum parsimony (MP), maximum likelihood (ML) and Bayesian analyses.

Phylogenetic Analyses

MP analyses were implemented in PAUP*4.0 (Swofford, 2000). Shortest trees were obtained using a heuristic search and 1,000 replicates of random taxon addition with tree-bisection-reconnection (TBR) branch swapping, saving all shortest trees per replicate. Bootstrap support (BS) for relationships (Felsenstein, 1985) was estimated from 1,000 bootstrap replicates using 10 random taxon additions per replicate, with TBR branch swapping and saving all trees.

For ML analyses we employed the program GARLI (Genetic Algorithm for Rapid Likelihood Inference; version 0.942) (Zwickl, 2000). GARLI conducts ML heuristic phylogenetic searches under the GTR model of nucleotide substitution, in addition to models that incorporate among-site rate variation, either assuming a gamma distribution (Γ) or a proportion of invariable sites (I), or both. Models of nucleotide substitution were determined using

MrModeltest (Nylander, 2004). The Akaike information criterion (AIC) was used to select GTR+I+G as an appropriate model based on the relative informational distance between the ranked models. Analyses were run with default options, except that the “significanttopchange” parameter was reduced to 0.01 to make searches more stringent. ML bootstrap analyses were conducted with the default parameters and 100 replicates. We performed a strict consensus of five replicate GARLI analyses and topological differences resulting in collapsed nodes were annotated on the representative ML tree.

Models of nucleotide substitution were determined using MrModeltest (Nylander, 2004). The Akaike information criterion (AIC) was used to select GTR+I+G as an appropriate model based on the relative informational distance between the ranked models. Bayesian analyses were implemented in MrBayes, version 3.1.2 (Huelsenbeck and Ronquist, 2001; Ronquist and Huelsenbeck, 2003). Two independent analyses each ran for 5 million generations, using four Markov chains, and with all other parameters at default values; trees were sampled every thousandth generation, with a burn-in of 200,000 generations. Stationarity of the Markov Monte Carlo chain was determined by the average standard deviation of split frequencies between runs (after 5 million generations the average standard deviation was 0.004%) and by examination of the posterior in Tracer, version 1.3 (Rambaut and Drummond, 2003). A majority-rule consensus of post burn-in trees was generated in PAUP*4.0 (Swofford, 2000), using the resulting posterior distribution of the trees.

Results and Discussion

Caryophyllid MIKC Complement

ML analysis of the ‘all MIKC’ data set revealed that 50 distinct MIKC-type loci representing ten major clades of MADS-box genes had been isolated from seven previously unrepresented taxa within the Caryophyllales (Figure 5-1). Almost all major lineages of the

ABCDE MIKC-type gene lineages are represented by these caryophyllid loci (with the exception of the eu*PLE* lineage, (see below). A-Function: Representatives of the eu*API* and eu*FUL* lineages were isolated from all 5 species of Aizoaceae and additionally two eu*FUL*-like loci were isolated from *D.napiforme* and *M. cordifolia*. B-function: Representatives of the eu*AP3*, *PI*, and *TM6* lineages were isolated from all five species of Aizoaceae and two eu*AP3* paralogs were isolated from *A. leptopus*. Two additional loci belonging to the B-sister lineage were identified from *P. oleracea* and *T. tetragonoides*. C- and D-function: Representatives of the eu*AG* lineage were recovered from all five species of Aizoaceae and two loci belonging to the *AGL11* lineage were isolated from *D. napiforme* and *T. tetragonoides*. E-function: Three *SEP* homologs were obtained from two species of Aizoaceae (*D. napiforme*, *M. cordifolia* and *T. tetragonoides* and in addition four *SEP* homologs were obtained from *A. leptopus*. Consequently four gene lineages within the *SEP* sub-family (*AGL2*, *FBP9*, *AGL3* and *AGL9*) are represented by caryophyllid loci isolated in this study.

The diversity of caryophyllid MADS-box genes isolated here is representative of the expected complement predicted by previous phylogenetic analyses, although this study provides some of the first caryophyllid ‘placeholders’ in lineages that previously were not represented by loci from the Caryophyllales. These include homologs from non-ABCDE function lineages *STMADS11*, *AGL15*, and *TM3*. *P. oleracea MADS1* and *T. tetragonoides MADS6* are the first B-sister homologs to be isolated from the Caryophyllales while *A. leptopus MADS6* is the first caryophyllid placeholder for the *FBP9* lineage of the *SEP* subfamily.

On the whole, the inclusion of these 54 new caryophyllid loci does not alter our understanding of the broad relationships between the different gene lineages in which they are included. The relative order of branching between some paralogous lineages remains uncertain

either because deeper level nodes lack support or because there is topological conflict between phylogenetic analyses using different optimality criterion (e.g. contrast the topology of the eu*API*, eu*FUL*, and *FUL*-like lineages in the MP, ML and Bayesian analyses in Figure 5-2; contrast with Litt et al., 2003). While broad taxon sampling, including caryophyllid taxa, is important to resolve these deeper level uncertainties, the most critical taxa to sample are those that are phylogenetically close to point of duplication i.e. mostly non-core and early diverging eudicot taxa. It is not surprising, therefore, that the inclusion of additional relatively derived caryophyllid loci does not clarify these deeper-level uncertainties.

Polygonales-specific Duplication in the Eu*AP3* Lineage

The isolation of two *AP3* paralogs in *Antigonon leptopus* (Polygonaceae) is notable given that two *AP3* paralogs have also been detected in another genus in the Polygonaceae, *Rumex acetosa*. This suggested a possible Polygonales-specific duplication in the eu*AP3* lineage. Phylogenetic analysis of this putative duplication is complicated by the much higher molecular substitution rates in the *AP3* homologs in *R. acetosa* versus *A. leptopus* as inferred by branch lengths. The MP analyses suggest two recent separate duplications as the paralogs in each species are recovered as sister to each other i.e. *Rumex RAD1* is sister to *Rumex RAD2* and *Antigonon MADS2* is sister to *Antigonon MADS4* (Figure 5-3a). In contrast the ML and Bayesian approaches suggest an older Polygonaceae-specific duplication with *Rumex RAD1* sister to *Antigonon MADS2* and *Rumex RAD2* sister to *Antigonon MADS4* (Figure 5-3b and 5-3c). The ML and Bayesian topologies would seem more credible given the inherent difficulties that long branches pose for MP phylogenetic analyses and the better performance of model-based ML and Bayesian approaches in situations of substitution rate heterogeneity (Gadagkar and Kumar, 2005). On the other hand, analysis of the *RAD1* and *RAD2* paralogs finds little evidence for neo or subfunctionalization at the mRNA expression level as both paralogs are apparently identically

expressed in both staminate and carpellate flowers of *Rumex acetosa* (Ainsworth et al., 1995). It is therefore currently unclear what selective forces are maintaining the co-existence of these paralogs if they are derived from an older duplication event.

Absence of the euPLE Lineage in Caryophyllales

Although representatives of most of the expected eudicot-specific lineages of ABCDE MIKC-type genes were isolated in this study, one notable exception is the absence of the euPLE lineage homologs in Caryophyllales (Figure 5-6). Additionally, euPLE homologs have not been isolated by five previous studies that report the isolation of euAG homologs which constitute the sister lineage to euPLE. A total of 11 caryophyllid taxa are therefore represented by euAG homologs, and yet no euPLE homologs have been detected. There are three possible explanations for this: 1) the euPLE homologs in Caryophyllales may have diverged in sequence such that they were un-amplifiable by the primers used in this and previous studies. This would seem unlikely as the primers used were able to amplify more distant related *AGL11* homologs within the *AGAMOUS* subfamily (*Delosperma MADS8* and *Tetragonia MADS17* in this study; *Phytolacca AG2*, (Kramer et al., 2004). 2) The euPLE and euAG lineages derive from a duplication that occurred after the divergence of the Caryophyllales within the core eudicots. This scenario remains possible as it is currently unclear where the duplication giving rise to euAG and euPLE lineages occurred. Only rosid and asterid lineages possess both paralogs suggesting that the duplication may have arisen just prior to the divergence of the rosid and asterid lineages; uncertainty as to the branching order of major eudicot lineages further complicates evaluation of this scenario. Additionally EM Kramer reports a possible PLE homolog in the early-diverging eudicot lineage *Gunnera* (pers comm.), which would make the following third explanation more probable. 3) The duplication giving rise to the euAG and euPLE lineages occurred at the base of the core eudicots as suggested by Kramer et al., (2004) but the euPLE lineage was subsequently

lost in the Caryophyllales. As highlighted previously there is widespread evidence for instances of paralog loss in lineages of MIKC-type gene lineages; in the *AGAMOUS* subfamily, a notable example is the apparent loss of *AGL11* lineage homologs in the Ranunculales (Kramer et al., 2004). This hypothesis would need to be explored at the genomic level to demonstrate that the PLE loci have indeed been lost.

Absence of Duplications Coinciding with the Inferred Origin of Petaloid Staminodes

It is evident from these phylogenetic analyses that there have been no duplications in the MADS-box gene lineages associated with the inferred point of origin of petaloid staminodes. In particular, there is no increase in gene complement in the *AGAMOUS*, *APETALA3* and *PISTILLATA* lineages, which, due to their roles in stamen and petal identity, are of particular interest with respect to the evolution of petaloid staminodes of Ruschoideae and Mesembryanthoideae. We therefore reject the hypothesis that the evolution of petaloid staminodes could be linked to duplication and subsequent neofunctionalization in key MADS-box gene lineages.

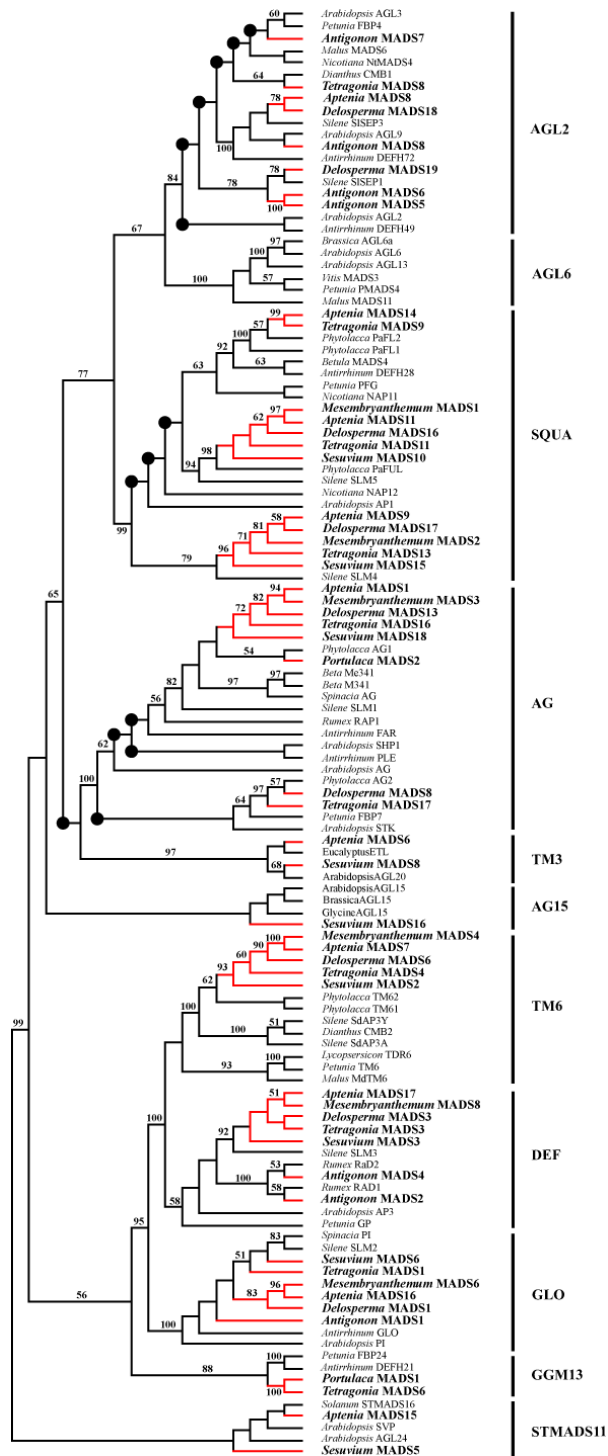


Figure 5-1. ML tree derived from analysis of a DNA dataset comprising 121 MADS-box gene loci (including 54 loci isolated by this study) Nodes with circles collapse in strict consensus of five trees; numbers above branches represent bootstrap support values, red branches leading to terminals in bold text signify loci isolated by this study. Ten major clades are revealed and labeled based on the nomenclature in (Becker and Theissen, 2003).

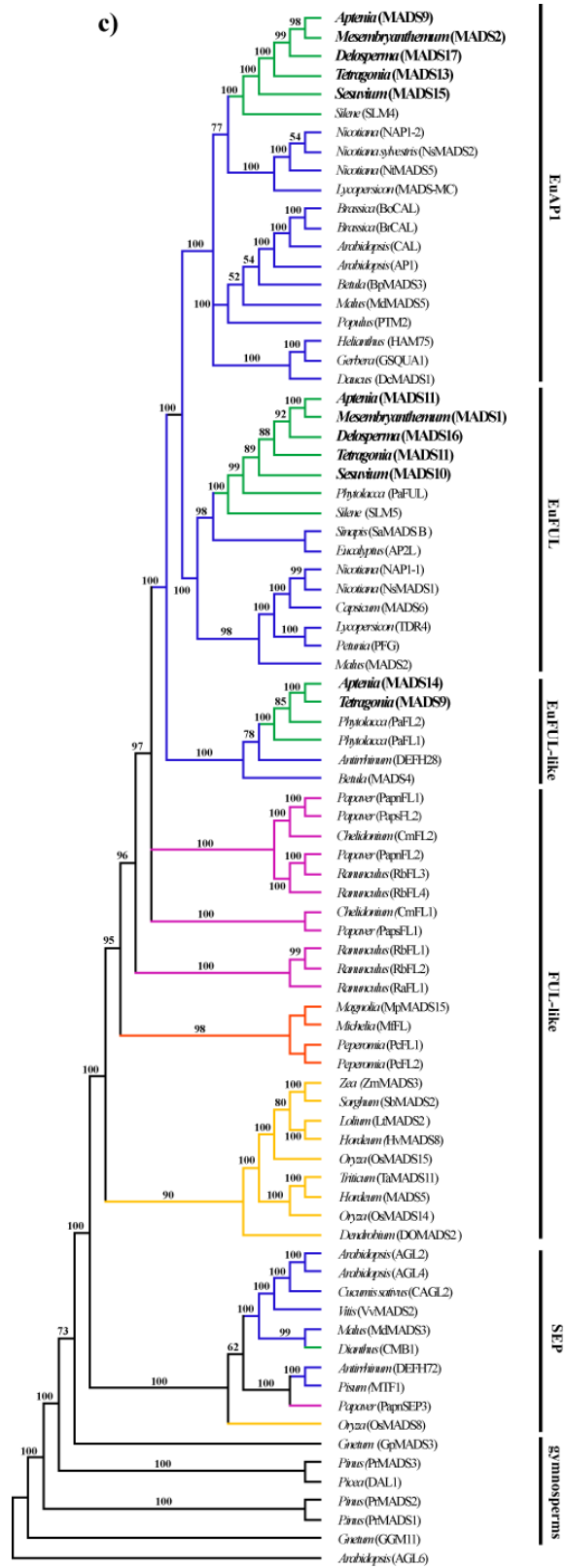


Figure 5-2. Continued

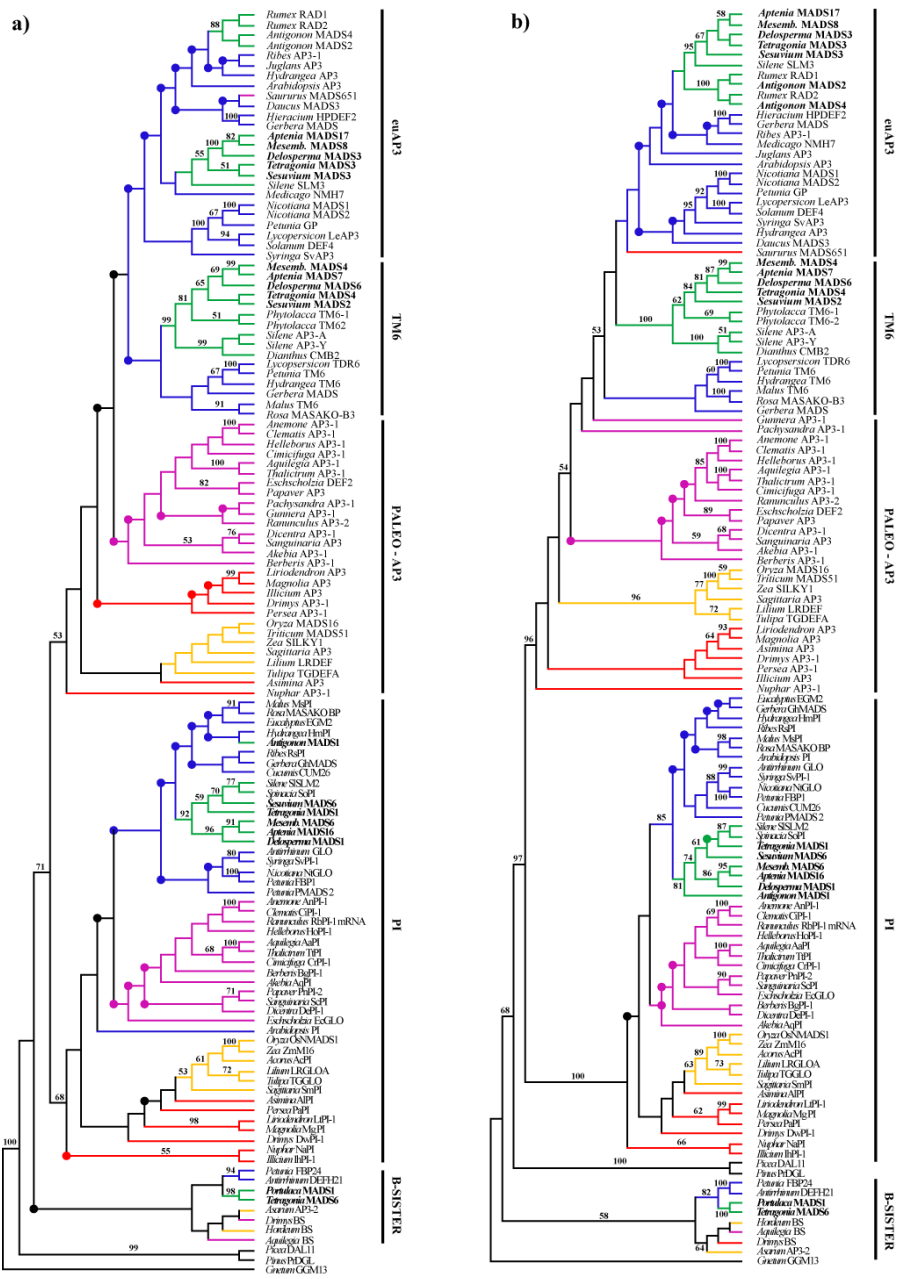


Figure 5-3. Trees derived from analyses of the ‘B-function’ DNA dataset comprising 127 MADS-box gene loci (including 19 loci isolated by the study). Lineages coded by organismal affinity: gymnosperms (black), magnoliids and basal angiosperms (red), monocots (yellow), non-core eudicots (pink), core eudicots (blue), caryophyllids (green). Loci isolated in this study are highlighted in bold text. a) one of five MP trees, numbers above branches are bootstrap support values b) ML tree; numbers above branches are bootstrap support values; nodes with circles collapse in strict consensus. c) 50% majority rule consensus tree derived from ‘post burn-in’ posterior distribution of the trees derived from bayesian analysis. Clades are labeled based on the nomenclature in (Stellari et al., 2004)

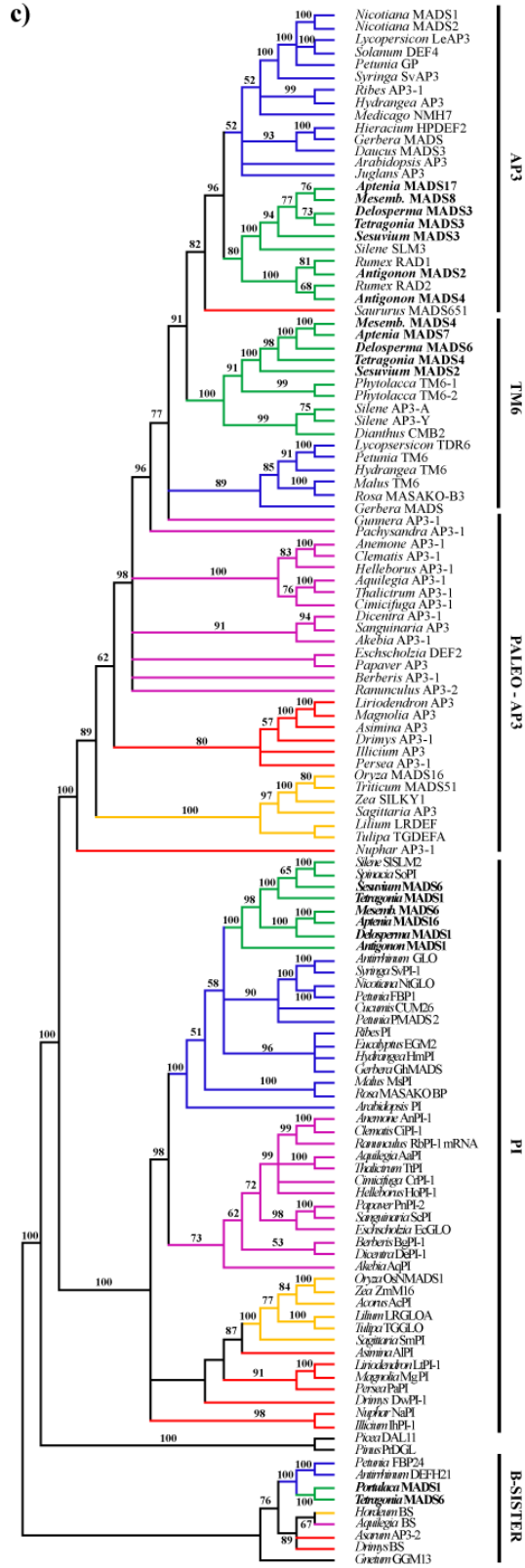


Figure 5-3. Continued

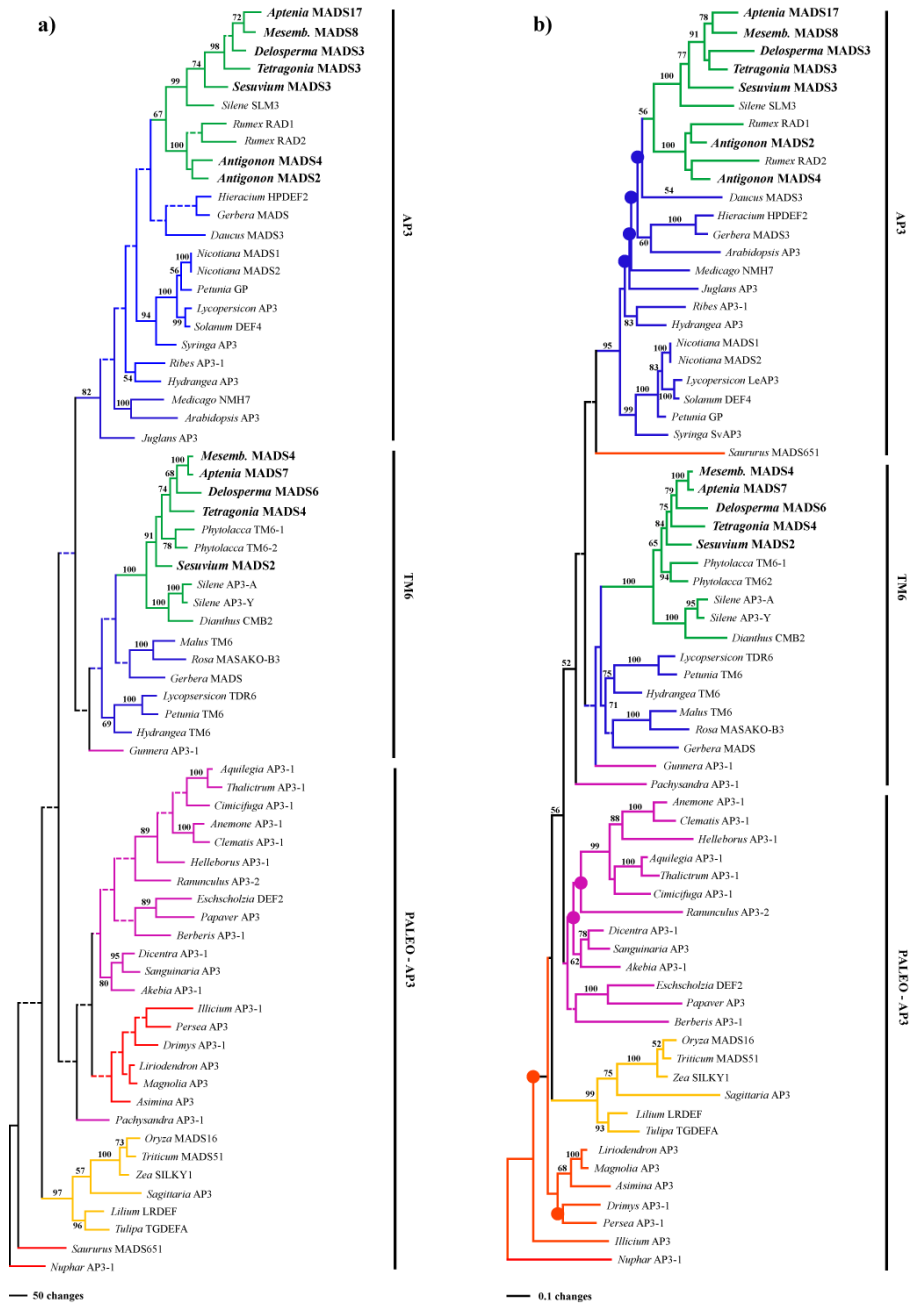


Figure 5-4. Trees derived from analyses of the *APETALA3* DNA dataset comprising 69 MADS-box gene loci (including ten loci isolated by the study). Lineages coded by organismal affinity: magnoliids and basal angiosperms (red), monocots (yellow), non-core eudicots (pink), core eudicots (blue), caryophyllids (green). Loci isolated in this study are highlighted in bold text. a) one of two MP trees, numbers above branches are bootstrap support values. b) ML tree; numbers above branches are bootstrap support values; nodes with circles collapse in strict consensus c) 50% majority rule consensus tree derived from ‘post burn-in’ posterior distribution of the trees derived from bayesian analysis. Clades are labeled based on the nomenclature in (Stellari et al., 2004)

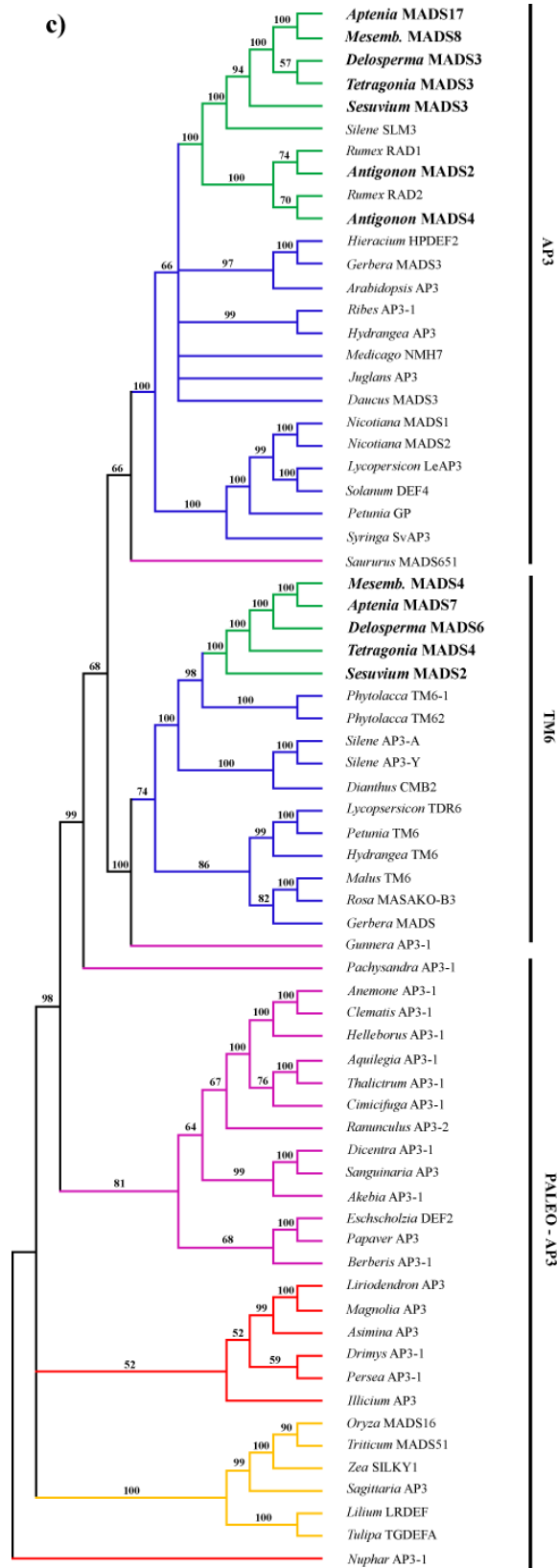


Figure 5-4. Continued

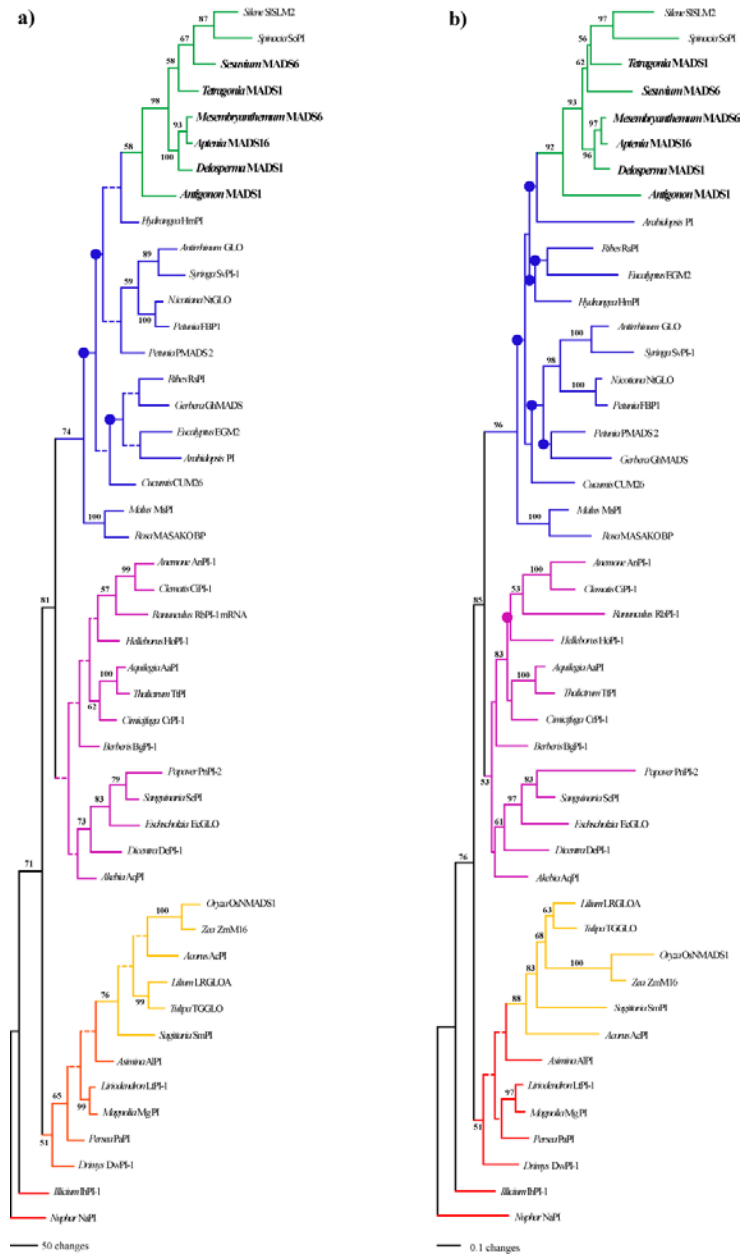


Figure 5-5. Trees derived from analyses of the *PISTILLATA* DNA dataset comprising 47 MADS-box gene loci (including 6 loci isolated by the study). Lineages coded by organismal affinity: magnoliids and basal angiosperms (red), monocots (yellow), non-core eudicots (pink), core eudicots (blue), caryophyllids (green). Loci isolated in this study are highlighted in bold text. a) one of 13 MP trees, numbers above branches are bootstrap support values. b) ML tree; numbers above branches are bootstrap support values; nodes with circles collapse in strict consensus. c) 50% majority rule consensus tree derived from ‘post burn-in’ posterior distribution of the trees derived from bayesian analysis. Clades are labeled based on the nomenclature in (Stellari et al., 2004).

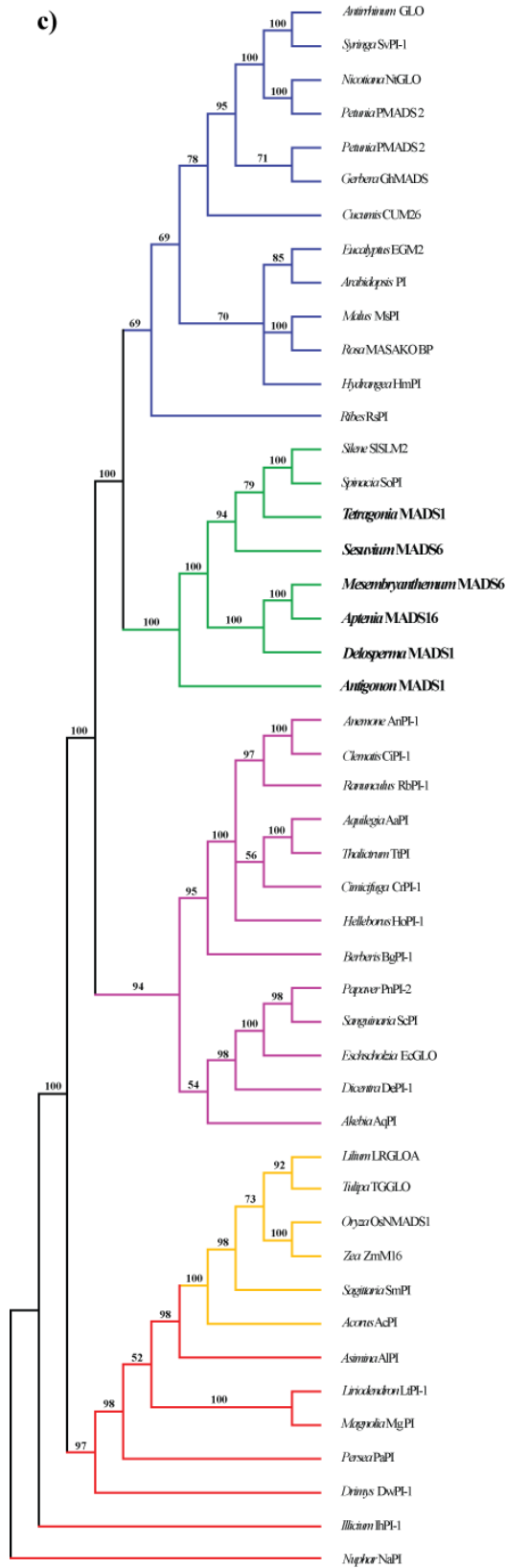


Figure 5-5 Continued

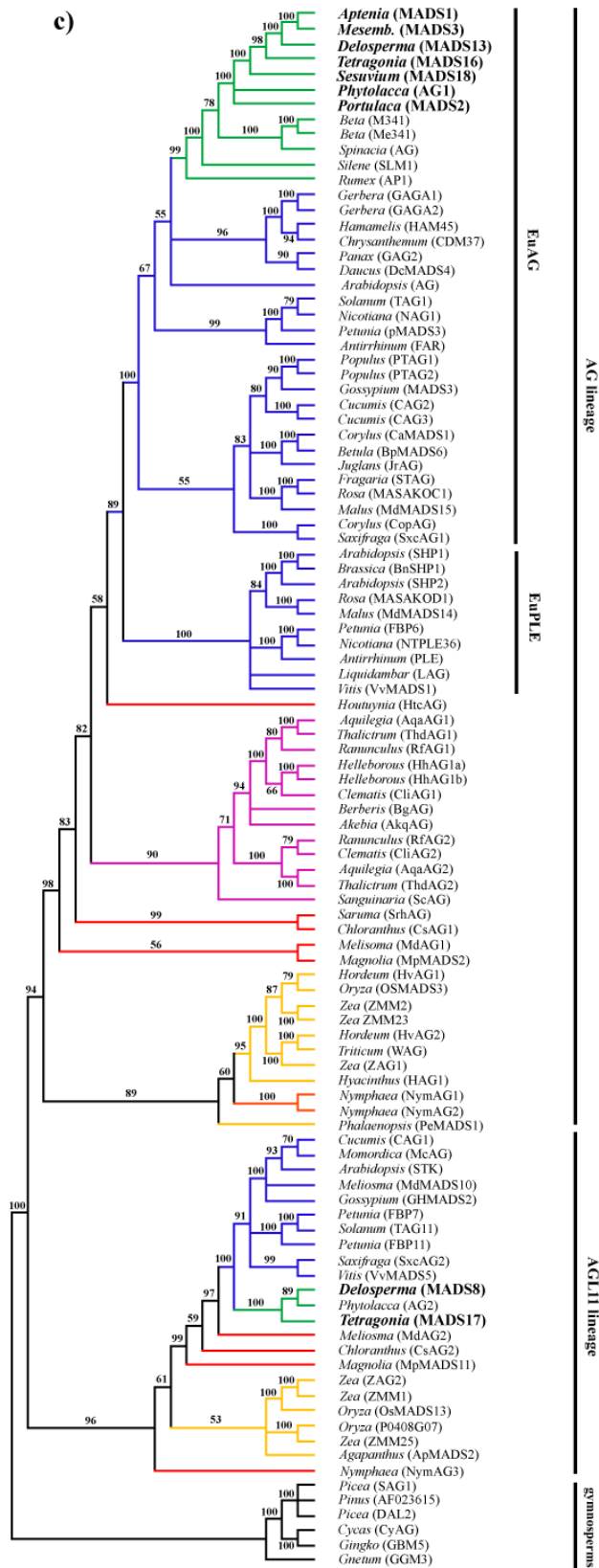


Figure 5-6. Continued

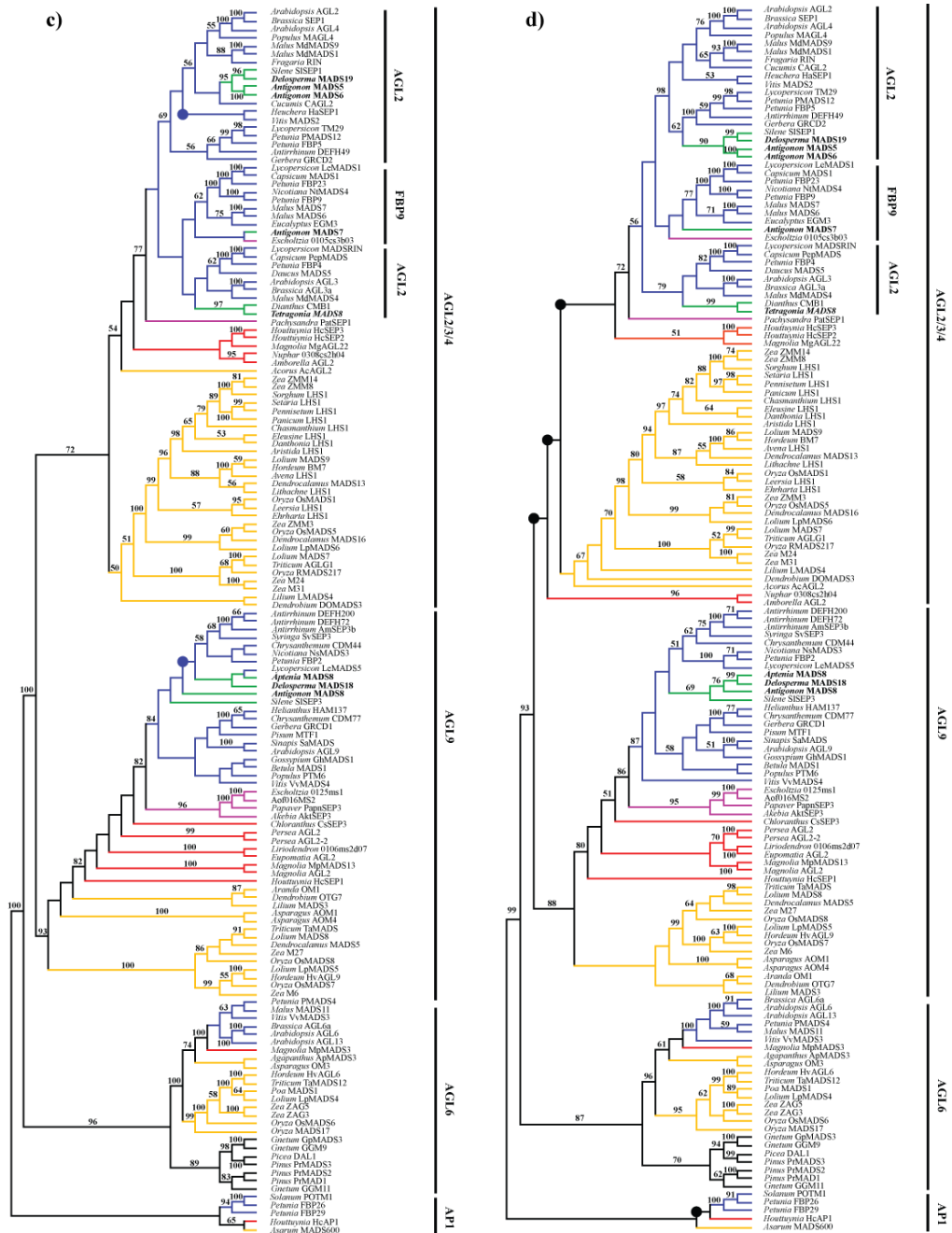


Figure 5-7. Trees derived from analyses of the ‘E-function’ DNA dataset comprising 151 MADS-box gene loci (including eight loci isolated by the study). Lineages coded by organismal affinity: gymnosperms (black), magnoliids and basal angiosperms (red), monocots (yellow), non-core eudicots (pink), core eudicots (blue), caryophyllids (green). Loci isolated in this study are highlighted in bold text. a) one of four MP trees, numbers above branches are bootstrap support values. b) ML tree; numbers above branches are bootstrap support values; nodes with circles collapse in strict consensus. c) 50% majority rule consensus tree derived from ‘post burn-in’ posterior distribution of the trees derived from bayesian analysis. Clades are labeled on the nomenclature in (Zahn et al., 2005)

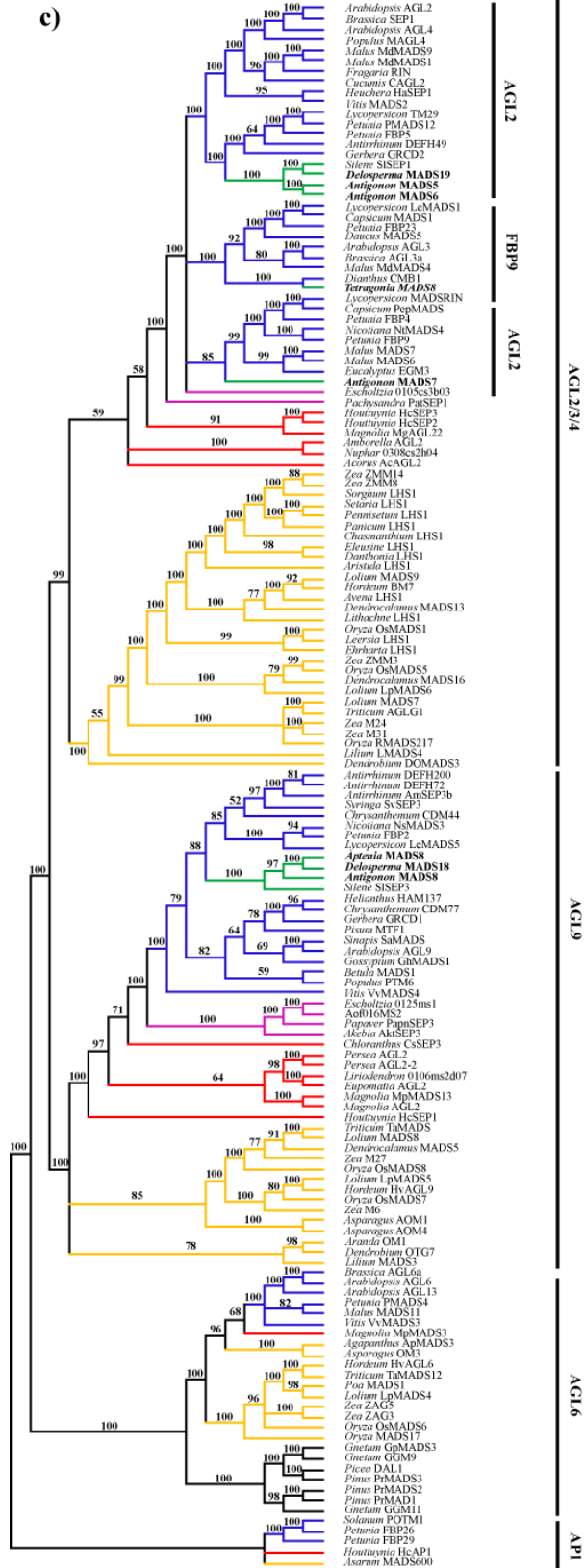


Figure 5-7. Continued

CHAPTER 6
PERIANTH EVOLUTION IN AIZOACEAE: NOT ALL CORE EUDICOT PETALS WERE
CREATED EQUAL

The existence of similar developmental genetic pathways in the petals of distantly related eudicot model organisms led to the proposal of a common petal identity program (Bowman 1997; Ambrose et al. 2000). According to this hypothesis, a petal identity program, regulated by *APETALA3* and *PISTILLATA* MADS-box genes, evolved to specify petals or petaloid morphology in an early angiosperm ancestor. This hypothesis is attractive from the evolutionary standpoint as a petal identity program could engender organ identity independently of position in the flower or historical homology of the organs. The observation that petaloid organs can occupy both first and second whorls of the flower and can be derived from different organs (bracts or stamens) could therefore be explained by simple heterotopic changes in the activity of an ancestral petal identity program. We test the concept of a common petal identity program in the Caryophyllid family Aizoaceae, which possesses two distinct petaloid organs, petaloid tepals and petaloid staminodes derived from bracts and stamens respectively. We assess to what extent the morphology of these organs in Aizoaceae can be attributed to their differing historical derivation and whether they share similar morphological features indicative of a common petal identity pathway. Furthermore we analyze the gene expression patterns of three MADS-box gene homologs *APETALA3*, *PISTILLATA* and *AGAMOUS* to assess the genetic evidence for a common petal identity program. We find little evidence at the morphological or genetic level for a shared petal identity program between petaloid tepals and staminodes. Moreover the petaloid organs in Aizoaceae exhibit unusual expression patterns of MADS-box genes, unlike that described in other core eudicot petals. We discuss these findings in comparison to developmental genetic data from other angiosperm taxa, and in the context of perianth evolution in the Caryophyllales. We suggest that both petaloid organs have unique genetic and morphological

attributes, implying that petaloid morphology has evolved independently of an ancestral petal identity program.

Introduction

Petals are the showy attractive organs that comprise the second whorl in the perianth of most core eudicot flowers. Several similarities in the genetic regulation of the second whorl petal (Coen and Meyerowitz, 1991) were revealed by comparison of two distantly related eudicot taxa *Antirrhinum majus* and *Arabidopsis thaliana*. First, in the absence of the C-function MADS-box gene *AGAMOUS* (*AG*) (*PLENA* in *A. majus*) co-activity of B-function MADS-box genes *APETALA3* (*AP3*) and *PISTILLATA* (*PI*) (*DEFICIENS* and *GLOBOSA* respectively in *A. majus*) is necessary for development of the petal in the second whorl of the flower (Bradley et al., 1993; Goto and Meyerowitz, 1994; Jack et al., 1992; Mizukami and Ma, 1992); Second, persistent co-activity of B-class MADS-box genes through late stages of petal development is necessary to maintain the expression of characteristic petal features (Bowman et al., 1991; Sommer et al., 1991; Zachgo et al., 1995). Third, heterotopic expression of B-function MADS-box genes in the first whorl of the flower is sufficient to induce ectopic petal morphology in the sepals (Coen and Meyerowitz, 1991; Krizek and Meyerowitz, 1996). From these observations it has been inferred that the common ancestor of *A. majus* and *A. thaliana* possessed a petal development pathway regulated by orthologs of *AP3/PI* and *DEF/GLO*. Furthermore, this has led to the suggestion of an ancestral petal identity program conserved at least in core eudicots and possibly across angiosperms (Kramer and Jaramillo, 2005): a concept that has been strengthened by additional taxon sampling. *AP3* and/or *PI* are implicated in the development of petals in additional angiosperm taxa; e.g., *Aquilegia* (Kramer et al., 2007), *Aristolochia* (Jaramillo and Kramer, 2004), *Gerbera* (Yu et al., 1999), *Lycopersicon* (de Martino et al., 2006), *Magnolia* (Kim et al.,

2005) *Nicotiana* (Liu et al., 2004), *Papaver* (Drea et al., 2007), *Petunia* (Vanderkrol et al., 1993), and *Silene* (Hardenack et al., 1994).

Central to the concept of a conserved petal identity program is an assumption that the role of B-class genes in petal development is conserved because, in the absence of C-class gene activity, B-class gene function is required for appearance of petal characteristics such as pigmentation, texture, ultra-structure, and epidermal cell shape. In other words, activity of B-class genes in petals is conserved in distantly related taxa because B-class gene orthologs evolved to regulate, in a common ancestor, a genetic program that engenders the expression of petal features (Baum and Whitlock, 1999; Kramer and Jaramillo, 2005). Conserved *AP3* and *PI* homolog co-activity in second-whorl petals could also be described as process homology *sensu* Gilbert and Bolker (2001). The concept of the petal identity program rests on the idea that the process homology of petals is best explained in correlation with the morphological homology of petals i.e. the appearance of homologous petal traits. However morphological homology, corresponding to ‘special characteristics’ *sensu* Remane (1952), is only one criterion by which petals may be considered homologous. Additional criteria include: 1) positional homology *sensu* Remane (1952), i.e., petals in core eudicots and other angiosperms may be homologous by the criterion of positional homology as they commonly occupy the same position in the second whorl of the flower and; 2) historical homology *sensu* Mayr (1982) i.e. core eudicot petals may be considered homologous if they are derived from the same structure that is present in the common ancestor (e.g. ‘andropetals’ derived from stamens). A key question then is the extent to which the process homology of petals can be explained by morphological homology as opposed to positional or historical homology.

Morphological homology, inherent in the concept of an angiosperm-wide petal identity program, has dominated the interpretation of comparative MADS-box gene expression data (e.g. Kim et al., 2005). However, both positional and historical homology criteria have also been invoked to explain the particular pattern expressions of MADS-box genes. For example, in an analysis of the evolution of the lodicules in Poaceae, Whipple et al. (2007) invoked positional homology and rejected morphological homology when they argued, “B-class genes specify second whorl identity in many angiosperms [despite the fact] that the details of second whorl morphology are variable”. In a similar rejection, Drea et al. (2007) contended that the common role for *AP3* and *PI* is in ‘specifying a spatially limited regional domain [the second and third whorls] within the flower’. In contrast, Kramer and Irish (2000) appeal to historical homology when they suggested that the expression of *AP3* and *PI* homologs in stamens “makes it likely that andropetals [stamen-derived petals] would also utilize these genes in their development”. In the context of the gynostemium in *Aristolochia*, Jaramillo and Kramer (2004) also invoke historical homology when they suggest that ‘B-class genes may serve as molecular markers for staminally derived tissue’. Finally, Chanderbali et al. (2006) suggested that the expression of *AG* in the second whorl of the perianth in *Persea* is a “genetic footprint” resulting from the historical derivation of the second whorl tepals from stamens.

That these interpretations are competing or co-existing in the literature reflects a number of issues: 1) petal identity is difficult to define from a comparative morphological standpoint (Endress, 1996; Jaramillo and Kramer, 2004; Kramer and Jaramillo, 2005); 2) variable floral structure, merosity and phyllotaxy obscures positional correspondence between floral organs (Endress, 1996); 3) historical homology of the perianth can be difficult to determine and the criteria for doing so have been questioned (Ronse De Craene, 2007, 2008); 4) limited taxon

sampling forces comparative analysis across vast phylogenetic distance over which our ability to define the nature of the homology between the perianth of distant taxa is diminished (Jaramillo and Kramer, 2007); 5) arguments that seek to explain process homology through the positional, historical, and morphological homology of the second perianth whorl are not exclusive as each may have explanatory power in different morphological structures, taxonomic groups, phylogenetic levels and episodes of angiosperm evolution. As subsequently discussed, however, explanations of process homology based on different homology criteria have distinct implications for our understanding of morphological evolution.

If process homology in the petals of angiosperms is explained through association with appearance of petal characteristics, then an ancestral petal identity program becomes a viable hypothesis. A petal identity program is appealing in the context of petal evolution because, as suggested by genetic manipulation in model organisms, it could operate in a homeotic fashion and engender organ identity independently of position in the flower or historical homology of the organ (Kramer and Jaramillo, 2005). The presence of petals in both first and second whorls of the flower and their derivation from different organs (e.g. ‘bracteopetals’ from bracts and ‘andropetals’ from stamens Tahktajan, 1991) could consequently be explained through heterotopic changes in the activity of a petal identity program (Kramer and Jaramillo, 2005). An ancestral petal identity program therefore advocates parallelism (the independent evolution of the same derived trait via the same developmental changes, *sensu* Patterson, 1982) and makes evolutionary transitions between different organs a more simple matter than could be envisioned by models of gradual modification (Rasmussen et al., 2009).

In contrast, explanations of process homology in petals based on positional or historical homology allow for convergence (the evolution of morphologically similar traits with a distinct

developmental basis, *sensu* Patterson 1982). If process homology in the second perianth whorl is better explained through positional homology then the repeated role of *AP3* and *PI* homologs in directing petal development could be due to repeated independent recruitment of the genes through position-dependent developmental constraint (Drea et al., 2007; Kramer et al., 1998). In this scenario, second whorl organs may share process homology because of position, yet similar morphological appearance would not necessarily be due to this process homology, but could be the result of convergent morphological differentiation. Similarly, if historical homology of organs in the second whorl best explains observed process homology then the conserved function of *AP3* and *PI* homologs could be attributed to a common derivation of second-whorl organs from stamens (whose development is also dependent in part on the activity of *AP3* and *PI* homologs, Kramer et al., 1998). This interpretation would predict conserved *AP3* and *PI* homolog activity in all stamen-derived petals (but not necessarily bract-derived petals) yet allow morphological similarity to be the result of convergent differentiation of developmental processes downstream of *AP3* and *PI*.

In the face of these competing interpretations, evaluating the concept of a petal identity program requires perianth variation with a pattern of character change that can be accurately reconstructed across a well-resolved organismal phylogeny. In addition, it requires an experimental system in which it is possible to assess perianth variation clearly from the perspective of several homology criteria. The angiosperm family Aizoaceae (Caryophyllales) is one such system, exhibiting two distinct types of perianth. The subfamilies Sesuvioideae and Aizoioideae both possess a perianth that is simple, comprising organs (termed petaloid tepals) that are petaloid on the adaxial side and sepaloid on the abaxial side. In contrast, the perianth of both the subfamilies Ruschoideae and Mesembryanthemoideae is differentiated, with an outer

whorl of sepals and an inner whorl of petals (termed petaloid staminodes). The term petaloid is applied here as a ‘homology-neutral’ term that simply describes the superficially similar appearance of these organs to each other and to petals in other core eudicots, without reference to specific characters or homology criteria.

Molecular phylogenetic studies indicate that Sesuvioideae and Aizoioideae form an early-diverging grade within Aizoaceae (Klak et al., 2003) such that the differentiated perianth of Ruschoideae and Mesembryanthemoideae is derived (Brockington et al., 2009). Importantly, the petaloid perianth in the early-diverging subfamilies is thought to derive from bracteal organs and thus is not homologous in a historical sense to what are considered to be stamen-derived petaloid staminodes present in the derived subfamilies. Furthermore the sepals in derived sub-families are derived from the petaloid tepals of early-diverging subfamilies although the petaloid appearance of the tepals has been lost in the evolution of the differentiated perianth in Ruschoideae and Mesembryanthemoideae, in which petaloid staminodes have assumed the attractive role.

The above pattern of perianth evolution makes Aizoaceae a valuable system in which to assess the concept of the petal identity program against an underlying conflict in historical homology. In this study we: (1) confirm the different historical derivation of the two types of petaloid organ (2) assess the extent to which the differing derivation of the petaloid organs influences their morphological appearance; (3) examine whether historically non-homologous petaloid organs share common characteristics consistent with a morphological concept of shared petal identity; (4) examine the expression patterns of homologs of the organ identity genes, *AGAMOUS* (*AG*), *APETALA3* (*AP3*) and *PISTILLATA* (*PI*), to assess whether the differing petaloid organs share a common developmental genetic program and; (5) compare these findings

with data from core eudicot model organisms and other angiosperm taxa to assess the applicability of a conserved petal identity program to Aizoaceae.

Methods

Plant Materials

Mesembryanthemum cordifolia, *Delosperma napiforme*, *Tetragonia tetragonoides* were grown in a greenhouse at the University of Florida. Flowering material of *Sesuvium portulacastrum* was collected from Cedar Key, Florida. Vouchered specimens are deposited at the University of Florida herbarium (FLAS).

Scanning Electron Microscopy

Ontogenetic analysis was performed on *S. portulacastrum* and *D. napiforme* to investigate the respective homology of the perianth organs and to provide a morphological framework to interpret RNA-RNA *in-situ* hybridizations. Developing inflorescences were dissected and fixed in freshly prepared FAA (3.7% formaldehyde, 50% ethanol, 5% acetic acid). Samples were dehydrated through absolute ethanol and critical-point dried using an Autosamdri-815B CPD (Tousimis Research, Rockville, Maryland, USA), then coated with platinum using an Emitech (Kent, UK) K550 sputter coater and examined using a Hitachi (Wokingham, UK) cold-field emission SEM S4700 II. Some images were colored using Adobe Photoshop (San Jose, California, USA).

RNA-RNA *In-situ* Hybridisation

RNA-RNA *in-situ* hybridizations were performed on two species in Aizoaceae representing two perianth types; *S. portulacastrum* and *D. napiforme*. Developing inflorescences were dissected and fixed in freshly prepared FAA (3.7% formaldehyde, 50% ethanol, 5% acetic acid) overnight at 4°C. Anti-sense and sense probes were designed to the C-terminus and 3'UTR region of the homologs of *AP3* (*SpAP3* and *DnAP3*), *PI* (*SpPI* and *DnPI*) and *AG* (*SpAG* and

DnAG) and synthesized using a DIG RNA labeling kit with a T3 polymerase (Roche, Indianapolis, USA). Probes were hydrolyzed to approximately 150bp. Probe hybridization, post-hybridization treatment and immuno-localization was performed as previously described (Malcomber and Kellogg, 2004). Colorimetric staining was performed with NBT/BCIP for 1-2 and slides were photographed using a Zeiss Axiocam MRc5 digital camera mounted on a Zeiss Axioskop 2 Plus microscope (Carl Zeiss MicroImaging, Thornwood, NY) with bright field illumination.

Relative-Quantitative RT-PCR

Relative-Quantitative RT-PCR (RQ-RT-PCR) was performed in four species representing all four subfamilies in Aizoaceae: *S. portulacastrum* (Sesuvioideae), *T. tetragonia* (Aizooideae), *Mesembryanthemum cordifolia* (Mesembryanthoideae) and *D. napiforme* (Ruschoideae). Flowers were dissected into separate pools of organs prior to RNA extraction (*S. portulacastrum*/*T. tetragonia*; Vegetative Leaves, Petaloid Tepals, Stamens, and Carpels; *Mesembryanthemum cordifolia*/*D. napiforme*; Sepals, Petaloid Staminodes, Stamens, and Carpels). For *S. portulacastrum* and *D. napiforme*, prior to organ dissection, flowers were separated into different size pools (<4mm, 5-8mm, >10mm) in order to assess gene expression levels at different stages of development. Only mature flowers of *T. tetragonia* were employed in RQ-RT-PCR analyses due to the small size of the flowers so expression data from *T. tetragonia* only represents late-stage gene expression. In the case of *M. cordifolia* flowers of different sizes were admixed prior to cDNA manufacture so expression data also predominantly represents late-stage gene expression. RNA extraction and cDNA manufacture was performed as in Chapter 5. RNA was normalized between different pools using a Nanodrop (Thermoscientific, Delaware, USA) prior to cDNA manufacture. We performed RQ-RT-PCR using a gene-specific primer pair (designed to *AG*, *AP3* and *PI* homologs) and using a specific primer pair to the 18S rRNA gene

following the protocol of QuantumRNA (Ambion, California, USA). The 18S rRNA gene was used as a control. All RT-PCR products were confirmed initially by size and subsequently by direct sequencing. Products were run on a 1.5% agarose gel and digitally photographed.

Results

Floral Ontogeny in *Sesuvium portulacastrum*

Tepal primordia arise in a quincuncial 2/5 arrangement (Figure 6-1, A-F). The primordia are crescent shaped with a broad base of insertion (Figure 6-1, A, B). The gynoecial primordium becomes visible prior to the emergence of distinct androecial primordia. Androecial primordia arise in a somewhat chaotic fasciculated pattern with a tendency to centrifugal initiation (Figure 6-1, I, J, K). The gynoecium develops with three carpels. Outer stamens develop and hide the inner stamens and developing carpel later in development (Figure 6-1, K, L).

The tepal primordia differentiate into an upper and lower zone early in development (Figure 6-3, A). In *S. portulacastrum*, an adaxial cross-zone gives rise to a ligule that marks the boundary between the upper and lower zones (colored green and pink, respectively, in Figure 6-3), allowing the two zones to be tracked through the ontogeny of the tepal. Early in development, the unifacial upper zone comprises the bulk of the tepal (Figure 6-3, B). Subsequently, however, the bifacial lower zone expands to form the bulk of the mature tepal (Figure 6-3, C-H). The petaloid lamina of the tepal is therefore derived from the lower zone while a distal unifacial tip represents the upper leaf zone (Figure 6-3, G). The derivation of the petaloid portion of the tepal from the lower leaf zone suggests homology between the lamina of the tepal and the leaf sheath of the vegetative leaf (Figure 6-3, L), which is also derived from a lower leaf zone. In turn, the lamina of the vegetative leaf (Figure 6-3, I), derived from the upper zone, is represented in the tepal by the reduced unifacial distal tip.

The correspondence between leaf sheath and perianth reveals that several morphological features in the perianth of *S. portulacastrum* are also present in the vegetative leaf sheath. 1) The perianth in *S. portulacastrum* is singular in its strong abaxial/adaxial differentiation, a condition that is also found in the leaf sheath (cf. Figure 6-1, M, N and Figure 6-3, G, H, J, K). 2) The epidermis of the showy adaxial tissue in the perianth has a simple convex cell type that initially seems unique within the context of the flower, but is actually identical to the epidermal cell type found on the adaxial surface of the leaf sheath (cf. Figure 6-1, M and Figure 6-3, M). 3) The distinctive flanges of delicate petal tissue, seen easily from the abaxial side of the perianth (Figure 6-3, H), correspond to the hyaline margins of tissue in the leaf sheath (Figure 6-3, K).

Floral Ontogeny in *Delosperma napiforme*

Sepals arise in a quincuncial 2/5 arrangement in *D. napiforme* (data not shown). Removal of the sepals reveals that five carpel primordia comprising the gynoecium are visible prior to the emergence of the initial androecial primordia, which arise in alternation with the carpel primordia (Figure 6-2, A, B). Further primordia arise outside of these inner androecial primordia in a centrifugal direction (Figure 6-2, C). Only the innermost primordia develop into fertile stamens (Figure 6-2, F, G); in a mature flower the fertile stamens form a single ring around the gynoecium (Figure 6-2, I, J, K). Subsequent centrifugally initiating primordia develop into sterile staminodes or petaloid staminodes (Figure 6-2, G, H, I); early in development these staminodes resemble stamens (Figure 6-2, L). Centrifugally initiated primordia are increasingly petaloid the further they are initiated from the inner fertile stamens (Figure 6-2, I). The petaloid staminodes are broad relative to the filament of the stamens and cover all fertile organs in development (Figure 6-2, I). The epidermal cells on the petals are undifferentiated (Figure 6-2, M) and resemble the epidermal cells on the stamen filament (Figure 6-2, N).

Expression of *AGAMOUS* Homologs

In general, expression of *AG* homologs was strong and easily detected by RNA-RNA *in-situ* hybridisation. In *S. portulacastrum* *SpAG*, is expressed early in the development of the androecium and gynoecium and continues through to the late stages of stamen and carpel differentiation (Figure 6-4, A-F). *SpAG* is also expressed in developing micro- and mega-sporangia (Figure 6-4, F). In *D. napiforme* *DnAG* is expressed in the meristem prior to the emergence of androecial and gynoecial primordia (Figure 6-4, G). Expression is strong in the developing carpel and in all members of the androecium: it is strongly expressed in the primordia that eventually form sterile staminodes as well as in fertile stamen primordia (Figure 6-4, H, I). Sections that simultaneously capture staminodes at varying stages of maturation reveal the dynamic change in expression of *DnAG* (Figure 6-4, I, J, K). In sterile staminodes *DnAG* is expressed throughout the organs until after they have reached approximately 100 μ M in length (Figure 6-4: J, staminode 3). After this stage in staminode maturation, expression of *DnAG* appears to become restricted in a distal direction until expression is restricted to the tip of the maturing sterile staminode (Figure 6-4, J, staminode 2; K, staminode 3). Later in development this restricted expression is lost (Figure 6-4, J, staminode 1, K, staminode 2 and 3). *DnAG* is strongly expressed in the ovary wall and the developing pollen and ovules (Figure 6-4, J, K, L).

RQ-RT-PCR mostly supports these data. Expression of *DnAG* is strong throughout stamen and carpel development, but although initially expressed in petaloid staminodes, expression weakens and is lost by the time flowers are greater than >10mm in diameter (Figure 6-7). *ApAG* is strongly expressed in stamens and carpels but not detected in the petaloid staminodes possibly due to the late stage flowers that were used to manufacture cDNA pools from *M. cordifolia*.

SpAG is expressed strongly throughout development of stamens and carpels and *TtAG* is strongly expressed in late-stage stamen and carpels of *T. tetragonoides* (Figure 6-7).

Expression of *PISTILLATA* Homologs

In general, expression of *PI* homologs was strong and easily detected. In *S. portulacastrum* *SpPI* expression is restricted to the androecium and absent from the developing carpels and tepals (Figure 6-5, A-F). Expression in the androecium persists through the late stages of stamen differentiation and is present in both filament and differentiated anther (Figure 6-5: E, F). *SpPI* expression is absent from developing ovules (Figure 6-5; F). In *D. napiforme*, *DnPI* expression is restricted to androecial primordia giving rise to fertile stamens and staminodes (Figure 6-5; G). Expression is initially strong in all androecial primordia. In fertile stamens, expression is maintained through differentiation of the filament and anther (Figure 6-5; I, K). Expression remains strong in the developing filament; within the anthers strong expression is restricted to the anther locule wall (Figure 6-5; I, K). In contrast, in primordia giving rise to outer staminodes, *DnPI* expression is initially strong but rapidly weakens in maturation (Figure 6-5; J, c.f. staminodes 1, 2 and 3) as expression becomes restricted in a distal direction (Figure 6-5; K c.f. staminodes 2, and 3) (in a similar manner to *DnAG*). Expression is lost by the time the staminodes reach ~300 μM in length (Figure 6-5, K – staminode 1). *DnPI* expression is absent from the ovules (Figure 6-5; I and K).

RQ-RT-PCR supports these data (Figure 6-7). *DnPI* is expressed strongly in stamens and petaloid stamens; expression weakens throughout petaloid staminodes but is maintained to late stages in stamen development. *AcPI* is expressed in stamen and petaloid staminodes. *SpPI* is expressed throughout stamen development and *TtPI* is expressed in stamens of late stage flowers.

Expression of *APETALA3* Homologs

In general, the expression of *AP3* homologs was weaker and harder to detect than the expression of *AG* and *PI* homologs. In *S. portulacastrum*, *SpAP3* expression is restricted to the androecium and absent from the developing carpels and tepals (Figure 6-6, A-F). Expression in the androecium persists through the late stages of stamen differentiation and is present in both filament and differentiated anther (Figure 6-6, D, E). *SpAP3* expression is strong in developing ovules (Figure 6-6, F). In *D. napiforme*, *DnAP3* expression is restricted to androecial primordia giving rise to fertile stamens and staminodes (Figure 6-6, G) and to the ovules. Expression is initially strong in all androecial primordia. In fertile stamens, expression is maintained through differentiation of the filament and anthers (Figure 6-6, I, J). In contrast, in primordia giving rise to staminodes, *DnAP3* expression is initially strong but weakens in maturation of staminodes (Figure 6-6, J, cf. staminodes 1, 2 and 3), and expression becomes restricted in a distal direction (Figure 6-5, K cf. staminodes 1, 2, and 3) (in a similar manner to *DnAG*). Expression is lost by the time the staminodes reach ~300 μ M in length (Figure 6-5, K – staminode 1). *DnAP3* is strongly expressed in the ovules (Figure 6-5, I and K).

RQ-RT-PCR supports this data (Figure 6-7). *DnAP3* is expressed throughout stamen development but although initially strongly expressed in petaloid staminodes, subsequently weakens through development. Weak *DnAP3* expression is also detected in carpels, consistent with expression in ovules detected by RNA-RNA *in situ* hybridization. *AcAP3* is detected in petaloid staminodes and stamens, with weak expression in carpels. *SpAP3* and *TtAP3* are both strongly detected in stamens with weak expression in carpels.

Discussion

Perianth Ontogeny and Historical Homology of Petaloid Organs in Aizoaceae

The distinct historical homology of the petaloid organs in Aizoaceae is an essential experimental feature of Aizoaceae as a system for testing the concept of the petal identity program. Here we summarize the evidence supporting the different derivation of petaloid tepals (in Sesuvioideae and Aizooideae) and petaloid staminodes (in Mesembryanthoideae and Ruschoideae).

The petaloid tepals of Sesuvioideae and Aizooideae meet traditional criteria of bract-derived petals, as the tepal primordia are crescent-shaped, have a broad base at insertion (Figure 6-1, B-D), and are supplied by three vascular traces (Hofmann, 1994). Ontogenetic analysis of the perianth in *S. portulacastrum* further supports a leaf-like development of petaloid tepals (Figure 6-3, A-L). Tepal primordia differentiate into an upper and lower zone; such differentiation is a well-established first stage in the morphogenesis of the leaves of many species of angiosperms (Kaplan, 1973). The relative expansion of these two zones reveals that the petaloid lamina of the tepal is derived from the lower zone and thus corresponds to the leaf sheath in the vegetative leaves of *S. portulacastrum*. The sepals of Mesembryanthemoideae and Ruschoideae are clearly homologous to the tepals in Sesuvioideae and Aizooideae. Sepal primordia in Mesembryanthemoideae and Ruschoideae exhibit similar differentiation into upper and lower zones (Payer, 1857) (although the lower zone does not undergo much expansion in development), occupy a similar position relative to the floral bracts, and have a similar quincuncial aestivation (Payer, 1857). In contrast to the tepals of Sesuvioideae and Aizooideae, however, the adaxial surface of the sepals of Mesembryanthemoideae and Ruschoideae is not petaloid.

The petaloid staminodes of Mesembryanthemoideae and Ruschoideae can be considered stamen-derived, according to traditional criteria, as they possess a singular vascular trace (Hofmann, 1994) and a narrow point of insertion (Figure 6-2, L). In addition, several lines of evidence peculiar to floral development in Aizoaceae support the interpretation of stamen-derived petaloid structures in Mesembryanthemoideae and Ruschoideae. 1) both petals and stamens develop from primordia initiating in a centrifugal direction (Figure 6-2, A-H) (Hofmann, 1994). 2) Centrifugal initiation of the androecium also occurs in the early-diverging subfamily Aizooideae (e.g. in the genus *Gunniopsis*), however in Aizooideae all centrifugally initiating primordia develop into fertile stamens (Hofmann, 1994). 3) Within the genus *Delosperma*, positionally homologous primordia can develop into petaloid staminodes or stamens, dependent on the species. For example, in *D. napiforme* all but the innermost primordia develop into petals (Figure 6-2, F, I, J, K), but in *D. apetala* only the outermost primordia develop into petals. 4) Stamens and petals are conceptually linked by intermediates, as floral organs developing closest to the fertile stamens are increasingly filamentous while outermost organs are increasingly petaloid (Hofmann, 1994). 5) The petaloid staminodes resemble stamens early in development (Figure 6-2, L).

Petal Identity: A Morphological or Functional Concept?

The concept of petal identity, suggested by the ectopic expression of petal characteristics in gain-of-function mutants, argues for a floral-specific genetic program that turns on a suite of petal characteristics. As a comparative concept, however, petal identity is problematic. There are no diagnostic morphological features that can define a comparative concept of petal identity across angiosperms (Kramer et al., 2007; Whipple et al., 2007), as the characteristics commonly attributed to petals are not always present, do not always co-occur, and are not always restricted to petals (Ronse De Craene, 2007, 2008). Petal identity is therefore applied to a diverse range of

variable perianth organs in absence of definable or consistent morphological similarity. We argue that in the absence of a strict demonstration of morphological homology, the comparative concept of petal identity is in general based on functional analogy. This perceived functional analogy is then masked by the use of intangible pseudo-morphological terms such as ‘petaloidy’ and ‘showiness’. That similar function does not necessarily reflect underlying homology is well documented by numerous examples of non-homologous yet functionally similar structures (e.g. wings of bats and flies, Bolker and Raff, 1996). Consequently, functional similarity can obscure underlying differences and has received rigorous criticism (Bolker and Raff, 1996). Such criticism is echoed in our analysis of the morphology of the perianth in Aizoaceae, which finds little morphological evidence to support homology between functionally equivalent and superficially similar petaloid organs found in different sub-families.

Implications of Correspondence between Leaf Sheath and Petaloid Tepal

In assessing the morphological concept of petal identity in Aizoaceae, we need to distinguish between morphological characters that have bearing on a comparative concept of petal identity, versus those that are related to the historical homology of the petaloid organ. Morphology that can be attributed to historical homology of the organ is difficult to incorporate within the conceptual framework of petal identity, because petal identity has been hypothesized to operate independently of the derivation of the floral organ (Kramer and Jaramillo, 2005). In practice it is easy to conflate historical and morphological homology, but the need for distinction is illustrated by the correspondence of the petaloid tepal and leaf sheath in *S. portulacastrum*. Viewed from the perspective of the organ identity concept, the petaloid tepal is chimeric with adaxial petal identity and abaxial sepal identity. However, with the exception of pigmentation, we find little tepal-specific morphological differentiation relative to the leaf sheath; both have the same strong adaxial/abaxial differentiation, epidermal cell morphology, and delicate margins (Figure 6-3, cf.

G, H, J, K). We suggest therefore that the chimeric morphology of the tepal should not be interpreted within the framework of organ identity, but is better interpreted as a largely derivative morphology (in essence, a pigmented leaf sheath) that is perceived as petaloid in the context of the flower.

Additionally, the correspondence of the petaloid tepal and leaf sheath is insightful due to the correspondance of the delicate petal-like tissue and hyaline margins of the leaf sheath (Figure 6-3, H and K). This observation suggests that petal-like tissue can have unexpected developmental origins. We speculate that hyaline margins may be pre-adapted for co-option as pigmented petal tissue as they are both delicate and, perhaps more significantly, achlorophyllous. The role of hyaline margins in the perianth is largely unstudied (see Rohweder, 1967, 1970; cited in Hoffman, 1994); however additional taxa within the Caryophyllales also exhibit a sepal-like perianth with delicate petaloid margins (e.g. *Polycarpon* (Figure 6-3, N) and *Hypertelis* (Figure 6-3, O)). The correspondence between hyaline margins and petal tissue implies that a petal-like appearance may be achieved differently depending on the historical derivation of the petaloid organ; this complicates our morphological comparison of petaloid tepals and staminodes. Although it is tempting to argue that a hyaline origin of delicate petal-like tissue in *S. portulacastrum* demonstrates non-homology with respect to the delicate tissue in petaloid staminodes of Aizoaceae, this risks conflating concepts of historical and morphological homology. Delicate tissue is commonly regarded as a distinctive feature of petals (Whipple et al., 2007); however delicacy is yet another intangible term without a defined histological basis. As such, there may still be morphological characteristics that are shared by the delicate tissue of the tepals and the petaloid staminodes in Aizoaceae.

Assessing Morphological Homology between Different Petaloid Organs in Aizoaceae

Given the uncertainty introduced by the different derivations of petaloid organs within Aizoaceae, what morphological characteristics should one evaluate in the framework of comparative petal identity? Despite their distinctive appearance, petals can have a very simple structure (Endress and Matthews, 2006) which makes it difficult to define discrete morphological characters with which to test homology. Perhaps the most useful characters then are those that have been shown to have adaptive significance to pollinator attraction and which may be present irrespective of the position or derivation of the petal. We focused on three such adaptive characteristics that have been demonstrated to enhance petal-pollinator interactions: conical cell morphology on the epidermis (Glover and Martin, 1998; Kevan and Lane, 1985; Noda et al., 1994), epidermal cuticular striation (Whitney et al., 2009), and pigmentation (Waser and Price, 1981). We surveyed the epidermis of *S. portulacastrum* and *D. napiforme* (Figure 6-1, 2, 3) and several additional genera in Aizoaceae: *Aizoon* with petaloid tepals has a similar cell type to *Sesuvium*; in *Tetragonia* all plant surfaces including petaloid tepals are covered in bladder cells (data not shown); *Mesembryanthemum* and *Mestoklema* have petaloid staminodes with similar cell type to *Delosperma* (data not shown); *Lampranthus* has petaloid staminodes with flattened tabular epidermal cells similar to *Delosperma* (Christensen and Hansen, 1998). With respect to epidermal morphology and cuticular striation, we find no similarity between the petaloid tepals and petaloid staminodes. In both petaloid staminodes and petaloid tepals the epidermal morphology is remarkably undifferentiated with an absence of conical cells and cuticular striations. This lack of differentiation is not necessarily a point of a similarity however, as the epidermal cell types in *D. napiforme* and *S. portulacastrum* most resemble those found on the organs to which they are historically homologous (stamen filaments in the case of the staminodes, and the adaxial surface of the leaf sheath in the case of petaloid tepals). It is only

with respect to pigmentation that the petaloid tepals and petaloid staminodes can be considered morphologically homologous.

In conclusion, we find that the morphological appearance of the petaloid organs in Aizoaceae can be largely explained through appeal to historical derivation. There are inherent limitations of assessing homology in simple and largely undifferentiated structures; however there is little evidence for morphological homology between petaloid staminodes and petaloid tepals to support a concept of shared petal identity in Aizoaceae. One exception is pigmentation, which is not a trivial similarity but the manifestation of several complex developmental pathways regulating processes such as pigment synthesis, manufacture of leuco- or chromoplasts, and the turning off of chloroplast synthesis (Irish, 2009). Therefore we next assess the evidence for process homology between petaloid staminodes and petaloid tepals

Assessing Process Homology between Petaloid Staminodes and Petaloid Tepals

The term ‘process homology’ as coined by Gilbert and Bolker (2001) refers to similarity in developmental pathways comprised of homologous proteins and related by common ancestry. Unfortunately, the developmental pathway that leads to the expression of petal characteristics in model organisms is still poorly characterized and here we can only assess process homology at the level of gene expression of the *AP3*, *PI* and *AG* homologs. We realize that the expression pattern of three gene homologs does not necessarily constitute process homology *per se* however these three genes perform critical roles in genetic pathways of organ identity in model organisms. Differences in the expression patterns of these genes would at least be suggestive of differences in process homology although we accept that genetic similarities may still exist at different hierarchical levels than that represented by MADS-box gene expression.

From the perspective of genetic programs of petal identity we expected the B-class gene homologs *SpAP3* and *SpPI* to be expressed in the petaloid adaxial lamina of the tepal and the

lower zone of the primordia from which the petaloid lamina is derived. Contrary to this expectation, *SpAP3* and *SpPI* are not expressed at any point in the development of the petaloid tepal but that expression of *SpAP3* and *SpPI* is restricted to the stamens, where they are expressed throughout the development of the filament and anthers. In contrast, in *D. napiforme*, *DnAP3* and *DnPI* are expressed not only in the filaments and anthers of fertile stamens, but also in the petaloid staminodes. Petaloid tepals and petaloid staminodes can also be distinguished at the level of *AG* homolog expression as *AG* homologs are expressed in petaloid staminodes but are not expressed in petaloid tepals. Therefore at the level of *AP3*, *PI* and *AG* homolog expression, we find no evidence for process homology between the petaloid tepals and petaloid staminodes. This supports our morphological interpretation that there is little to unite petaloid tepals and petaloid staminodes within the framework of a shared petal identity program.

Implications of *AP3* and *PI* Homolog Expression Patterns

The petaloid appearance of the tepal is not dependent on *SpAP3* or *SpPI* activity. To our knowledge this is the first evidence that demonstrates the complete absence of *AP3* and *PI* homologs in a petaloid organ within the core eudicots, although previous studies have also conceptually decoupled petal identity and B-class gene expression in other angiosperm taxa. On the basis of late stage RT-PCR Geuten et al. (2006) suggest that *AP3* homologs but not *PI* homologs are expressed in the petaloid sepals of *Impatiens hawkeri* (Balsaminaceae). However, late stage RT-PCR alone is a potentially misleading method of assaying gene expression with respect to organ identity (Jaramillo and Kramer, 2007). Jaramillo and Kramer (2004) found expression of *AP3* and *PI* homologs in the showy uniseriate perianth of *Aristolochia*, but noted that, in contrast to model organisms, the onset of expression occurs late in the differentiation of the perianth and is not correlated with the showiest parts of the perianth. Park et al. (2004, 2003) demonstrated that *AP3* and *PI* homologs are not expressed in the outermost petaloid perianth

whorl in the homochlamydeous flowers of *Asparagus*. Silencing of the PI homolog in *Aquilegia* suggests that *AqvPI* is required for petal identity in the second whorl but not the petaloid first whorl (Kramer et al., 2007). Finally, Whipple et al., (2007) found expression of *AP3* and *PI* homologs irrespective of a petaloid appearance in the second whorl of members of Poales. The absence of *SpAP3* and *SpPI* activity in the petaloid tepals of *Sesuvium portulacastrum* extends these observations to the core eudicots, and contradicts earlier hypotheses (Kramer and Irish, 1999, 2000) that all petaloid organs in core eudicots might share a common *AP3* and *PI* dependent petal identity pathway.

The spatial and temporal expression patterns of *DnAP3* and *DnPI* within the petaloid staminodes also bear on the concept of a core eudicot petal identity program. Expression of *DnAP3* and *DnPI* is initially strong in the primordia but is subsequently restricted to the distal tip of the developing staminode. Signal through *in-situ* hybridisation is undetectable by the time petaloid staminodes reach ~500µM in length. This expression pattern differs from that of stamens as in both *S. portulacastrum* and *D. napiforme*, the *AP3* and *PI* homologs are expressed throughout filament and anther development. RNA-RNA *in-situ* hybridization can become unreliable at later stages of organ development due to diffuse signal caused by vacuolarization and cell expansion (Kramer and Jaramillo, 2005). However we have several reasons to reject this artifactual explanation: 1) We were able to detect strong *AP3* and *PI* homolog expression in expanded stamen filaments of both *S. portulacastrum* and *D. napiforme* (Figure 6-5, E, K and Figure 6-6, E) 2) We detected spatially distinct patterns in temporally separated staminodes despite very slight differences in overall length of the staminode (Figure 6-5, K) 3) Strength of signal does not correlate with cell size (data not shown) 4) The *in-situ* hybridization data is supported by temporal changes in gene expression detected by RQ-RT-PCR (Figure 6-7).

This pattern of expression is of interest because it is similar to that reported in the petaloid organs of Ranunculales (Kramer and Irish, 1999). Constant expression until late stages of petal development is necessary for the maintenance of petal identity in *A. thaliana* and *A. majus*. Given inconstant expression of B-class homologs in *Ranunculus* and *Papaver*, Kramer and Irish (1999) hypothesized that the developmental genetic processes operating in the petals in Ranunculales were different from petals in core eudicot species. They suggested that these developmental differences might be the consequence of the independent evolution of petals in the Ranunculales and/or the phylogenetic position of the order outside of core eudicots, prior to the fixation of a petal identity program. However, the theory of Developmental Systems Drift offers an alternative explanation (Kramer and Jaramillo, 2005; True and Haag, 2001). Our description of a similar pattern within Aizoaceae suggests that even within core eudicots there may be considerable variation in *AP3* and *PI* expression in stamen-derived petaloid organs. Following the argumentation of Kramer and Irish (1999), the detection of this pattern *within* the core eudicots argues against the notion of a core eudicot petal identity program that has simply been turned on in the petaloid staminodes of Aizoaceae.

Implications of AG Homolog Expression Patterns

The specification of petal identity by *AP3* and *PI* homologs in *A. thaliana* and *A. majus* is contingent on an absence of *AG* homolog activity; however, the expression of *AG* homologs is rarely examined when assessing evidence for a conserved petal identity program. The expression pattern of *DnAG* in petaloid staminodes further limits our expectation of a typical eudicot petal identity program operating in the petaloid staminodes. In *D. napiforme*, *DnAG* is expressed not only in the gynoecium and androecium, but also in the petaloid staminodes. This finding is not surprising from the perspective of historical homology as the petals in *D. napiforme* are derived from stamens, and thus one might expect *DnAG* to be retained in the development of the

staminodes (Chanderbali et al, 2006). The spatial expression pattern is consistent with this interpretation because although *DnAG* is expressed early on it is subsequently lost perhaps allowing staminodes to become sterile rather than developing into fertile stamens. However, *DnAG* expression in the staminodes is unexpected in comparison with the petals of *A. thaliana* and *A. majus*. *AG* homologs are not expressed during the development of the petals of these model species and yet traditionally the petals of these species are also considered to be stamen-derived. The expression of *DnAG* in staminodes is therefore a further point of non-homology with respect to the petals of other core eudicots.

Notably, in the petaloid staminodes of *D. napiforme*, the strong expression of *DnAP3* and *DnPI* seems entirely coincident with strong *DnAG* expression. All three genes exhibit the same patterns of strong early expression and subsequent loss. At no point in the development of the petaloid staminodes are *DnAP3* and *DnPI* strongly co-expressed in absence of *DnAG* expression. This co-incident expression of *DnAG*, *DnAP3* and *DnPI* conceptually limits the opportunity for a *DnAP3*- and *DnPI*- driven petal identity pathway unless the co-activity of *DnAG*, *DnAP3* and *DnPI* is decoupled. The ‘quartet model’ of MADS-box protein interactions (Saedler and Theissen, 2001), in which the co-activity of *AP3* and *PI* and *AG* is mediated by additional *SEPELLATA* (*SEP*) MADS-box proteins, provides a possible mechanism for a decoupling of *DnAG*, *DnAP3* and *DnPI* activity. For example, in *Gerbera* it has been discovered that a specific *SEP* locus is required for mediating *C* function. Antisense knockdown of this locus, *GRCD1*, results in the transformation of stamens into petaloid staminodes. However, no *C* function-specific *SEP* has been described in Caryophyllids, or other core eudicots for that matter. This raises another possibility - that transient, early expression of the B+C code in staminodia commits them to an alternative organ identity. Notably, the down-regulation of B and C genes

does not result in the organs reversion to tepal identity but, rather, their development into a completely distinct fourth identity. It will be important, therefore, to examine other floral MADS box genes to determine what loci might be involved in distinguishing these organs from stamens on the one hand and tepals on the other. Alternatively, the similar co-incident expression and loss of *DnAG*, *DnAP3* and *DnPI* might simply signify the wholesale turning off of a stamen developmental program.

Evolution of the Aizoaceae Perianth in the Context of the Caryophyllales

We have assessed the different perianth structures in Aizoaceae from the perspective of historical, morphological and process homology and find numerous anomalies that are difficult to explain from the perspective of a common petal identity program: 1) lack of shared morphological features between petaloid staminodes and petaloid tepals, 2) a potentially different mechanism for the origin of petaloid tissue in tepals, 3) absence of *AP3* and *PI* homologs from the petaloid tepals of Sesuvioideae and Ruschoideae, 4) co-incident expression of *AP3*, *PI* and *AG* homologs in petaloid staminodes of Ruschoideae and Mesembryanthoideae, and 5) loss of *AP3*, *PI* and *AG* homologs through the development of the petaloid staminodes. So far we have discussed our data in the context of Aizoaceae with some reference to other core eudicot model organisms, however the unique evolutionary history of the Caryophyllales provides additional insight.

From the character reconstruction analyses it is evident that early in the evolution of the Caryophyllales, one whorl of perianth was lost such that the simple uniseriate perianth of the Sesuvioideae/Aizoaceae type predominates throughout the Caryophyllales (Brockington et al., 2009). Traditionally it has been assumed that the inner petal whorl of the perianth was lost such that the uniseriate tepals in Caryophyllales correspond to the sepals of other core eudicots (Hofmann, 1994). The absence of *AP3* and *PI* homolog expression in the petaloid tepals of

Aizoaceae is consistent with this interpretation as core eudicot sepals also lack B-class gene function. This appeal to historical homology suggests that tepals (corresponding to sepals) have reacquired petaloid characteristics (as in Sesuvioideae and Aizoioideae), independently of an *AP3* and *PI* dependent petal identity program. If the petaloid appearance in the tepals of Sesuvioideae and Aizoioideae have been achieved independently of *AP3* and *PI* homologs this may well be the case in the numerous other lineages of the Caryophyllales which possess showy organs that are positionally or historically homologous to the tepals of Aizoaceae e.g the tepals of Molluginaceae, Nyctaginaceae and *Hypertelis* and the inner perianth whorls of Portulacaceae, Montiaceae, and Didieraceae. A sepal-derived interpretation of the petaloid tepals in Sesuvioideae and Aizoioideae therefore predicts widespread convergent evolution of petaloid organs in additional lineages of Caryophyllales, independent of the *AP3* and *PI* dependent genetic programs operating in other core eudicots.

Character reconstruction analyses suggest that following a loss of a perianth whorl, multiple separate origins of a differentiated perianth result from the recruitment of staminodes to function as petals e.g the petaloid staminodes in Aizoaceae and the petals of Caryophyllaceae, *Corbichonia* and *Glinus* (Molluginaceae) (Brockington et al., 2009). Arguably, this is precisely the pattern of perianth evolution that the concept of an ancestral petal identity program is intended to explain: “once such a homeotic petal identity program evolved, deactivation and reactivation of the genetic pathway could produce independent losses and gains of petaloid organs’ (Kramer and Jaramillo, 2005). A loss of petals, early in the evolution of the core Caryophyllales, would seem to necessitate loss of an *AP3* and *PI* driven petal identity pathway. However the absence of *AP3* and *PI* homologs from the tepals and sepals in Aizoaceae implies that an *AP3* and *PI* dependent petal identity pathway was not maintained by spatial redeployment

to the tepals at least at the point of divergence of Aizoaceae. Therefore it is not clear how, following the complete loss of the second whorl organs, an *AP3* and *PI* dependent pathway would then be maintained. This is perhaps reflected by genetic differences in the development of stamen-derived petals in Aizoaceae compared with Caryophyllaceae. Hardenack et al. (1994) describes the expression of *AP3* and *PI* homologs early in the development of the petals in *Silene* but the expression of the *AG* homolog *SLMI* is clearly absent from all stages of petal development, similar to other core eudicots. This signifies that in lineages within the Caryophyllales, independent recruitment of stamens to function as petals has entailed dissimilar developmental genetic processes; it is difficult to reconcile these observations with a petal identity program that has been maintained across the Caryophyllales despite losses and gains of petals. Thus far the petaloid staminodes of Aizoaceae appear to be novel floral organs, uniquely derived within the family, and exhibiting a unique developmental genetic program with respect to the stamen derived petals of Caryophyllaceae and other core eudicots.

Conclusion

In this study we have analyzed two different perianth structures each possessing functionally similar petaloid organs of differing historical homology. We found little morphological evidence for a concept of petal identity that unites these different petaloid structures. This finding was supported by expression data suggesting dissimilar developmental genetic processes operating in petaloid staminodes versus petaloid tepals. We therefore reject the hypothesis that heterotopic expression of an *AP3*- and *PI*- driven petal identity pathway underlies superficially similar appearance of petaloid staminodes and petaloid tepals. Furthermore the gene expression patterns in these petaloid organs do not match those of the petals in any other core eudicot organisms studied to date. Consequently we reject the hypothesis

that a core eudicot petal identity program operates in Aizoaceae and suggest that, even within core eudicots, not all petals were created equal.

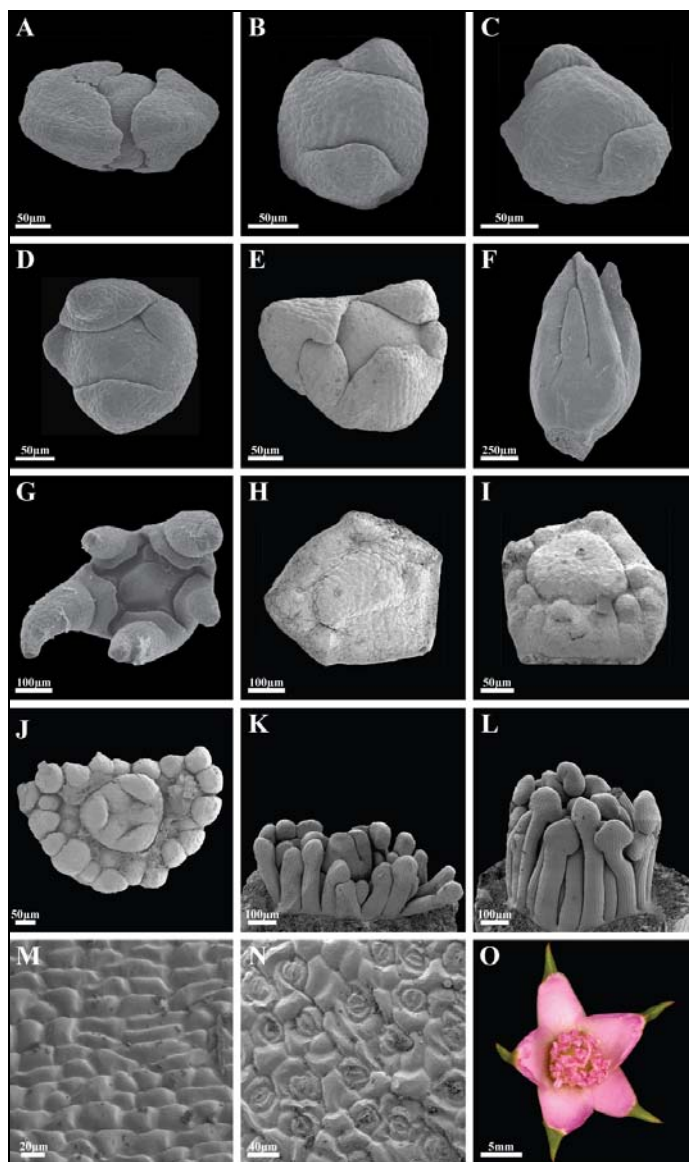


Figure 6-1 Floral Development in *Sesuvium portulacastrum*. (A-F). Early development of the pentamerous uniseriate perianth. (A) Meristem enclosed by floral bracts. (B) Emergence of first two members of perianth. (C and D) Emergence of third and fourth tepal primordia. (E) Five tepal primordia in 2/5 quincuncial arrangement. (F) Five tepals enclosing floral meristem. (G-L) Development of the androecium and gynoecium. (G) Tepals parted to reveal underlying development of androecium and gynoecium. (H and I) Tepals removed to reveal developing carpel primordia in the center of the flower surrounded by early stamen primordia. (J) Tricarpellate gynoecium is revealed together with fasciculated androecial development. (K) Developing stamens beginning to enclose gynoecium, (L) Stamens with clear anther and filament differentiation enclose the gynoecium. (M) Cell type on the adaxial petaloid epidermis of mature tepal. (N) Stomata on the abaxial sepaloid epidermis of the mature tepal. (O) Mature floral form of *Sesuvium portulacastrum*.

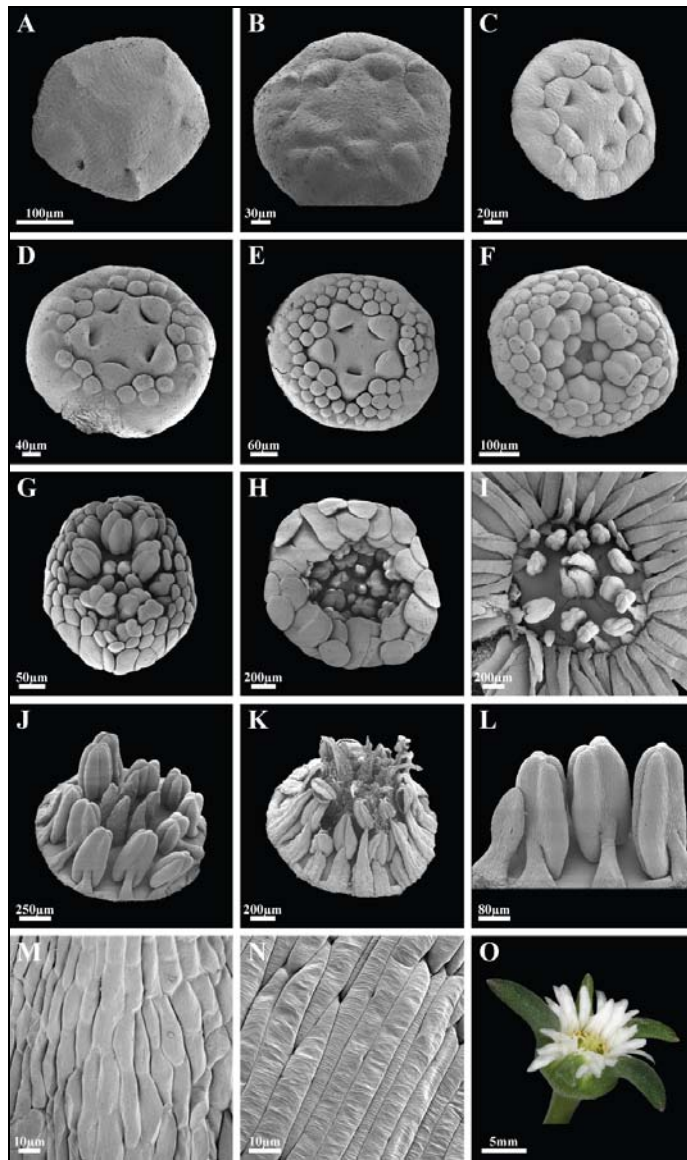


Figure 6-2. Floral development in *Delosperma napiforme* (outer sepals removed). (A) floral meristem prior to emergence of androecial and gynoecial primordia. (B and C) Five carpel primordia emerge at the centre of the meristem. (D and E) Further androecial primordia initiate to the outside of existing stamen primordia in a centrifugal fashion. (F) Inner androecial primordia differentiate into stamens with anthers clearly visible. (G) Outer androecial primordia differentiate into sterile lamina petal structures. (H) Petals clearly visible enclosing underlying fertile stamens and carpels. (I) Mature flower opened to reveal multiple petal whorls surrounding single whorl of fertile stamens and five-carpellate gynoecium. (J) Outer petals removed to reveal single whorl of developing differentiated stamens surrounding gynoecium. (K) Outer petals removed to reveal stamens and carpels at anthesis. (L) Stamens flanked on the left by a developing sterile staminode. (M) Cell type on the epidermis of the mature stamen filament. (N) Cell type on the epidermis of the mature petals. (O) Mature floral form of *Delosperma napiforme*.

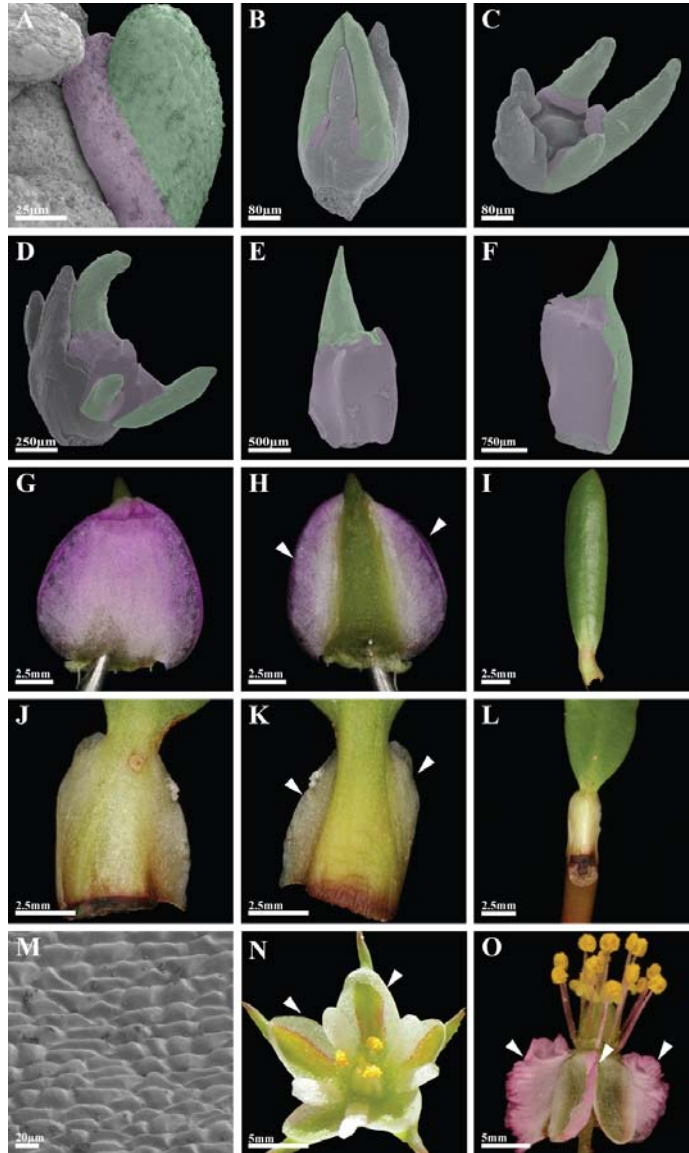


Figure 6-3. Correspondence between perianth and leaf sheath in *Sesuvium portulacastrum*. (A-F) Expansion of the lower leaf zone through development of the tepals. (A) Single primordium with distinct upper (green) and lower (pink) zones. (B and C) Early in development the upper leaf zone forms the bulk of the tepal. (D, E and F) Expansion of lower leaf zone. (F) Lower leaf zone forms the bulk of the tepal and upper leaf zone forms distal tip of the tepal. (G and H) Adaxial and abaxial surface of a mature tepal with distal tip (arrow in H). (I) Vegetative leaf illustrating the leaf lamina and leaf sheath. (J) Adaxial surface of the leaf sheath. (K) Abaxial surface of the leaf sheath. Comparison of (K) with (H) demonstrates relationship between petaloid flanges of tepal and marginal tissue of the leaf sheath (arrows). (L) Leaf sheath attached to the shoot node. (M) Cell type on the adaxial surface of the leaf sheath. (N) Petaloid margins in *Polycarpon tetraphyllum* (arrows). (O) Petaloid margins in *Hypertelis salsoloides* (arrows).

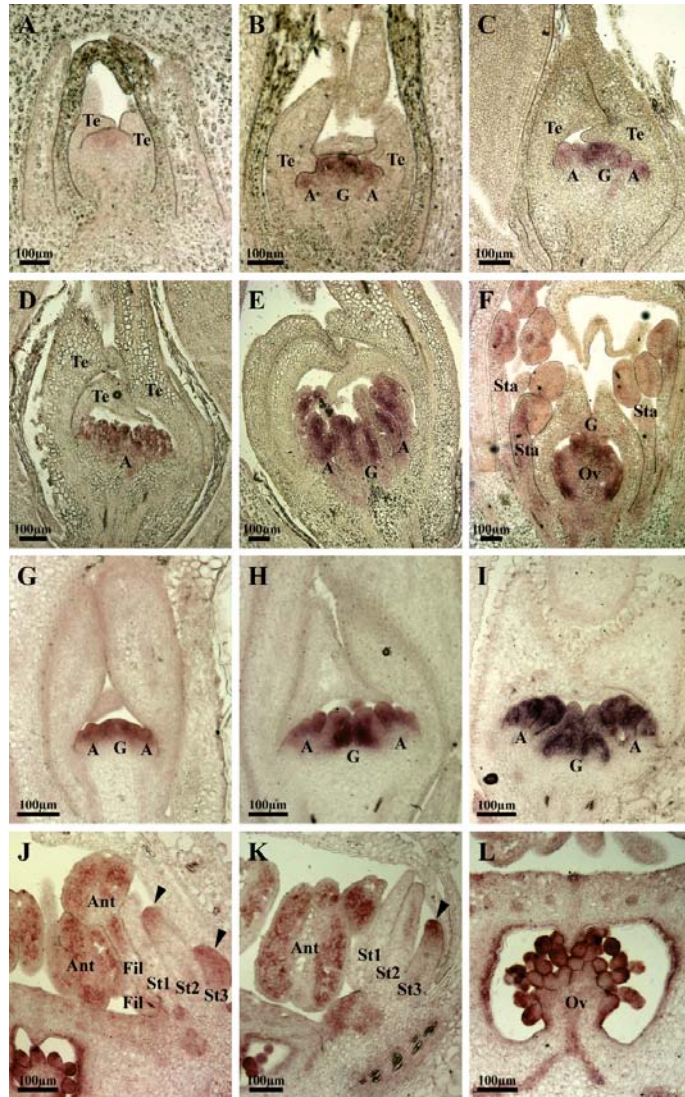


Figure 6-4. Expression of *AGAMOUS* (*AG*) homologs in *Sesuvium portulacastrum* (A-F) and *Delosperma napiforme* (G-L). Tepal (Te), Androecium (A), Gynoecium (G), Stamen (Sta), Filament (Fil), Anther (Ant), Staminode (St), Ovary (Ov). (A) Weak *SpAG* expression in the centre of the meristem, absent from tepals. (B and C) *SpAG* expression in gynoecium and androecium. (D) *SpAG* expression in androecium and absence in tepals. (E) *SpAG* expression in carpels and stamens. (F) *SpAG* expression in the developing ovules; weak expression in filaments and anthers of differentiated stamens. (G) *DnAG* expression in the carpel and stamen primordia. (H) *DnAG* expression in carpel and stamen primordia and in outer first and second primordia that form petaloid staminodes. (I) *DnAG* expression in gynoecium and all fertile and sterile members of the androecium. (J) *DnAG* expression strong in anthers and filaments of inner stamens; lost from developing staminode 1; expression restricted to the tip of staminode 2 (black arrow), strong expression in emerging staminode 3 (~100µM in length) (black arrow). (K) Expression of *DnAG* in anthers; absent now in staminodes 1 and 2; expression restricted to distal tip of staminode 3 (~200µM in length). (L) *DnAG* expression in developing ovules.

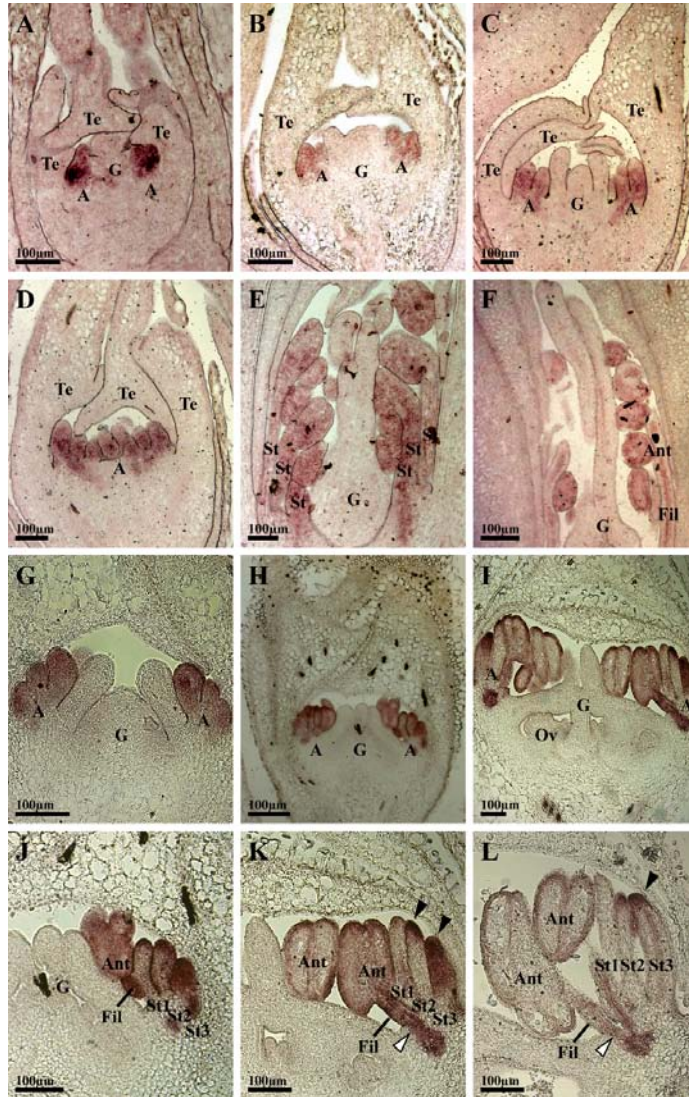


Figure 6-5. Expression of *PISTILLATA* (*PI*) homologs in *Sesuvium portulacastrum* (A-F) and *Delosperma napiforme* (G-L). Tepal (Te), Androecium (A), Gynoecium (G), Stamen (Sta), Filament (Fil), Anther (Ant), Staminode (St), Ovary (Ov). (A) Strong *SpPI* expression marks the site of origin of stamens; no expression developing tepals. (B and C) *SpPI* expression in developing androecium. (D) Section across the androecium show *SpPI* expression maintained in developing androecium and absence in tepals. (E) *SpPI* expression in differentiating stamens; absent in the carpel (F) *SpPI* in expression mature stamens; absent from carpels and developing ovules. (G, H and I) *DnPI* expression in emerging and developing androecial primordia. (J) Expression maintained in anthers and filament; expression in innermost staminodes (1 and 2) weaker than outermost staminode (3). (K) Expression maintained in anther and filament (white arrow), expression weak in staminode 1; restricted to tip in staminode 2; strong in staminode 3 (~150µM in length). (L) Expression of *DnPI* absent now in staminodes 1; expression almost entirely lost in staminode 2 and restricted to the distal tip of staminode 3 (~250uM in length); *DnPI* expression absent in developing ovules.

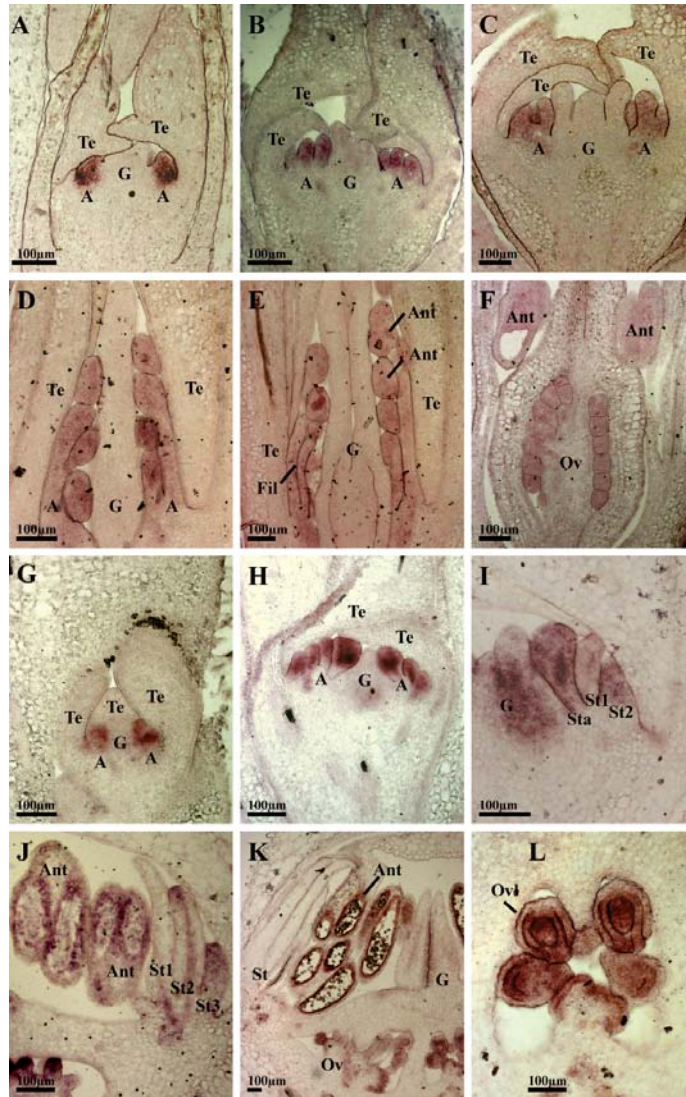


Figure 6-6. Expression of *APETALA3* (*AP3*) homologs in *Sesuvium portulacastrum* (A-F) and *Delosperma napiforme* (G-L). Tepal (Te), Androecium (A), Gynoecium (G), Stamen (Sta), Filament (Fil), Anther (Ant), Stamimode (St), Ovary (Ov), Ovules (Ovl). (A) Strong *SpAP3* expression marks the site of origin of stamens; no expression in developing tepals. (B and C) *SpAP3* expression in developing androecium. (D and E) *SpAP3* expression in differentiating stamens; absent in the carpel. (F) *SpAP3* expression in developing ovules. (G, H and I) *DnAP3* expression in emerging and developing androecial primordia. (I) Expression in developing placenta, expression maintained in anthers and filament; expression in staminode 1 weaker than in staminode 2. (J) Expression strong in locule walls, absent in staminode 1, expression restricted to distal tip of staminode 2, stronger in staminode 3. (K) Expression absent in all staminodes, maintained in anther locule wall and in ovules. (L) *DnAP3* expression strong in developing ovules.

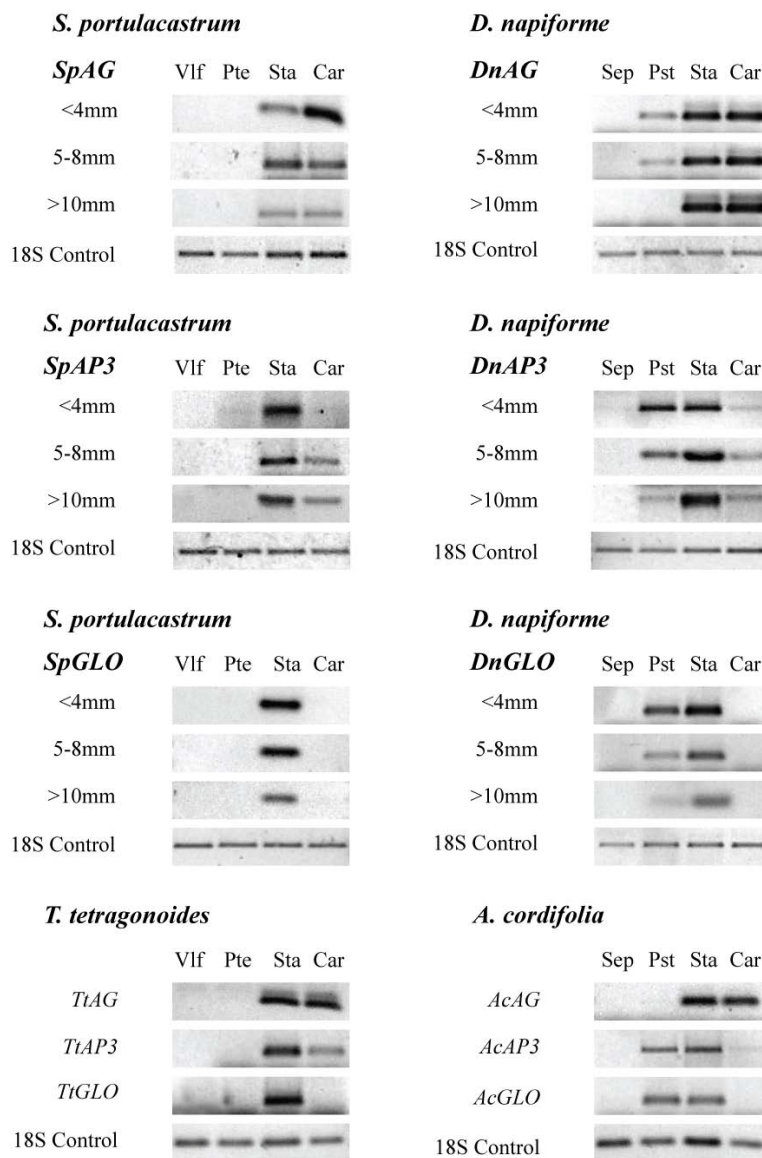


Figure 6-6. RQ-RT-PCR data for four species of Aizoaceae and three gene homologs (*AG*, *AP3*, and *PI*). *S. portulacastrum* and *D. napiforme* are examined at three different stages of floral size (<4mm, 5-8mm, >10mm in diameter). *T. tetragonoides* was assessed at the mature flower only and *M. cordifolia* was assessed using admixed flowers of different sizes. (Vlf = vegetative leaf, Sep = sepals, Pte = petaloid tepals, Pst = petaloid staminode, Car = carpel). 18S rRNA was employed as a control.

REFERENCES

- Ainsworth, C, S Crossley, V Buchananwollaston, M Thangavelu, J Parker 1995 Male and female flowers of the dioecious plant sorrel show different patterns of MADS-box gene-expression. *Plant Cell* 7: 1583-1598.
- Albert, VA, SE Williams, MW Chase 1992 Carnivorous Plants: Phylogeny and Structural Evolution. *Science* 257: 1491-1495
- Alvarez-Buylla, ER, S Pelaz, SJ Liljegren, SE Gold, C Burgeff, GS Ditta, LR de Pouplana, L Martinez-Castilla, MF Yanofsky 2000 An ancestral MADS-box gene duplication occurred before the divergence of plants and animals. *Proceedings of the National Academy of Sciences of the United States of America* 97: 5328-5333.
- Angenent, GC, J Franken, M Busscher, A Vandijken, JL Vanwent, HJM Dons, AJ Vantunen 1995 A novel class of MADS box genes is involved in ovule development in *Petunia*. *Plant Cell* 7: 1569-1582.
- APG II 2003 An update of the angiosperm phylogeny group classification for the orders and families of flowering plants: APG II. *Botanical Journal of the Linnean Society* 141: 399-436.
- Applequist, WL, RS Wallace 2001 Phylogeny of the portulacaceous cohort based on ndhF sequence data. *Systematic Botany* 26: 406-419
- Arnold, KE, IPF Owens, NJ Marshall 2002 Fluorescent signaling in parrots. *Science* 295: 92-92.
- Bate-Smith, E 1962 The phenolic constituents of plants and their taxonomic significance. *Botanical Journal of the Linnean Society* 58: 95-173.
- Baum, DA, BA Whitlock 1999 Plant development: Genetic clues to petal evolution. *Current Biology* 9: R525-R527.
- Beale, G, J Price, V Sturgess 1941 A survey of anthocyanins. VII. The natural selection of flower colour. *Proceedings of the Royal Society of London. Series B, Biological Sciences* 130: 113-126.
- Beck, E, H Merxmuller, H Wagner 1962 Uber die Art der anthocyane bei Plumbaginaceen, Alsinoiden und Molluginaceen. *Planta* 58: 220-224.
- Becker, A, G Theissen 2003 The major clades of MADS-box genes and their role in the development and evolution of flowering plants. *Molecular Phylogenetics and Evolution* 29: 464-489.
- Behnke, HD 1994 Sieve Element Plastids: Their Significance for the Evolution and Systematics of the Order. Pages 87-121 in HD Behnke and TJ Mabry, eds. *Caryophyllales: Evolution and Systematics*. Springer, Berlin.
- Behnke, HD 1997 Sarcobataceae - a new family of Caryophyllales. *Taxon* 46: 495-507.

- Bessey, CE 1915 The phylogenetic taxonomy of flowering plants. *Annals of the Missouri Botanical Garden* 2: 108-164.
- Birkinshaw, C, R Edmond, C Hong-Wa, C Rajeriarison, F Randriantafika, G Schatz 2004. Red lists for Malagasy plants II: Asteropeiaceae. Missouri Botanical Garden, Antananarivo University.
- Bischoff, H. 1876. *Das Caryophyllinenroth* Inaugural Dissertation. Universitat Tubingen.
- Bittrich V 1993 Halophytaceae. Pages 320-321 in K Kubitzki, JG Rohwer, V Bittrich, eds. *Flowering plants, Dicotyledons, Magnoliid, Hamamelid, and Caryophyllid families*. Springer-Verlag, Berlin; New York.
- Bittrich, B, M Amaral 1991 Proanthocyanidins in the testa of centrospermous seeds. *Biochemical Systematics and Ecology* 19: 319-321.
- Blackwell, WH and Powell MJ 1981 A preliminary note on pollination in the Chenopodiaceae. *Annals of the Missouri Botanical Garden* 68: 524-526
- Blattner, FR 1999 Direct amplification of the entire ITS region from poorly preserved plant material using recombinant PCR. *Biotechniques* 27: 1180
- Bolker, JA, RA Raff 1996 Developmental genetics and traditional homology. *Bioessays* 18: 489-494.
- Bollback, JP 2006 SIMMAP: Stochastic character mapping of discrete traits on phylogenies. *BMC Bioinformatics* 7: -
- Bowman, JL, DR Smyth, EM Meyerowitz 1989 Genes directing flower development in *Arabidopsis*. *Plant Cell* 1: 37-52.
- Bowman, JL, DR Smyth, EM Meyerowitz 1991 Genetic interactions among floral homeotic genes of *Arabidopsis*. *Development* 112: 1-20.
- Bradley, D, R Carpenter, H Sommer, N Hartley, E Coen 1993 Complementary floral homeotic phenotypes result from opposite orientations of a transposon at the *PLENA* locus of *Antirrhinum*. *Cell* 72: 85-95.
- Braun, A 1864 ebersicht der Natürlichen Systems nach der Anordnung Derselben. Pages 22-67 in P Ascherson, ed. *Flora der Provinz Brandenburg, der Altmark und des Herzogthums Magdeburg*. Hirschwald, Berlin.
- Brockington, SF, E Mavrodiev, J Ramdial, A Dhingra, PS Soltis, DE Soltis 2008 Keep the DNA Rolling: Multiple Displacement Amplification of archival plant DNA extracts. *Taxon* 53: 944-948

Brockington, SF, Frohlich M, PJ Rudall, DE Soltis, PS Soltis 2007 Differing patterns of MADS-box gene expression associated with shifts in petaloidy within Aizoaceae (Caryophyllales). 2007. Page 191 in Program and Abstract Book, Plant Biology and Botany Congress, Chicago: pp191.

Brockington, SF, R Alexandre, J Ramdial, MJ Moore, S Crawley, A Dhingra, K Hilu, DE Soltis, PS Soltis 2009 Phylogeny of the caryophyllales sensu lato: Revisiting hypotheses on pollination biology and perianth differentiation in the core caryophyllales. *International Journal of Plant Sciences* 170: 627-643.

Buxbaum, F 1950-55 *Morphology of Cacti*. Pasadena, Abbey Garden Press.

Carolin R 1987 A review of the family Portulacaceae. *Australian Journal of Botany* 35: 383-412.

Carpenter, R, ES Coen 1990 Floral homeotic mutations produced by transposon-mutagenesis in *Antirrhinum majus*. *Genes & Development* 4: 1483-1493.

Chanderbali, AS, S Kim, M Buzgo, Z Zheng, DG Oppenheimer, DE Soltis, PS Soltis 2006 Genetic footprints of stamen ancestors guide perianth evolution in *Persea* (Lauraceae). *International Journal of Plant Sciences* 167: 1075-1089.

Chase, MW, DE Soltis, RG Olmstead, D Morgan, DH Les, BD Mishler, MR Duvall, RA Price, HG Hills, YL Qiu, KA Kron, JH Rettig, E Conti, JD Palmer, JR Manhart, KJ Sytsma, HJ Michaels, WJ Kress, KG Karol, WD Clark, M Hedren, BS Gaut, RK Jansen, KJ Kim, CF Wimpee, JF Smith, GR Furnier, SH Strauss, QY Xiang, GM Plunkett, PS Soltis, SM Swensen, SE Williams, PA Gadek, CJ Quinn, LE Eguiarte, E Golenberg, GH Learn, SW Graham, SCH Barrett, S Dayanandan, VA Albert 1993 Phylogenetics of seed plants - an analysis of nucleotide-sequences from the plastid gene *rbcL*. *Annals of the Missouri Botanical Garden* 80: 528-580.

Christensen, K, H Hansen 1998 Sem-studies of epidermal patterns of petals in angiosperms. *Opera Botanica* 135: 1-91.

Clement, J, T Mabry 1996 Pigment evolution in the Caryophyllales: A systematic overview. *Botanica Acta* 109: 360-367.

Clement, J, T Mabry, H Wyler, A Dreiding 1994 Chemical review and evolutionary significance of the betalains. in: H-D Behnke, T Mabry eds. *Caryophyllales: Evolution and systematics*. Springer, Berlin.

Coen, ES, EM Meyerowitz 1991 The war of the whorls - genetic interactions controlling flower development. *Nature* 353: 31-37.

Couvreur, TLP, JE Richardson, MSM Sosef, RHJ Erkens, LW Chatrou 2008 Evolution of Syncarpy and other morphological characters in African Annonaceae: A posterior mapping approach. *Molecular Phylogenetics and Evolution* 42: 302-318

Couvreur, TLP. 2008. Revealing the secrets of African Annonaceae: Systematics, evolution and biogeography of the syncarpous genera *Isolona* and *Monodora*. Pages 15-33 D. Phil. Thesis, Wageningen University.

- Cronquist, A 1981 An integrated system of classification of flowering plants. Columbia University Press, New York.
- Cronquist, A 1988 The evolution and classification of flowering plants. New York Botanical Garden, Bronx.
- Cronquist, A, RF Thorne 1994 Nomenclatural and taxonomic history. Pages 87-12 in HD Behnke and TJ Mabry, eds. Caryophyllales: Evolution and Systematics. Springer, Berlin.
- Cuenoud, P, V Savolainen, LW Chatrou, M Powell, RJ Grayer, MW Chase 2002 Molecular phylogenetics of Caryophyllales based on nuclear 18S rDNA and plastid *rbcL*, *atpB*, and *matK* DNA sequences. American Journal of Botany 89: 132-144.
- Dahlgren, R 1975 A system of classification of the angiosperms to be used to demonstrate the distribution of characters. Botaniska Notiser 128: 119-147.
- de Martino, G, I Pan, E Emmanuel, A Levy, VF Irish 2006 Functional analyses of two tomato *apetala3* genes demonstrate diversification in their roles in regulating floral development. Plant Cell 18: 1833-1845.
- Dean, FB, S Hosono, L Fang, X Wu, AF Faruqi, P Bray-Ward, Z Sun, Q Zong, Y Du, J Du, M Driscoll, W Song, SF Kingsmore, M Egholm, RS Lasken 2002 Comprehensive human genome amplification using multiple displacement amplification. Proceedings of the National Academy of Sciences of the United States of America U S A 99: 5261-5266.
- Dhingra, A, KM Folta 2005 ASAP: Amplification, Sequencing and Annotation of Plastomes. BMC Genomics 6: 176.
- Di Gregorio, J, J Dipalma 1966 Anthocyanin in *Dionaea muscipula* (Ellis) (Venus Flytrap). Nature 212: 1264-1265.
- Ditta, G, A Pinyopich, P Robles, S Pelaz, MF Yanofsky 2004 The *SEP4* gene of *Arabidopsis thaliana* functions in floral organ and meristem identity. Current Biology 14: 1935-1940.
- Douglas, NA, PS Manos. 2007. Molecular phylogeny of Nyctaginaceae: Taxonomy, biogeography, and characters associated with a radiation of xerophytic genera in North America. American Journal of Botany. Vol. 94.
- Downie, SR, DS Katz-Downie, KJ Cho 1997 Relationships in the Caryophyllales as suggested by phylogenetic analyses of partial chloroplast DNA ORF2280 homolog sequences. American Journal of Botany 84: 253-273.
- Downie, SR, JD Palmer 1994 A chloroplast DNA phylogeny of the Caryophyllales based on structural and inverted repeat restriction site variation. Systematic Botany 19: 487-487.
- Doyle, J, J Doyle 1987 Genomic plant DNA preparation from fresh tissue-CTAB method. Phytochemical Bulletin 19: 11.

- Drabkova, L, J Kirschner, C Vlcek 2002 Comparison of seven DNA extraction and amplification protocols in historical herbarium specimens of Juncaceae. *Plant Molecular Biology Reporter* 20: 161-175.
- Drea, S, LC Hileman, G De Martino, VF Irish 2007 Functional analyses of genetic pathways controlling petal specification in poppy. *Development* 134: 4157-4166.
- Duminil, J, MH Pemonge, RJ Petit 2002 A set of 35 consensus primer pairs amplifying genes and introns of plant mitochondrial DNA. *Molecular Ecology Notes* 2: 428-430.
- Egea-Cortines, M, H Saedler, H Sommer 1999 Ternary complex formation between the MADS-box proteins *SQUAMOSA*, *DEFICIENS* and *GLOBOSA* is involved in the control of floral architecture in *Antirrhinum majus*. *EMBO Journal* 18: 5370-5379.
- Ehrendorfer, E 1976 Closing remarks: Systematics and evolution of centrospermous families. *Plant Systematics and Evolution* 126: 99-106.
- Eichler, A 1875-1878 Blüthendiagramme I/II. Engelmann, Leipzig, Germany
- Endress, M, V Bittrich 1993 Molluginaceae in K Kubitski ed The families and genera of vascular plants. Vol. 2. Springer Berlin.
- Endress, PK 2002. Morphology and angiosperm systematics in the molecular era *Botanical Review* 68: 545–570.
- Endress, PK 1994 Diversity and evolutionary biology of tropical flowers. Cambridge University Press, Cambridge.
- Endress, PK, ML Matthews 2006 Elaborate petals and staminodes in eudicots: Diversity, function, and evolution. *Organisms Diversity and Evolution* 6: 257-293.
- Favaro, R, A Pinyopich, R Battaglia, M Kooiker, L Borghi, G Ditta, MF Yanofsky, MM Kater, L Colombo 2003 MADS-box protein complexes control carpel and ovule development in *Arabidopsis*. *Plant Cell* 15: 2603-2611.
- Fay, MF, KM Cameron, GT Prance, MD Lledo, MW Chase 1997 Familial relationships of *Rhabdodendron* (Rhabdodendraceae) plastid *rbcL* sequences indicate a caryophyllid placement. *Kew Bulletin* 52: 923-932.
- Felsenstein, J 1978 Cases in which parsimony or compatability methods will be positively misleading. *Systematic Zoology* 27: 401-410.
- Felsenstein, J 1985 Confidence-limits on phylogenies - an approach using the bootstrap. *Evolution* 39: 783-791.
- Fior, S, PO Karis, G Casazza, L Minuto, F Sala 2006 Molecular phylogeny of the Caryophyllaceae (Caryophyllales) inferred from chloroplast *matK* and nuclear rDNA ITS sequences. *American Journal of Botany* 93: 399-411.

- Friedman, J, SCH Barrett 2008 A phylogenetic analysis of the evolution of wind pollination in the angiosperms. *International Journal of Plant Sciences* 169: 49-58.
- Gadagkar, SR, S Kumar 2005 Maximum likelihood outperforms maximum parsimony even when evolutionary rates are heterotachous. *Molecular Biology and Evolution* 22: 2139-2141.
- Gadkar, V, MC Rillig 2005 Application of phi29 DNA polymerase mediated whole genome amplification on single spores of arbuscular mycorrhizal (am) fungi. *FEMS Microbiol Lett* 242: 65-71.
- Gandia-Herrero, F, J Escribano, F Garcia-Carmona. 2005. Betaxanthins as pigments responsible for visible fluorescence in flowers *Planta*. Vol. 222. 1-12
- Giannasi, DE, G Zurawski, G Learn, MT Clegg 1992 Evolutionary relationships of the Caryophyllidae based on comparative *rbcl* sequences. *Systematic Botany* 17: 1-15.
- Gilbert, SF, JA Bolker 2001 Homologies of process and modular elements of embryonic construction. *Journal of Experimental Zoology* 291: 1-12.
- Glover, BJ, C Martin 1998 The role of petal cell shape and pigmentation in pollination success in *Antirrhinum majus*. *Heredity* 80: 778-784.
- Goto, K, EM Meyerowitz 1994 Function and regulation of the *Arabidopsis* floral homeotic gene *PISTILLATA*. *Genes and Development* 8: 1548-1560.
- Graham, SW, RG Olmstead 2000 Utility of 17 chloroplast genes for inferring the phylogeny of the basal angiosperms. *American Journal of Botany* 87: 1712-1730.
- Hardenack, S, D Ye, H Saedler, S Grant 1994 Comparison of mads box gene-expression in developing male and female flowers of the dioecious plant white campion. *Plant Cell* 6: 1775-1787.
- Hershkovitz, MA 1993 Revised circumscriptions and subgeneric taxonomies of *Calandrinia* and *Montiopsis* (Portulacaceae) with Notes on Phylogeny of the portulacaceous Alliance. *Annals of the Missouri Botanical Garden* 80: 333-365
- Hershkovitz, MA, EA Zimmer 1997 On the evolutionary origins of the cacti. *Taxon* 46: 217-232.
- Hilu, KW, T Borsch, K Muller, DE Soltis, PS Soltis, V Savolainen, MW Chase, MP Powell, LA Alice, R Evans, H Sauquet, C Neinhuis, TAB Slotta, JG Rohwer, CS Campbell, LW Chatrou 2003 Angiosperm phylogeny based on *matK* sequence information. *American Journal of Botany* 90: 1758-1776.
- Hofmann, U 1973 Morphologische Untersuchungen zur Umgrenzung und Gliederung der Aizoaceen. . *Botanische Jahrbücher für Systematik* 93: 247-324.
- Hofmann, U 1994 Flower morphology and ontogeny. in: H.-D. Behnke and T. J. Mabry [eds.], *Caryophyllales: Evolution and Systematics* 123-166. Springer, Berlin.

- Hofmann, U 1994 Flower morphology and ontogeny. Pages 123-166 in HD Behnke and TJ Mabry, eds. Caryophyllales: Evolution and Systematics. Springer, Berlin.
- Huelsenbeck, JP, F Ronquist 2001 MrBayes: Bayesian inference of phylogenetic trees. *Bioinformatics* 17: 754-755.
- Hunziker, JH, R Pozner, A Escobar 2000 Chromosome number in *Halophytum ameghinoi* (Halophytaceae). *Plant Systematics and Evolution* 221: 125-127.
- Irish, VF 2003 The evolution of floral homeotic gene function. *Bioessays* 25: 637-646.
- Irish, VF, EM Kramer 1998 Genetic and molecular analysis of angiosperm flower development. *Advances in Botanical Research*, Vol 28: 197-230.
- Irish, VF, IM Sussex 1990 Function of the *APETALA1* gene during *Arabidopsis* floral development. *Plant Cell* 2: 741-753.
- Jack, T, GL Fox, EM Meyerowitz 1994 *Arabidopsis* homeotic gene *APETALA3* ectopic expression - transcriptional and posttranscriptional regulation determine floral organ identity. *Cell* 76: 703-716.
- Jack, T, LL Brockman, EM Meyerowitz 1992 The homeotic gene *APETALA3* of *Arabidopsis thaliana* encodes a MADS box and is expressed in petals and stamens. *Cell* 68: 683-697.
- Jansen, RK, C Kaitanis, C Sasaki, SB Lee, J Tomkins, AJ Alverson, H Daniell 2006 Phylogenetic analyses of *Vitis* (Vitaceae) based on complete chloroplast genome sequences: Effects of taxon sampling and phylogenetic methods on resolving relationships among rosids. *BMC Evolutionary Biology* 6
- Jaramillo, MA, EM Kramer 2004 *APETALA3* and *PISTILLATA* homologs exhibit novel expression patterns in the unique perianth of *Aristolochia* (Aristolochiaceae). *Evolution and Development* 6: 449-458.
- Jaramillo, MA, EM Kramer 2007 The role of developmental genetics in understanding homology and morphological evolution in plants. *International Journal of Plant Sciences* 168: 61-72.
- Jaramillo, MA, EM Kramer 2007 The role of developmental genetics in understanding homology and morphological evolution in plants. *International Journal of Plant Sciences* 168: 61-72.
- Judd, WS, CS Campbell, EA Kellogg, PF Stevens 2007 *Plant systematics: A phylogenetic approach*. Sinauer Associates, Sunderland.
- Kaplan, DR. 1973. The problem of leaf morphology and evolution in the monocotyledons *Quarterly Review of Biology*.
- Kevan, P, M Lane 1985 Flower petal microtexture is a tactile cue for bees. *Proceedings of the National Academy of Sciences of the United States of America* 82: 4750-4752.

Kim, S, J Koh, MJ Yoo, HZ Kong, Y Hu, H Ma, PS Soltis, DE Soltis 2005 Expression of floral MADS-box genes in basal angiosperms: Implications for the evolution of floral regulators. *Plant Journal* 43: 724-744.

Kim, ST, MJ Yoo, VA Albert, JS Farris, PS Soltis, DE Soltis 2004 Phylogeny and diversification of B-function MADS-box genes in angiosperms: Evolutionary and functional implications of a 260-million-year-old duplication. *American Journal of Botany* 91: 2102-2118.

Klak, C, A Khunou, G Reeves, T Hedderson 2003 A phylogenetic hypothesis for the Aizoaceae (Caryophyllales) based on four plastid DNA regions. *American Journal of Botany* 90: 1433-1445.

Komaki, MK, K Okada, E Nishino, Y Shimura 1988 Isolation and characterization of novel mutants of *Arabidopsis thaliana* defective in flower development. *Development* 104: 195-&.

Kramer, EM, L Holappa, B Gould, MA Jaramillo, D Setnikov, PM Santiago 2007 Elaboration of b gene function to include the identity of novel floral organs in the lower eudicot *Aquilegia*. *Plant Cell* 19: 750-766.

Kramer, EM, MA Jaramillo 2005 Genetic basis for innovations in floral organ identity. *Journal of Experimental Zoology Part B-Molecular and Developmental Evolution* 304B: 526-535.

Kramer, EM, MA Jaramillo, VS Di Stilio 2004 Patterns of gene duplication and functional evolution during the diversification of the *AGAMOUS* subfamily of MADS-box genes in angiosperms. *Genetics* 166: 1011-1023.

Kramer, EM, RL Dorit, VF Irish 1998 Molecular evolution of genes controlling petal and stamen development: Duplication and divergence within the *APETALA3* and *PISTILLATA* MADS-box gene lineages. *Genetics* 149: 765-783.

Kramer, EM, VF Irish 1999 Evolution of genetic mechanisms controlling petal development. *Nature* 399: 144-148.

Kramer, EM, VF Irish 2000 Evolution of the petal and stamen developmental programs: Evidence from comparative studies of the lower eudicots and basal angiosperms. *International Journal of Plant Sciences* 161: S29-S40.

Kramer, EM, VS Di Stilio, PM Schluter 2003 Complex patterns of gene duplication in the *APETALA3* and *PISTILLATA* lineages of the Ranunculaceae. *International Journal of Plant Sciences* 164: 1-11.

Krizek, BA, EM Meyerowitz 1996 Mapping the protein regions responsible for the functional specificities of the *Arabidopsis* MADS domain organ-identity proteins. *Proceedings of the National Academy of Sciences of the United States of America* 93: 4063-4070.

Krizek, BA, EM Meyerowitz 1996 The *Arabidopsis* homeotic genes *APETALA3* and *PISTILLATA* are sufficient to provide the B class organ identity function. *Development* 122: 11-22.

- Kubitzki, K, C Bayer 2003 Flowering plants, Dicotyledons: Malvales, Capparales, and non-betalain Caryophyllales. Springer, Berlin; New York.
- Kubitzki, K, C Bayer 2007 Flowering Plants. Eudicots: Berberidopsidales, Buxales, Crossosomatales, Fabales p.p., Geraniales, Gunnerales, Myrtales p.p., Proteales, Saxifragales, Vitales, Zygophyllales, Clusiaceae Alliance, Passifloraceae Alliance, Dilleniaceae, Huaceae, Picramniaceae, Sabiaceae. Springer, Berlin; New York.
- Kubitzki, K, JG Rohwer, V Bittrich 1993 Flowering plants, Dicotyledons: Magnoliid, Hamamelid, and Caryophyllid families. Springer-Verlag, Berlin; New York.
- Kuhn, U 1993 Chenopodiaceae. in: K Kubitzki, J Rohwer, V Bittrich eds. The families and genera of vascular plants. Vol. II. Springer-Verlag.
- Lage, JM, JH Leamon, T Pejovic, S Hamann, M Lacey, D Dillon, R Seagraves, B Vossbrinck, A Gonzalez, D Pinkel, DG Albertson, J Costa, PM Lizardi 2003 Whole genome analysis of genetic alterations in small DNA samples using hyperbranched strand displacement amplification and array-cgh. *Genome Research* 13: 294-307.
- Lasken, RS, M Egholm 2003 Whole genome amplification: Abundant supplies of DNA from precious samples or clinical specimens. *Trends Biotechnology* 21: 531-535.
- Litt, A, VF Irish 2003 Duplication and diversification in the *APETALA1/FRUITFULL* floral homeotic gene lineage: Implications for the evolution of floral development. *Genetics* 165: 821-833.
- Liu, Y, N Nakayama, M Schiff, A Litt, VF Irish, SP Dinesh-Kumar 2004 Virus induced gene silencing of a DEFICIENS ortholog in *Nicotiana benthamiana*. *Plant Molecular Biology* 54: 701-711.
- Mabry, T 1964 The betacyanins, a new class of red violet pigments, and their phylogenetic significance. Roland Press, New York.
- Mabry, T 1976 Pigment dichotomy and DNA-RNA hybridization data for centrosperous families. *Plant Systematics and Evolution* 126: 79-94.
- Mabry, T 1980 Betalains. in: E Bell, B Charwood eds. *Encyclopedia of plant physiology, secondary plant products*. Vol. 8. New series. Springer-Verlag, Berlin.
- Maddison, W, D Maddison 2008 Mesquite: A modular system for evolutionary analysis. Version 2.5 <http://mesquiteproject.org>.
- Maddison, W., and D. Maddison. 2008. Mesquite: a modular system for evolutionary analysis. Version 2.5 <http://mesquiteproject.org>.
- Malcomber, ST, EA Kellogg 2004 Heterogeneous expression patterns and separate roles of the SEPALLATA gene leafy hull sterile1 in grasses. *Plant Cell* 16: 1692-1706.

- Malcomber, ST, EA Kellogg 2005 *SEPALLATA* gene diversification: Brave new whorls. Trends in Plant Science 10: 427-435.
- Manhart, J, JH Rettig 1994 Gene sequence data. in: H-D Behnke, T Mabry eds. Caryophyllales: Evolution and Systematics. Springer, Berlin.
- Mayr, E 1982 Growth of biological thought. The Belknap Press of Harvard University Press, Cambridge.
- Mazel, CH, TW Cronin, RL Caldwell, NJ Marshall 2004 Fluorescent enhancement of signaling in a mantis shrimp. Science 303: 51-51.
- Mears, J 1976 Guide to research in plant taxonomy. Chemical Plant Taxonomy Newsletter 25: 11-14.
- Meyerowitz, EM, JL Bowman, LL Brockman, GN Drews, T Jack, LE Sieburth, D Weigel 1991 A genetic and molecular-model for flower development in *Arabidopsis thaliana*. Development: 157.
- Milby TH 1980 Studies in the Floral Anatomy of *Claytonia* (Portulacaceae). American Journal of Botany 67: 1046-1050
- Mizukami, Y, H Ma 1992 Ectopic expression of the floral homeotic gene *AGAMOUS* in transgenic *Arabidopsis* plants alters floral organ identity. Cell 71: 119-131.
- Moore, MJ, CD Bell, PS Soltis, DE Soltis 2007 Using plastid genome-scale data to resolve enigmatic relationships among basal angiosperms. Proceedings of the National Academy of Sciences of the United States of America 104: 19363-19368.
- Morton, CM, KG Karol, MW Chase 1997 Taxonomic affinities of *Physena* (Physenaceae) and *Asteropeia* (Theaceae). Botanical Review 63: 231-239.
- Nelson, B, GT Prance 1984 Observations on the pollination of *Rhabdodendron macrophyllum* (Spruce ex Benth.) Huber. Acta Amazonica 14: 411-426
- Ng, M, MF Yanofsky 2001 Function and evolution of the plant MADS-box gene family. Nature Reviews Genetics 2: 186-195.
- Noda, K, BJ Glover, P Linstead, C Martin 1994 Flower color intensity depends on specialized cell-shape controlled by a myb-related transcription factor. Nature 369: 661-664.
- Norman, C, M Runswick, R Pollock, R Treisman 1988 Isolation and properties of cDNA clones encoding *SRF*, a transcription factor that binds to the c-FOS serum response element. Cell 55: 989-1003.
- Nyffeler, R. 2007. The closest relatives of cacti: Insights from phylogenetic analyses of chloroplast and mitochondrial sequences with special emphasis on relationships in the tribe Anacampseroteae. American Journal of Botany: 94 89-101

- Nylander, J 2004 Mrmodeltest v2. Program distributed by the author. Evolutionary Biology Centre Uppsala Univ.
- Park, JH, Y Ishikawa, R Yoshida, A Kanno, T Kameya 2003 Expression of AODEF, a B-Functional MADS-box gene, in stamens and inner tepals of the dioecious species *Asparagus officinalis* L. Plant Molecular Biology 51: 867-875.
- Park, JH, Y Ishikawa, T Ochiai, A Kanno, T Kameya 2004 Two GLOBOSA-like genes are expressed in second and third whorls of homochlamydeous flowers in a *Asparagus officinalis* L. Plant and Cell Physiology 45: 325-332.
- Payer, J-B 1857 Traite d'organogenie comparee de la fleur. Masson, Paris.
- Pelaz, S, GS Ditta, E Baumann, E Wisman, MF Yanofsky 2000 B and C floral organ identity functions require *SEPALLATA* MADS-box genes. Nature 405: 200-203.
- Piatelli, M 1981 The betalains: Structure, biosynthesis, and chemical taxonomy. in: C EE ed. The biochemistry of plants. Vol. 7. Academic Press.
- Pinard, R, A de Winter, GJ Sarkis, MB Gerstein, KR Tartaro, RN Plant, M Egholm, JM Rothberg, JH Leamon 2006 Assessment of whole genome amplification-induced bias through high-throughput, massively parallel whole genome sequencing. BMC Genomics 7 -
- Pinyopich, A, GS Ditta, B Savidge, SJ Liljegren, E Baumann, E Wisman, MF Yanofsky 2003 Assessing the redundancy of MADS-box genes during carpel and ovule development. Nature 424: 85-88.
- Pnueli, L, M Abuabeid, D Zamir, W Nacken, Z Schwarzsommer, E Lifschitz 1991 The MADS-box gene family in tomato - temporal expression during floral development, conserved secondary structures and homology with homeotic genes from *Antirrhinum* and *Arabidopsis*. Plant Journal 1: 255-266.
- Pollock, R, R Treisman 1991 Human *SRF*-related proteins - DNA-binding properties and potential regulatory targets. Genes & Development 5: 2327-2341.
- Prance, GT 2003 Rhabdodendraceae. In K Kubitzki, C Bayer eds. The families and genera of vascular plants 5: 339-341. Springer, Berlin. .
- Preston, JC, EA Kellogg 2006 Reconstructing the evolutionary history of paralogous *APETALA1/FRUITFULL*-like genes in grasses (poaceae). Genetics 174: 421-437.
- Price, J, V Sturgess 1938 A survey of anthocyanins. VI. Biochemical Journal 32: 1658-1660.
- Raghunathan, A, HR Ferguson, Jr., CJ Bornarth, W Song, M Driscoll, RS Lasken 2005 Genomic DNA amplification from a single bacterium. Applied Environmental Microbiology 71: 3342-3347.

- Rambaut, A, A Drummond. 2003 Tracer. Ver 1. <http://tree.Bio.Ed.Ac.Uk/software/tracer/> March 2008
- Rasmussen, DA, EM Kramer, EA Zimmer 2009 One size fits all? Molecular evidence for a commonly inherited petal identity program in ranunculales. *American Journal of Botany* 96: 96-109.
- Remane, A 1952 Die Grundlagen des natürlichen Systems, der vergleichenden Anatomie und der Phylogenetik. Akademische Verlagsgesellschaft, Leipzig.
- Rettig, JH, HD Wilson, JR Manhart 1992 Phylogeny of the Caryophyllales - gene sequence data. *Taxon* 41: 201-209.
- Riechmann, JL, BA Krizek, EM Meyerowitz 1996 Dimerization specificity of Arabidopsis MADS domain homeotic proteins *APETALA1*, *APETALA3*, *PISTILLATA*, and *AGAMOUS*. *Proceedings of the National Academy of Sciences of the United States of America* 93: 4793-4798.
- Robinson, G, R Robinson 1933 A survey of anthocyanins: Notes on the distribution of leucoanthocyanins. *Biochemical Journal* 27: 206-212.
- Rohweder, O 1967 Centrospermenstudien 3. Blütenentwicklung und Blütenblau bei Silenoideen (Caryophyllaceae). *Botanische Jahrbücher für Systematik* 86: 130-185.
- Rohweder, O, K Huber (1974) Centrospermenstudien. 7. Beobachtungen und Anmerkungen zur Morphologie und Entwicklungsgeschichte einiger Nyctaginaceae. *Botanische Jahrbücher für Systematik* 90: 447-468
- Ronquist, F, JP Huelsenbeck 2003 MrBayes 3: Bayesian phylogenetic inference under mixed models. *Bioinformatics* 19: 1572-1574.
- Ronse De Craene, L 2008 Homology and evolution of petals in the core eudicots. *Systematic Botany* 33: 301-325.
- Ronse De Craene, LP 2007 Are petals sterile stamens or bracts? The origin and evolution of petals in the core eudicots. *Annals of Botany* 100: 621-630.
- Ronse De Craene, LP 2007 Are petals sterile stamens or bracts? The origin and evolution of petals in the core eudicots. *Annals of Botany* 100: 621-630.
- Ronse De Craene, LP 2008 Homology and evolution of petals in the core eudicots. *Systematic Botany* 33: 301-325.
- Ronse De Craene, LP, EF Smets, P Vanvinckenroye 1998 Pseudodiplostemony and its implications for the evolution of the androecium in the Caryophyllaceae. *Journal of Plant Research* 111: 25-43.
- Saedler, H, G Theissen 2001 Plant biology. Floral quartets. *Nature* 409 525-529.

- Sasaki, N, K Wada, T Koda, K Kasahara, T Adachi. 2005. Isolation and characterization of cDNAs encoding an enzyme with glucosyltransferase activity Plant and Cell Physiology.
- Sato, M, M Ohtsuka, Y Ohmi 2005 Usefulness of repeated genomic phi29 DNA polymerase-based rolling circle amplification kit, for generation of large amounts of plasmid DNA. Biomolecular Engineering 22: 129-132.
- Schaefer, HM, GD Ruxton 2008 Fatal attraction: Carnivorous plants roll out the red carpet to lure insects. Biology Letters 4: 153-155.
- Schmitz-Linneweber, C, RM Maier, JP Alcaraz, A Cottet, RG Herrmann, R Mache 2001 The plastid chromosome of spinach (*Spinacia oleracea*): Complete nucleotide sequence and gene organization. Plant Molecular Biology 45: 307-315.
- Shan, HY, N Zhan, CJ Liu, GX Xu, J Zhang, ZD Chen, HZ Kong 2007 Patterns of gene duplication and functional diversification during the evolution of the *API/SQUA* subfamily of plant MADS-box genes. Molecular Phylogenetics and Evolution 44: 26-41.
- Sharma, HP 1954 Studies in the order Centrospermales I Vascular anatomy of certain species of Portulacaceae. Journal of the Indian Botanical Society 33: 98-111
- Sharma, HP 1963 Contributions to the morphology of the Nyctaginaceae. 2: Floral anatomy of some species. Proceedings of the Indian Academy of Sciences 57: 149-163.
- Shimada, S, H Otsuki, M Sakuta 2007 Transcriptional control of anthocyanin biosynthetic genes in the Caryophyllales. Journal of Experimental Botany 58: 957-967.
- Shimada, S, YT Inoue, M Sakuta. 2005. Anthocyanidin synthase in non-anthocyanin-producing Caryophyllales species Plant Journal. Vol. 44.
- Soltis DE, PS Soltis, PK Endress, MW Chase 2005 Phylogeny and Evolution of Angiosperms. Sinauer, Sunderland.
- Soltis, DE, PS Soltis, MW Chase, ME Mort, DC Albach, M Zanis, V Savolainen, WH Hahn, SB Hoot, MF Fay, M Axtell, SM Swensen, LM Prince, WJ Kress, KC Nixon, JS Farris 2000 Angiosperm phylogeny inferred from 18S rDNA, *rbcL*, and *atpB* sequences. Botanical Journal of the Linnean Society 133: 381-461.
- Soltis, PS, DE Soltis, MW Chase 1999 Angiosperm phylogeny inferred from multiple genes as a tool for comparative biology. Nature 402: 402-404.
- Sommer, H, JP Beltran, P Huijser, H Pape, WE Lonng, H Saedler, Z Schwarzsommer 1990 *DEFICIENS*, a homeotic gene involved in the control of flower morphogenesis in *Antirrhinum majus* - the protein shows homology to transcription factors. EMBO Journal 9: 605-613.
- Sommer, H, W Nacken, P Beltran, P Huijser, H Pape, R Hansen, P Flor, H Saedler, Z Schwarzsommer 1991 Properties of *DEFICIENS*, a homeotic gene involved in the control of flower morphogenesis in *Antirrhinum majus*. Development: 169-175.

- Stafford, HA. 1994. Anthocyanins and betalains: Evolution of the mutually exclusive pathways Plant Science
- Stellari, GM, MA Jaramillo, EM Kramer 2004 Evolution of the *APETALA3* and *PISTILLATA* lineages of MADS-box-containing genes in the basal angiosperms. Molecular Biology and Evolution 21: 506-519.
- Strack, D, T Vogt, W Schliemann. 2003. Recent advances in betalain research Phytochemistry. Vol. 62.
- Swofford, D 2000 PAUP: Phylogenetic analysis using parsimony and other methods, version 4.
- Takhtajan, A 1980 Outline of the classification of flowering plants (Magnoliophyta). Botanical Review 46: 225-359.
- Takhtajan, AL 1991 Evolutionary trends in flowering plants. Columbia University Press, New York.
- Tanaka, Y, N Sasaki, A Ohmiya 2008 Biosynthesis of plant pigments: Anthocyanins, betalains and carotenoids. Plant Journal 54: 733-749.
- Theissen, G, A Becker, A Di Rosa, A Kanno, JT Kim, T Munster, KU Winter, H Saedler 2000 A short history of MADS-box genes in plants. Plant Molecular Biology 42: 115-149.
- Thompson, JD, TJ Gibson, F Plewniak, F Jeanmougin, DG Higgins 1997 The Clustal X windows interface: Flexible strategies for multiple sequence alignment aided by quality analysis tools. Nucleic Acids Research 25: 4876-4882.
- Thorne, R 1976 A phylogenetic classification of the Angiospermae. Evolutionary biology 9: 35-106.
- Thorne, R 1992 An updated classification of the flowering plants. Aliso 13: 365-389.
- Trobner, W, L Ramirez, P Motte, I Hue, P Huijser, WE Lonig, H Saedler, H Sommer, Z Schwarzsommer 1992 GLOBOSA - a homeotic gene which interacts with *DEFICIENS* in the control of *Antirrhinum* floral organogenesis. EMBO Journal 11: 4693-4704.
- True, J, H Haag 2001 Developmental systems drift and flexibility in evolutionary trajectories. Evolution of Development 3: 109-119.
- Vandenbussche, M, J Zethof, E Souer, R Koes, GB Tornielli, M Pezzotti, S Ferrario, GC Angenent, T Gerats 2003 Toward the analysis of the *Petunia* MADS-box gene family by reverse and forward transposon insertion mutagenesis approaches: B, C, and D floral organ identity functions require *SEPALLATA*-like mads box genes in petunia. Plant Cell 15: 2680-2693.
- Vanderkrol, AR, A Brunelle, S Tsuchimoto, NH Chua 1993 Functional-analysis of *Petunia* floral homeotic mads box gene *PMADSI*. Genes & Development 7: 1214-1228.

- Vanvinckenroye P, E Cresens, LPR Decraene, E Smets (1993) A Comparative Floral Developmental Study in *Pisonia*, *Bougainvillea* and *Mirabilis* (Nyctaginaceae) with Special Emphasis on the Gynoecium and Floral Nectaries. Bulletin du Jardin Botanique National de Belgique 62: 69-96.
- Vanvinckenroye, P, E Smets 1996 Floral ontogeny of five species of *Talinum* and of related taxa (Portulacaceae). Journal of Plant Research 109: 387-402.
- Vogt, T 2002 Substrate specificity and sequence analysis define a polyphyletic origin of betanidin 5- and 6-o-glucosyltransferase from *Dorotheanthus bellidiformis*. Planta 214: 492-495.
- Vogt, T, E Zimmermann, R Grimm, M Meyer, D Strack 1997 Are the characteristics of betanidin glucosyltransferases from cell-suspension cultures of *Dorotheanthus bellidiformis* indicative of their phylogenetic relationship with flavonoid glucosyltransferases? Planta 203: 349-361.
- Waser, NM, MV Price 1981 Pollinator choice and stabilizing selection for flower color in *delphinium-nelsonii*. Evolution 35: 376-390.
- Whipple, CJ, MJ Zanis, EA Kellogg, RJ Schmidt 2007 Conservation of B class gene expression in the second whorl of a basal grass and outgroups links the origin of lodicules and petals. Proceedings of the National Academy of Sciences of the United States of America 104: 1081-1086.
- Whitney, HM, M Kollé, P Andrew, L Chittka, U Steiner, BJ Glover 2009 Floral iridescence, produced by diffractive optics, acts as a cue for animal pollinators. Science 323: 130-133.
- Wikstrom N, V Savolainen, MW Chase 2001 Evolution of the angiosperms: calibrating the family tree. Proceedings of the Royal Society London B Biological Series 268: 2211-2220.
- Williams, SE, VA Albert, MW Chase 1994 Relationships of Droseraceae: A Cladistic Analysis of rbcL Sequence and Morphological Data. American Journal of Botany 81: 1027-1037
- Wyman, SK, RK Jansen, JL Boore 2004 Automatic annotation of organellar genomes with dogma. Bioinformatics 20: 3252-3255.
- Yanofsky, MF, H Ma, JL Bowman, GN Drews, KA Feldmann, EM Meyerowitz 1990 The protein encoded by the *Arabidopsis* homeotic gene *AGAMOUS* resembles transcription factors. Nature 346: 35-39.
- Yu, DY, M Kotilainen, E Pollanen, M Mehto, P Elomaa, Y Helariutta, VA Albert, TH Teeri 1999 Organ identity genes and modified patterns of flower development in gerbera hybrida (asteraceae). Plant Journal 17: 51-62.
- Zachgo, S, ED Silva, P Motte, W Trobner, H Saedler, Z Schwarzsommer 1995 Functional-analysis of the *Antirrhinum* floral homeotic *DEFICIENS* gene in-vivo and in-vitro by using a temperature-sensitive mutant. Development 121: 2861-2875.

Zahn, LM, HZ King, JH Leebens-Mack, S Kim, PS Soltis, LL Landherr, DE Soltis, CW dePamphilis, H Ma 2005 The evolution of the *SEPALLATA* subfamily of MADS-box genes: A preangiosperm origin with multiple duplications throughout angiosperm history. *Genetics* 169: 2209-2223.

Zahn, LM, JH Leebens-Mack, JM Arrington, Y Hu, LL Landherr, CW dePamphilis, A Becker, G Theissen, H Ma 2006 Conservation and divergence in the *AGAMOUS* subfamily of MADS-box genes: Evidence of independent sub- and neofunctionalization events. *Evolution and Development* 8: 30-45.

Zwickl, D 2000 Genetic algorithm approaches for the phylogenetic analysis of large biological sequence datasets under the maximum likelihood criterion. PhD Thesis University of Texas at Austin

BIOGRAPHICAL SKETCH

Samuel Fraser Brockington was born 27 July 1979 in Manchester, England, son of Ian Fraser Brockington and Diana Hilary Pink. He attended King Edwards School, Edgbaston, Birmingham. Subsequently he taught at St Marks School, Jane Furse, South Africa before attending the University of Edinburgh where he was awarded a First Class degree in Biology with honors in Plant Science. After attending a Tropical Botany Field Course run by Walter. S. Judd of the University of Florida, he subsequently entered the graduate program at the Department of Botany and Florida Museum of Natural History at the University of Florida in 2003. He complete his PhD in 2009. He goes on to a Marie Curie Fellowship at the Department of Plant Science at the University of Cambridge, England.